Quantification of pathology in Lewy body disease: the impact of multiple pathologies on clinical phenotype

Lauren Walker
MRes Medical and Molecular Biosciences

Institute of Neuroscience
Newcastle University
Campus for Ageing and Vitality
Newcastle-upon-Tyne
NE4 5PL

Thesis submitted for the degree of Doctorate of Philosophy in Newcastle University
October 2015

Abstract

Introduction: Pathologies characteristic of Alzheimer's disease (i.e. hyperphosphorylated tau (HP-τ) and β amyloid (Aβ) plaques) often co-exist in patients with dementia with Lewy bodies and Parkinson's disease dementia, in addition to lesions positive for α-synuclein. Post-translational modifications of Aβ and α-synuclein, namely pyroglutamylated amyloid-β (pE(3)-Aβ) and α-synuclein phosphorylated at serine-129 (pSer129 α-syn) have also been implicated in disease pathogenesis, and with recent studies pointing to a synergistic relationship between HP-τ, Aβ and α-synuclein, interactions between these protein aggregations may have clinical implications. The aim of this study was to determine whether quantitative neuropathological assessment can be a useful tool in detecting subtle changes in pathology load in cases with mixed Alzheimer's disease (AD) and Lewy body disease (LBD) (mixed AD/LBD) presenting with either AD or LBD. In addition, the impact that multiple pathological lesions have on the pathological profile and clinical phenotype of cases with LBD was investigated.

Methods: *Post-mortem* brain tissue from cases that fulfilled neuropathological criteria for mixed AD/LBD was analysed by immunohistological staining and quantitative image analysis, measurements of cortical thickness were taken and *APOE* status determined to detect differences between different clinical phenotypes, with 'pure' AD, DLB and control samples for comparison. HP-τ, Aβ, pE(3)-Aβ and pSer129 α-syn pathology loads were quantitatively measured in a cohort of LBD cases and the influence of individual and combined pathology loads on end stage motor dysfunction, as measured by part III of the Unified Parkinson's Disease Rating Scale (UPDRS), was determined.

Key findings: In neuropathologically mixed AD/LBD cases, both the amount and the topographical distribution of pathological protein aggregates differed between distinct clinical phenotypes. Aβ, individually and in combination with α-syn, may be associated with UPDRS scores in DLB cases, and both pE(3)-Aβ and HP-τ correlated positively with pSer129 α-syn in multiple regions in LBD cases.

Conclusions: This study demonstrated the potential importance of quantitative neuropathological assessment in clinico-pathological studies and suggests co-existing pathologies may play a role in neurodegeneration. In addition to supporting studies that suggest a synergistic relationship between Aβ and HP-τ with pSer129 α-syn, this study also introduces pE(3)-Aβ as a potential contributor, making it an interesting target for future study and therapeutic design.

Acknowledgements

I would like to acknowledge all those that have helped me throughout my PhD. First and foremost I would like to thank my supervisor Professor Johannes Attems for giving me the opportunity to pursue a PhD in this exciting field of research and for his constant support, enthusiasm, guidance and good humour throughout the past three years. Also, special thanks to my second supervisor Professor Alan Thomas for providing guidance on the clinical aspects of this project.

I feel privileged to have completed my PhD in such an inspiring and supportive group of people. I am eternally grateful to Mrs Mary Johnson, Mrs Ros Hall and Mrs Lynne Ramsay for the endless teaching, advice when things weren't going according to plan and expertise in immunohistochemical and histological techniques. Special thanks to my fellow researchers particularly Dr Kirsty McAleese for her support and friendship (and excellent cake!) and Mr Daniel Erskine for his friendship, advice and general enthusiasm for life! All of these people helped to create a stimulating and friendly environment which was a pleasure to work in.

I extend my appreciation to Dr Carmen Martin-Ruiz, Dr Craig Parker and Mrs Claire Kolenda for their assistance in the *APOE* genotyping and Dr Sean Colloby for continuous statistical advice. In addition, thanks to my progression advisors Professor Raj Kalaria and Dr Christopher Morris for their guidance during my studies and Mr Arthur Oakley for sharing his expertise in microscopy and interesting anecdotes of his time in research.

Many thanks to all of the staff at the Newcastle Brain Tissue Resource for their assistance during my studies. This research would not have been possible if not for the generosity of the donors and families to whom I am especially grateful.

I would like to thank my friends who have listened tirelessly to my stories about work and reminded me that there is a life outside of the laboratory. Finally, heartfelt thanks go to my family for the constant love and support over the years, especially recently during the more stressful times of my PhD.

My PhD was funded by National Institute for Health Research (NIHR) Biomedical Research Unit based at the Institute of Neuroscience at Newcastle University.

Lauren Walker
October 2015

Original publication

The study described in Chapter 3 is based on the following original publication

Walker L, McAleese KE, Thomas AJ, Johnson M, Martin-Ruiz C, Parker C, Colloby SJ, Jellinger K and Attems J. Neuropathologically mixed Alzheimer's and Lewy body disease: burden of pathological protein aggregates differs between clinical phenotypes. *Acta Neuropathologica* 2015 129 (5): 729-48.

Contents

List of figures and tables

List of Abbreviations

3R	3 repeat tau
4R	4 repeat tau
Aβ	Amyloid-beta
AβSer8	Amyloid beta phosphorylated at serine 8
ADRDA	Alzheimer's Disease and Related Disorders Association
AGD	Agyrophilic grain disease
ALP	Autophagy-lysosome pathway
APES	3-aminopropyltriethoxysilane
APOE	Apoliopoprotein
APP	Amyloid precursor protein
α-syn	α-synuclein
AD	Alzheimer's disease
APES	3-Aminopropyltriethoxysilane
BA	Brodmann area
CA	Cornu ammonis
Ca^{++}	Calcium
CAA	Cerebral amyloid angiopathy
cAD	Mixed AD/LBD clinically presenting with Alzheimer's disease
CaMK-II	Calcium/calmodulin-dependent kinase II
CBD	Corticobasal degeneration
Cdk5	Cyclin-dependant kinase 5
cDLB	Mixed AD/LBD clinically presenting with dementia with Lewy bodies
CERAD	Consortium to Establish a Registry for Alzheimer's disease
CFV	Cresyl fast violet
CJD	Creutzfeldt–Jakob disease
CK1	Casein kinase 1
CNS	Central nervous system
CPS	Combined pathology score

CPC	Clinico-pathological correlation
cPDD	Mixed AD/LBD clinically presenting with Parkinson's disease dementia
CR	Cognitive reserve
CSF	Cerebral spinal fluid
CTX	Cortex
CWMR	Cerebral white matter rarefaction
DAB	3,3 diaminobezidine
DLB	Dementia with Lewy bodies
DNA	Deoxyribonucleic acid
DOPAC	3,4-dihydroxyphenylacetic acid
ELISA	Enzyme-linked immunoabsorbant assay
EOD	Early onset dementia
EPS	Extrapyramidal symptom
FAD	Familial Alzheimer's disease
FTLD	Fronto-temporal lobar degeneration
FUS	Fused in sarcoma RNA binding protein
GCI	Glial cytoplasmic inclusion
GBA	Glucocerebrosidase
GSK-3β	Glycogen synthase-3β
HP-τ	Hyperphosphorylated tau
HRP	Horseradish peroxidase
IPS	Individual pathology score
IHC	Immunohistochemistry
iLBD	Incidental Lewy body disease
LB	Lewy body
LC	Locus coeruleus
LI	Large image
LN	Lewy neurite
LBD	Lewy body disease
LBV-AD	Lewy body variant of Alzheimer's disease
LOD	Late onset dementia
LRRK2	Leucine-rich repeat kinase 2
LT	Lewy thread
MAP	Microtubule associated protein

MCI	Mild cognitive impairment
MDS	Movement disease society
MTL	Medial temporal lobe
MMSE	Mini mental state examination
MND	Motor neurone disease
MRI	Magnetic resonance imaging
nbM	Nucleus basalis of Meynert
NBTR	Newcastle Brain Tissue Resource
NIA-AA	National Institute on Ageing - Alzheimer's Association
NCI	Neuronal cytoplasmic inclusion
NC	Negative controls
NFT	Neurofibrillary tangle
NI	No inclusion
NII	Neuronal intranuclear inclusion
NINCDS	National Institute of Neurological and Communicative Disorders and Stroke
NT	Neuropil thread
NIA-AA	National Institute on Ageing – Alzheimer's Association
pAD	'pure' Alzheimer's disease
pDLB	'pure' dementia with Lewy bodies
PD	Parkinson's disease
PDD	Parkinson's disease dementia
pE(3)-Aβ	Pyruglutmylated amyloid-beta
PET	Positron emission tomography
PiB	^{11}C-labelled Pittsburgh compound B
PKA	Cyclic AMP dependant protein kinase
PP	Phosphatase
PSEN1	Presenilin-1
PSEN2	Presenilin-2
pSer129 α-syn	α-synuclein phosphorylated at serine-129
PSP	Progressive supranuclear palsy
QC	Glutaminyl cyclase
r_s	Spearman's rank correlation
RBD	Rapid eye movement sleep behaviour disorder
RGB	Red green blue threshold

ROI	Region of interest
RT-PCR	Real-time Polymerase Chain Reaction
SI	Single image
SN	Substantia nigra
SNCA	α-synuclein
SPECT	Single photon emission computed tomography
SQ	Semi-quantitative
TBS	Tris buffered saline
TMA	Tissue Micro Array
TPD	Transactive response DNA binding protein
μm	Micrometre
UPDRS	Unified Parkinson's Disease Rating Scale
UPS	Ubiquitin proteasome system
VP	Vascular pathology
WM	White matter

Chapter 1. Introduction

1.1 Ageing and chronic disease

The increase in life expectancy due to improved treatment options for many acute and chronic diseases has to be regarded as one of the greatest medical achievements of the 20th century. For the first time in history, 11 million people in the UK are aged 65 or over, which has doubled from 7% to 14% of the total population within the last 46 years (Large, 2014, Prince et al., 2015). In addition, the report by the National Office of Statistics highlighted that in the current UK population there is a higher proportion of people aged 60 years or over compared to those under the age of 18 (Large, 2014). This demographic transition is a result of high to low mortality rates and a steady decline in birth rate, and this increase in population ageing is continuing into the 21st century.

Population ageing has already had an impact on society as chronic, non-communicable diseases in the elderly population such as neurodegenerative diseases accounting for age related dementias, diabetes, cerebrovascular disease and chronic respiratory disease. These age associated diseases are reaching epidemic proportions worldwide accounting for up to 23% of the global disease burden (Prince et al., 2015). This has introduced a unique set of challenges as the potential financial and social costs of non-communicable diseases, particularly affecting carers and the healthcare system, have the ability to affect economic growth and many governments are prioritising strategies to address this issue (Daar et al., 2007).

1.2 Epidemiology of dementia

Dementia is a clinical syndrome and is an umbrella term for the neurodegenerative diseases that cause progressive deterioration in cognitive ability and capacity for independent living (Prince et al., 2013) and it is important to track the global prevalence of this emerging pandemic. With this in mind, the World Health Organisation in collaboration with Alzheimer's Disease International issued a report in 2012 and estimated the prevalence of dementia would reach 115.4 million by 2050, highlighting the urgent need to invest in health and social systems to improve care and services and to increase the priority given to dementia in the health research agenda (World Health Organisation and Alzheimer's Disease International, 2012). The worldwide

dementia pandemic is reflected by respective data of the UK population, as currently 835,000 people in the UK are affected by dementia with an annual cost to the National Health Service of £26 billion (Alzheimer's Society, 2014). In recognition of this, the UK government announced a challenge on dementia which promised to improve the care of people with dementia and increase the funding for dementia research (Department of Health, 2012). Neurodegenerative diseases that cause dementia are not fatal *per se* but rather predispose patients to other fatal illnesses, with bronchopneumonia and ischaemic heart disease accounting for 61.5% of deaths in patients with dementia (Brunnstrom and Englund, 2009).

1.3 Early onset and age related dementia

Dementia can occur in 2 forms: early onset dementia (EOD) which refers to dementia that becomes clinically manifested before the age of 65 and late onset dementia (LOD) which typically occurs in people over the age of 65. EOD is much less frequent than LOD as it has been estimated that between 2% and 10% of all dementia cases occur before the age of 65 (Prince, 2009). EODs are also referred to as familial dementia as they can be inherited in a Mendelian fashion and are more likely to arise from a single gene defect. Genetic studies have linked mutations in several genes that are associated with EO Alzheimer's disease (AD) and Parkinson's disease (PD) which are summarised in table 1.1. In contrast, LOD is considered to be sporadic in nature with complex genetic and environmental risk factors, many of which are unknown (Masellis et al., 2013). LOD or sporadic dementia is attributed to neurodegenerative diseases of the central nervous system resulting in the impairment of normal neuronal and synaptic function and subsequent loss of vulnerable neuronal populations that frequently involve anatomically related systems (Jellinger, 2009). The focus of this thesis is on neurodegenerative diseases associated with age related dementia.

Neurodegenerative disease	Mutation (variant)	Model
Alzheimer's disease	*APP*	Autosomal dominant
	PSEN1	Autosomal dominant
	PSEN2	Autosomal dominant
	APOE	Individuals heterozygous or homozygous for ε4 have increased risk
	TREM2	rs75932628 variant causes R47H substitution associated with increased risk for AD. N.B. homozygous mutations in TREM2 result in Nasu-Hakola disease of which early onset dementia is a clinical characteristic
Parkinson's disease	*SNCA* (*A30P*) (*E46K*) (*A53T*) (*H50Q*) (*G51D*)	All autosomal dominant point mutations
	SNCA duplications *SNCA* triplications	Age of onset and severity of the disease phenotype correlating with the SNCA copy number, suggesting a gene-dose effect
	Parkin	Autosomal recessive
	LRRK2	Autosomal dominant
	DJ1	Autosomal recessive
	PINK1	Autosomal recessive
	ATP13A2	Autosomal recessive
	VPS35	Autosomal dominant
	HTRA2	Autosomal dominant
	PLA2G6	Autosomal recessive
	GBA	Risk locus
	MAPT	Mutations are associated with parkinsonism
	Ataxin3	Mutations cause syndromes of which parkinsonism is a feature
	Ataxin2	Mutations cause syndromes of which parkinsonism is a feature

Table 1.1 Genetic mutations linked to Alzheimer's disease and Parkinson's disease. Abbreviations: *APP*; amyloid precursor protein, *PSEN1*; presenilin-1, *PSEN2*; presenilin-2, *APOE*; apolipoprotein, *TREM2*; Triggering Receptor Expressed On Myeloid Cells 2, *SNCA*; α-synuclein, *LRRK2*; leucine-rich repeat kinase 2, *GBA*; glucocerebrosidase, *PINK*; PTEN induced putative kinase 1, *MAPT*; Microtubule-Associated Protein Tau, ATP13A2; Adenosine triphosphate 13A2, *VPS35*; Vacuolar protein sorting-associated protein 35, *HTRA2*; serine protease HtrA2, PLA2G6, phospholipase A2 group VI. For reviews see (Hernandez et al., 2016, Scheltens et al., 2016).

1.4 Patho-mechanisms of neurodegeneration

Most neurodegenerative diseases occur sporadically and the aetiology is thought to be multifactorial with genetic and environmental factors playing a role (Elbaz et al., 2007). One unifying characteristic of neurodegenerative diseases is the mis-folding of particular proteins into a stable alternative conformation and accumulation in tissues of fibrillar deposits resulting in neuronal cell death. (Carrell and Lomas, 1997, Dobson, 1999). There are several recognised ways

in which neuronal cells can die including apoptosis and necrosis. Apoptosis is described as programmed cell death where the cell itself stimulates a cascade of events that lead to the destruction of the neurone (Friedlander, 2003). In contrast necrosis is a result of acute ischemia or traumatic injury to the brain leading to the direct cause of the demise of the cell (Friedlander, 2003). Although the apoptotic cell death process has been implicated in neurodegenerative diseases it can be argued that due to the acute nature and rapid time course it might not be the most relevant mechanism of cell death. Necrosis on the other hand has an extended duration with a time course of days or even weeks, which might better fit the clinical phenotype and gradual accumulation of toxic proteins associated with many neurodegenerative diseases (Graeber and Moran, 2002).

Under physiological conditions the native protein exists in a soluble state. However, under pathological conditions the protein undergoes mis-folding into pathogenic species (dimers, trimers and oligomers) that undergo further conformational changes to form higher order aggregates in the form of β-pleated sheets (protofibrils and amyloid fibrils). These structures then form the basis for the formation of pathological inclusions seen in neurodegenerative diseases (Figure 1.1). The type and topographical locations of these lesions are the basis of neuropathological classification systems used to define specific neurodegenerative diseases (Table 1.2). The formation of protein aggregate that is the most neurotoxic remains a topic of debate (De Felice et al., 2004). Studies conducted by Guillozet and colleagues and Imhof and colleagues suggested quantification of insoluble Aβ is not a good clinical correlate of dementia (Guillozet et al., 2003, Imhof et al., 2007), whilst LaFerla and colleagues and Haass and colleagues indicated that soluble oligomeric forms of Aβ correlate with *ante-mortem* cognitive decline (Haass and Selkoe, 2007, LaFerla et al., 2007).

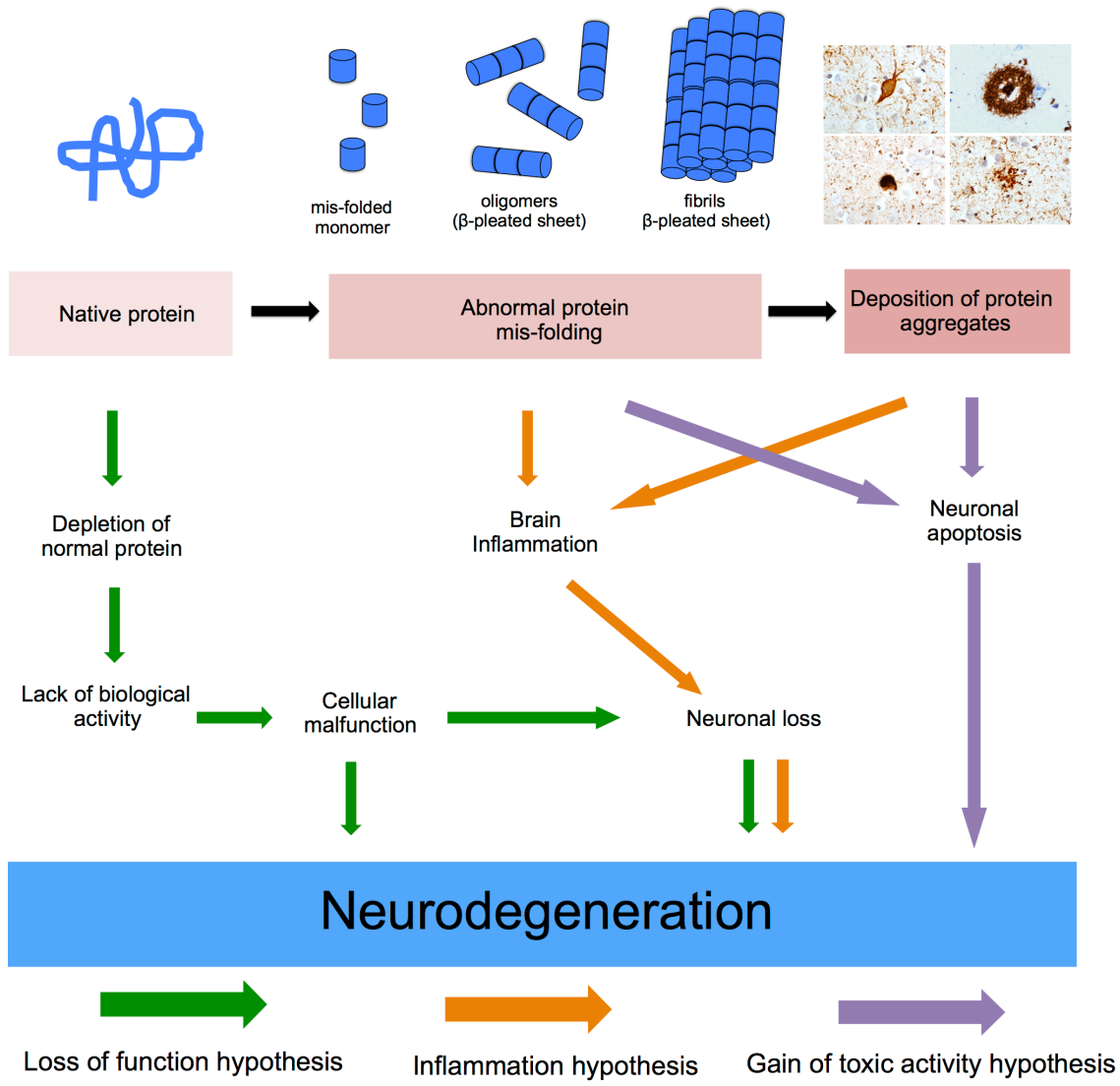

Figure 1.1 Proposed common pathomechanisms for neurodegenerative diseases associated with protein mis-folding and aggregation. Adapted from (Soto, 2003).

Neurodegenerative disease	Misfolded protein	Signature lesion	Localisation
Alzheimer's disease	HP-τ (3R, 4R) β-amyloid (1-40, 1-42) HP-τ (3R, 4R) and β-amyloid (1-40, 1-42)	NFT, NT Aβ plaque neuritic plaque	Neuronal cell bodies (NFT) and processes (NT) extracellular HP-τ - dystrophic neurites, β-amyloid - extracellular
Lewy body diseases			
Parkinson's disease	α-synuclein	LB, LN	Neuronal cell bodies (LB) and processes (LN)
Dementia with Lewy bodies	α-synuclein	LB, LN	Neuronal cell bodies (LB) and processes (LN)
Multiple system atrophy	α-synuclein	GCI	Cytoplasm of glial cells
Frontotemporal lobar degeneration			
Tauopathies			
Pick's disease	HP-τ (3R)	Pick bodies	Neuronal cell bodies
Corticobasal degeneration	HP-τ (4R)	Astrocytic plaque	distal segments of astrocytes
Progressive supranuclear palsy	HP-τ (4R)	Globose NFT	Neuronal cell body
	HP-τ (4R)	Tufted astrocyte	Astrocytic cell body
Agyrophilic grain disease	HP-τ (4R)	Grains	Neuronal processes
Others			
FTLD-TDP	TDP-43	NCI (NII)	Neuronal cytoplasm and intranuclear
FTLD-UPS	Ubiquitin	NCI (NII)	Neuronal cytoplasm and intranuclear
FTLD-FUS	FUS protein	NCI (NII)	Neuronal cytoplasm and intranuclear
FTLD-ni	none known	none known	none known

Table 1.2 Major neurodegenerative diseases classified by their signature pathological lesions, including type of mis-folded protein and the cellular localisation protein aggregates. Abbreviations: HP-τ, hyperphosphorylated tau; 3R, 3 repeat tau; 4R, 4 repeat tau; NFT, neurofibrillary tangle; NT, neuropil thread; LB, Lewy body; LN, Lewy neurite; GCI, glial cytoplasmic inclusion; FTLD, frontotemporal lobar degeneration; TDP, n; NCI, neuronal cytoplasmic inclusion; NII, neuronal intranuclear inclusion; UPS, ubiquitin proteasome system; FUS, fused in sarcoma RNA binding protein; ni, no inclusion.

Although the triggers are not yet fully understood (Jellinger, 2003, Forman et al., 2004, Selkoe, 2004), it is an attractive idea to speculate that neurodegenerative diseases share common pathomechanisms causing the deposition of different pathologic protein aggregations and resulting in the different syndromes seen in clinics. Three central hypotheses have been suggested:

1) The loss of function hypothesis suggests the loss of normal neuronal activity arises when native proteins are depleted during mis-folding and aggregation (Soto, 2003). One example concerns the debate surrounding TDP-43 mediated neurodegeneration typically associated with motor neurone disease (MND) and Frontotemporal lobar degeneration (FTLD). Physiological TDP-43 is expressed in the nucleus of neurones where its main function is to regulate RNA processing (Polymenidou et al., 2011). However, in patients with MND/FTLD, TDP-43 positive inclusions are typically found in the cytoplasm alongside loss of nuclear expression of the protein, which suggests loss of physiological function could potentially play a role in neurodegeneration (Xu, 2012) (Figure 1.1).

2) The most widely accepted theory of neurodegeneration of the ageing brain is gain of toxic function hypothesis (Soto, 2003). *In vitro* studies to support this theory have suggested that aggregates of mis-folded proteins can directly induce neuronal apoptosis (Loo et al., 1993, El-Agnaf et al., 1998, Lunkes and Mandel, 1998). In addition, evidence has emerged that implicates oligomeric forms of Aβ and soluble forms of hyperphosphorylated tau (HP-τ) in synaptic dysfunction and loss of neurones (Yoshiyama et al., 2007, Shankar et al., 2008, Koffie et al., 2012, Kopeikina et al., 2012). As synaptic dysfunction has been shown to be the strongest pathological correlate of cognitive decline (DeKosky and Scheff, 1990, Terry et al., 1991), impairments in synaptic plasticity due to aggregation of mis-folded proteins strengthens the idea of unifying mechanisms by which tissue degeneration and cell death occur in neurodenegerative disorders (Figure 1.1).

3) According to the brain inflammation hypothesis, abnormal protein aggregates can induce a cascade of events that result in the production of neurotoxic irritants leading to synaptic changes and neuronal death (Soto, 2003). Inducers, sensors, transducers and effectors of neurodegeneration may be generated in a disease specific manner, although there may be considerable overlap in the mechanisms common to multiple neurodegenerative diseases (McGeer and McGeer, 1995, Wyss-Coray and Mucke, 2002). Proteins specific to the immune system including complement inhibitors and inflammatory cytokines have been detected surrounding protein deposits (McGeer et al., 1988, Kawamata et al., 1992). In addition, i*n vitro* studies have suggested that aggregated forms of pathogenic proteins are capable of activating microglia and astrocytes resulting in the release of inflammatory proteins (Peyrin et al., 1999, Yates et al., 2000). Although the studies mentioned imply neuroinflammation plays an active role in the neurodegenerative process, a contrasting theory suggests activation of the immune system in response to the accumulation of pathogenic protein accumulation is a protective mechanism. A study conducted by Wyss-Coray and colleagues

demonstrated that inhibiting C3 complement component (a key inflammatory protein activated in AD) in a mouse model resulted in a 2- to 3- fold increase in Aβ plaques indicating complement activation may act as part of a defence mechanism against Aβ and is potentially beneficial in neurodegenerative diseases (Wyss-Coray et al., 2002) (Figure 1.1).

In addition to the overproduction of abnormal protein deposits in the brain leading to perturbed cellular function and eventual cell death, impairments to protein quality control systems facilitating the degradation and/or removal of toxic proteins from the brain may result in accumulation of pathological protein aggregates, presenting as a key step in the pathological cascade that leads to spreading neurodegeneration. Mis-folded proteins are primarily degraded by the multi-component ubiquitin proteasome system (UPS) and the autophagy-lysosome pathway (ALP) (Ciechanover, 2005, Rubinsztein, 2006). Dysfunction in the UPS has been strongly implicated in the pathogenesis of PD as it has been shown that proteasome structure and function are altered in the substantia nigra (SN) in PD patients compared to age matched control subjects (McNaught et al., 2003). Alternatively it has been hypothesised the UPS system plays a role in Lewy body formation (Olanow and McNaught, 2006), as the aggresomal inclusions cannot clear unwanted proteins due to impairment of the proteasomal function and/or the overwhelming production of damaged proteins and expands to become a Lewy body (Olanow et al., 2004).

In addition to the UPS system, mis-folded proteins i.e α-synuclein (α-syn) can also be cleared by the autophagy lysosome pathway (ALP) (Webb et al., 2003, Cuervo et al., 2004). As autophagy utilises intracellular lysosomes to degrade mis-folded proteins, defective or depleted lysosomes are implicated in pathogenesis of PD (Alvarez-Erviti et al., 2010, Dehay et al., 2010). Interestingly, neuropathological examination of patients with Gaucher's disease (the most predominant lysosomal storage disorder of which parkinsonism is a clinical feature) revealed numerous α-syn positive inclusions in the hippocampus (Wong et al., 2004) indicating impairment of the ALP system may be a common mechanism by which aggregated proteins accumulate resulting in neurodegeneration.

Reduced elimination of toxic proteins from the brain could also contribute to the accumulation of respective proteins in the CNS (Attems and Jellinger, 2013b). Failure of the perivascular drainage system results in the accumulation of Aβ (mainly Aβ40) in the walls of blood vessels as cerebral amyloid angiopathy (CAA) (Weller et al., 2000, Hawkes et al., 2014).

1.5 Neurodegenerative diseases

Regardless of the mechanism resulting in neurodegeneration and the accumulation of insidious protein aggregations, the classification of neurodegenerative diseases is underpinned by the combination of the molecular composition and topographical localisation of pathological lesions identified at *post-mortem* examination and the presence of specific clinical features.

1.5.1 Alzheimer's disease

Alzheimer's disease (AD) is the leading cause of dementia caused by neurodegenerative disease accounting for between 50%-80% of cases (Blennow et al., 2006, Mayeux and Stern, 2012). Clinically, AD is characterised by chronic and irreversible decline in cognition of insidious onset which renders the patient unable to perform activities of daily living, as outlined by a collaborative report by the National Institute of Neurological and Communicative Disorders and Stroke (NINCDS) and Alzheimer's Disease and Related Disorders Association (ADRDA) (McKhann et al., 1984). More recently the National Institute on Ageing (NIA) and Alzheimer's Association (AA) charged a task force to update these guidelines. In addition to the core features of an amnestic presentation and impairments in visuospatial abilities and language functions, the revised criteria also include consideration of magnetic resonance imaging (MRI), positron emission tomography (PET) imaging and cerebral spinal fluid (CSF) bio-markers (Jack et al., 2011, McKhann et al., 2011). A diagnosis of probable AD is only given when there is no evidence of clinical symptoms associated with other diseases of which dementia can be a feature.

AD is a complex and heterogeneous disorder classified as either early onset (with age of onset under the age of 65) or late onset (over the age of 65). Familial early onset can be characterised by mendelian inheritance, however

early onset patients have been reported without any family history (termed sporadic early onset AD) (Bagyinszky et al., 2014). Three main mutations are involved in early onset AD namely *APP*, *PSEN1* and *PSEN2* (Campion et al., 1999). Ageing is the most prominent risk factor associated with late onset AD, however other factors have been implicated in increased risk including people who are heterozygous or homozygous for ε4 on the apolipoprotein (*APOE*) gene located on chromosome 19 of the which confers a 3 fold and 12-18 fold increase in risk respectively (Corder et al., 1993, Verghese et al., 2011). Observational studies have also implicated potentially modifiable risk factors for AD including cardiovascular risk factors (e.g. hypertension (Kloppenborg et al., 2008), diabetes (Biessels et al., 2006) and obesity (Beydoun et al., 2008)). Epidemiological data suggests that individuals with higher educational attainment and sustained cognitive activity are less vulnerable to AD (Stern, 2006, Amieva et al., 2014), which has been linked to an increase in cognitive reserve (CR). The CR hypothesis postulates that the capacity to tolerate pathology caused by AD, without associated changes to clinical expression differs between individuals (Stern, 2006). It also suggests that only if a specific critical threshold is breached, functional deficits emerge. Whether this is due to a reduced susceptibility or an increased ability to compensate for dysfunctional neuronal networks remains to be determined.

Macroscopic changes of AD brains include a slight reduction in brain weight in addition to the characteristic atrophy of the medial temporal lobe (inclusive of entorhinal cortex, hippocampus and temporal lobe) and frontal lobe. Loss of both grey and white matter leads to the enlargement of the ventricles in particular the inferior horn of the lateral ventricles (Halliday et al., 2003, Attems and Jellinger, 2013b).

The hallmark pathological lesions associated with AD are mainly constituted of intracellular accumulations of hyperphosphorylated tau protein and extracellular Aβ, forming neurofibrillary tangles (NFTs) and neuropil threads (NTs), and Aβ plaques respectively. Each type of protein accumulation has a different topographical pattern of distribution.

In its physiological state microtubule associated protein (MAP) tau can been found in abundance in the axons of neurones where it regulates the interaction between microtubule motor proteins and microtubules, and controls the movement of axonal organelles i.e. mitochondria and vesicles, maintaining the functionality and viability of the neurone (Hong et al., 1998). Human tau protein is encoded on chromosome 17q21 which consists of 16 exons, and alternate splicing of exons 2, 3 and 10 producing six isoforms ranging from 352-441 amino acids in length (Binder et al., 1985, Ingram and Spillantini, 2002). Each isoform differs by the number of tubulin binding repeats they possess (either 3 or 4, known as 3R or 4R respectively) and the presence or absence of either one or two 29 amino acid long inserts at the N-terminal portion of the protein (Binder et al., 1985). Although the functionality of the six isforms is largely similar they are differentially expressed during development. In the adult human brain 3R and 4R isoforms are expressed in a 1:1 ratio and deviations from this are characteristic of neurodegenerative tauopathies (Hong et al., 1998).

To allow effective axonal transport, tau is in a constant state of flux, on and off the microtubules between phosphorylated and dephosphorylated states. Dysregulation of the phosphorylation/dephosphorylation system is observed in AD brains (Grundke-Iqbal et al., 1986). Whether it is triggered by an increased rate of phosphorylation and/or a decreased rate in dephosphorylation is yet to be fully determined, it results in a 3-4 fold increase of hyperphosphorylated tau compared to normally aged brains (Grundke-Iqbal et al., 1986, Ksiezak-Reding et al., 1992, Kopke et al., 1993). Tau phosphorylation (which detaches tau from the microtubule) is mediated by numerous kinases, the key candidate protein kinases associated with AD being glycogen synthase-3β (GSK-3β), cyclin-dependant kinase 5 (cdk5), casein kinase 1 (CK1), cyclic AMP dependant protein kinase (PKA), and calcium/calmodulin-dependent kinase II (CaMK-II). There are currently over 80 potential phosphorylation sites on the longest tau isoform (Hanger, 2015), with over 40 being implicated in the pathogenesis of AD (Hanger et al., 2009). Current therapeutic strategies are aimed at the specific and complete inhibition of individual tau kinases and as it is thought the relationship between phosphorylation site and putative kinase is not mutually exclusive, this can be an additional challenge to designing effective treatments (Hanger et al., 2009).

Downregulation of phosphatases ((PPs) involved in attaching tau to the microtubule) have also been implicated in the pathogenesis of AD. PP-2A is the most active enzyme in de-phosphorylating tau to its physiological state, followed by PP5 (Liu et al., 2005a). Experiments investigating the expression and activity of both phosphates in AD revealed activity levels and mRNA expression were decreased by 30% in PP2-A and activity levels but not mRNA expression of PP5 were decreased by 20% compared to aged-matched controls (Gong et al., 1995, Liu et al., 2005b).

Although hyperphosphorylation is the most prominent post-translational modification of tau, other modifications include glycosylation, ubiquitination, glycation, polyamination and nitration have been suggested as components of the highly insoluble paired helical filaments that are characteristic of the AD brain. Despite recent advances in developing a suitable ligand to allow imaging of HP-$_T$ in-vivo (Fodero-Tavoletti et al., 2011, Chien et al., 2013, Cook et al., 2015) NFTs (depositions of HP-$_T$ in the cell soma forming cytoplasmic inclusions) and NTs (aggregations of HP-$_T$ in axons and dendrites) are best visualised in human *post-mortem* brain tissue using immunohistochemistry using antibodies against HP-$_T$ (i.e AT8). In AD patients, NFTs and NTs are most predominantly found in the hippocampus, entorhinal cortex and layers III and VI of the isocortex (for review see: Attems and Jellinger, 2013b) (Figure 1.2).

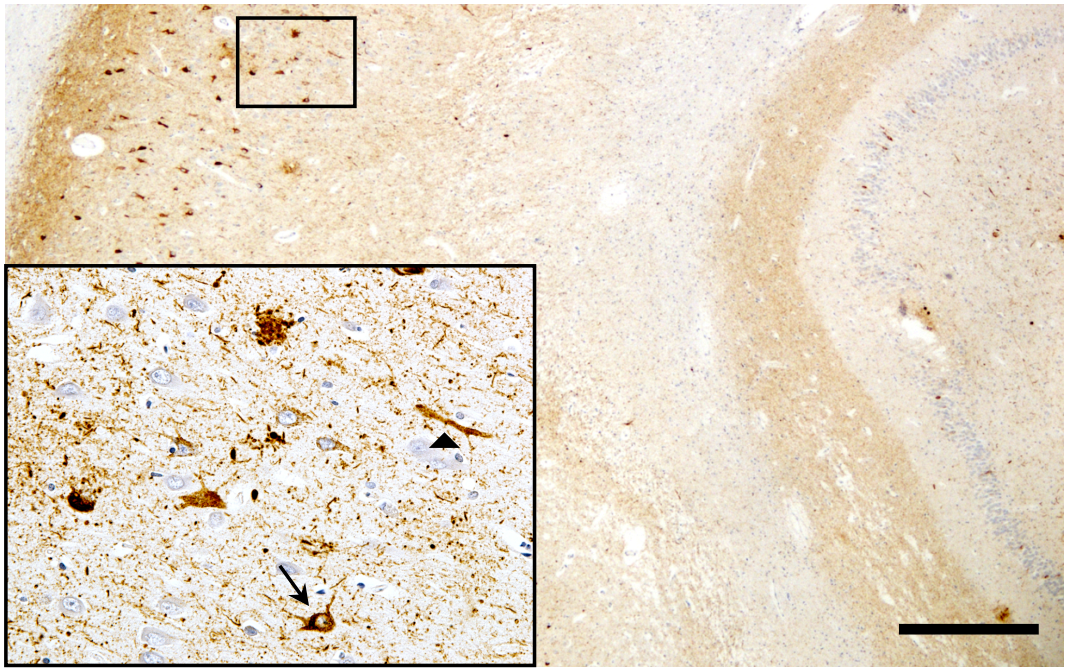

Figure 1.2 Neurofibrillary tangles (arrow) and neupil threads (arrowhead) immunopositive for HP-τ (AT8) antibody in the CA1 region of the hippocampus of an AD case. Scale bar represents 500µm.

The formation of NFTs encompasses 3 stages in which tau phosphorylation sites follows a consistent pattern and corresponds to the degree of cytopathology (Augustinack et al., 2002). Early stages are characterised by delicate fibrillary inclusions within affected neuronal bodies. Following this, the entire neuronal cytoplasm is filled with neurofibrillary material and the nucleus dislocated forming the classical NFT. Finally the neurone degenerates and a ghost tangle is formed where a large number of filaments without any relationship to the soma or nucleus are located freely in the parenchyma (Figure 1.3) (Bancher et al., 1989). Progressive fibril formation and tangle formation has been suggested to run in parallel to a profile shift from 4R tau-positive pre tangles to 3R tau-positive ghost tangles with mature NFTs expressing both 3R and 4R tau (Uchihara, 2014) (Figure 1.3).

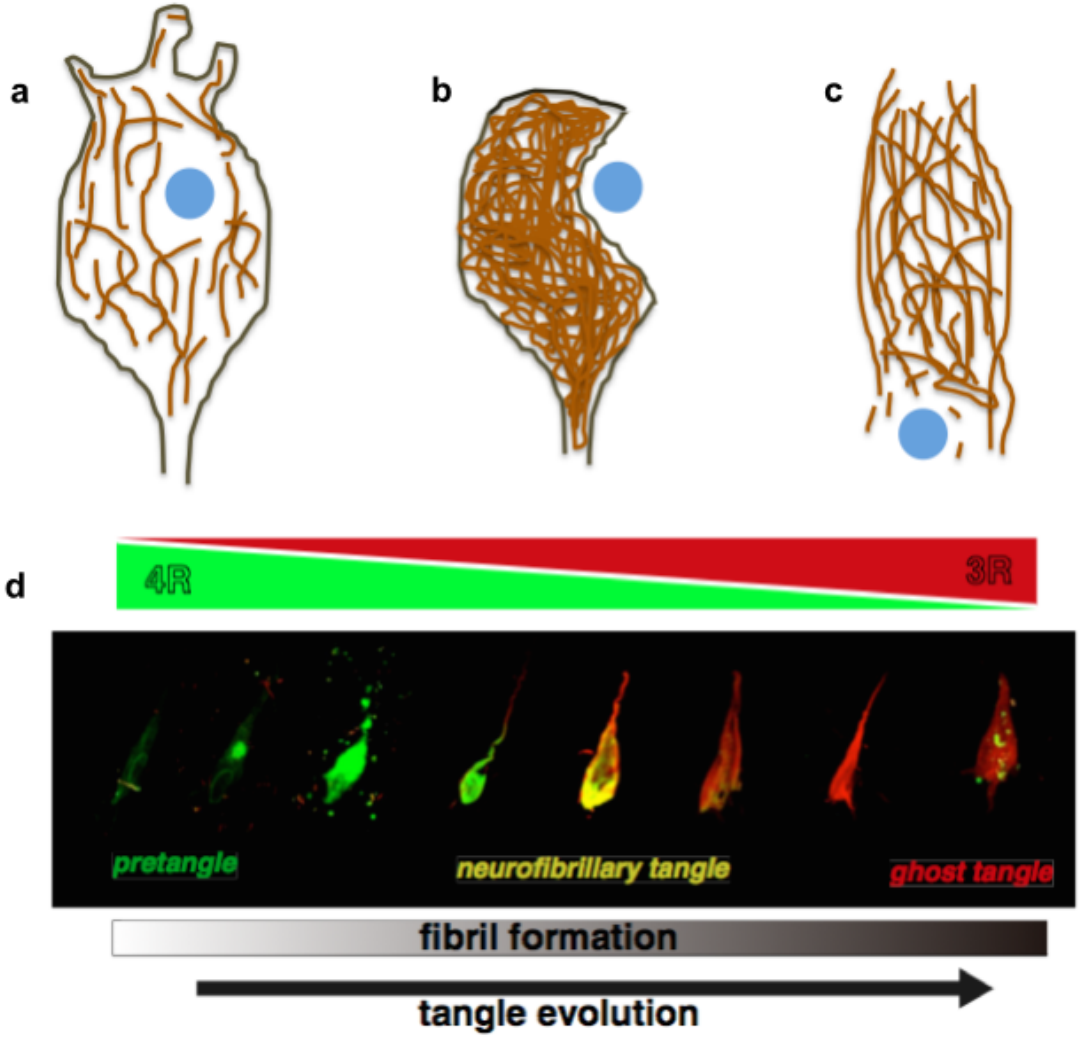

Figure 1.3 Illustration of the stages associated with the formation of neurofibrillary tangles. Pre-tangle stages are characterised by the accumulation of delicate fibrillary inclusions within the affected neurone (a). As the amount of tau pathology increases the classical NFT is formed and the nucleus of the neurones is dislocated (b). Finally a ghost tangle is formed when the neurone degenerates fully, leaving remaining filaments to exist freely in the parenchyma without any relationship to the soma or nucleus (c). The evolution from pre tangles to ghost tangles can be observed by the profile shift from 4R tau to 3R tau as visualised by double label immunofluoresence (d) Adapted from (Uchihara, 2014).

HP-τ pathology is commonly seen in aged individuals; in both demented and non-demented subjects (Tomlinson et al., 1970). Therefore, to make a definite diagnosis of AD (which can only be done at *post-mortem* examination) the topographical pattern of HP-τ (both NFTs and NTs) deposition was described in human *post-mortem* tissue, which highlighted the stepwise progression of HP-τ pathology throughout the brain termed Braak stages (Braak and Braak, 1991, Braak et al., 2006, Alafuzoff et al., 2008). Several studies have demonstrated a good correlation between advanced Braak stages and clinical severity (Bancher et al., 1996, Gertz et al., 1996, Gold et al., 2000) validating its inclusion in the diagnostic criteria in the neuropathological assessment of AD (Montine et al., 2012a). Using tissue sections immunostained with AT8 antibody, brain regions involved in each Braak stage are described as follows: -

- Braak stage 0 - All regions must be described as AT8 negative.
- Braak stage + - Few immunopositive cell bodies (tangles or pre-tangles) can be seen in any section but not sufficient to apply a positive Braak stage.
- Braak stage I - Transentorhinal region is immunopositive for AT8 of at least mild density (Alafuzoff et al., 2008).
- Braak stage II - Involvement of the both anterior and posterior hippocampus with HP-τ pathology being of at least moderate density. From this stage only moderate pathology on the specified region will classify the case at the higher stage.
- Braak III - In addition to previous stages, HP-τ immunopositivity may extend to the adjoining neocortex, specifically the occipito-temporal gyrus (at least moderate density).
- Braak IV - Denotes involvement of the middle temporal gyrus with at least moderate density of HP-τ pathology.
- Braak V - Widespread HP-τ pathology throughout the neocortex with the involvement of the peristriate region of the occipital cortex (at least moderate density).
- Braak VI - Immunopositivity of layer V of the striate area (BA17 - primary visual cortex) of at least moderate density.

Another hallmark pathological lesion involved in the pathogenesis of AD are accumulations of Aβ which form plaques in the parenchyma. Aβ is a 4kDa peptide which has isoforms terminating at corboxy terminus 40 ($A\beta_{40}$) and 42 ($A\beta_{42}$). The physiological role of Aβ in non-disease states is unclear, however evidence suggests it may be involved in learning and memory as Aβ 1-42 facilitated induction and maintenance of long term potentiation in hippocampal slices (Morley et al., 2010). Depositions of Aβ in the brain are considered to be a result of a gradual and chronic imbalance in the production and clearance of Aβ from the brain (Selkoe, 2001a). Aβ is derived by proteolytic cleavage of the transmembrane protein, amyloid-β precursor protein (*APP*) (Selkoe, 2001b) (Figure 1.4). The Aβ peptide sequence is located at the junction between the integral membrane domain and the extracellular domain of *APP* (Kang et al., 1987). There are two pathways in which *APP* can produce amyloid fragments the amyloidgenic and non-amyloidgenic pathways. In AD, *APP* is cleaved by two proteases. Firstly β secretase cleaves *APP* at its extracellular domain leaving fragment C99 which then undergoes further cleavage by γ secretase liberating the Aβ peptide. The alternative proteolytic pathway of *APP*, which is more dominant in healthy controls, involves processing of *APP* by α secretases. The cleavage site for α secretase lies within the Aβ sequence and therefore processing down this pathway precludes Aβ formation. Aβ can be degraded by multiple enzymes i.e. neprilysin and insulin degrading enzyme. In addition to degradation Aβ can be cleared from the brain parenchyma through interstitial fluid and perivascular spaces (Weller et al., 2009).

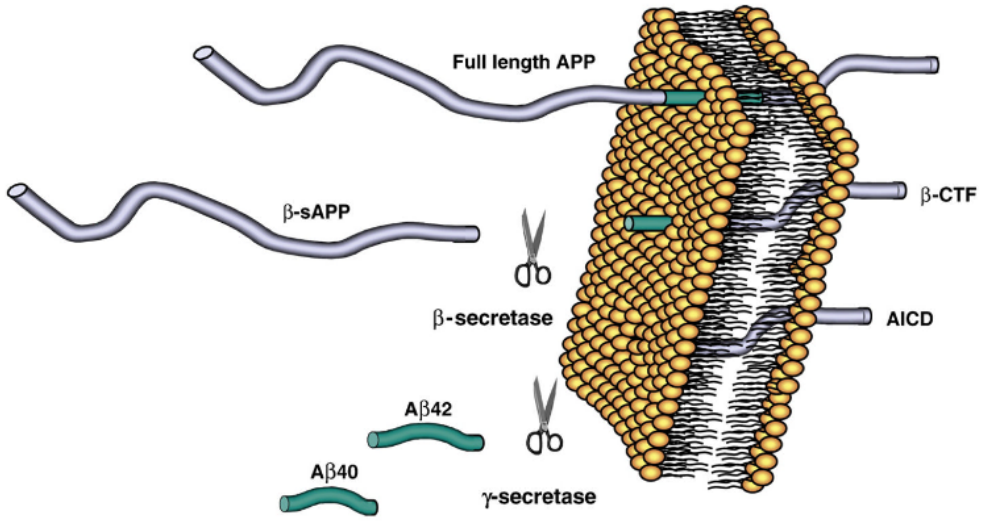

Figure 1.4 Schematic of amyloid precursor processing resulting in the production of Aβ. Taken from (Hampel et al., 2010).

The amyloid cascade hypothesis has dominated research into the pathogenesis of AD for more than 20 years. The hypothesis postulates that the production and deposition of Aβ in the brain parenchyma is the upstream event which induces a sequence of events triggering NFT formation and eventual cell death (Hardy and Higgins, 1992) (Figure 1.5). Evidence in support of this theory stems from patients with trisomy 21 (Down's syndrome) which leads to early $A\beta_{42}$ production and subsequent accumulation of Aβ plaques, microgliosis, astrogliosis and NFTs which are indistinguishable from those seen in AD (Selkoe, 2000). In addition, Scheuner and colleagues demonstrated, using *in vitro* experiments, that familial forms of the AD, attributed to mutations in Presenilin genes 1 and 2 (both of which are homologous proteins that form the catalytic active site of γ secretase), are associated with an increase of extracellular $A\beta_{42}$ (Scheuner et al., 1996). However, evidence that the amyloid hypothesis contributes to age related sporadic AD is less convincing. One key argument against the amyloid hypothesis is the poor correlation between amyloid burden and cognitive decline observed in AD (however several studies have suggested oligomeric forms of $A\beta_{42}$ correlate with cognitive dysfunction in AD (McLean et al., 1999, Naslund et al., 2000)), whilst NFTs, neurone number, are a more accurate predictor of cognitive status in AD (DeKosky and Scheff,

1990, Giannakopoulos et al., 2003). Another key consideration is the discordance of the topographical distribution of Aβ deposits in relation to HP-*T*. Braak and Braak demonstrate NFTs are present in the entorhinal cortex (Stage I) of non-demented individuals in the absence of Aβ plaques (Braak and Braak, 1991, Braak et al., 2006), whilst Thal has suggested the temporal cortex is the first brain region to be affected by Aβ pathology (Thal et al., 2002b). In addition, there is evidence for human transmission of Aβ pathology as Jaunmuktane and colleagues observed in a small autopsy study (n=8) of iatrogenic Creutzfeldt–Jakob disease (CJD) moderate to severe grey matter and vascular Aβ similar to that observed in AD (Jaunmuktane et al., 2015). None of these cases had pathogenic mutations, *APOE* ε4 or other high-risk alleles associated with EOAD, suggesting the otherwise healthy individuals may be at risk of iatrogenic transmission of Aβ pathology in addition to CJD. A final criticism is the failure of clinical trials targeting the clearance of Aβ, most notably the Elan AN1792 active immunisation study which was halted as a result of several cases of meningoencephalitis. Several of the patients were followed after immunisation and failed to show any clinical improvement despite evidence of a reduced Aβ plaque burden at *post-mortem* examination (Holmes et al., 2008).

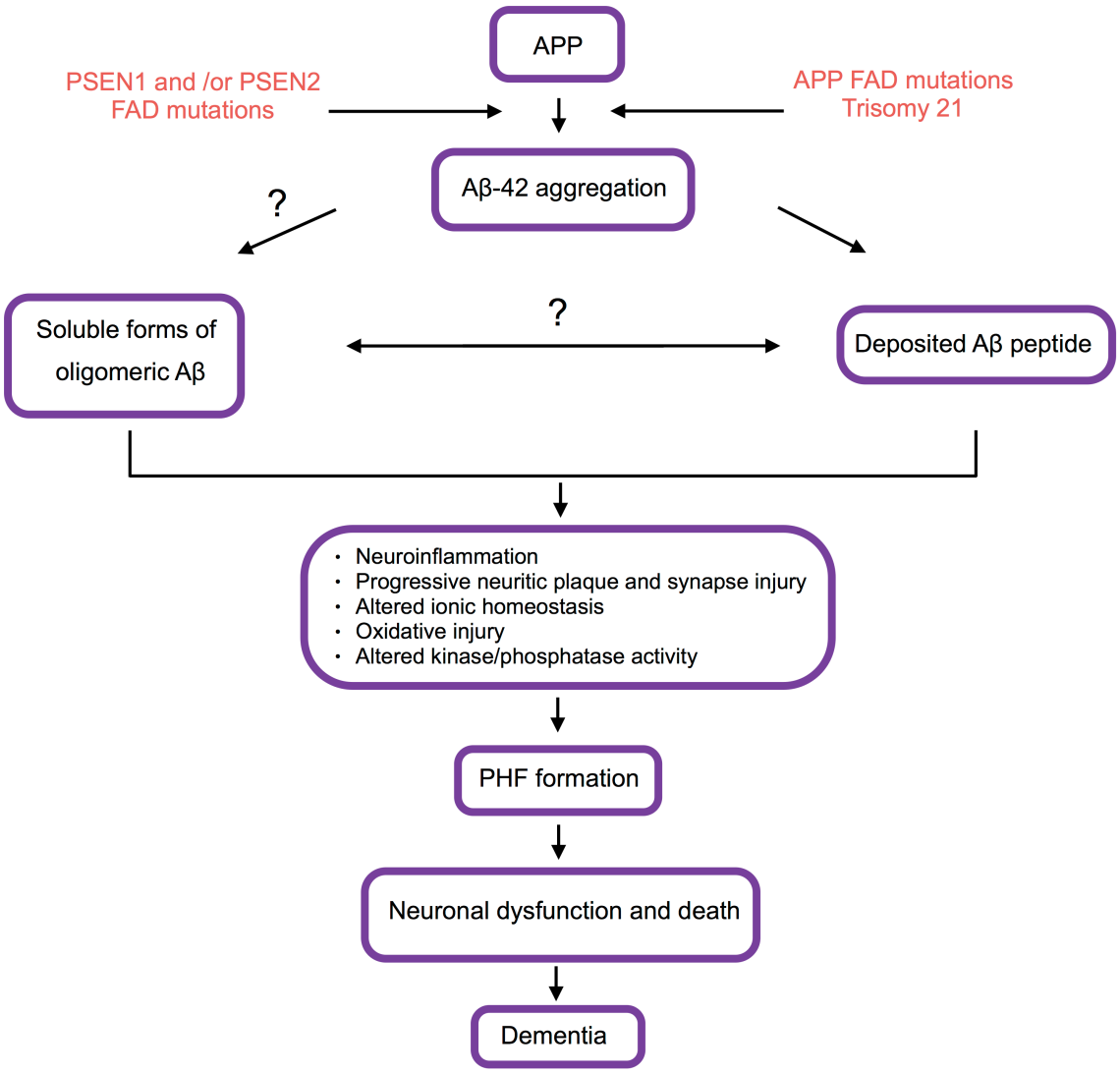

Figure 1.5 The amyloid hypothesis proposes that the production of Aβ is the upstream event that ultimately leads to the formation of neurofibrillary tangle formation and subsequent cell death and dementia. Adapted from (Hardy and Higgins, 1992).

Aβ can be visualised *in vivo* using positron emission tomography (PET) with most research studies conducted in humans utilising ^{11}C-labelled Pittsburgh compound B (PiB) as a ligand (Klunk et al., 2004). However, PiB has a relatively short physical half life (20 minutes) therefore use of this in a clinical setting would require a cyclotron on site making the isotope an unfeasible option. Other imaging ligands including flutemetamol, florbetapir, and florbetaben labelled with ^{18}F are currently undergoing clinical trials to determine their accuracy to label fibrillary amyloid and ability to distinguish AD from control cases (O'Brien and Herholz, 2015).

Despite recent advancements in imaging techniques, Aβ aggregates are best visualised in *post-mortem* tissue using immunohistochemical techniques. Using antibodies directed against Aβ (i.e. 4G8) several types of plaques can be detected (Figure 1.6). Diffuse deposits are usually between 50μm and several 100μm in size with ill defined borders and can be described as 'lake like', 'fleecy' and 'sub-pial band like' (Thal et al., 2002b, Duyckaerts et al., 2009). Aβ plaques on the other hand are more spherical and can be classified as being focal, cored or neuritic plaques. In addition to Aβ aggregates, neuritic plaques are also immunopositive for HP-τ in surrounding dystrophic neuronal processes and correlate well with clinical dementia (Attems and Jellinger, 2013b).

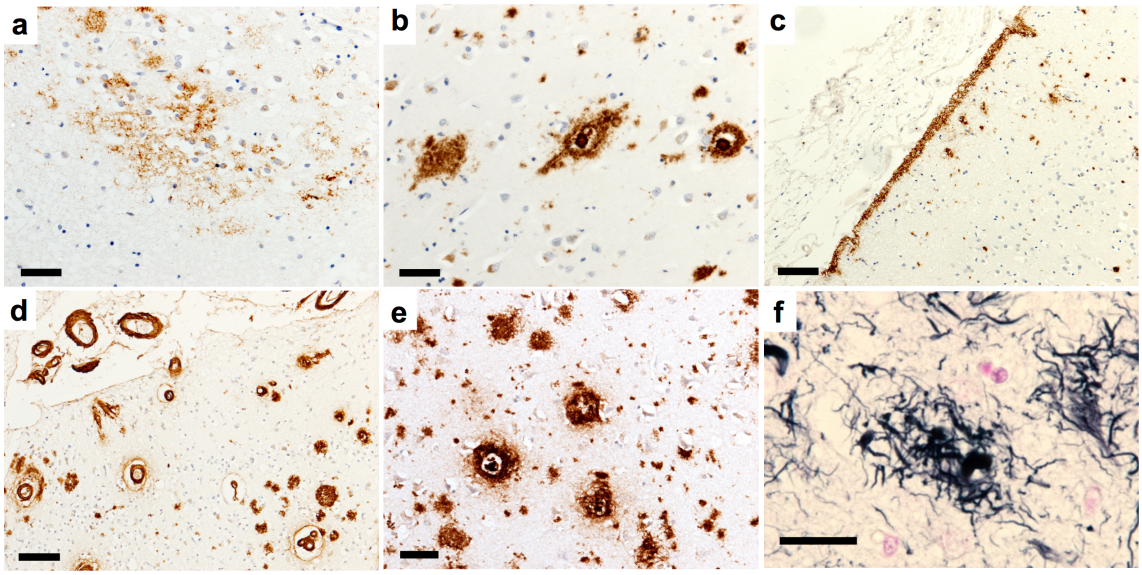

Figure 1.6 Photomicrographs of different Aβ depositions: fleecy amyloid (a), cored and focal plaques (b), supial deposits (c), cerebral amyloid angiopathy (CAA) in leptomeningeal vessels and cortical vessels (d), focal and cored plaques immunopositive for pyroglutamylated Aβ (e) and neuritic plaques with dystrophic neurites (f). (a-c) stained with 4G8 antibody, (e) stained with pE(3)Aβ and (f) stained with gallyas. Scale bars: 50μm in a,b and e; 100μm in c and and 20 μm in f.

The assessment of the distribution of Aβ in the brain parenchyma has become standard practice when assessing *post-mortem* tissue from elderly subjects and particularly those that have dementia. Following the observation of a distinct sequence of Aβ in the medial temporal lobe (MTL) (Thal et al., 2000) Thal and colleagues investigated whether Aβ deposition outside the MTL followed a hierarchical pattern of deposition in neuropathologically confirmed AD cases and age-matched controls with and without AD-related pathology (Thal et al., 2002b). Five phases of Aβ deposition emerged: -

- Phase 1 - Aβ deposition exists exclusively in the neocortex.
- Phase 2 - In addition to the neocortex Aβ deposits are seen in limbic regions including entorhinal cortex, CA1 (cornu ammonis 1) of the hippocampus, cingulate gyrus, insular cortex and the amygdala.
- Phase 3 - Subcortical regions are now affected including the caudate and putamen of the striatum, basal forebrain nuclei, thalamus, hypothalamus and claustrum.

- Phase 4 - Aβ has progressed to the brainstem including the inferior olivary nucleus, the reticular formation of the medulla oblongata and SN.
- Phase 5 - Additional brainstem regions including the locus coeruleus (LC) of the pons are affected and finally Aβ deposits can be seen in the cerebellum.

As part of the neuropathological diagnostic criteria for AD, the importance of Thal phasing is becoming increasingly recognised in the rapidly evolving field of AD biomarkers e.g. amyloid cerebral spinal fluid (CSF) markers and PiB-PET imaging. The correlation between Aβ Thal phases and 11C-PiB imaging was investigated recently in multi-disciplined study including neuropathological, clinical and imaging data (Murray et al., 2015). The study which utilised 35 cases all with *ante-mortem* amyloid imaging revealed a transition between Thal phases 1 to 2 corresponding to 1C-PiB standard uptake value ratio of 1.4, which is a clear cut off for amyloid detection regardless of clinical diagnosis. This study supports the link between PiB imaging and Thal phases as markers of amyloid deposition and clinical characteristics of AD; however it also demonstrated the pre-mortem clinical status of these patients was driven by Braak tangle stage.

Similar to tau protein, it is becoming apparent post-translational modifications of Aβ may play a role in the pathogenesis of AD. *In vitro* and *in vivo* experiments revealed the existence of various N- and C-terminal variants of Aβ (Prelli et al., 1988, Miller et al., 1993). One particular peptide that is gaining interest is pyroglutamylated Aβ (pE(3)Aβ) which has been shown to have a greater propensity to aggregate into plaques, is more stable and demonstrates an increased neuronal toxicity compared to full length Aβ (Russo et al., 2002, Wirths et al., 2009). Following its discovery, pE(3)Aβ was found to constitute 15-20% of total Aβ in AD cases (Mori et al., 1992).

The generation of pE(3)Aβ is a multi-step process involving the removal of the first two amino acids, aspartate and alanine to expose the N-terminal of glutamate at position 3 of the Aβ peptide. Subsequently, glutamate is modified to the N-terminal pyroglutamate by dehydration catalysed by glutaminyl cyclase (QC) activity.

Multiple studies have been conducted into the putative role pE(3)Aβ may play in the pathogenesis of AD including the development of mouse models that produce high levels of pE(3)Aβ and display neurological deficits characteristic of AD. In particular Wirths and colleagues developed the TBA2 mouse model which expresses $A\beta_{Q3\text{-}42,}$ with glutamine at residue 3 of Aβ instead of the naturally occurring glutamate, facilitating the conversion to pE(3)Aβ. Intra-neuronal pE(3)Aβ deposits and plaques were observed predominantly in the hippocampus and cerebellum with robust cell loss, in particular Purkinje cells, and neurological impairments demonstrated in these mice highlighting the potential toxicity of pE(3)Aβ *in vitro* (Wirths et al., 2009). Building on this work, Wittnam and colleagues investigated the influence of elevated pE(3)Aβ levels on existing AD pathology by crossing a novel transgenic mouse model (TBA42) with an established model of AD (5XFAD) (Wittnam et al., 2012). The resulting FAD42 mice displayed an aggravated behavioural phenotype compared to the single transgenic animals and subsequent elevated plaque load as quantified by ELISA provides an argument for a seeding effect of pE(3)Aβ on FAD42 mice.

Recently it was reported that tau is required for the neurotoxicity of pE(3)Aβ and suggested Aβ oligomers containing pE(3)Aβ may confer tau-dependant neuronal death establishing a functional connection between Aβ and tau in AD (Nussbaum et al., 2012). This proposed connection between tau and pE(3)Aβ was further supported when our group in Newcastle reported an association between protein aggregates in frontal and entorhinal cortices in human *post-mortem* tissue as well as frontal pE(3)Aβ predicting the severity of clinical dementia (Mandler et al., 2014). These studies taken together point to pE(3)Aβ playing a central role in AD, inducing neuronal death directly and indirectly with a putative synergistic effect on tau pathology.

Cerebral amyloid angiopathy (CAA) describes the pathological changes that occur in the cerebral blood vessels resulting from the deposition of Aβ (Revesz et al., 2003) **(**Figure 1.6)**.** CAA exists in two forms, the first (CAA type 1) affecting capillaries, with or without the involvement of leptomeningeal and cortical arteries, arterioles, veins and venules. The second (CAA type 2) exhibits Aβ pathology in the leptomeningeal and cortical vessels, but not in capillaries (Thal et al., 2002a). The accumulation of β-amyloid in the vessel

walls is thought to occur by two mechanisms. Incorporation of Aβ into vessel walls may be the result of the failure of the perivascular drainage system to clear Aβ (via the basement membrane) whilst capillary CAA is thought to be the failure of transendothelial clearance of Aβ via *APOE* ε4 complexes (Weller et al., 2000). CAA is common in the ageing brain but is also thought to have an association with AD as shown in a population study conducted by Vonsattel and colleagues where 50% of all cases displayed CAA pathology, whilst 87% of the subgroup of AD cases were positive for CAA pathology (Vonsattel et al., 1991). Attems and colleagues found that CAA increased with increasing AD pathology and this was more pronounced in the occipital lobe followed by the frontal, temporal and parietal lobes. The association between CAA and cognitive decline was influenced by concomitant AD pathology suggesting that CAA alone is not a major independent cause for cognitive decline in the elderly (Attems et al., 2005, Attems et al., 2007).

AD is characterised by the presence of both HP-$_T$ and Aβ, but in symptomatic cases there is convergence between the two in the form of neuritic plaques. In addition to the central core positive for Aβ, neuritic plaques also contain dystrophic neurites positive for HP-$_T$ (Figure 1.6). Neuritic plaques have been shown to be more strongly associated with AD compared to other forms of parenchymal Aβ (Nagy et al., 1995) suggesting targeting neuritic changes rather general Aβ may be more effective when designing therapeutics that could have a beneficial outcome in patients with AD. Age adjusted assessment of neuritic plaques was provided by the Consortium to Establish a Registry for Alzheimer's Disease (CERAD) (Mirra et al., 1991). These criteria are based on semi-quantitative assessment denoting neuritic plaque pathology in the middle frontal gyrus, superior/ middle temporal gyri, and inferior parietal lobe as sparse, moderate or frequent.

In addition to hallmark pathological lesions of NFT's and Aβ plaques, loss of neurones and extensive synapse loss in the neocortex are closely related to the pathological and clinical progression of AD. Studies by Masliah and colleagues have demonstrated a 45% decrease in presynaptic boutons in parietal, temporal and mid-frontal cortex in AD cases compared to controls by quantifying synaptophysin, an immunohistochemical marker directed against synaptic

proteins, using electron microscopy. They argued that disruption in neurone-to-neurone communication contributed to cognitive loss in AD (Masliah et al., 1989). More specifically, stereological assessment of synaptic volume density measured in layers III and V suggests neuronal and synaptic loss in the central nervous system (CNS) is a result of neurodegeneration such as AD rather than a consequence of normal ageing (Scheff et al., 2001).

All three internationally used staging systems for HP-τ, (i.e., Braak stages), Aβ (i.e., Thal phases) and neuritic plaque (i.e., CERAD scores) pathology respectively, are taken into consideration when deciding on the level of AD neuropathological change in *post-mortem* tissue. Recently revised criteria from the National Institute on Ageing - Alzheimer's Association (NIA- AA) provide guidelines for assigning the level of AD neuropathological change by suggesting an 'ABC' scoring system (A - for assessment of amyloid β, B - for Braak staging of HP-τ pathology and C - for CERAD scoring of neuritic plaques (Hyman et al., 2012, Montine et al., 2012b)). A summary of the 'ABC' scoring system is illustrated in Figure 1.7.

Level of AD neuropathologic change					
Thal phase for Aß-plaques	A	0 or 1	B 2	3	C	CERAD
0	0	Not	Not	Not	0	neg
1 or 2	1	Low	Low	Low	0 or 1	neg or A
1 or 2	1	Low	Intermediate	Intermediate	2 or 3	A or B
3	2	Low	Intermediate	Intermediate	any C	neg or A to C
4 or 5	3	Low	Intermediate	Intermediate	0 or 1	neg or A
4 or 5	3	Low	Intermediate	High	2 or 3	B or C
		Braak 0-II	Braak III-IV	Braak V-VI		

Figure 1.7 The level of AD neuropathologic change is determined by taking into account individual scores for Thal phases for Aβ plaques (A) Braak stages for HP-$_T$ pathology (B) and CERAD scores for neuritic plaque pathology (C). Taken from (Attems and Jellinger, 2013b).

1.5.2 Lewy body disease

Lewy body diseases (LBDs) are a collection of neurodegenerative disorders with aggregations of α-syn being the characteristic hallmark lesion in all diseases, including PD, Parkinson's disease dementia (PDD) and dementia with Lewy bodies (DLB) (Spillantini et al., 1997). The human gene encoding α-syn lies on chromosome 4q21.3-q22 and structurally α-syn protein is 140aa in length which can be divided into three regions with distinct characteristics (Beyer, 2006). The three mis-sense mutations known to cause familial PD (A30P, E46K and A53T) all lie in the amphiphathic region (Figure 1.8).

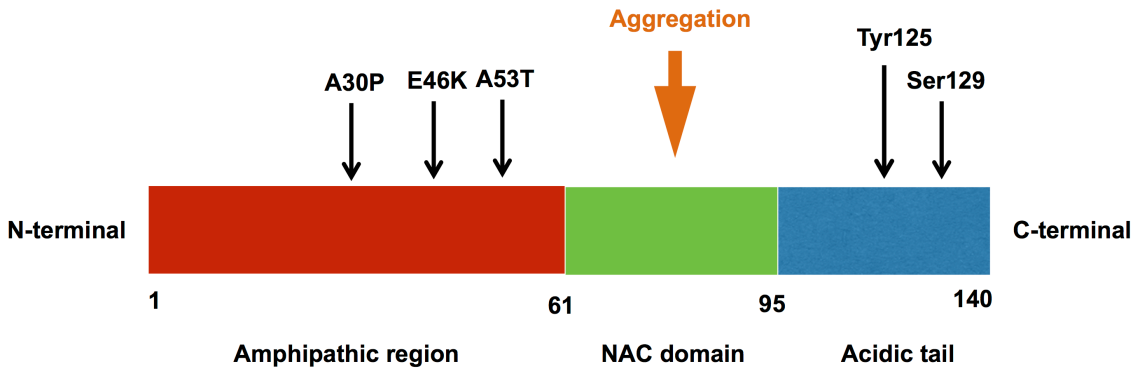

Figure 1.8 Structure of α-syn, which is divided into three distinct regions: the Amphipathic region, NAC domain and Acidic tail. Modified from (Venda et al., 2010).

Physiologically α-syn is thought to be a lipid binging protein highly enriched at the presynaptic terminals (Bendor et al., 2013), where it binds to the external surface of synaptic vesicles, potentially playing a role in neurotransmission. Under pathological conditions α-syn undergoes a conformational change from random coil to a cross-β structure similar to that seen in AD lesions (Serpell et al., 2000, Goedert et al., 2013). The lesions containing α-syn associated with LBDs are Lewy bodies (LBs), (intraneuronal cytoplasmic α-syn inclusions) and Lewy neurites (LNs), (α-syn accumulated in neuronal processes). Electron microscopy has revealed LBs and LNs are made up of unbranched α-syn filaments with a length of 200-600nm and a width of 5-10nm (Spillantini et al., 1998). Two types of LBs have been described: - brainstem LBs have an acidophilic and argyrophilic core with a pale stained halo, classically seen using H&E staining. Typically they are 8-30μm in diameter and predominantly seen in pigmented neurones of the SN. Cortical LBs are eosinophilic, rounded, angular or reniform structures without a halo (for review see: Attems and Jellinger, 2013b) (Figure 1.9).

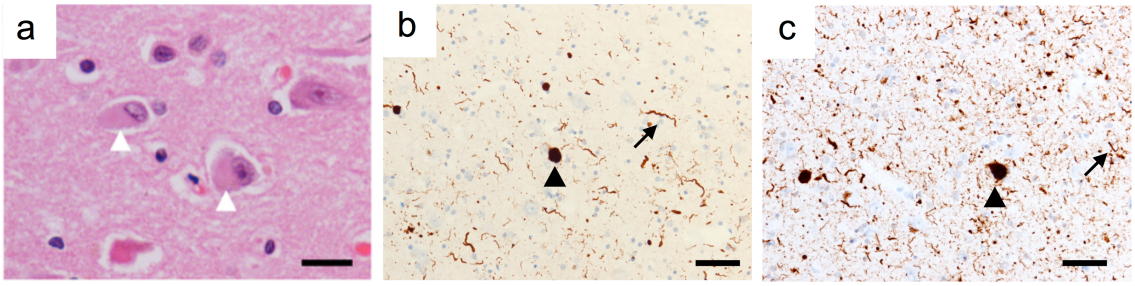

Figure 1.9 Photomicrographs of Lewy body pathology. Classical cortical Lewy bodies are rounded eosinophilic inclusions in neuronal cells as seen by H&E stain (white arrowheads) (a). Lewy bodies (black arrowheads) and Lewy neurites (black arrows) can be visualised using antibodies against full length recombinant α-syn (b) and α-syn phosphorylated at serine 129 (c). Images b and c are both taken from the amygdala of the same DLB patient demonstrating immunohistochemistry of α-syn phosphorylated at serine 129 reveals a more abundant load of α-syn than phosphorylation independent antibodies, with more thread and dot like structures. Scale bars: 20μm in a and 50μm in b and c. Image a taken from (Attems and Jellinger, 2013b)

There is conflicting evidence surrounding the toxic effects of α-syn in LBDs. Several studies have highlighted the importance of cortical LB/LNs in cognitive decline as measured by Mini Mental State Examination (MMSE) in LBDs (Hurtig et al., 2000, Irwin et al., 2012, Howlett et al., 2014). However, a large study consisting of 1720 autopsied brains revealed approximately 50% of cases with widespread α-syn pathology lacked any clinical signs of dementia and/or parkinsonism (Parkkinen et al., 2008). This data was further supported by two more recent studies by Greffard and colleagues and Parkkinen and colleagues who demonstrated that neither distribution or densities of LBs in the brainstem or cortex correlate with nigral cell loss (Greffard et al., 2010, Parkkinen et al., 2011). It has been suggested that α-syn sequestered into LBs represent a failed cytoprotective event resulting from protein clearing mechanisms in response to accumulating toxic oligomeric intermediate α-syn species (Alafuzoff and Parkkinen, 2014). The role of oligomers as the toxic form α-syn is yet to be fully elucidated with the most common hypothesis of the mechanism by which oligomers exert their cytotoxicity is by creating pores in membranes increasing permeability to ions from extracellular space leading to cell death (Volles et al., 2001, Danzer et al., 2007).

Post-translational modifications in the C-terminal region of α-syn such as oxidation, nitration and phosphorylation influence the propensity of α-syn to aggregate in vivo (Hashimoto et al., 1999, Giasson et al., 2000). Hyperphosphorylation of Ser129 by G protein-coupled receptor kinase is the main post-translational modification of filamentous α-syn and has been demonstrated to be in abundance in LBs and LNs (Fujiwara et al., 2002). Other kinases demonstrated to promote phosphorylation at ser129 are casein kinase-1 (CK-1) and CK-2 (Okochi et al., 2000). Investigations into the involvement of α-syn phosphorylated at ser129 (pSer129 α-syn) in the formation of LBs is of current interest since it was found by several groups that 90% of α-syn is phosphorylated at this residue in LBD in contrast to normal brains where only 4% of total α-syn is phosphorylated (Fujiwara et al., 2002, Anderson et al., 2006). However, the pathological relevance of phosphorylation of α-syn at this residue remains unanswered. This was investigated by Lue and colleagues who demonstrated biochemically detectable pSer129 α-syn preceded the presence of histologically identified Lewy pathology in brain homogenates from 128 autopsy cases, suggesting the phosphorylation of α-syn at Serine 129 is an early event and potentially important in the pathogenesis of LBD (Lue et al., 2012). Following this, Walker and colleagues defined changes in solubility properties of pSer129 α-syn with increased Lewy body formation (Walker et al., 2013). They found higher accumulation of insoluble pSer129 α-syn in the cingulate cortex (where LB pathology is observed earlier in disease progression) compared to the temporal cortex which is in line with the topographical distribution of LB pathology (Braak et al., 2003, McKeith et al., 2005, Beach et al., 2009). Immuohistochemistry of pSer129 α-syn has revealed far more abundance of α-syn than phosphorylation-independent antibodies, and in addition to LBs and LNs more threads and dot-like structures similar to argyophilic grains (Lewy dots) are immunopositive (Saito et al., 2003, Obi et al., 2008) (Figure 1.9).

1.5.2.1 Parkinson's disease

PD is the second most common neurodegenerative disorder following AD with 0.3% of the population in industrialised countries being diagnosed with PD and this number increasing to 1% in the population over the age of 60 (de Lau and Breteler, 2006). Primarily it was considered as a motor disorder with the four cardinal features common to PD being tremor at rest, rigidity, akinesia and postural instability (Jankovic, 2008). In clinical practice PD is diagnosed with the presence of these motor features, in combination with the exclusion of other neurodegenerative disease and a response to levodopa (Rao et al., 2003). Gross assessment of PD progression is evaluated using several rating scales including Hoehn and Yahr (Hoehn and Yahr, 1967) and the Unified Parkinson's disease Rating Scale, which is the most established tool for assessing disability and impairment (Goetz et al., 2008). In addition to motor symptoms, recently the clinical spectrum of PD has been recognised to be more extensive incorporating non-motor features such as constipation, anosmia, sleep disturbances and depression (Chaudhuri et al., 2006) with studies speculating the appearance of these symptoms prior to the emergence of typical motor features represent the prodromal phase of the disease (Hawkes et al., 2010, Postuma et al., 2012, Postuma, 2014).

Macroscopical changes indicative of PD include the depigmentation of the SN due to depletion of neuromelanin containing dopaminergic neurones (Figure 1.10a). Dopaminergic neurones in the SN project to the basal ganglia and synapse onto the striatum forming the nigrostriatal pathway (Figure 1.10b). Motor dysfunction associated with PD patients emerges when 60% of dopaminergic neurones are lost in the SN leading to reduced projections to the striatum (Damier et al., 1999). This subsequently leads to a loss of inhibition to the output nuclei including the internal globus pallidus and SN pars reticulata. The loss of inhibition to the subthalamic nucleus also increases the relative excitation to the output, which in turn inhibits the thalamic projection regions to the motor cortex, resulting in the akinetic-rigid symptoms associated with PD (Halliday, 2014).

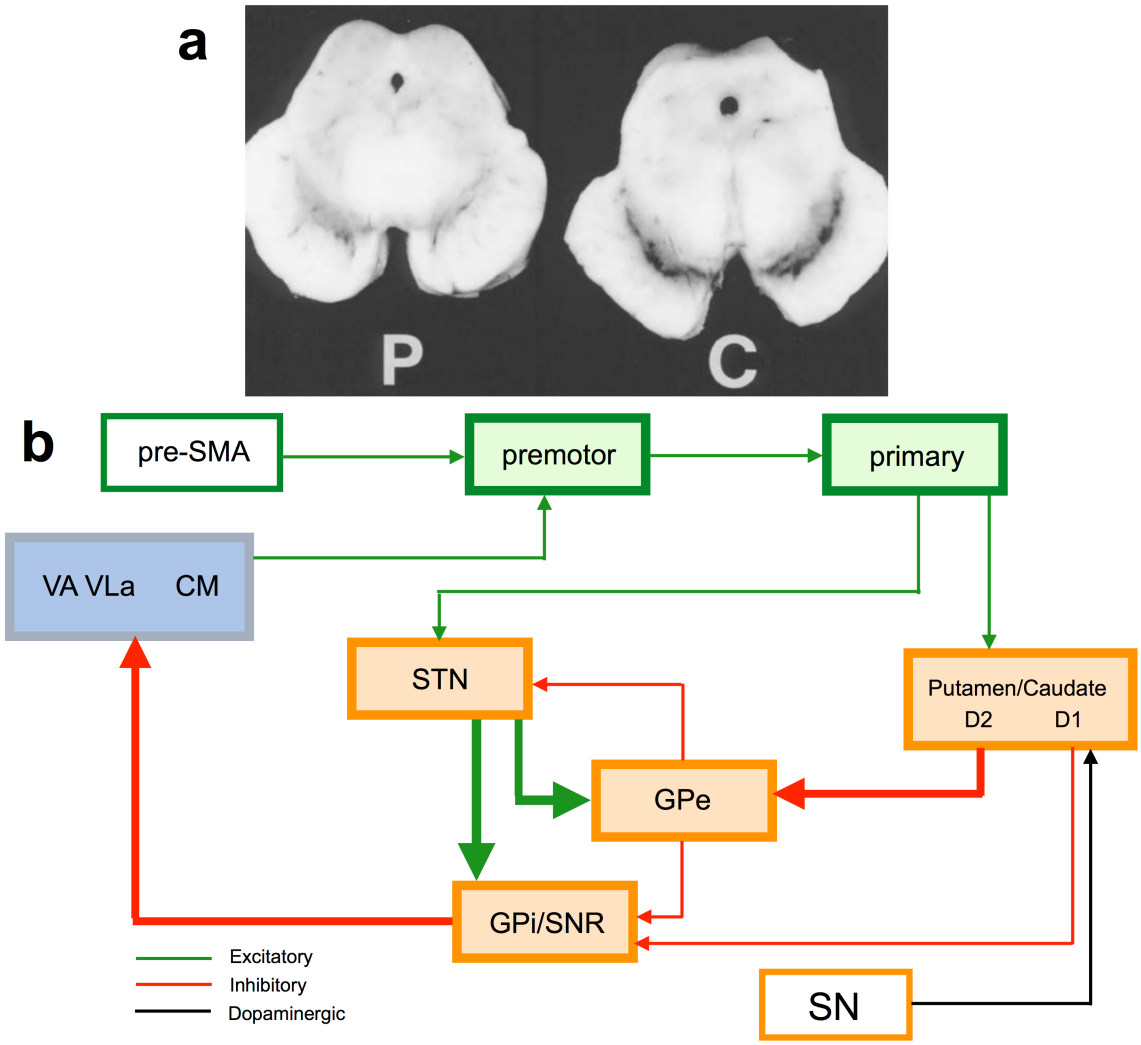

Figure 1.10 (a) Photograph illustrating the loss of pigmented neurones caused by depletion of neuromelanin in the dopaminergic neurones of the Substantia nigra (SN) of a patient with Parkinson's disease (P) compared to a control (C) patient. Image (a) taken from (Mackenzie, 2001). (b) Simplified schematic illustrating the nigrostriatal circuits that are affected by cell loss in the SN. Abbreviations: SN, substantia nigra; GPi, internal globus pallidus; GPe, external globus pallidus; STN, sub thalamic nucleus; VA, ventral anterior thalamus; VLa, ventral lateral anterior thalamus; CM, thalamic caudal intralaminar nuclei; pre-SMA, pre-supplementary motor cortex. Image (b) adapted from (Halliday, 2014).

A number of biomarkers for the diagnosis of PD are currently under investigation. Olfactory impairment, a cardinal symptom in PD, occurs in up to 96% of patients where it appears as a prodromal marker typically preceding the emergence of motor disturbance (Boesveldt et al., 2008, Attems et al., 2014b). The sensitivity and specificity of using olfactory testing to differentiate between PD and non-PD has been reported to be between 79% to up to 100% highlighting the importance of future development of olfactory testing in the differential diagnosis of PD (Doty et al., 1995, Katzenschlager et al., 2004). Candidate imaging biomarkers including positron emission tomography (PET), or single photon emission computed tomography (SPECT) can identify ligand binding that correlates with the loss of dopaminergic neurones projecting from the SN to the striatum (Rakshi et al., 1999, Colloby et al., 2012), however these methods are unable to distinguish PD from other neurodegenerative disorders associated with SN degeneration such as progressive supranuclear palsy, corticobasal degeneration, multiple systems atrophy and DLB. In addition, investigations into non-cerebral tissue markers have detected α-syn in skin biopsies with deposits located in skin and intraepidermal small nerve fibres (Miki et al., 2010, Doppler et al., 2014). However, although specificity for α-syn was high in this study as 0/35 of control subject biopsies has cutaneous α-syn deposits, sensitivity was fairly low with α-syn positive biopsies demonstrated in only 16/31 PD cases (Doppler et al., 2014).

1.5.2.2 Parkinson's disease dementia

A frequent complication of PD is the development of dementia, with an estimated 80% of patients with the motor disorder reporting symptoms associated with a dementia syndrome in the advanced stages of the disease, and a six fold increased risk of developing dementia compared to healthy controls (Aarsland et al., 2001a). In addition to the patient, PDD can impose greater burden on caregivers as it is associated with increased nursing home placement and mortality (Aarsland et al., 2000, Levy et al., 2002b). The Sydney Multicentre Study is a longitudinal study which highlighted the progression of PD patients to PDD by prospectively following 136 patients diagnosed with PD over a 20 year period. Of the 100 patients that came to autopsy at the time of the report, 75% were reported to have had dementia during life, in addition to dementia being present in 83% of the surviving

participants, raising question as to whether dementia is an inevitable complication of PD (Hely et al., 2008). In all longitudinal studies to date there have been subjects that were dementia-free at time of death (Docherty and Burn, 2010). Further investigations as to whether this is due to an increased threshold e.g patients that have a higher cognitive reserve, or whether they would have developed dementia should they have lived to an older age will help to address these questions. In 2007 the Movement Disorder Society recruited a task force to identify the epidemiological, clinical, auxiliary and pathological features of PDD (Emre et al., 2007).

Identification of clinical features and risk factors that may identify patients that will progress to dementia in the later stages of PD is of interest to clinicians and may have a potential impact on disease management. Although the biggest risk factor for dementia in PD is advancing age (Levy et al., 2002a, Kempster et al., 2010) other factors linked to PDD include male sex and low education (Levy et al., 2000) and visual hallucinations (Aarsland et al., 2003) (Levy et al., 2002a). Mild cognitive impairment (MCI) is common in non-demented patients with PD and has been described as a potential prodromal state to PDD and potential risk factor (Goldman and Litvan, 2011). In a large population based study that identified new cases of Parkinsonism in the UK (CamPaIGN study), Foltynie and colleagues reported 36% of their incident PD cases were cognitively impaired but not demented based on their MMSE scores documenting the existence of cognitive dysfunction even in the early stages of PD (Foltynie et al., 2004). There has been significant heterogeneity regarding the specific diagnostic criteria of PD-MCI, with some patients exhibiting non amnestic deficits in numerous cognitive domains such as executive dysfunction, attention and visuospatial function whilst others experience more amnestic deficits (Goldman and Litvan, 2011). To address this, the Movement Disorder Society commissioned a task force to refine the criteria to support future research and to identify patients at the early stages of PD who are at risk of developing dementia (Litvan et al., 2012). The proposed inclusion criteria includes a diagnosis of PD based on the UK Brain Bank criteria (Gibb and Lees, 1988), gradual decline in the context of established PD and cognitive deficits that are not sufficient to interfere with independent living.

1.5.2.3 Dementia with Lewy bodies

Dementia with Lewy bodies (DLB) is the second most common cause of neurodegenerative dementia after AD accounting for 4.2% of all cases of dementia in the community which increases to 7.5% in secondary care (Vann Jones and O'Brien, 2014). Age of onset for the disease is thought to be between 50 and 83 with rapid symptom progression within 1-2 years of onset (McKeith, 2002). DLB shares common clinical and pathological features with PD and PDD and all three are part of the LBD spectrum. The clinical distinction between DLB and PDD is based on the time of dementia onset in relation to extrapyramidal symptoms (EPS); in PDD EPS precede the onset of dementia by at least 12 months whereas in DLB dementia is concomitant with or precedes EPS (McKeith et al., 2005). To date there are no neuropathological criteria that can distinguish DLB from PDD (McKeith et al., 1996, McKeith et al., 2005, Emre et al., 2007, Lippa et al., 2007, Savica et al., 2013).

The clinical profile of patient with DLB centres around a non amnestic dementia of which core features of deficits in executive dysfunction, recurrent well-formed visual hallucinations, fluctuating cognition and spontaneous Parkinsonism are observed (McKeith et al., 2005). Two core features are required for a diagnosis of probable DLB, but diagnostic accuracy is improved with the presence of more than two core features. In addition to one or more core features, if a patient experiences suggestive features of DLB e.g REM sleep behaviour disorder or has severe neuroleptic sensitivity the a probable clinical diagnosis of DLB can be made (McKeith et al., 1996, McKeith et al., 2005). Many patients report symptoms of recurrent falls and syncope which may reflect the involvement of the autonomic nervous system (McKeith, 2002). The most recent criteria for the clinical diagnosis of DLB were provided in the third report of the DLB consortium to include further supportive and suggestive features for the clinical diagnosis are illustrated in Table 1.3.

1. *Central feature* (essential for a diagnosis of possible or probable DLB)

   - Dementia defined as progressive cognitive decline of sufficient magnitude to interfere with normal social or occupational function
   - Prominent or persistent memory impairment may not necessarily occur in the early stages but is usually evident with progression.
   - Deficits on tests of attention, executive function, and visuospatial ability may be especially prominent.

2. *Core* features (two core features are sufficient for a diagnosis of probable DLB, one for possible DLB)

   - Fluctuating cognition with pronounced variations in attention and alertness
   - Recurrent visual hallucinations that are typically well formed and detailed
   - Spontaneous features of Parkinsonism.

3. *Suggestive features* (If one or more of these is present in the presence of one or more core features, a diagnosis of probable DLB can be made. In the absence of any core features, one or more suggestive features is sufficient for possible DLB. Probable DLB should not be diagnosed on the basis of suggestive features alone.

   - REM sleep behaviour disorder
   - Severe neuroleptic sensitivity
   - Low dopamine transporter uptake in basal ganglia demonstrated by SPECT or PET imaging

4. *Supportive* features (commonly present but not proven to have diagnostic specificity)

   - Repeated falls and syncope
   - Transient, unexplained loss of consciousness
   - Severe autonomic dysfunction, e.g., orthostatic hypotension, urinary incontinence
   - Hallucinations in other modalities
   - Systematised delusions
   - Depression
   - Relative preservation of medial temporal lobe structures on CT/MRI scan
   - Generalised low uptake on SPECT/PET perfusion scan with reduced occipital activity
   - Abnormal (low uptake) MIBG myocardial scintigraphy
   - Prominent slow wave activity on EEG with temporal lobe transient sharp waves

Table 1.3 Clinical diagnostic criteria for DLB as outlined by (McKeith et al., 2005).

As with AD, the greatest risk factor for the development of DLB is advancing age (McKeith et al., 1996). In addition to age there are a number of other factors that infer risk of developing DLB. Several studies have linked a mutation in the glucocerebrosidase gene, most commonly associated with the glycolipid storage disorder Gaucher's disease to an increased risk of DLB and PDD. Mata and colleagues found *GBA* mutations exert a 3% population-attributable risk in individuals of a European ancestry, whilst in a multi-centre study Nalls and colleagues utilised tissue samples from 721 DLB cases, 151 PDD cases and 1962 control cases matched of age, sex and ethnicity and found a significant association between *GBA1* mutation carrier status and DLB, highlighting *GBA* as a significant risk factor for DLB (Mata et al., 2008, Nalls et al., 2013). In a retrospective case-control study Boot and colleagues evaluated 19 candidate risk factors, and in agreement with other studies found patients with DLB were more likely to be older, male, and have a history of depression, stroke or a family history of PD (Boot et al., 2013).

Similar to PD and PDD the most prominent macroscopical feature associated with DLB the depigmentation of the SN caused by the loss of dopaminergic neurones, however other macroscopic changes are observed in patients with DLB. Some structural changes seen in DLB are similar to those seen in AD with widespread cerebral atrophy being a feature of both (Attems and Jellinger, 2013b). DLB does differ from AD in the relative preservation of the medial temporal lobe, which can be visualised by magnetic resonance imaging (Burton et al., 2009). T1-weighted MRI assessing cortical thickness has been used to further distinguish DLB from other dementing disorders as Watson and colleagues found focal areas of cortical thinning in the posterior regions of the brain including inferior parietal, posterior cingulate and fusiform gyrus whereas areas susceptible to cortical thinning in AD cases included the temporal and parietal lobes extending to the frontal cortex (Watson et al., 2014). Taken together these data can potentially be applied as a diagnostic tool in the future diagnosis of DLB.

There are currently several neuropathological staging systems in use for the assessment of α-syn pathology and diagnosis of LBD:

1) Braak staging for the assessment of α-syn related pathology inclusive of LBs and LNs suggest the sequence of α-syn deposition encompasses 6 stages depending on disease severity (Braak et al., 2003):

- Stage 1 - IX/X motor nucleus of the medulla oblongata
- Stage 2 - Pathology of stage 1 with the addition of lesions in the LC.
- Stage 3 - α-syn lesions can be seen in the SN of the midbrain.
- Stage 4 - Pathology of stage 3 plus lesions in the transentorhinal region and CA2 of the hippocampus
- Stage 5 - Higher order sensory association areas of the neocortex and frontal cortex are now affected.
- Stage 6 - Pathology of stage 5 in addition to lesions in the first order sensory association of the neocortex, premotor and motor regions.

According to this system cases with PD would reach stage 3 with DLB and PDD reaching at least stage 4.

2) The Newcastle-McKeith criteria distinguishes between:

- Brainstem-predominant - regions affected include IX/X motor nucleus, LC and SN.
- Limbic (transitional) - including the amygdala, transentorhinal and cingulate cortex.
- Diffuse neocortical - temporal, frontal and parietal lobes are affected.

3) Leverenz and colleagues modified the Newcastle-McKeith criteria to include a subtype that classifies cases that lack α-syn pathology in any other brain regions with the exception the amygdala, known as amygdala predominant LB disease (Leverenz et al., 2008), which increased the number of classifiable cases from 51% to 96% (Alafuzoff and Parkkinen, 2014).

4) Although these staging systems are the most widely used to assess α-syn in LBD, a study conducted by Beach and colleagues suggested these systems fall short of adequately describing the full histopathologic range and variability of LBD (Beach et al., 2009). They argued the current staging systems fail to account for subjects that have α-syn pathology confined to the olfactory bulb or pass through the limbic-predominant pathway bypassing the brainstem. Furthermore, it is now known α-syn pathology frequently extends beyond the brainstem nuclei to the spinal cord and peripheral nervous system (Bloch et al., 2006, Braak and Del Tredici, 2008). They propose a unified staging system to allow the classification of a much greater proportion of cases:

- I. Olfactory bulb only
- IIa. Brainstem predominant
- IIb. Limbic predominant
- III. Brainstem/limbic
- IV. Neocortical

1.6 Cerebral multi-morbidity

The traditional method used to ascertain the diagnosis of a neurodegenerative disease is based on a consensus clinico-pathological diagnosis; where the combination of signature neuropathological lesions identified at *post-mortem* examination (see table 1.2 for overview) and clinical symptoms observed during life lead to a clinico-pathological diagnosis. The neuropathological diagnosis of neurodegenerative disorders is based on the most prevalent pathology, however, it is becoming increasingly clear that multiple pathologies frequently co-exist in the brains of the demented elderly, suggesting the clinical picture of dementia results from a multi-morbid condition rather than one disease process (Jellinger and Attems, 2007, Attems and Jellinger, 2013b). The presence of multiple pathologies within the same brain may bring into question the idea of neurodegenerative disorders being distinct disease entities. In an attempt to address these issues Armstrong proposed three possible models (Armstrong, 2012):

1) Discrete model - This model requires the majority of cases to be distinct clinical and pathological entities with minimal overlap. In addition to this there should be positive correlations between clinical and pathological features of the disease.
2) Overlap model - This model suggests diseases may be relatively distinct but exhibit a degree of overlap in their clinical and pathological presentations e.g. AD can share features with normal ageing and vascular dementia (Jellinger and Attems, 2007).
3) Continuum model - this model postulates that the degree of overlap between clinical and pathological features of each disease is so extensive that it represents a continuum, suggesting no two cases are identical with each displaying a varying levels of 'neurodegeneration'.

A question arising from these models is whether the pathologic lesions characteristic of neurodegenerative disease are a result of age related changes or are disease specific. For example Aβ can occur in normal processing pathways of the brain (Mullan and Crawford, 1993) and both Aβ and HP-τ can be present in the brains of non-demented elderly as well as in dementing disorders other than AD (Mann and Jones, 1990, Alafuzoff, 2013).

Cerebrovascular disease is common in AD as demonstrated by study conducted by Nagata and colleagues who concluded that vascular pathology (VP) (inclusive of lacunar infarcts, white matter lesions and old micro-bleeds) were present in up to 90% of elderly Japanese patients (Nagata et al., 2012).

1.6.1 Prevalence of cerebral multi-morbidity

The observations that multiple pathologies of potentially differing aetiologies co-exist in the same brain has induced a number of cross-sectional studies to try and establish the prevalence of mixed pathologies in the ageing brain.

In a large autopsy study conducted in Vienna, of the 1500 demented elderly cases only 52% exhibited 'pure' AD, 7% atypical AD, 16-20% AD harbouring concomitant cerebrovascular lesions, 9% AD with additional LB pathology, 2.4% with mixed AD and vascular encephalopathy and 2% exhibiting 'pure' vascular dementia. Other dementing disorders were assigned to 16.1% of the remaining cases with 1% showing no specific pathology (Jellinger and Attems, 2007).

In 2008, a multi-centre study lead by the BrainNet Europe consortium utilised cerebral tissue from 9 brain banks with a total of 3,303 cases analysed (1,667 female: 1,636 male, mean age 74.14 SD± 12.07 years) (Kovacs et al., 2008). The proportion of cases that were reported to have multiple pathological lesions associated with more than one neurodegenerative disease including those with AD, vascular pathology (VP), agyrophilic grain disease (AGD) and synucleinopathies was 55.3%. Mixed pathology was most frequently reported in PD cases (92%) followed by AGD (67%), LBD (61%), vascular pathology (65%) and AD (43%). Whilst PSP, CBD, FTLD-U and CJD did show mixed pathology to a lesser extent 22%, 21%, 9% and 2% respectively. An important finding from this study was the under appreciation of mixed pathologies in a multitude of neurodegenerative diseases in particular LBDs.

Another study conducted by Dugger and colleagues further investigated the degree of concomitant pathologies among all Parkinsonian disorders using data from the Arizona Study of Ageing and Neurodegenerative Disorders (AZSAND) study (Dugger et al., 2014). Of the 140 neuropathological confirmed PD cases

44% had cerebral white matter rarefaction (CWMR), 38% had concomitant AD pathology, 25% had agyrophilic grains, 24% had CAA and 9% had PSP. Of the 90 DLB cases 89% had AD-related pathology, 51% CWMR, 50% CAA, 21% Argyophilic grains and 1% PSP. PSP, MSA and CBD also demonstrated similar heterogeneity with many of the cases analysed fulfilling neuropathological criteria for more than one disease.

As with all neurodegenerative disorders, the prevalence of mixed pathologies increases with age. In a large autopsy series consisting of 1,110 cases (mean age 83.3±5.6 years, 90% over 70 years) conducted by Jellinger and Attems, the prevalence of AD with vascular pathology increased from 7.8% to 32.9% from the 7th to the 10 decade, whilst conversely the prevalence of 'pure' AD increased from 32.2% in the 7th decade to 45.1% in the 9th decade, whilst in the 10th decade decreased to 39.2% (Jellinger and Attems, 2010).

1.6.2 Clinical relevance of cerebral multi-morbidity

To date a plethora of studies concerning mixed pathologies have focussed on the co-existence of AD and VP (Skoog et al., 1999, Ince, 2001, Jellinger, 2002, de la Torre, 2004, Jellinger and Attems, 2005). Studies into the clinical relevance of the co-existence of AD related pathology and VP have been largely inconsistent. Some studies indicate there is a positive correlation between increasing Braak stages and increasing severity of VP (Jellinger and Attems, 2003, Kovacs et al., 2008). As part of the Nun study (a longitudinal study of ageing and AD) Snowdon and colleagues demonstrated the presence of cerebrovascular disease in patients with AD had a poorer cognitive function and higher prevalence of dementia than those without cerebral infarcts (Snowdon, 2003). Conversely, others suggest a small amount of VP does not impact cognitive decline in severe AD cases (Lee et al., 2000, Jellinger, 2001). The inconsistency of the data regarding the relationship between AD and VP may be due in part to the lack of consensus in the classification of vascular lesions. However, research is progressing to develop a staging system that can address this issue (Deramecourt et al., 2012). Another consideration may be the existence of a threshold of concomitant VP pathology that needs to be breached before the impact of combined pathologies on clinical phenotype can be seen (Gold et al., 2007).

Historically AD and DLB were distinguished by the presence of Aβ plaques and NFTs versus LBs. However, a large proportion of AD cases (50%) exhibit concomitant Lewy body pathology in addition to plaques and tangles, but do not fulfil neuropathological criteria for a diagnosis of AD (Marsh and Blurton-Jones, 2012). This subpopulation of patients, termed Lewy body variant of Alzheimer's disease (LBV-AD), experience a more rapid decline in cognition and a shorter survival time from the onset of clinical symptoms compared to classical AD and DLB groups (Olichney et al., 1998, Serby et al., 2003, Kraybill et al., 2005)

1.7 Synergism between pathological lesions

Given the overlap in pathology in neurodegenerative diseases, research is currently undertaken to elucidate putative interactions between these proteins.

1.7.1 Aβ and α-syn

The potential relationship between α-syn and Aβ has been studied (Masliah et al., 2001, Compta et al., 2011, Marsh and Blurton-Jones, 2012). Using *post-mortem* brain tissue from 40 PD cases and 20 controls Lashley and colleagues used a combination of semi-quantitative and morphometric assessment to determine Aβ plaque load and LB density respectively, and found a significant correlation between Aβ plaque load, in particular the diffuse plaque load and overall LB burden (Lashley et al., 2008). More recently Swirski and colleagues measured Aβ40, Aβ42, α-syn and pSer129 α-syn by sandwich enzyme-linked immunoabsorbant assay (ELISA) in midfrontal, cingulate, parrahippocampal cortex and thalamus in a cohort of PD, PDD, DLB and control cases, and found insoluble levels of pSer129 α-syn was positively correlated with soluble and insoluble levels of Aβ (Swirski et al., 2014). In parallel experiments, exposure of SH-SY5Y cells transfected with wild-type human *SNCA* cDNA to aggregated Aβ42 significantly increased the phosphorylation of pSer129 α-syn suggesting the concentration levels of pSer129 α-syn is directly related to Aβ.

1.7.2 HP-τ and α-syn

As HP-τ is frequently seen as a concomitant pathology in other neurodegenerative disorders other than AD in particular LBD, research to elucidate a potential interaction between HP-τ and α-syn is ongoing.

In 2003, Giasson and colleagues demonstrated α-syn can initiate the polymerization of HP-τ *in vitro.* In addition to this tau inclusions were observed in approximately 50% of Ala53Thr transgenic mice expressing human α-syn which lead to severe motor dysfunction (Giasson et al., 2003, Lee et al., 2004). Further evidence to support this work was provided by Badiola and colleagues, who used mouse primary cortical neurones to demonstrate overexpression of HP-τ increased the number of α-syn aggregates and enhanced α-syn toxicity (Badiola et al., 2011). At the cellular level the co-occurrence of HP-τ and α-syn has been shown using double immunofluorescence Figure 1.11 (Ishizawa et al., 2003, Colom-Cadena et al., 2013).

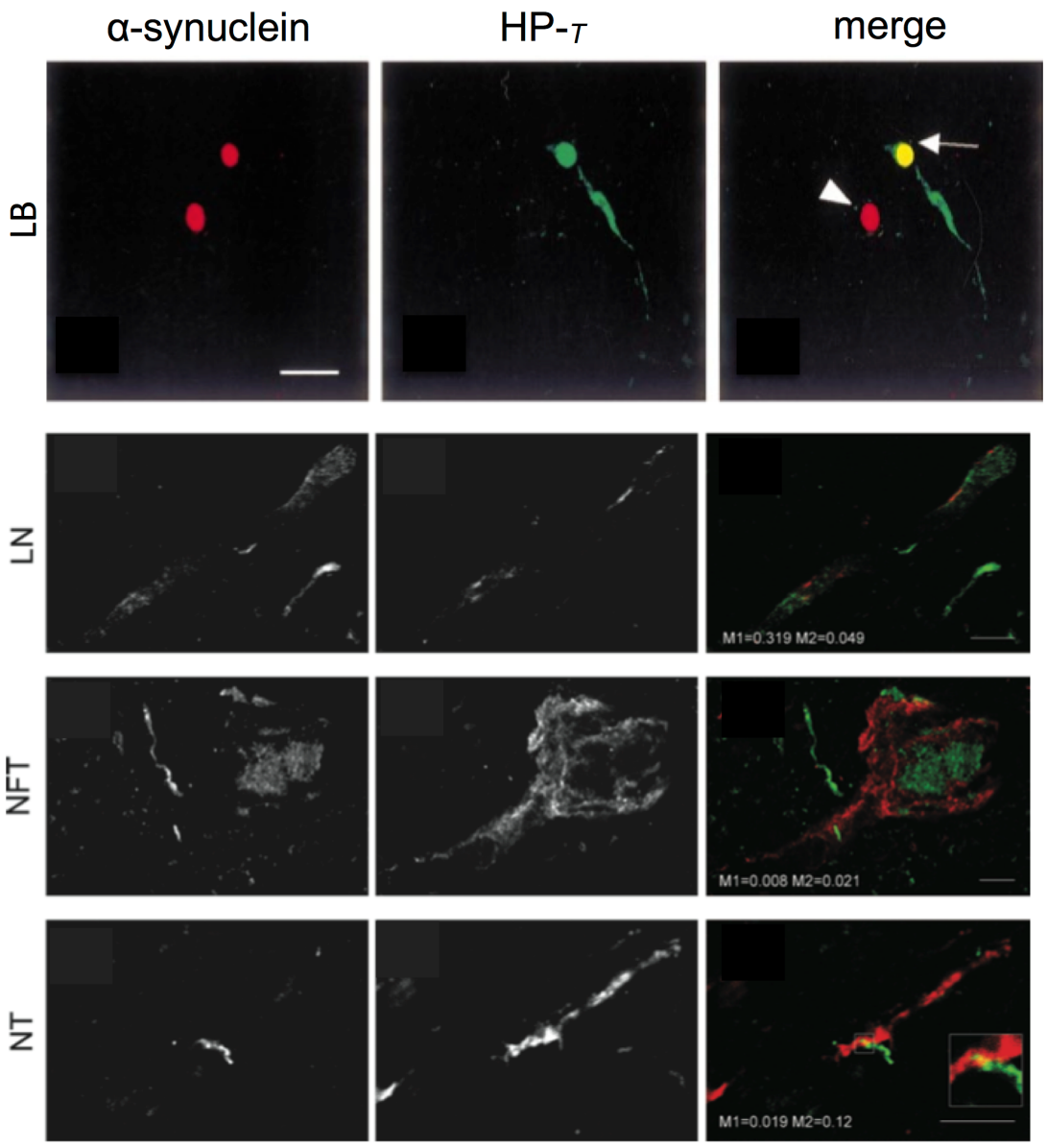

Figure 1.11 Co-localisations of HP-τ (green) and α-syn (red) and merged images in Lewy bodies (LB), Lewy neurites (LN), neurofibrillary tangles (NFT) and neuropil threads (NT). Image adapted from (Colom-Cadena et al., 2013) and (Ishizawa et al., 2003).

1.7.3 Aβ, HP-τ and α-syn

A limitation to these experiments is the study of these pathological protein aggregates in isolation, as it does not accurately reflect the mixed pathology load frequently seen in brains of the demented elderly. Clinton and colleagues addressed this limitation by generating a mouse model that expressed Aβ, HP-τ and α-syn pathologies by crossing 3xTg-AD mice with mice expressing the A53T mutation in α-syn. The resulting DLB-AD mice exhibited all three pathological lesions at a higher load and an acceleration in cognitive decline as measured using the Barnes maze test compared to the single transgenic animals (Clinton et al., 2010). As data that fully recapitulates these findings in the human brain is still lacking (Colom-Cadema and colleagues found a correlation between Aβ and α-syn, but not between HP-τ and α-syn in a cohort of DLB cases (Colom-Cadena et al., 2013)), future work will help to elucidate the mechanistic link between multiple pathologies.

1.8 Clinico-pathological correlative studies (CPCs)

Clinico-pathological correlative studies (CPCs) are critically important in dementia research. Although neuropathology is paramount in dementia research, a more multi-disciplinary approach seems mandatory to achieve further progress in the field and direct future research projects. Autopsy studies provide cross sectional data, which on its own cannot be related to the clinical features of dementia, and therefore clinical symptoms need to be compared to hallmark pathological lesions to address the question of the relevance of morphological abnormalities to cognitive status.

1.8.1 CPCs in AD

A plethora of CPC have been performed on dementing disorders. In AD, numerous studies have assessed the association between Aβ plaques, HP-τ and synaptic connections and cognitive decline as measured by MMSE (Tomlinson et al., 1970, Crystal et al., 1993, Bancher et al., 1996, Haroutunian et al., 1999). Using staging patterns and topographical distribution of aggregated proteins, there is a complex but predictable relationship between AD pathological hallmarks in particular NFT's and NT's and cognitive impairment (Nelson et al., 2012)

1.8.2 CPCs in PD

Using data from a clinical study conducted by Lewis and colleagues that identified 4 distinct clinical subtypes of PD (Lewis et al., 2005), Selikhova and colleagues analysed the distribution of pathology using a semi-quantitative methodology. Lewy body pathology, amyloid plaques and CAA were assessed in each of the 4 subtypes: 1. patients with younger disease onset, 2. tremor dominant patients, 3. non-tremor dominant with significant cognitive impairment and 4. rapid disease progression but no cognitive impairment (Selikhova et al., 2009). The non-tremor dominant subgroup had a significantly higher mean pathological grading of cortical LBs than all of the other groups and more cortical Aβ burden and CAA than the early disease onset and tremor dominant groups.

1.8.3 CPCs in DLB

A CPC using a semi-quantitative methodology for assessing pathology has indicated we may be able to tease out distinct clinicopathological subgroups of DLB, as a subset of DLB cases with rapid eye movement sleep behaviour disorder (RBD) was identified that had lower Braak neurofibrillary stage (IV vs VI) and lower neuritic plaque scores (18 vs 85%) compared to those without RBD, but no differences in α-syn distribution (Dugger et al., 2012). Schneider and colleagues also used a semi-quantitative approach and found neocortical but not limbic or nigral predominant DLB was related to dementia. Concomitant Alzheimer's pathology had an additive effect in the decline in cognition in neocortical DLB cases (Schneider et al., 2012).

1*.8.4 Challenges of CPCs*

There are also problems facing researchers who undertake CPCs. Most studies are subject to selection bias as brain bank donors are mainly those with end stage dementia and are from countries with the most advantageous socioeconomic conditions and are therefore not representative of a worldwide population (Nelson et al., 2012). Another challenge facing CPCs in AD is the molecular, anatomic and clinical changes do not progress in a uniform manner (Han et al., 2000, Murray et al., 2011).

1.9 Semi-quantitative vs Quantitative neuropathological assessment

Many CPCs rely on semi-quantitative assessment to define the burden of pathological protein aggregates in a given brain region of *post-mortem* brains. For semi-quantitative assessment of HP-τ and α-syn several internationally recognised staging systems are used which are based on a 4 and 5-tiered scales (absent, mild, moderate, severe (and very severe)) respectively (McKeith et al., 2005, Alafuzoff et al., 2008). Due to the heterogeneity of Aβ deposits in the human brain Aβ assessment is dichotomous, based on the presence or absence of immunopositivity (Alafuzoff et al., 2009b). Although semi-quantitative evaluation is extremely valuable when classifying neurodegenerative diseases, it lacks the accuracy to detect subtle differences in pathology loads, particularly in later stages of disease when pathology burden in considerable. For example, the amount of HP-τ immunopositivity differed by nearly 100% between cases that are classified as having severe pathology when assessed semi-quantitatively (Attems and Jellinger, 2013b). Furthermore, semi-quantitative assessment can be inherently subjective, produces ordinal rather than continuous data and inter-rater reliability may be questionable when more than one person is assessing the same cohort of cases (Rizzardi et al., 2012).

On the other hand, quantitative neuropathological assessment negates the problem of inter-rater reliability and may be useful when assessing more delicate neuropathological lesions such as NTs and LBs. In the 90+ study, a prospective longitudinal population based study of ageing and dementia, quantitative measures of both Aβ and HP-τ in the neocortex and hippocampus were strongly associated with the presence of dementia, whereas using semi-quantitative values this association was not observed (Robinson et al., 2011). Another study utilising quantitative techniques by McAleese and colleagues, found HP-τ burden in the overlying cortex independently predicted age related white matter changes as seen on MRI in a cohort of AD and control cases. These findings suggest an alternative pathogenesis of white matter changes in AD other than the normal assumption of small vessel disease, and may have implications in future treatment strategies (McAleese et al., 2015).

A study demonstrating the importance of quantification techniques in AD identified 3 distinct clinico-pathological subtypes of AD. In the large-scale study 11% of cases were found to have hippocampal sparing AD whilst 14% demonstrated limbic predominant AD in addition to those with typical AD (Murray et al., 2011). Moreover, these distinct subgroups of AD could be predicted *intra vitam* by MRI. Patterns of atrophy were measured in each of the subtypes and the ratio of hippocampal to cortical volumes allowed discrimination between limbic predominant, hippocampal sparing and classical AD subtypes (Whitwell et al., 2012). Taken together the prediction of different subtypes of AD during life could have significant impacts on the choice of therapeutics by the treating clinician.

Common methods employed for quantifying neuropathological lesions include unbiased stereological estimation (Ohm et al., 1997), grid counting estimates of the numbers of plaques and tangles per unit area (Rogers and Morrison, 1985) and grading plaque and tangle densities using a numerical scale (Arnold et al., 1991). However, a plethora of new technologies are emerging to aid high-throughput analysis of pathological lesions in the human brain. Neltner and colleagues have developed a highly accurate and reproducible digital pathology and image analysis method that will reliably quantify AD neuropathological changes (Neltner et al., 2012). Whilst Smid and colleagues reported a correlation between pre-mortem [F-18]FDDNP PET with cortical neuropathology as determined *post-mortem* by quantifying 3-dimensional whole brain coronal slices (Smid et al., 2013). Manual methods of quantification are time-consuming, therefore any advances in automated quantification techniques will only aid our ability to assess large cohorts of patients with the aim identifying clinico-pathological subtypes of neurodegenerative disease not previously detected using semi-quantitative methodology.

1.10 Study outline

The main aim was to investigate the use of quantitative neuropathological assessment in clinico-pathological assessment of LBD cases that have multiple pathological lesions, and to investigate the impact multiple pathologies have on each other and clinical features associated with LBD.

My main research objectives were:

- To determine whether quantification of pathological lesions in cases that fulfil neuropathological criteria for mixed AD/LBD can distinguish between cases with different clinical phenotypes. In addition, to investigate how these cases compare against 'pure' forms of AD and DLB (Chapter 3).

- To Investigate individual pathologies observed in LBD (HP-*T*, Aβ and α-syn) or a combination of these pathologies associate with motor impairment in cohort of LBD cases (Chapter 4).

- To explore possible associations between HP-*T*, Aβ and pE(3)Aβ and pSer129 α-syn in a cohort of LBD cases (Chapter 5).

Chapter 2. Materials and Methods

2.1 Introduction

This chapter describes the histological, immunohistochemical, and molecular techniques employed to assess human *post-mortem* brains of aged individuals.

Clinico-pathological correlations were conducted using corresponding clinical data to investigate how the presence of single and multiple pathologies affects the clinical phenotype of dementia in Lewy body diseases and to better characterise cases with mixed AD/LBD.

2.2 Study Cohort

Cases were selected for the study on the basis that they fulfilled clinical and neuropathological criteria for DLB, PDD, or both AD and LBD, the latter being classified as mixed AD/LBD (e.g. High AD neuropathologic change (Montine et al., 2012a) and neocortical LBD (McKeith et al., 2005). Control cases were included in the analysis of cortical thickness. In addition a subset of cases with minimal amounts of α synuclein pathology but no clinical dementia during lifetime were selected (PD) to complete the spectrum of LBD cases to include cases with brainstem and limbic pathology. To the best of my knowledge all of the cases in this study did not carry a genetic mutation associated with early onset neurodegeneration. Characteristics of the study cohort are shown in table 2.1

2.3 Clinical assessment

During life, patients underwent cognitive evaluation including Mini-Mental State Examination (MMSE) (Folstein et al., 1975) as a measure of cognitive function. If more than one MMSE was available the rate of cognitive decline was calculated. Rate of cognitive decline was determined as described previously (Olichney et al., 1998) (i.e. taking the initial MMSE score, minus the final MMSE score divided by the time interval between testings). The Unified Parkinson's Disease Rating Scale (UPDRS) part III was employed to efficiently assess motor dysfunction typically associated with PD (Goetz, 2003, Goetz et al., 2008).

	Case Number	Disease cat.	Clinical diagnosis	Age	Sex	Age at onet (dementia)	PM delay (hours)	Fixation length (weeks)	Brain weight	Braak	Thal	CERAD	McKeith	Braak LB	APOE genotype	Chapters used
	1	mixed AD/DLB	AD	79	F	66	46	12	900	6	5	Frequent	Neocortical	6	E3/E4	3
	2	mixed AD/DLB	AD	82	M	75	12	4	1410	6	5	Frequent	Neocortical	6	E4/E4	3
	3	mixed AD/DLB	AD	63	F	49	38	16	818	5	5	Frequent	Neocortical	6	E3/E3	3
	4	mixed AD/DLB	AD	77	M	66	78	8	1312	6	4	Frequent	Neocortical	6	E3/E3	3
	5	mixed AD/DLB	AD	88	F	73	84	7	1034	6	5	Frequent	Neocortical	6	E3/E4	3
	6	mixed AD/DLB	AD	62	M	54	28	7	1335	6	5	Frequent	Neocortical	6	E3/E3	3
	7	mixed AD/DLB	AD	73	M	69	7	12	1129	6	5	Frequent	Neocortical	6	E4/E4	3
	8	mixed AD/DLB	AD	77	F	70	51	12	1072	6	5	Frequent	Neocortical	6	E3/E4	3
Mean				**75.13**	**4M:4F**	**65.75**	**43**	**9.75**	**1126.25**							
SE mean				**3**		**3.23**	**9.9**	**1.37**	**75.15**							
	9	mixed AD/DLB	DLB	80	F	73	51	14	N/A	6	5	Frequent	Neocortical	6	E3/E4	3
	10	mixed AD/DLB	DLB	68	M	59	48	124	N/A	6	5	Frequent	Neocortical	5	E3/E4	3
	11	mixed AD/DLB	DLB	75	F	70	78	8	1180	6	5	Frequent	Neocortical	6	E3/E3	3
	12	mixed AD/DLB	DLB	80	F	68	17	7	1014	5	5	Frequent	Neocortical	6	E3/E4	3
	13	mixed AD/DLB	DLB	83	M	68	48	7	1228	6	5	Frequent	Neocortical	6	NA	3
	14	mixed AD/DLB	DLB	78	M	77	17	9	1308	6	5	Frequent	Neocortical	6	E4/E4	3
	15	mixed AD/DLB	DLB	78	M	72	18	8	1065	6	5	Frequent	Neocortical	6	E3/E4	3
	16	mixed AD/DLB	DLB	67	M	61	46	4	1382	6	5	Frequent	Neocortical	6	E3/E4	3
Mean				**76.13**	**5M:3F**	**68.5**	**40.36**	**22.63**	**1196.17**							
SE mean				**2.05**		**2.13**	**8.82**	**14.52**	**57.36**							
	17	mixed AD/DLB	PDD	68	M	62	11	2	1425	6	5	Frequent	Neocortical	6	E3/E3	3
	18	mixed AD/DLB	PDD	75	M	63	28	17	1180	5	5	Frequent	Neocortical	6	E3/E4	3
	19	mixed AD/DLB	PDD	77	M	73	6	8	1250	6	5	Frequent	Neocortical	6	E3/E4	3
Mean				**73.33**	**3M:0F**	**66**	**15**	**9**	**1285**							
SE mean				**2.72**		**3.15**	**6.66**	**4.36**	**72.86**							
	20	AD	AD	77	F	**64**	63	5	975	6	5	Frequent	Negative	Negative	NA	3
	21	AD	AD	83	M	**77**	12	16	1250	6	4	Frequent	Negative	Negative	NA	3
	22	AD	AD	86	F	**75**	69	69	1087	6	5	Frequent	Negative	Negative	NA	3
	23	AD	AD	84	F	**75**	47	16	956	6	5	Frequent	Negative	Negative	NA	3
	24	AD	AD	81	F	**80**	50	9	1131	6	5	Frequent	Negative	Negative	NA	3
Mean				**82.2**	**1M:4F**	**74.2**	**48.2**	**23**	**1079.8**							
SE mean				**1.53**		**2.71**	**9.91**	**11.69**	**53.83**							

Table 2.1 Characteristics of the study cohort. Abbreviations: PM, *post-mortem*; CERAD, Consortium to Establish a Registry for Alzheimer's disease; LB, Lewy body; AD, Alzheimer's disease; DLB, dementia with Lewy bodies; F, female; m, male; SE, standard error; PDD, Parkinson's disease dementia; PD, Parkinson's disease.

	Case Number	Disease cat.	Clinical diagnosis	Age	Sex	Age at onet (dementia)	PM delay (hours)	Fixation length (weeks)	Brain weight	Braak	Thal	CERAD	McKeith	Braak LB	APOE genotype	Chapters used
	25	DLB	DLB	89	M	NA	88	85	1255	3	NA	Sparse	Neocortical	NA	NA	4,5
	26	DLB	DLB	88	F	80	16	12	NA	3	NA	Moderate	Neocortical	NA	NA	4,5
	27	DLB	DLB	78	F	NA	120	7	1225	5	NA	Frequent	Diffuse	NA	NA	4,5
	28	DLB	DLB	75	F	72	64	5	1010	6	NA	Frequent	Diffuse	NA	NA	4,5
	29	DLB	DLB	75	M	68	18	3	1300	2	NA	Negative	Limbic	NA	NA	4,5
	30	DLB	DLB	77	M	74	29	4	1380	2	NA	Moderate	Neocortical	NA	NA	4
	31	DLB	DLB	78	F	75	96	5	1090	3	NA	Sparse	Neocortical	NA	NA	4,5
	32	DLB	DLB	91	F	84	84	3	1150	5	NA	Frequent	Limbic	NA	NA	4,5
	33	DLB	DLB	75	F	70	78	7	1180	6	NA	Frequent	Neocortical	NA	NA	4,5
	34	DLB	DLB	71	M	68	68	4	1300	3	NA	Sparse	Neocortical	NA	NA	4,5
	35	DLB	DLB	78	M	75	83	7	1280	1	NA	Negative	Limbic	NA	NA	4,5
	36	DLB	DLB	76	M	68	76	41	1110	2	NA	Sparse	Neocortical	NA	NA	4,5
	37	DLB	DLB	70	M	NA	50	50	1155	2	NA	None	Neocortical	NA	NA	4,5
	38	DLB	DLB	74	M	66	42	8	1610	4	NA	Sparse	Neocortical	NA	NA	4
	39	DLB	DLB	77	M	73	8	4	1290	2	0	Negative	Neocortical	6	NA	3,4,5
	40	DLB	DLB	71	M	64	8	10	1359	2	1	Sparse	Neocortical	6	NA	3,4,5
	41	DLB	DLB	72	M	64	89	14	1406	3	0	Negative	Neocortical	6	NA	3,4,5
	42	DLB	DLB	77	M	66	46	13	1328	3	0	Negative	Neocortical	6	NA	3,4,5
	43	DLB	DLB	81	F	77	44	11	1314	4	1	Moderate	Neocortical	6	NA	4,5
	44	DLB	DLB	73	F	67	99	9	1108	3	3	Negative	Neocortical	6	NA	4,5
	45	DLB	DLB	78	M	72	8	13	1138	3	3	Moderate	Neocortical	6	NA	4,5
	46	DLB	DLB	81	M	NA	24	5	1273	4	NA	Sparse	Neocortical	NA	NA	4,5
	47	DLB	DLB	81	M	77	26	8	1331	3	3	Moderate	Neocortical	6	NA	4,5
Mean				**77.65**	**15M:8F**	**71.58**	**54.96**	**14.26**	**1254.18**							
SE mean				**1.17**		**3.04**	**7.07**	**4**	**28.19**							
	48	PDD	PDD	69	M	64	17	6	1430	2	NA	Negative	Limbic	NA	NA	4,5
	49	PDD	PDD	69	F	NA	46	6	1488	2	NA	Negative	Neocortical	NA	NA	4
	50	PDD	PDD	69	M	61	96	4	1350	0	NA	Negative	Neocortical	NA	NA	4,5
	51	PDD	PDD	81	M	73	40	10	1400	2	NA	Negative	Neocortical	NA	NA	4,5
	52	PDD	PDD	79	M	NA	64	6	1250	4	NA	Negative	Neocortical	NA	NA	4
	53	PDD	PDD	75	M	73	40	5	1315	3	NA	Sparse	Diffuse	NA	NA	4,5
	54	PDD	PDD	78	M	NA	48	6	1350	3	NA	Negative	Limbic	NA	NA	4,5

Table 2.1 continued

	Case Number	Disease cat.	Clinical diagnosis	Age	Sex	Age at onet (dementia)	PM delay (hours)	Fixation length (weeks)	Brain weight	Braak	Thal	CERAD	McKeith	Braak LB	APOE genotype	Chapters used
	55	PDD	PDD	79	M	70	30	4	1610	3	NA	Sparse	Neocortical	NA	NA	4,5
	56	PDD	PDD	77	M	70	17	6	1380	2	NA	Negative	Neocortical	NA	NA	4,5
	57	PDD	PDD	68	M	62	11	4	1425	5	NA	Frequent	Neocortical	NA	NA	4,5
	58	PDD	PDD	68	F	60	69	20	1260	3	NA	Negative	Neocortical	NA	NA	4,5
	59	PDD	PDD	75	M	63	28	18	1180	5	NA	Frequent	Neocortical	NA	NA	4,5
	60	PDD	PDD	73	M	68	31	5	1315	0	NA	Negative	Limbic	NA	NA	4,5
	61	PDD	PDD	75	M	67	83	5	1398	1	NA	Negative	Neocortical	NA	NA	4
	62	PDD	PDD	70	F	70	9	4	1058	4	NA	Moderate	Neocortical	6	NA	4,5
	63	PDD	PDD	74	M	NA	34	7	1210	4	NA	Frequent	Neocortical	6	NA	4,5
	64	PDD	PDD	87	F	84	60	18	1155	3	2	Negative	Neocortical	6	NA	4
	65	PDD	PDD	75	F	73	18	8	1202	3	4	Moderate	Neocortical	6	NA	4
	66	PDD	PDD	83	M	79	71	9	1253	4	5	Moderate	Neocortical	6	NA	4
	67	PDD	PDD	86	M	85	44	10	1118	3	4	Moderate	Neocortical	5	NA	4
	68	PDD	PDD	76	M	58	68	8	1339	3	1	Negative	Neocortical	5	NA	4
Mean				**75.52**	**16M:5F**	**69.41**	**44**	**8.05**	**1308.86**							
SE mean				**1.24**		**2.86**	**5.35**	**1.05**	**28.72**							
	69	PD	PD	76	M	/	49	7	1450	1	NA	Sparse	Neocortical	NA	NA	5
	70	PD	PD	82	M	/	7	4	1270	2	NA	Negative	Neocortical	NA	NA	5
	71	PD	PD	81	M	/	52	8	1460	3	0	Negative	Limbic	4	NA	5
	72	PD	PD	80	M	/	88	14	1497	1	NA	Sparse	Limbic	NA	NA	5
	73	PD	PD	90	M	/	18	14	1194	2	0	Negative	Limbic	4	NA	5
	74	PD	PD	92	F	/	45	12	1063	1	0	Negative	Limbic	5	NA	5
	75	PD	PD	70	M	/	48	7	1358	2	0	Negative	Limbic	4	NA	5
Mean				**81.57**	**6M:1F**		**43.86**	**9.43**	**1327.43**							
SE mean				**2.88**			**9.86**	**1.48**	**60.42**							
	76	Control	Control	94	F	/	15	10	1171	2	1	Negative	Negative	0	NA	3
	77	Control	Control	70	F	/	72	10	1567	0	0	Negative	Negative	2	NA	3
	78	Control	Control	70	M	/	39	7	1034	1	1	Negative	Negative	0	NA	3
	79	Control	Control	78	F	/	34	8	1179	0	1	Negative	Negative	0	NA	3
	80	Control	Control	96	F	/	29	11	1124	3	1	Negative	Limbic	3	NA	3
	81	Control	Control	86	M	/	50	13	1070	4	4	Moderate	Negative	0	NA	3
	82	Control	Control	65	F	/	47	8	1236	1	0	Negative	Negative	0	NA	3
	83	Control	Control	85	M	/	45	7	1192	1	2	Negative	Negative	0	NA	3
Mean				**80.5**	**3M:5F**		**41.375**	**9.25**	**1196.93**							
SE mean				**4.1**			**5.92**	**0.75**	**57.86**							

Table 2.1 continued

2.4 Tissue preparation

2.4.1 Tissue acquisition

Human *post-mortem* brain tissue from 83 cases was obtained from Newcastle Brain Tissue Resource (NBTR) in accordance with the approval of the joint Ethics Committee of Newcastle and North Tyneside Health Authority and following NBTR brain banking procedures.

2.4.2 Tissue sampling for routine diagnosis

At autopsy the left hemisphere, brainstem and cerebellum were snap frozen between copper plates at -120^{o}C, whilst the right hemisphere, brainstem and cerebellum were immersion fixed in 4% aqueous formalin for 4-124 weeks.

Following fixation, the right hemisphere was dissected in coronal planes approximately 0.7cm intervals and subjected to standard macroscopic examination (abnormal/pathological findings were recorded). Sub-dissection was performed to obtain routine tissue blocks, required to determine neuropathological diagnosis. Tissue blocks were processed through increasing concentrations of alcohol (to dehydrate the tissue) and chloroform (to clear the tissue) before being embedded into paraffin wax suitable for long-term storage. This study used several blocks that were also used for routine diagnostic purposes including frontal, temporal, entorhinal, parietal and occipital cortices and hippocampus (see Figure 2.1) as well as midbrain and pons.

Subsequently, all brains underwent standard assessment by a neuropathologist to determine neuropathological diagnosis (criteria are outlined in introduction section 1.9). Following a detailed analysis of the clinical notes, a consensus clinico-pathological diagnosis was determined for each of the cases.

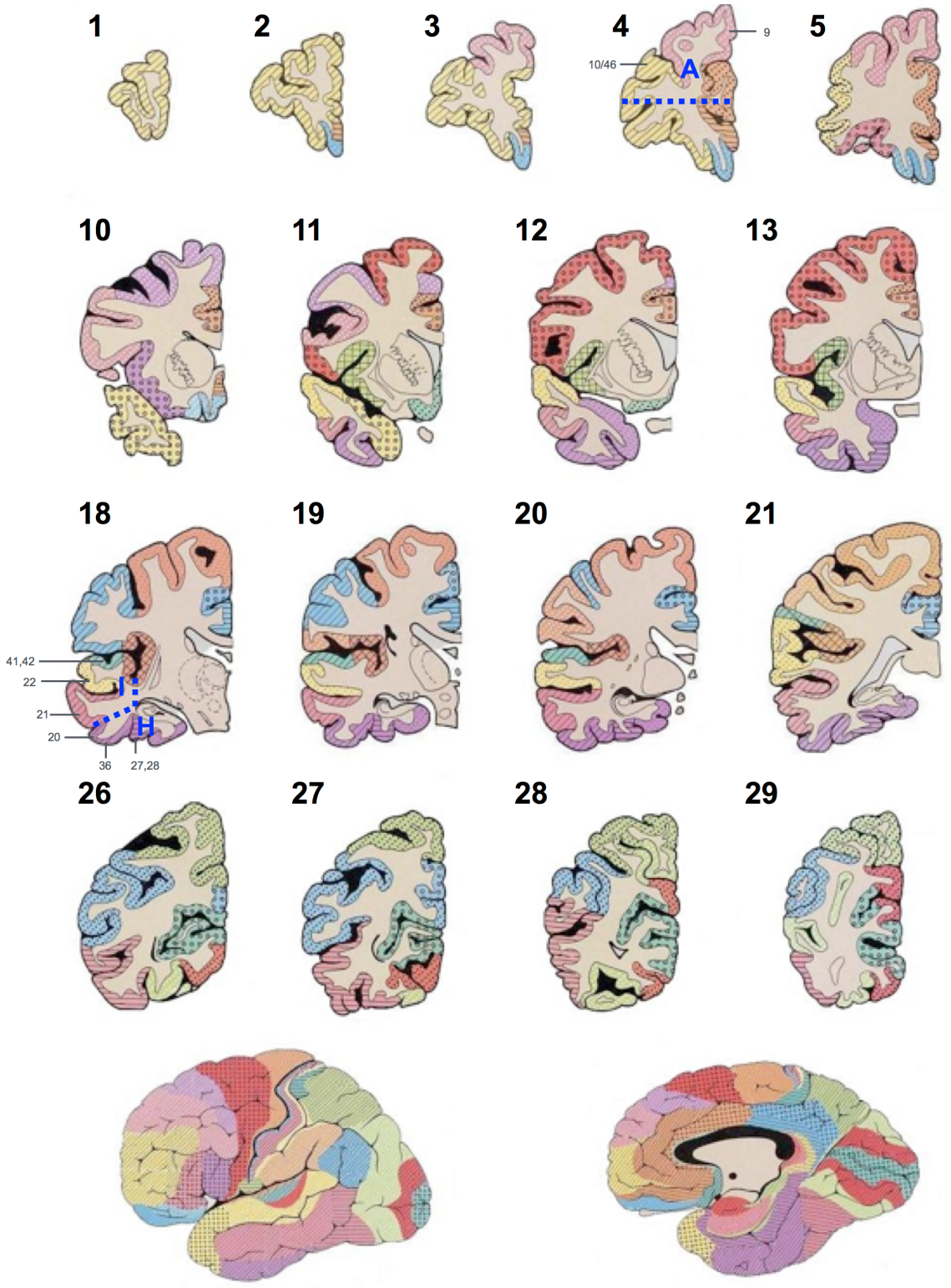
1
2
3
4
9
10/46
A
5
10
11
12
13
18
41,42
22
I
21
H
20
36
27,28
19
20
21
26
27
28
29

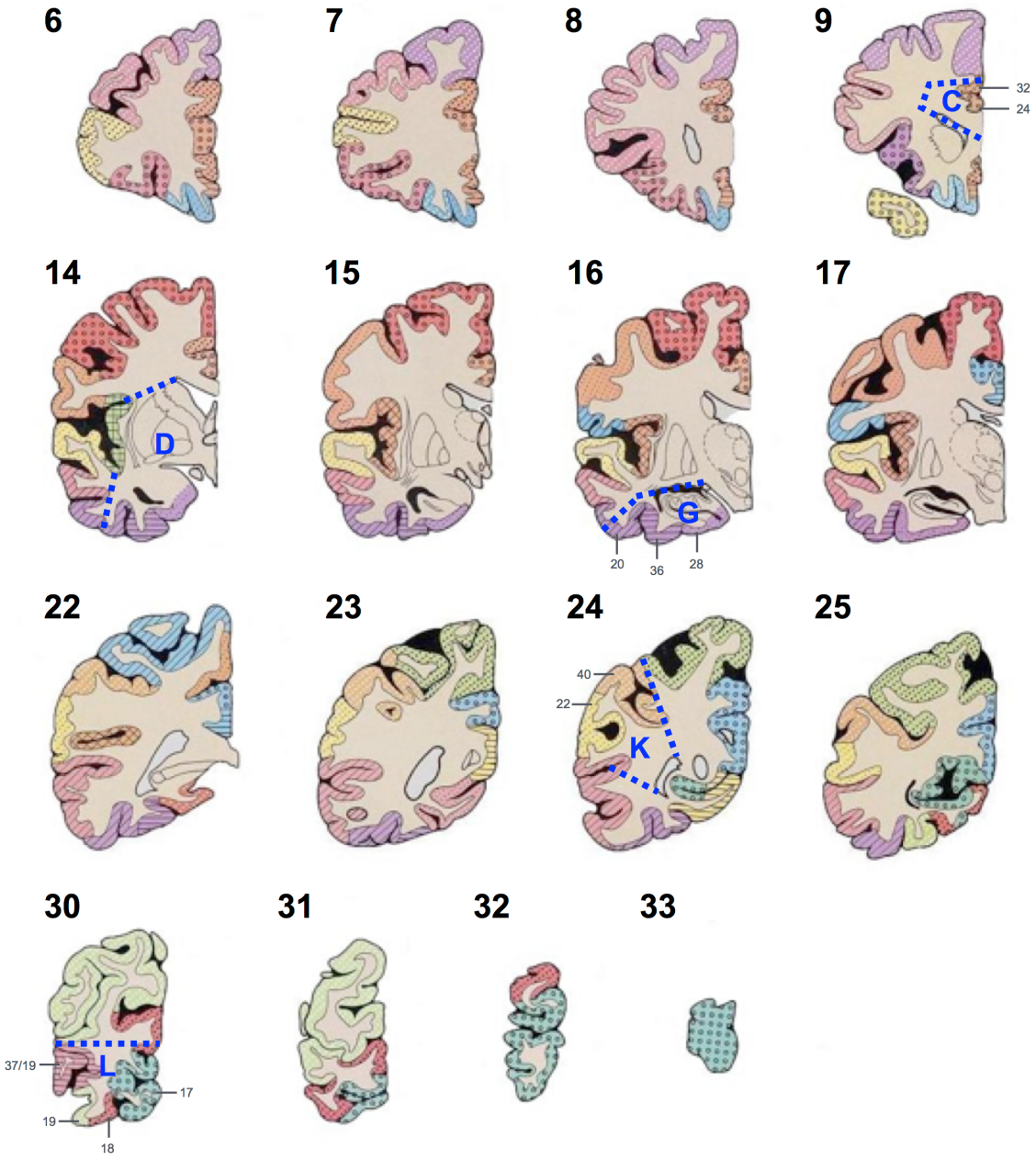

Figure 2.1. Schematic illustrating the coronal levels and diagnostic blocks used in this study. Block lettering illustrate coronal levels, blue lettering and blue dashed lines represent diagnostic blocks and sub-dissection lines. Small grey lettering and colour coding illustrates Brodmann areas. Adapted from the Newcastle Brain map (Perry and Oakley, 1993).

2.5 Brain Regions

2.5.1 Frontal cortex

Frontal cortex comprises 25-33% of the brain (Smith and Jonides, 1999) and enables us to engage in higher cognitive functions including short term working memory and executive functioning (Stuss and Alexander, 2000, Andres, 2003, Stuss, 2011). Within the frontal lobe lies the primary motor cortex, located just rostral of the central sulcus which mediates voluntary movement of the limbs with neurones projecting to the spinal cord (Dum and Strick, 1991, Watts and Mandir, 1992) along with the premotor area and supplementary motor area.

2.5.2 Temporal cortex

The temporal cortex is subdivided into several anatomical regions. The superior temporal gyrus plays a central role in hearing and speech perception and contains the primary auditory cortex, BA 41 and 42, whilst the middle and inferior temporal gyri are implicated in language, memory processing and visual perception (Onitsuka et al., 2004) and are amongst the first neocortical regions to be affected in AD (Convit et al., 2000). Declarative memories are encoded in the medial temporal lobe which is comprised of the perirhinal, entorhinal and parahippocampal cortices and hippocampus (Alvarez and Squire, 1994, Squire et al., 2004). The hippocampus is composed of interconnecting subfields each with distinctive histological characteristics including four fields of the Cornu Ammonis (CA1-4) and is one of the earliest affected regions affected by AD pathology (Braak and Braak, 1991, Braak et al., 2006).

2.5.3 Parietal cortex

The parietal lobe represents 20% of the cerebral cortex and is divided into two regions. The somatosensory cortex is located in the post-central gyrus and is integral in processing sensory information with connections to the basal ganglia and thalamus (Kunzle, 1977), whilst the posterior parietal cortex projects to various subcortical regions and is involved in numerous cognitive functions including attention and episodic memory (Wheeler and Buckner, 2004, Hutchinson et al., 2014).

2.5.4 Occipital cortex

The occipital lobe contains the primary visual cortex (V1), which can be mapped to Brodmann area 17, and is the main area in the brain responsible for processing visual information, receiving visual stimulus from the retina via the lateral geniculate nucleus (Jones, 1998).

2.5.5 Cingulate cortex

Located in the forebrain and as part of the limbic system, it has been proposed that the cingulate cortex is associated with emotion (Papez, 1995, Hadland et al., 2003). In addition, neuro-imaging studies in humans have implicated pain-related activation, specifically in the anterior cingulate cortex (Morrison and Downing, 2007).

2.5.5 Corpus striatum

The corpus striatum (inclusive of the caudate nucleus and putamen) is the largest component of a collection of subcortical regions found on both sides of the thalamus termed the basal ganglia and is implicated in the fine tuning and execution of motor responses (Graybiel et al., 1994).

2.5.6 Amygdala

Historically, the amygdala was considered part of the basal ganglia, however more recently the amygdala has been shown to be associated with olfactory pathways and is regarded as part of the limbic system (Swanson, 2003). Involved in regulation of responses to emotion, the amgydala also plays a crucial role in the acquisition and storage of hippocampal-dependant memories (Phelps, 2004).

2.5.7 Brain Stem

The SN is situated in the midbrain which is a part of the brainstem and contains neuromelanin pigmented cells which synapse onto cells in the striatum forming the nigro-striatal pathway (York, 1970). The SN is affected early in PD as the severity of the selective loss of dopaminergic neurones in the ventrolateral part of the substantial nigra pars compacta can be related to disease duration (Hassler, 1938, Fearnley and Lees, 1991). The LC is a pontine nucleus which is located in the pons and is the largest group of noradrenergic neurones in the

central nervous system (Dahlstroem and Fuxe, 1964), and is involved in the pathways controlling arousal and autonomic function (Samuels and Szabadi, 2008).

2.6 Tissue Micro Array

In addition to brain regions being sampled for routine diagnostics, for each case tissue was sampled to compose a Tissue Micro-Array (TMA) tissue block to enable quantification of pathological lesions in a large quantity of cases. TMA is commonly used as a high-throughput technique in cancer research to facilitate the comprehensive analysis of hundreds of tumour tissue samples to a high degree of accuracy (Kononen et al., 1998, Bubendorf et al., 2001). This technique has been adapted previously in our laboratory and has been fine tuned to accurately assess neuropathological lesions in human *post-mortem* brains (Attems et al., 2014a, McAleese et al., 2015). Forty cylindrical tissue cores were sampled from human *post-mortem* cerebral tissue from pre-defined brain regions important in the routine assessment of neurodegenerative diseases (see section 2.5).

Areas that were sampled for the TMA were taken from paraffin embedded (donor) blocks containing: - pre-frontal cortex (block A, Brodmann area 9 (BA), 10/46), mid-frontal cortex (block B, BA8, 9), cingulate gyrus (block C, BA24, 32), caudate, putamen, external globus pallidus, amgydala and insular cortex (all block D), motor cortex (block E, BA4), thalamus (block F), entorhinal cortex (block G), temporal cortex (block I, BA21, 22, 41/42), parietal cortex (block K, BA22, 40) and occipital cortex (block L, BA17, 18, 19, 19/37) (Figure 2.2).

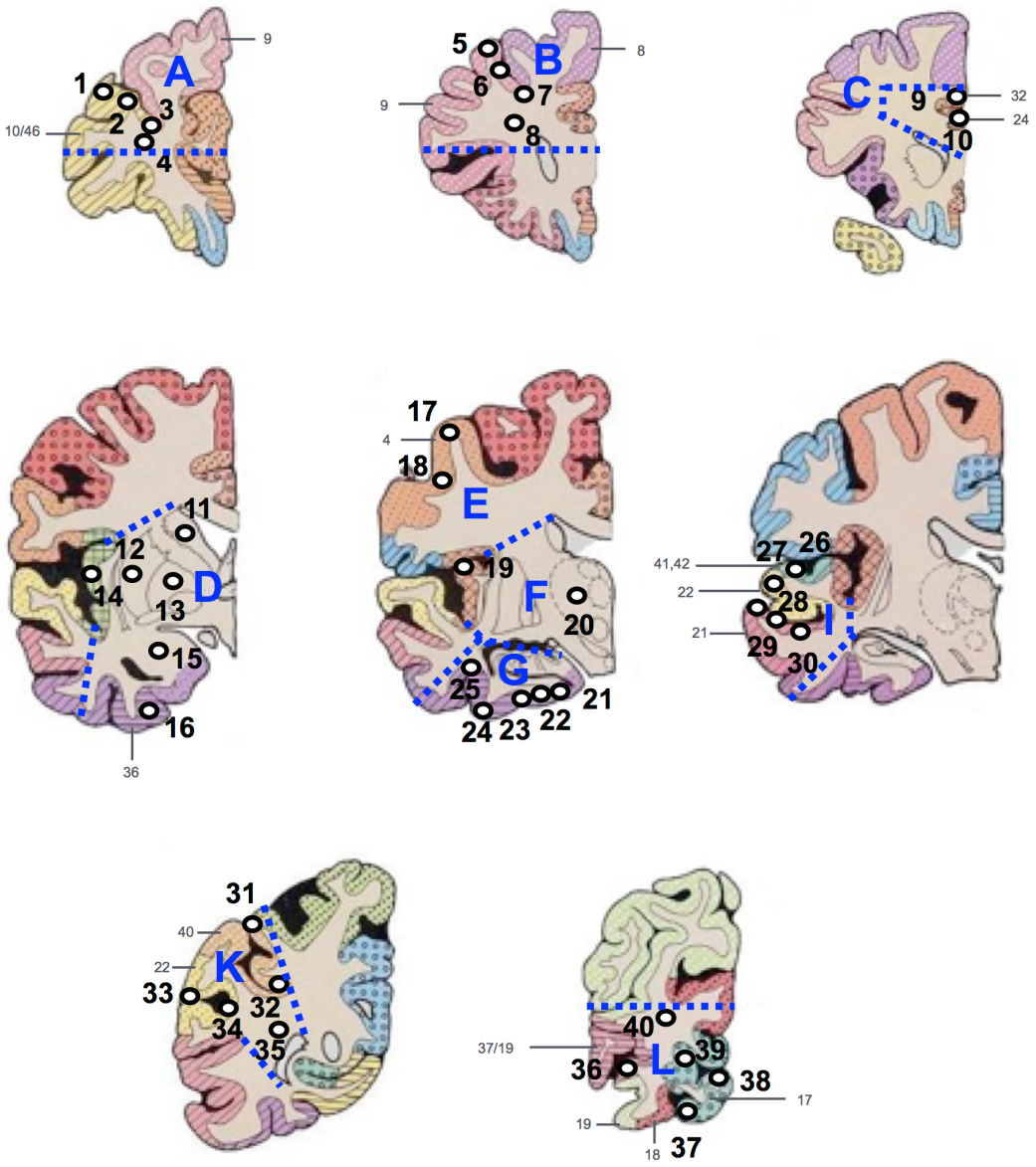

Figure 2.2 Diagram illustrating the locations where each of the Tissue Micro Array (TMA) tissue cores were extracted from each diagnostic tissue block. Tissue cores 1-4 were taken from the pre-frontal cortex (block A), 5-8 from mid-frontal cortex (block B), 9 and 10 from the cingulate cortex (block C), caudate, putamen, external globus pallidus, amygdala and insular cortex (11-16, all block D), 17 and 18 from motor cortex (block E), thalamus (20 - block F), 21-25 from entorhinal cortex (block G), 26-30 from temporal cortex (block I), 31-35 from parietal cortex (block K) and 36-40 from occipital cortex (block L). Blue lettering denotes diagnostic tissue block and blue dashed lines represent sub-dissection lines. White circles and black numbers represent the tissue cores with numeric label. Grey numbers and colour coding represent Brodmann areas. Adapted from the Newcastle Brain map (Perry and Oakley, 1993).

Fixed paraffin donor blocks were warmed for 1 hour at 37^{o}C to aid tissue removal. 3mm cylindrical tissue cores were taken from predefined positions using a hand held tissue sampler (Tissue-Tek ® Quick-Ray™ TMA system, Sakura, California, USA). The tip of the hand held punch was inserted at the correct position through the depth of the tissue in the donor block and removed along with the cylindrical tissue core (Figure 2.3a). Each tissue core was then inserted into the correct 'hole' in a single, regular sized pre-made recipient TMA paraffin block (4cm x 3cm - made to perfectly match the Tissue-Tek ® Quick-Ray™ TMA system) in numerical order (Figure 2.3b.) If any donor blocks are missing, empty 'holes' in recipient block were filled with molten wax. Each of the punches were pushed securely in to the recipient block by hand and the block incubated at 37^{o}C to reduce the wax-tissue interface when sectioning.

An in-house silicone mould, made specifically to fit the TMA recipient block, was preheated to 60^{o}C for one hour and 2-4 mls of molten paraffin wax placed into the base. The recipient TMA block was placed tissue face down onto the molten wax and left for 5 minutes before a further 15 minutes incubation at 37^{o}C to anneal (Figure 2.3c). The block was allowed to cool fully before the silicone mould was removed and excess was removed. TMA sections were then cut and mounted onto glass slides (Figure 2.3d).

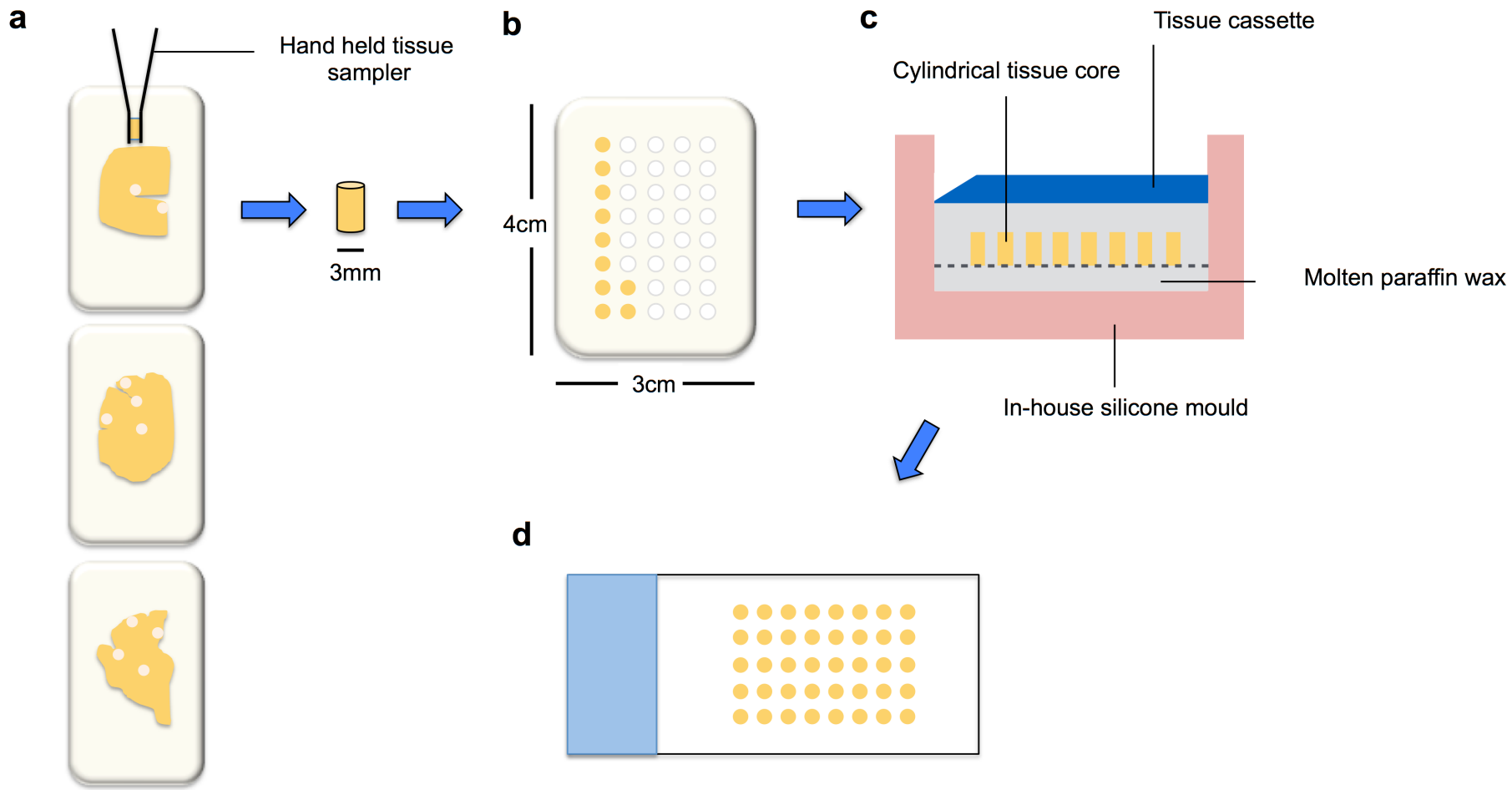

Figure 2.3 Schematic illustrating the production of the Tissue Micro Array (TMA) block. 3mm cylindrical tissue cores are taken from pre-defined positions from fixed paraffin embedded donor blocks using a hand held tissue sampler **(a)**. Each core is then inserted into the correct hole in a pre-made recipient block in numerical order **(b)**. The completed recipient block is then placed face down in a mould specifically made to fit the block with 2-4 mls of molton wax in the bottom, and left to anneal **(c)**. TMA sections are then cut at 6µm and mounted onto glass slides **(d)**.

For the purpose of this study only selected brain regions were used as outlined in Table 2.2.

Brain region	Coronal level	Brodmann area	Diagnostic block	Format	TMA tissue core numbers
Frontal	4-5	8, 9, 10/46	A	D and TMA	1-3,5-7
Temporal	18	21,22,41/42	I	D and TMA	26-30
Parietal	24	22,40	K	D and TMA	31-34
Occipital	30	17,18,19,19/37	L	D and TMA	36-39
Caudate	14	N/A	D	D and TMA	11
Putamen	14	N/A	D	D and TMA	12
External globus pallidus	14	N/A	D	TMA	13
Thalamus	16	NA	F	TMA	20
Amygdala	14	N/A	D	D	15
Cingulate	9	24,32	C	D and TMA	9-10
Hippocampus	18	N/A	H	D	N/A
Entorhinal	16	20,28,36	G	TMA	21-25
Substantia Nigra	N/A	N/A	N	D	N/A
Locus coeruleus	N/A	N/A	P	D	N/A
Motor cortex	16	4	E	TMA	17/18

Table 2.2 Brain regions in this study and topographical locations. Abbreviations; D, diagnostic slide; TMA, tissue micro array slide; N/A, not applicable. Coronal levels, Brodmann areas and diagnostic blocks are illustrated in Figures 2.1 and 2.2

2.7 Tissue sectioning, mounting and dewaxing

To aid tissue adhesion slides were pre-treated with 4% 3-aminopropyltriethoxysilane (APES) or superfrost plus slides (Thermo Shandon, Cheshire, UK) were used when required. To prepare the APES coated slides, clean glass slides were placed into racks and immersed into 4% solution of APES (Sigma-Aldrich, Dorset, UK) made up in acetone for 5 minutes, followed by 5 minutes in acetone before a final 5 minutes immersed in the 4% APES solution. Slides were then drained, rinsed in distilled water and dried at 37^{o}C and stored until used. For both the routine diagnostic and TMA sections, tissue blocks were serially sectioned at 6μm on a rotary microtome (HM325, Thermo Scientific, Hemel Hempstead, UK), and mounted onto glass slides. Mounted sections were then dried in an oven at 37^{o}C for two days, followed by 1 hour at 60^{o}C to aid adhesion, before being left to cool and stored until use.

Sections were then placed into the 60^{o}C oven for 10 minutes to aid dewaxing and deparaffinised in two changes of xylene (for 5 minutes each) before being rehydrated through a series of alcohols (2 x 100%, 1 x 75% and 1 x 50% for 2 minutes each) to water.

2.8 Histology

2.8.1 Cresyl Fast Violet

Cresyl Fast Violet (CFV) stains Nissl substance in *post-mortem* neuronal tissue and was used to visualise neuronal somata and nuclei. Following dewaxing and rehydration, sections were placed in a solution of 1% acid alcohol and rinsed in 3 changes of water. Sections were immersed in CFV solution preheated to 60^{o}C for 10 minutes then cooled for 5 minutes and rinsed. CFV staining solution was prepared by combining 20ml stock solution (0.2% w/v cresyl fast violet in distilled water), 500ml acetate buffer (13.5ml acetic acid, 23.5g sodium acetate in 2000ml distilled water, pH 4.5) and 500ml of distilled water. Sections were then differentiated in 95% alcohol until background was pale purple, dehydrated through a series of alcohols (70%, 95% and 2 x 100%) to xylene and mounted with a coverslip using DPX (CellPath, Newtown, UK).

2.8.2 Haematoxylin

Haematoxylin is one of the principal stains used in diagnostic histology and is a useful nuclear counterstain in immunohistochemistry (IHC). Following the routine IHC protocol below, sections were immersed in haematoxylin solution for 30 seconds. Haematoxylin solution was made up by adding the following to 700mls of distilled water: 0.5g sodium iodate, 50g aluminium potassium sulphate, 5g haematoxylin, 40mls acetic acid and 300mls glycerin. Sections were washed well in tap water and differentiated quickly in 1% acid alcohol before being rinsed again in tap water. Sections were immersed in Scott's tap water substitute (ammonia water) until nuclei turned blue and rinsed in tap water before being dehydrated through a series of alcohols (70%, 95% and 2 x 100%) to xylene and mounted with a coverslip using DPX.

2.9 Immunohistochemistry

All immunohistochemistry (diagnostic slides and TMA slides) was performed to visualise pathological protein aggregations using the protocol below. Samples were immunostained in as few batches as possible to minimise variability in staining. Sections underwent antigen retrieval to reveal epitopes masked as a consequence of formalin fixation and immunostained for a battery of antibodies listed in table 2.3

Antibody	Target	Host	Manufacturer	Working dilution (in TBS)	Antigen retrieval	Single label (SL)/ doubel label (DL) protocol
AT8	hyperphosphorylated tau Ser202/205 (HP-т)	Mouse	Innogenetics, Gent, Belgium	1:4000	Immersion in 0.01m.L-1 citrate buffer (pH6) and microwaving for 10 minutes	SL
4G8	β amyloid 17-24	Mouse	Covance, Alnwick, UK	1:15,000	Immersion in concentrated Formic acid for 1 hour	SL
8/4D	pyroglutamylated β amyloid (pE(3)-Aβ)	Mouse	AFFiRiS, Vienna, Austria	1:1000	Decloaking for 2 minutes in 0.01mol.L-1 EDTA	SL + DL
α-syn	α-synuclein	Mouse	Leica, Newcastle-upon-Tyne, UK	1:200	Decloaking for 2 minutes in 0.01mol.L-1 EDTA	SL
α-syn [pSer129]	α-synuclein phosphorylated at serine 129	Mouse	Abcam, Cambridge, UK	1:500	Decloaking for 2 minutes in 0.01mol.L-1 EDTA	SL
Tau [pSer396]	hyperphosphorylated tau Ser396 (HP-т)	Rabbit	Life technologies, Paisley, UK	1:4000	Decloaking for 2 minutes in 0.01mol.L-1 EDTA	DL

Table 2.3 List of primary antibodies, working dilution and antigen retrieval procedures used in immunohistochemistry. Abbreviations; TBS, Tris buffered saline; SL, single label immunohistochemistry and DL double label immunohistochemistry.

Antigen retrieval was performed by one of three techniques depending on the antibody: 1) Microwave antigen retrieval was performed by immersing slides in 0.01m.L-1 citrate buffer and microwaving on full power (900w, SLS, Hessle, UK) for 10 minutes, following which sections were left to cool for 20 minutes and rinsed in tap water. 2) Decloaking was performed by immersing slides in 0.01mol.L-1 EDTA (pH 8) for one and a half minutes in the Menapath Access Retrieval Unit (Menarini diagnostics, Berkshire, UK) or 3) immersed in concentrated (99%) Formic acid for 1 hour. Sections were quenched for endogenous peroxidase by incubation in 3% hydrogen peroxide and immunohistochemistry was performed using a MENAPATH HRP polymer detection kit (Menarini diagnostics, Berkshire, UK) following instructions supplied by the manufacturer.

Sections were rinsed well with Tris Buffered Saline (TBS) and incubated at room temperature for 1 hour with primary monoclonal antibodies at optimal dilution in TBS. Slides were then washed 3 times with TBS for 5 minutes with the final rinse in TBS with 1% Tween (VWR, Lutterworth, UK). The universal probe was applied and incubated for 30 minutes at room temperature and washes were performed again as previously described. Sections were then incubated with the Horseradish peroxidase (HRP) - polymer reagent at room temperature for 30 minutes before a final 3 rinses in TBS. Following this, sections were reacted with 3,3 diaminobezidine (DAB) with a ratio of 1 drop of DAB chromagen concentrate (32µm) to 1ml DAB substrate for 2-4 minutes. Sections were washed thoroughly in tap water before a counterstain of haematoxylin was applied to identify cell nuclei (section 2.8.2). Sections were then taken through increasing concentrations of alcohol (70%, 95% and 2 x 100%) to xylene and mounted with a coverslip with DPX.

2.10 Immunofluorescence

Fixed sections from frontal cortex were dewaxed and rehydrated through a series of alcohols to water and subjected to antigen retrieval in a pressure cooker immersed in 0.01mol.L-1 EDTA pH 8 for two minutes followed by cooling under running tap water for 10 min. Primary mouse and rabbit antibodies were made up in TBS according to the dilutions in table 2.3, pooled, applied to the sections and incubated overnight in a dark, humid chamber at 4^{o}C. Following 3 rinses in TBS, Alexa Fluor® 488 Goat Anti-Mouse IgG (fluoresces green, Invitrogen, dilution 1:200) was made up in TBS and applied to the sections for 30 minutes in a dark humid chamber. Sections were rinsed again in 3 changes of TBS and Alexa Fluor® 594 Goat Anti-Rabbit IgG (fluoresces red, Invitrogen, dilution 1:200) was applied and incubated for 30 minutes in a dark, humid chamber. Sections were then rinsed 3 times in TBS before being mounted with a coverslip using Vectashield hardset mounting medium containing DAPI (4',6-diamino-2-phenylindole) (Vector laboratories, Peterborough, UK) to visualise all neuronal nuclei. Control tissue sections were included, each with the omission of one of the primary antibodies to ensure antibodies were specific to their targeted antigen. Visualization of dual labelled sections confirmed no cross-reactivity of the antibodies. Immunofluorescence was visualized using Nikon 90i microscope and DsFi1 camera (Nikon).

2.11 Image Analysis

2.11.1 Image acquisition - Diagnostic slides

Diagnostic slides used for experiments in Chapter 3 were stained as described in section 2.9. Image analysis was performed using AT8, 4G8 and α-syn stained slides from frontal (Brodmann areas (BA) 9,10 and 46), temporal (BA 20, 21, 22, 41 and 42), parietal (BA 40), occipital (BA 17, 18 and 19) and cingulate (BA 24) cortices, posterior hippocampus, striatum (i.e., caudate nucleus, putamen; at the level of the amygdala), amygdala, SN (at the level of oculomotor nerve) and LC. Of note, great care was taken to minimise any variation among cases regarding the specific topographical localisation on which analyses were performed.

Multiple adjacent single images (SI) were captured at x200 magnification using a Nikon Eclipse 90i microscope and DsFi1 camera (Nikon, Surrey UK) with a fully motorised stage coupled to a PC and combined to one large image (LI) by NIS elements software v 3.0 (Nikon). If necessary, LI were subjected to manual setting of regions of interest (ROI; see below).

The size of measured areas was dependant on the assessed brain region; in each cortical region six LI were assessed and each LI encompassed a cortical strip which included all cortical layers and consisted of 8 adjacent SI forming a rectangle of 0.34mm x 3mm (of note, one SI measures 0.34mm x 0.43mm but in the final LI individual SI overlap by 0.03mm). If necessary, ROI were set to exclude white matter and meningeal structures (Figure 2.4a). It has been previously shown that densities of pathological protein aggregates (e.g., Aβ) differ between gyri and sulci (Gentleman et al., 1992, McParland, 2013) and therefore three gyri and three sulci were assessed per cortical region. Taking into consideration variation of pathology across the section, six measurements per slide (five for the cingulate) were felt to be sufficient to produce a reliable mean value for the slide, as analysis of the whole slide would be too time consuming. In addition, the majority of sections contained at least three gyri and three sulci therefore quantitative values were comparable between slides. In the hippocampus, 1 x 2 SI resulting in a rectangle of 0.34mm x 0.8mm were taken from hippocampal subfields CA2, CA3 and CA4 and 1 x 4 SI resulting in a

rectangle of 0.34mm x 1.54mm was taken in CA1. If necessary, ROI were set to encompass the pyramidal cell layer only in CA1-3 while the entire LI of CA4 was used for analysis (Figure 2.4b). Hippocampal subfields CA1-4 were chosen as they are implicated in Braak's staging of neurofibrillary pathology (Braak et al., 2006). In each the caudate nucleus, putamen and amygdala, three LI (0.88mm x 1.17mm), which were composed of 3 x 3 SI, were analysed entirely (Figure 2.4c). Three LI have been used previously to accurately quantify pathological lesions in the caudate and putamen (Colloby et al., 2012). Four SI (0.34mm x 0.43mm) were taken from the SN and were analysed without further setting of an ROI (Figure 2.4d). One SI covering the entire LC was used for analysis after setting an appropriate ROI to ensure that immunopositivity was measured in the LC only (Figure 2.4e).

The measurement of immunopositivity and subsequent calculation of the percentage area covered by immunopositivity was performed using an automated methodology. Red, Green and Blue (RGB) thresholds that determine the pixels that are included in the binary layer used for measurement were standardised separately for each AT8, 4G8 and α-syn immunopositivity and thresholds were set at a level that was reached by immunopositive pathological structures only (except *APP*); see below). RGB intensity values are measured on a scale between 0 and 255 (see NIS elements version 3.0, user guide, 2008, Nikon, Surrey UK) and were set as follows; AT8: R25-170, G27-156, B11-126; 4G8: R50-180, G20-168, B8-139, α-syn: R15-161, G7-139, B4-133. Thereby, unspecific background staining did not reach the threshold and was not included into the measurement. In addition to RGB thresholds, we set a restriction threshold for the assessment of 4G8 immunopositivity that excluded the measurement of immunopositive signals of a size below 100μm^2; this was necessary to ensure that physiological, cellular *APP* that is stained with 4G8 antibody was not included in the measurement. Of note, the exclusion of areas below 100μm^2 implies that pathological Aβ depositions of less than 100μm^2 were not included into the measurement. However, diffuse Aβ depositions and Aβ plaques are typically larger than 100μm^2 (Duyckaerts et al., 2009). On the limited occasions that the defined threshold for pathology was not appropriate due to section being out of focus, i.e. if a section lay unevenly on slide, the image was re-taken with the focus adjusted manually the threshold was

adjusted accordingly to ensure all pathological lesions were included in the binary layer and included in the final measurement.

Raw data was exported into Excel and the amount of immunopositivity (load) was stated as the percentage of the total measured area that was covered by immunopositive signals. The respective values are expressed as HP-$_T$ load (AT8), Aβ (4G8) and α-syn load.
Mean frontal, temporal, parietal, occipital and cingulate loads (i.e. mean value of 6 LI loads) were calculated. Loads of individual hippocampal subfields and caudate nucleus and putamen were used to calculate a mean hippocampal and a mean striatal load, respectively. No mean subfield values were calculated for the amygdala, SN and LC.

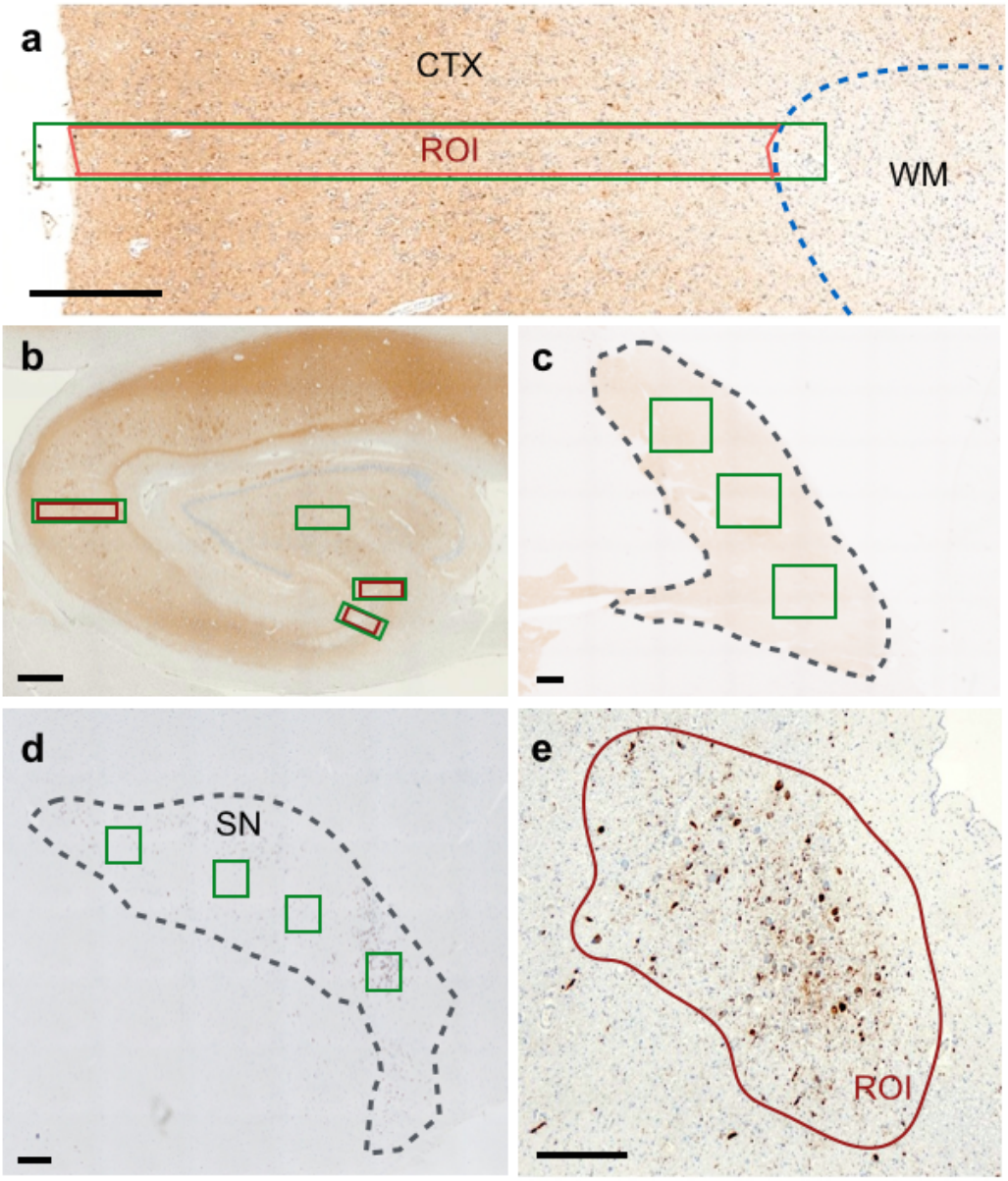

Figure 2.4 Examples of regions of interest (ROI) delineating the area used for quantification of protein aggregates in diagnostic slides. For assessment of cortical regions (a) 8 individual images were taken at X200 magnification forming 1 large image (area covered: 0.34mm x 3mm, green rectangle) that encompassed a cortical strip including all layers of the cortex (CTX). A ROI (red rectangle) was manually applied to exclude white matter (WM - delineated by blue dotted line) and meningeal structures (a). For assessment of the hippocampus (b) 2 individual images resulting in 1 rectangular image (green rectangle, area covered: 0.34mm x 0.8mm) were taken at X200 magnification in hippocampal subfields (CA2, CA3 and CA4) and 4 individual images resulting in a rectangle of 0.34mm x 1.54mm (green rectangle) were taken in CA1. ROI (red rectangles) were set to encompass the pyramidal cell layer only in CA1-3 whilst the entire image in CA4 was assessed. For quantification in the caudate ((c) delineated by grey dotted line), 3 areas were selected for assessment, with each area comprising of 9 individual images at X200 magnification forming 1 large image (area covered: 0.88mm x 1.17mm). For quantification of the substantia nigra of the midbrain ((d) delineated by grey dotted line), four single images (area covered in one single image: 0.34mm x 0.43mm) were taken at X200 magnification, and a mean of all four values was calculated for the final measurement. For the assessment of the locus coeruleus a ROI (red line) was placed manually to ensure quantification was limited to the locus coeruleus only (e). Scale bars represent 500µm in a-d and 100µm in e.

2.11.2 Image acquisition - TMA

TMA slides used in Chapters 4 and 5 were produced as outlined in section 2.6 and stained following the standardised protocol described in section 2.9 Immunohistochemically stained sections were analysed using an automated system consisting of a Nikon Eclipse 90i microscope, DsFi1 camera and NIS Elements software v 3.0 (Nikon). Sections were placed onto the microscope in the correct orientation to position tissue core 1 in the top left field of view. To capture images of each of the 40 tissue cores on the TMA slide, the microscope was positioned in the centre of the first tissue core at x20 magnification for guidance and brought into focus at x100 magnification. The co-ordinates of this first tissue core was then mapped using a macro designed to take LIs comprised of 3 x 3 SIs measuring 1.7mm^2. The microscope was then positioned over the centre of the second tissue core and the process repeated until the positions of all 40 tissue cores had been mapped. If any of the tissue cores are were missing or too damaged to be included in the analysis the tissue core number was noted and this was factored into the analysis (see below). Once all 40 tissue cores were mapped, the microscope was directed to the co-ordinates of the first tissue core and the images of all tissue cores were automatically taken in sequence. ROIs were applied to individual images if necessary to exclude any white matter or abnormalities in the tissue (e.g. folded tissue or tears). Raw data was exported into Excel and the measurement of immunopositivity (load) and subsequent calculation of the percentage area covered by immunopositivity was performed by multiplying the binary area fraction covering by immunopositivity by 100. For brain regions that had more than one tissue core, mean values were calculated.

2.12 Cortical thickness

Cortical thickness measurements were performed on frontal, temporal, parietal, occipital and cingulate cortex. Measurements were taken at the same sites used for quantification of pathological lesions as described in section 2.11.1 Three gyri and three sulci were selected in each of the cortical regions and four areas assessed from the cingulate (two gyri, BA 24 and BA32 and either side of the sulcus in between) (Figure 2.5) Images were captured using Nikon Eclipse 90i microscope and DsFi1 camera (Nikon) at x20 magnification. Five measurement lines were orientated perpendicular to the pial surface at equally

spaced intervals of each gyrus encompassing all cortical layers ending at the white matter as described by Kolasinski et al (Kolasinski et al., 2012). Measurements were taken from each side of each sulcus (total of 5 per sulcus). This was performed to avoid artefact that may result from sections being cut obliquely with the cortex appearing thicker than actual size, as described previously (Foster et al., 2014). Cortical thickness was determined by the mean of all lines in each region analysed.

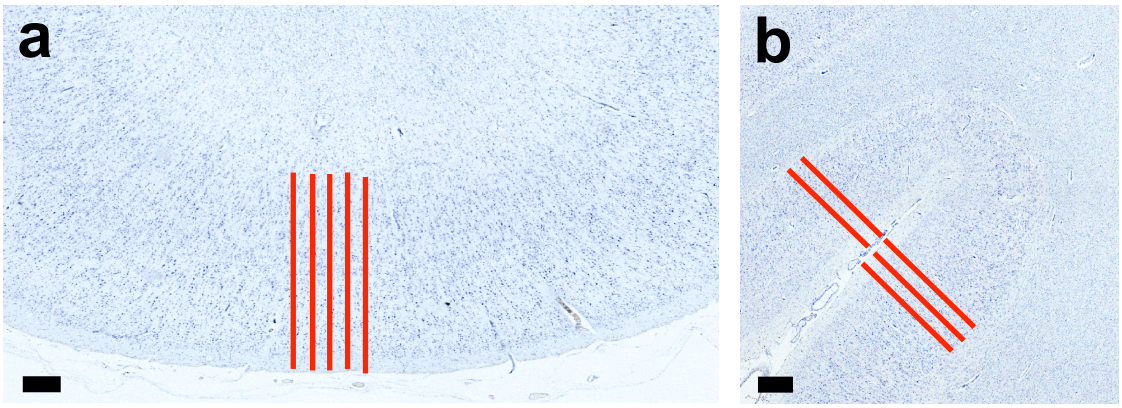

Figure 2.5 Cortical thickness was measured in frontal, temporal, parietal, occipital and cingulate cortex. Up to six points were measured per region with a mean of all points taken as the final cortical thickness value. Five measurement lines were placed at equally spaced intervals perpendicular to the pial surface ending at the white matter in each gyrus (a). Five measurements were taken in total from each sulcus (b). Both scale bars represent 500µm.

2.13 *APOE* genotyping

APOE genotyping was determined for cases fulfilling neuropathological criteria for mixed AD/LBD. Genomic DNA (deoxyribonucleic acid) was extracted from frozen tissue taken from the left lateral cerebellum using the QIAamp DNA Mini-kit and QIAGEN EZ1 advanced XL automated system (Qiagen, Manchester, UK) according to manufacturer's instructions. Genotyping of *APOE* polymorphisms (rs429358 and rs7412) was determined by Real-Time PCR (Calero et al., 2009) using the 7900HT fast Real-Time PCR system (Applied Biosystems, Paisley, UK) as previously described (Calero et al., 2009).

2.13.1 Acquisition of frozen tissue

Frozen tissue from 19 neuropathologically mixed AD/LBD cases was acquired from the NBTR. DNA was extracted using the QIAamp DNA Mini-kit and QIAGEN EZ1 advanced XL automated system (both Qiagen, Manchester, UK) according to manufacturer's instructions.

2.13.2 DNA extraction

Briefly, 50µg of frozen tissue from the left lateral cerebellum of each case was added to 1ml of TE (Tris/EDTA) tissue lysis buffer, 1% sodium dodecyl sulfate (SDS) and 50µl proteinase K solution (the latter provided with the QIAamp DNA Mini-kit) and incubated at 60^{o}C overnight to facilitate cell lysis. TE Lysis buffer was made up by combining 10ml of 1M TrisCl pH 7.5 stock solution (12.7g TrisCl, 2.63g Tris base, 100ml mq water) and 2ml 500mM EDTA pH 8.0, in 1L mq water. Homogenisation was completed by repeated vortexing. 200µl of cell lysate was loaded into each column and DNA was isolated using the QIAGEN EZ1 advanced XL automated system producing 100µl of isolated DNA eluted into AE buffer supplied by the manufacturer of the kit. DNA purity and concentration was measured using a Nanodrop.

2.13.3 Quantitative real-time Polymerase Chain Reaction (RT-PCR)

PCR is a universal technique used in molecular biology to amplify DNA sequences. The sequences of the primers use in RT-PCR are provided in table 2.4 and amplification process is outlined in figure 2.6. *Power* SYBR® Green PCR Master Mix (Applied Biosystems, Paisley, UK) containing AmpliTaq DNA Polymerase was used to amplify DNA. DNA samples were diluted to 20ng/µl and 25µl of each sample was loaded in a 96 well plate (Eppendorf, Stevenage, UK). Each PCR reaction mixture was prepared using the Eppendorf epMotion® and contained 1 x *Power* SYBR® Green PCR Master Mix, 0.3µM of each primer and 20ng of genomic DNA (prepared on ice). All reactions were added to a 384 well plate (Applied Biosystems, Paisley, UK) in duplicate.

The PCR amplification protocol was performed using a 7900HT Real-Time PCR system and consisted of: -

Initial denaturation step - AmpliTaq Gold® DNA Polymerase activation 95^{o}C for 10 minutes

40 cycles consisting of

Denaturation - 95^{o}C for 15 seconds

Annealing and elongation - 62^{o}C for 1 minute

As SYBR® Green binds to double-stranded DNA and fluoresces it allows the quantification of the double stranded DNA at the end of each elongation step, giving an amount of the double stranded DNA preset. The “cycle threshold”, or Ct value (i.e. number of PCR cycles necessary to achieve a threshold level of fluorescence) was used as the informative Real Time PCR read-out to distinguish between *APOE* haplotypes as indicated in Figure 2.8

Primer	Orientation	Nucleotide Sequence 5'- 3'	Length (bp)
ApoE_112C	Forward	CGGACATGGAGGACGTGT	18
ApoE_112R	Forward	CGGACATGGAGGACGTGC	18
ApoE_158C	Reverse	CTGGTACACTGCCAGGCA	18
ApoE_158R	Reverse	CTGGTACACTGCCAGGCG	18

Table 2.4 Primer sequences used in *APOE* genotyping

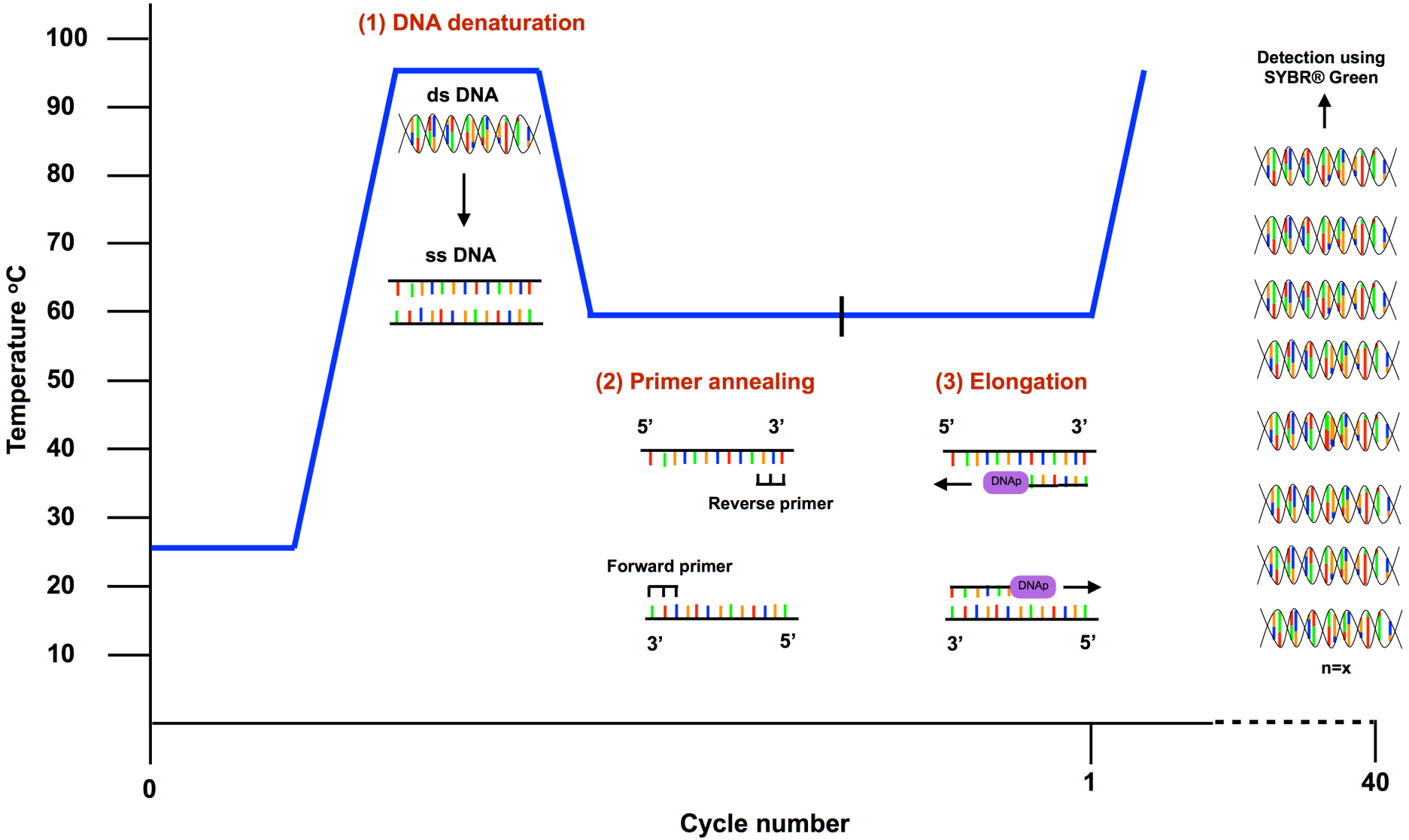

Figure 2.6 Illustration outlining the steps involved in polymerase chain reaction (PCR). After the initial activation step where AmpliTaq Gold® DNA Polymerase is activated, double stranded deoxyribonucleic acid (ds DNA) is heated to 95°C for 15 seconds to produce single stranded (ss) DNA **(1)**. Following this the temperature is dropped to 62°C forward and reverse primers anneal to their complementary sequences **(2)**. DNA polymerase (DNAp) then binds to the annealed primers and extends the DNA at the 3' end of the chain **(3)**. Annealing and elongation takes 1 minute. Following the completion of the first cycle, this process is repeated for a total of 40 cycles where sufficient quantity of the target sequence has been produced for detection using the fluorescent tag SYBR® Green which binds to ds DNA.

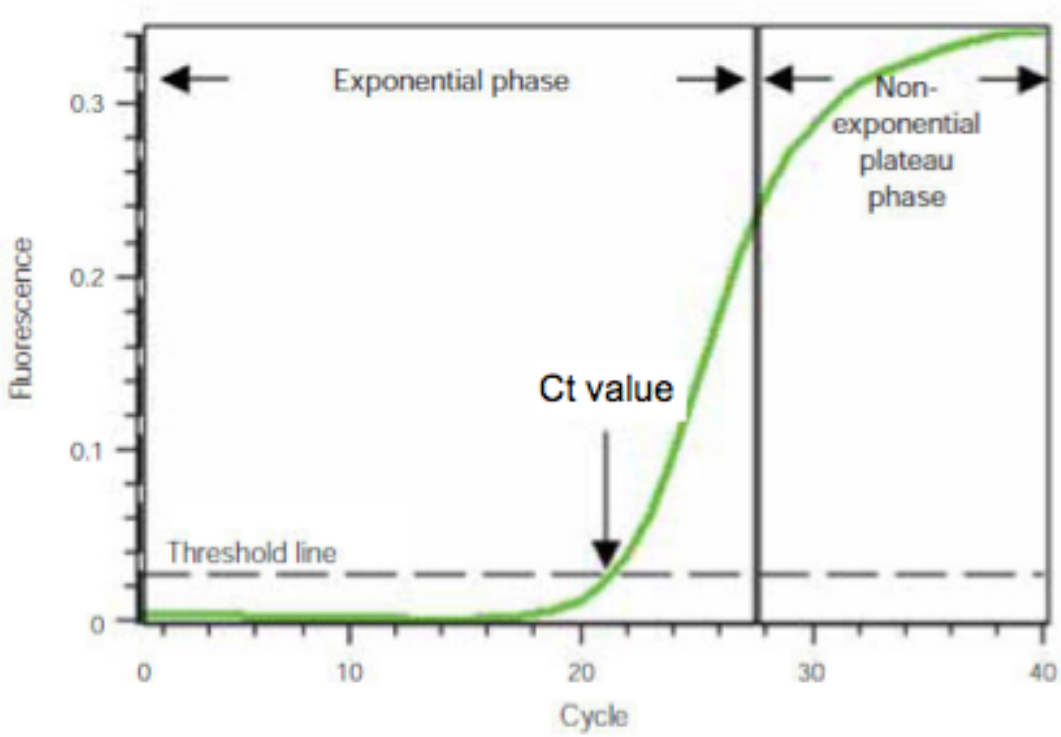

Figure 2.7. Amplification plot. Baseline-subtracted fluorescence versus number of PCR cycles (from http://www.bio-rad.com/en-uk/applications-technologies/qpcr-real-time-pcr)

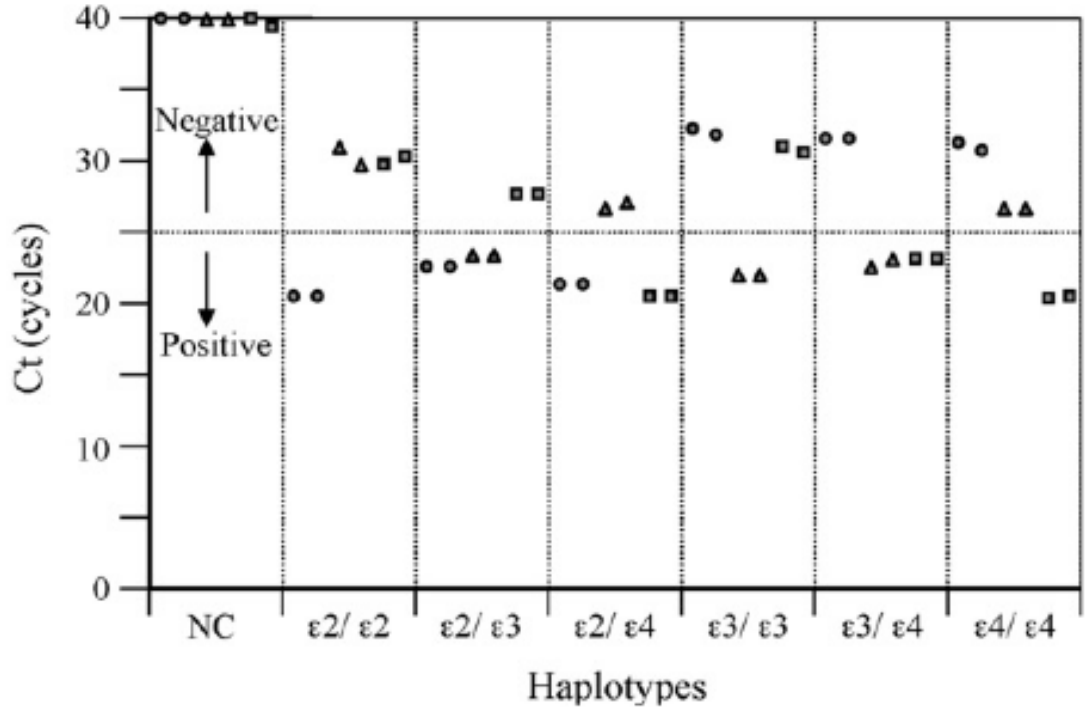

Figure 2.8. Amplification plots (haplotypes vs. Ct) in a 7900HT Real-Time PCR system of the six different *APOE* haplotypes in the human population and negative controls (NC) (E2: circles, E3: triangles and E4: squares) from (Calero et al., 2009).

2.14 Statistical analyses

Statistical analysis was conducted using the Statistical Package for Social Sciences (SPSS v 22, IBM). Data was tested for normality using Kolmogorov-Smirnov Test test followed by visual inspection of variable histograms. Kruskal Wallis and Friedman's tests were employed to determine overall group differences. A paired t test (Mann-Whitney U) was used to determine whether the difference in pathology burden was significant between the two clinical groups and Wilcoxon test was used to assess differences between related samples. Allele frequencies were calculated using the allele counting method. Hardy-Weinberg equilibrium was tested by a χ^2 goodness of fit test, using the following equation: -

$$p^2 + 2pq + q^2 = 1$$

where p is the frequency of the "A - dominant allele" and q is the frequency of the "a - recessive allele" in the population (Norton and Neel, 1965). Fisher's exact test was employed to assess differences in *APOE* allele frequencies between phenotypes. Spearman's rank correlation co-efficient was used to determine associations between variables. Linear regression was employed to determine whether particular pathogenic proteins influenced each other and clinical phenotype. A p-value of <0.05 was considered significant.

Chapter 3 - Neuropathologically mixed Alzheimer's disease and Lewy body disease: burden of pathological protein aggregates differs between clinical phenotypes.

3.1 Introduction

In neurodegenerative diseases, the neuropathological diagnosis is based on the most prevalent pathology found in the *post-mortem* brain, as this pathology is usually considered to be the main underlying pathology causing a clinical syndrome, most frequently dementia. Several internationally recognised staging systems assess the topographical distribution of associated pathological protein aggregates. In AD, Braak NFT staging (I–VI) (Braak and Braak, 1991, Braak et al., 2006) and Thal amyloid phases (1–5) (Thal et al., 2002b) are used to assess the topographical distribution of NFTs/NTs and β-amyloid deposits respectively, whilst Consortium to Establish a Registry for Alzheimer's Disease (CERAD) criteria are used to score neuritic plaques (neg, A, B or C) (Mirra et al., 1991). In DLB, the most common staging systems employed to assess α-syn pathology (i.e. LB and LN) are Braak LB staging (I–VI) (Braak et al., 2003) and Newcastle-McKeith criteria which distinguish between brainstem predominant, limbic (transitional) and neocortical LBD, respectively (McKeith et al., 2005). However, multiple pathological protein aggregates are frequently seen in human *post-mortem* brains and hence mixed pathology is common (Armstrong et al., 2005, Jellinger, 2007a, Jellinger, 2007b, Schneider et al., 2007, Kovacs et al., 2008, Rahimi and Kovacs, 2014). Mixed dementia on the other hand is less frequent and neuropathologically should only be diagnosed if criteria for more than one full blown disease are met. In such mixed dementia cases, the severity of each characteristic neuropathological lesion may have independently been the cause for clinical dementia.

There are a subset of cases that are neuropathologically classified as mixed AD/DLB because they fulfil neuropathological criteria for both AD (i.e. high AD neuropathologic change (Montine et al., 2012b)) and DLB (i.e. neocortical LBD (McKeith et al., 1996, McKeith et al., 2005)). Clinically, a proportion of these cases were diagnosed as AD, whereas others were diagnosed as DLB or PDD. Current semi-quantitative neuropathological assessment encompasses a 4-5 tiered scale (absent, mild, moderate, severe (very severe)) and when applied to

mixed AD/DLB cases fails to differentiate between different clinical phenotypes (AD vs DLB vs PDD). Therefore, it was investigated whether respective differences could be detected using a quantitative methodology.

3.2 Aims

The aims of this study were to : -

- Determine whether quantification of pathological protein aggregations associated with AD and DLB (HP-*T*, Aβ and α-syn) could be detected in cases that fulfil neuropathological criteria for AD and DLB/PDD but differ in their clinical presentations (AD vs DLB vs PDD).
- Investigate if the hierarchical distribution HP-τ, β-amyloid and α-syn loads in cortical and limbic regions in neuropathologically mixed AD/DLB cases that presented clinically with AD (cAD), DLB (cDLB) or PDD (cPDD) was similar to 'pure' forms of AD (pAD) or DLB (pDLB).
- Investigate whether there are any differences in basic clinical characteristics between different clinical phenotypes i.e. age of onset of cognitive decline, final MMSE scores and rates of cognitive decline in cAD, cDLB and cPDD and age of onset of motor symptoms in cDLB and CPDD.
- Investigate if there are differences in cortical thickness between cAD, cDLB and cPDD.
- Determine the *APOE* genotypes and allele frequencies for all mixed AD/DLB cases and investigate if there are differences between different clinical phenotypes.

3.3 Methods

3.3.1 Study cohort

Brain tissue from 28 donors were included in this study (mean age, 76.11; male 17; female, 11) from the Newcastle Brain Tissue Resource (NBTR). 19 cases were identified as fulfilling neuropathological criteria for mixed AD/DLB and of these cases 8 (42.1 %) were clinically diagnosed as AD (cAD), 8 (42.1 %) as DLB (cDLB) and 3 (15.8 %) as PDD (cPDD). In addition, 5 'pure' AD cases (pAD) and 4 'pure' DLB (pDLB) cases were selected for comparison. Cases were classified 'pure' AD or DLB if they had minimal concomitant pathology (i.e. pAD cases had no α-syn pathology and DLB cases had no/low AD neuropathologic change (Montine et al., 2012a). Patient demographic information (neuropathological criteria) is provided in Table 3.1. cAD and pAD cases did not exhibit core (i.e. spontaneous cognitive fluctuations, spontaneous motor Parkinsonism, complex, persistent visual hallucinations) nor suggestive (i.e. REM sleep behaviour disorder, neuroleptic sensitivity, positive dopaminergic imaging) features of LBD, respectively.

Case	Age	Sex	PM delay (hours)	Fix length (weeks)	Clinical Diagnosis	Thal Phase	Braak stage	CERAD	Cerebral amyloid angiopathy (CAA) score	Cerebral amyloid angiopathy (CAA) type	Alzheimer's disease neuropathologic change (NIA-AA)	Braak LB stage	McKeith criteria	APOE genotype
1	79	F	46	12	AD	5	6	Frequent	1	1	High	6	Neocortical	E3/E4
2	82	M	12	4	AD	5	6	Frequent	2	1	High	6	Neocortical	E4/E4
3	63	F	38	16	AD	5	5	Frequent	2	2	High	6	Neocortical	E3/E3
4	77	M	78	8	AD	4	6	Frequent	4	2	High	6	Neocortical	E3/E3
5	88	F	84	7	AD	5	6	Frequent	4	1	High	6	Neocortical	E3/E4
6	62	M	28	7	AD	5	6	Frequent	3	2	High	6	Neocortical	E3/E3
7	73	M	7	12	AD	5	6	Frequent	3	2	High	6	Neocortical	E4/E4
8	77	F	51	12	AD	5	6	Frequent	1	1	High	6	Neocortical	E3/E4
Clinical AD mean (±SE)	75.13 (3.13)	m:f = 4:4	43 (9.9)	9.75 (1.37)										
9	80	F	51	14	DLB	5	6	Frequent	0	0	High	6	Neocortical	E3/E4
10	68	M	48	124	DLB	5	6	Frequent	1	2	High	5	Neocortical	E3/E4
11	75	F	78	8	DLB	5	6	Frequent	0	0	High	6	Neocortical	E3/E3
12	80	F	17	7	DLB	5	5	Frequent	1	2	High	6	Neocortical	E3/E4
13	83	M	48	7	DLB	5	6	Frequent	2	1	High	6	Neocortical	NA
14	78	M	17	9	DLB	5	6	Frequent	2	2	High	6	Neocortical	E4/E4
15	78	M	18	8	DLB	5	6	Frequent	2	1	High	6	Neocortical	E3/E4
16	67	M	46	4	DLB	5	6	Frequent	2	2	High	6	Neocortical	E3/E4
Clinical DLB mean (±SE)	76.13 (2.05)	m:f = 5:3	40.38 (7.64)	22.63 (14.52)										
17	68	M	11	2	PDD	5	6	Frequent	4	1	High	6	Neocortical	E3/E3
18	75	M	28	17	PDD	5	5	Frequent	1	2	High	6	Neocortical	E3/E4
19	77	M	6	8	PDD	5	6	Frequent	2	2	High	6	Neocortical	E3/E4
Clinical PDD mean (±SE)	73.33 (2.73)	m:f = 3:0	15 (6.66)	9 (4.36)										
21	77	F	63	5	AD	5	6	Frequent	3	1	High	0	Negative	NA
22	83	M	12	16	AD	4	6	Frequent	2	1	High	0	Negative	NA
23	86	F	69	69	AD	5	6	Frequent	1	2	High	0	Negative	NA
24	84	F	47	16	AD	5	6	Frequent	2	2	High	0	Negative	NA
25	81	F	50	9	AD	5	6	Frequent	2	2	High	0	Negative	NA
Pure AD mean (±SE)	82.2 (1.53)	m:f = 1:4	48.2 (9.92)	23 (11.69)										
26	77	M	8	4	DLB	0	2	Negative	2	2	No	6	Neocortical	NA
27	72	M	89	13	DLB	0	3	Negative	0	0	No	6	Neocortical	NA
28	64	M	8	9	DLB	1	2	Sparse	1	2	Low	6	Neocortical	NA
29	77	M	46	12	DLB	0	3	Negative	0	0	No	6	Neocortical	NA
Pure DLB mean (±SE)	72.5 (3.07)		37.75 (19.29)	9.5 (2.02)										
Total mean (±SE)	76.11 (1.29)	m:f = 17:11	39.43 (4.85)	15.68 (4.60)										

Table 3.1 Patient demographics. Abbreviations: CAA, cerebral amyloid angiopathy; NIA-AA, NIA-AA, National Institute on Aging - Alzheimer's Association; LB, Lewy body; AD, Alzheimer's disease; DLB, dementia with Lewy bodies; cAD, neuropathologically mixed AD/DLB presenting clinically with Alzheimer's disease; SE, standard error; m, male; f, female; cDLB, neuropathologically mixed AD/DLB presenting clinically with dementia with Lewy bodies; cPDD, neuropathologically mixed AD/DLB presenting clinically with Parkinson's disease dementia. N/A; not available.

3.3.2 Tissue preparation

Paraffin-embedded blocks containing frontal, temporal, parietal and occipital cortices, cingulate and hippocampus, striatum (including caudate nucleus and putamen), amygdala, midbrain and LC were sectioned at 6μm and mounted onto 4 % 3-aminopropyltriethoxysilane (APES)-coated glass slides. Sections were immunostained for monoclonal antibodies against HP-τ (AT8, dilution 1:4000, Innogenetics, Ghent, Belgium) Aβ (4G8, dilution 1:15,000, 4G8, Signet Labs, Dedham, MA, USA) and α-syn (α-syn, dilution 1:200, Leica, Newcastle-upon-Tyne, UK) as described in section 2.9.

3.3.3 Semi-quantitative assessment

Blind to clinical diagnoses, neuropathological diagnoses were based on semi-quantitative assessment (Alafuzoff et al., 2008, Alafuzoff et al., 2009a, Whitfield et al., 2014) and assigned using accepted international neuropathological criteria including neuritic Braak stages (Braak et al., 2006), Thal amyloid phases (Thal et al., 2002b), CERAD scores (Mirra et al., 1991), NIA-AA scores (Montine et al., 2012b) and McKeith criteria (McKeith et al., 2005). Cerebral amyloid angiopathy (CAA) was scored according to the method described by Olichney and colleagues (Olichney et al., 1995).

3.3.4 Quantitative assessment

Image analysis was performed using AT8 (HP-τ), 4G8 (Aβ) and α-syn stained slides from frontal (Brodmann areas (BA) 9,10 and 46), temporal (BA 20, 21, 22, 41 and 42), parietal (BA 40), occipital (BA 17, 18 and 19) and cingulate (BA 24) cortices, posterior hippocampus, striatum (i.e. caudate nucleus, putamen; at the level of the amygdala), amygdala, SN (at the level of oculomotor nerve) and LC. Of note, great care was taken to minimise any variation among cases regarding the specific topographical localisation on which analyses were performed. The mean load (expressed as a percentage area covered by immunopositivity) of each protein aggregate was obtained according to section 2.11.1.

3.3.5 Cortical thickness measurements

In addition, 6μm section were taken from frontal, temporal, parietal, occipital and cingulate cortices and stained with CFV as described in section 2.8.1. Cortical thickness measurements were taken according to the protocol outlined in section 2.12.

3.3.6 APOE genotyping

Except for one cDLB case which had no frozen tissue available, all mixed AD/ DLB cases underwent *APOE* genotyping using Real-time PCR according to the protocol in section 2.13.

3.3.7 Statistical analysis

The Statistical Package for Social Sciences software (SPSS ver. 21) was used for statistical evaluation. Since the data were not normally distributed (Kolmogorov–Smirnov $p < 0.01$), we used Kruskal–Wallis to determine overall group differences and a non-parametric paired *t* test (Mann–Whitney *U*) to assess individual differences in pathological burden between clinical phenotypes. Friedman's test with post hoc Wilcoxon signed-rank test was employed to assess differences in pathological burden between individual cortices within each clinical phenotype. Allele frequencies were calculated using the allele counting method. Hardy–Weinberg equilibrium was tested by a χ^2 goodness-of-fit test, and Fisher's exact test was employed to assess differences in *APOE* allele frequencies between phenotypes.

3.4 Results

3.4.1 Cerebral amyloid angiopathy

Of the mixed AD/DLB cases, CAA with capCAA was present in 9 cases whilst 15 cases showed CAA without capillary involvement. There were no differences in the type of CAA between cAD, cDLB and cPDD although there was an increased severity of CAA in cAD group with 50 % of cases having a score of 3 or 4 whilst none of the cDLB cases had a score higher than 2 (Table 3.1).

3.4.2 Semi-quantitative analysis

Using routine semi-quantitative scoring criteria, no significant differences in the severity of HP-τ, Aβ and α-syn were seen between cAD, cDLB and cPDD since —not surprisingly—scores were “severe” in most areas except for the three cPDD cases which showed considerably lower HP-τ in cingulate and frontal cortices (Table 3.2).

		Frontal			Temporal			Parietal			Occipital			Cingulate			Hippocampus			Striatum			Substantia nigra			Locus coeruleus		
Case Number	Clinical phenotype	HP-$_T$	Aβ	α-syn	HP-$_T$	Aβ	α-syn	HP-$_T$	Aβ	α-syn	HP-$_T$	Aβ	α-syn	HP-$_T$	Aβ	α-syn	HP-$_T$	Aβ	α-syn	HP-$_T$	Aβ	α-syn	HP-$_T$	Aβ	α-syn	HP-$_T$	Aβ	α-syn
1	AD	3	3	2	3	NA	NA	3	3	2	3	NA	0	3	3	3	3	2	3	1	3	2	2	1	0	2	0	1
2	AD	3	3	1	3	3	2	3	3	1	3	NA	1	3	3	2	3	2	2	1	3	0	2	1	1	2	1	1
3	AD	3	3	NA	3	3	2	NA	NA	NA	3	3	NA	3	3	3	3	2	3	NA	NA	NA	2	0	NA	2	0	2
4	AD	3	3	3	3	3	3	3	3	3	2	1	1	3	3	3	3	3	3	3	3	3	3	1	1	2	0	2
5	AD	2	3	1	3	3	1	3	3	1	3	3	1	3	3	2	3	2	2	2	1	2	2	2	1	3	1	3
6	AD	3	3	1	3	3	1	3	3	0	3	3	0	3	3	3	3	3	3	2	3	1	2	2	0	2	2	3
7	AD	3	3	1	3	3	3	3	3	3	3	3	1	3	3	3	3	3	3	2	3	NA	2	1	1	3	1	3
8	AD	3	3	1	3	3	1	3	3	1	3	3	1	3	3	3	3	2	3	3	2	NA	2	2	1	3	NA	2
mean (±SE)		2.88 (0.13)[a]	3 (0)	1.43 (0.3)	3 (0)	3 (0)	1.83 (0.4)	3 (0)	3 (0)	1.57 (0.43)	2.86 (1.42)	2.67 (0.33)	0.71 (0.18)	3 (0)[b]	3 (0)	2.75 (0.16)	3 (0)	2.38 (0.18)	2.71 (0.18)	1.8 (0.37)	2.6 (0.4)	1.6 (0.5)	2.13 (0.13)	1.25 (0.25)	2.63 (0.18)	2.38 (0.18)	0.71 (0.29)	2.13 (0.3)
median		3	3	1	3	3	1.5	3	3	1	3	3	1	3	3	3	3	2	3	2	3	2	2	1	3	2	1	2
interquartile range		3-3	3-3	1-2	3-3	3-3	1-3	3-3	3-3	1-3	3-3	2.5-3	0-1	3-3	3-3	2.25-3	3-3	2-3	2-3	1-2.5	2-3	0.5-2.5	2-2	1-2	2-3	2-3	0-1	1.25-3
9	DLB	3	3	2	3	3	3	3	3	NA	3	3	0	2	3	3	3	3	3	2	2	2	1	1	NA	1	1	3
10	DLB	3	3	1	3	3	3	3	3	0	3	3	0	3	3	0	3	2	1	1	3	1	2	1	2	2	0	1
11	DLB	3	3	2	NA	NA	NA	3	2	NA	3	2	NA	NA	NA	NA	3	NA	2	3	3	0	NA	NA	NA	NA	NA	NA
12	DLB	3	3	2	3	3	3	3	3	2	3	NA	1	3	3	3	3	2	3	1	3	2	2	2	3	3	1	2
13	DLB	3	3	1	3	2	3	3	2	2	NA	NA	NA	3	3	3	3	1	3	1	2	3	1	0	2	0	0	0
14	DLB	3	3	2	3	3	1	3	2	1	3	3	1	3	2	3	3	3	3	NA	NA	3	2	2	3	2	0	3
15	DLB	3	3	0	3	3	1	3	3	0	3	3	2	3	3	1	3	2	1	1	3	1	2	2	3	2	0	3
16	DLB	3	3	3	3	3	2	3	3	3	3	2	2	3	2	3	3	3	3	2	2	2	2	2	2	2	2	2
mean (±SE)		3 (0)	3 (0)	1.57 (0.37)	3 (0)	2.86 (0.14)	2.17 (0.4)	3 (0)	2.71 (0.18)	1.33 (0.49)	3 (0)	2.67 (0.33)	1 (0.37)	2.86 (0.14)[c]	2.17 (0.18)	2.29 (0.47)	3 (0)	2.2 (0.37)	2.2 (0.5)	1.33 (0.33)	2.75 (0.25)	1.8 (0.37)	1.71 (0.18)	2.13 (0.45)	2.5 (0.22)	1.71 (0.4)	0.5 (0.34)	2 (0.43)
median		3	3	2	3	3	2.5	3	3	1.5	3	3	1	3	3	1	3	2	3	1	3	2	2	2.46	2.5	2	0	2
interquartile range		3-3	3-3	1-2	3-3	3-3	1-3	3-3	2-3	0-2.25	3-3	2-3	0-2	3-3	2-3	1-3	3-3	1.5-3	1-3	1-1	2.25-3	1-2.25	1-2	0.75-3	2-3	1-2	0-1.25	1-3
17	PDD	1	3	2	3	3	3	3	3	3	2	NA	1	1	3	3	3	2	3	0	2	3	1	1	3	1	1	3
18	PDD	1	3	2	3	3	2	2	3	1	3	3	1	2	3	3	3	2	3	1	2	2	2	1	1	3	1	1
19	PDD	2	3	2	3	3	3	3	3	2	3	3	3	1	3	2	3	3	3	NA	NA	NA	3	2	3	3	1	3
mean (±SE)		1.5 (0.5)[a]	3 (0)	2 (0)	3 (0)	3 (0)	2.67 (0.33)	2.67 (0.33)	3 (0)	2 (0.58)	2.67 (0.33)	3 (0)	1.67 (0.67)	1.33 (0.33)[bc]	3 (0)	2.67 (0.33)	3 (0)	2.33 (0.33)	3 (0)	0.5 (0.5)	2 (0)	2.5 (0.5)	2 (0.58)	1.33 (0.33)	2.33 (0.67)	2.33 (0.67)	1 (0)	2 (1)
median		1.5	3	2	3	3	3	3	3	2	3	3	1	1	3	2	3	2	3	0.5	2	2.5	2	1	3	3	1	2
interquartile range		1-1.5	3-3	2-2	3-3	3-3	2-3	2-3	3-3	1-2	2-3	3-3	1-1	1-1	3-3	2-3	3-3	2-2	3-3	0-0.5	2-2	2-2.5	1-2	1-1	1-3	1-3	1-1	1-2

Table 3.2 Semi-quantitative (SQ) assessment of hyperphosphorylated tau (HP-τ), β-amyloid (Aβ) and α-synuclein (α-syn) in clinical Alzheimer's disease (cAD) clinical dementia with Lewy bodies (cDLB) and clinical Parkinson's disease dementia (cPDD) cases. Areas assessed were frontal, temporal, parietal, occipital, cingulate, hippocampus, striatum, substantia nigra (SN) and locus coeruleus (LC). Mean, median and interquartile ranges are given 0, no pathology; 1, mild pathology; 2, moderate pathology; 3, severe pathology. Scores were "severe" in most areas except for the three cPDD cases which showed lower HP-τ in cingulate and frontal cortices.

[a]cPDD < cAD $p<0.05$
[b]cPDD < cAD $p<0.05$
[c]cPDD < cDLB $p<0.05$

3.4.3 Clinical characteristics

There were no overt differences in age of dementia onset between the clinical groups, however, the cDLB and cPDD had a shorter survival time from the onset of cognitive decline compared to the cAD group (cDLB mean 7.5 years, SE ±1.52; cPDD mean 7.33 years, SE ±2.4; cAD mean 9.38 years, SE ±1.31; Table 3.3). The onset of dementia in pure AD cases was 8.45 years later than in cAD (pure AD, 74.2 years SE ±2.71; cAD, 65.75 years SE ±3.32; Table 3.3). As expected, cPDD cases had an earlier onset of EPS (mean 64.33 years, SE ±4.33) than the cDLB cases (mean 71.83 years, SE ±2.44; Table 3.3).

cAD cases had lower final MMSE scores (mean: 6.0, SE ±3.21) compared to cDLB (mean: 8.43, SE ±3.64) and cPDD (mean: 8.0, SE ±3.56) as well as a higher rate of cognitive decline (mean: −7.17, SE ±2.8) compared to cDLB (mean: −3.83, SE ±0.94) and cPDD (mean: −3.5, SE ±1.32; Table 3.3).

Case Number	Age of Onset (cognitive decline)	Duration of cognitive decline (yrs)	Final MMSE	Rate of cognitive decline - MMSE (per year)	Presence of motor symptoms (y/n)	Age of Onset (motor symptoms)	Duration of motor symptoms (yrs)	Visual hallucinations (y/n)
Mixed AD/DLB - cAD								
1	66	10	10	-2.71	n	NA	NA	n
2	75	7	0	-9.5	n	NA	NA	n
3	49	14	0	NA	n	NA	NA	n
4	66	10	0	NA	n	NA	NA	n
5	73	15	10	-2.5	n	NA	NA	n
6	54	8	22	NA	n	NA	NA	n
7	69	4	NA	-14	n	NA	NA	n
8	70	7	0	-4.17	n	NA	NA	n
mean (±SE)	65.75 (3.23)	9.38 (1.31)	6 (3.21)	-7.17 (2.8)		NA	NA	
Mixed AD/DLB - cDLB								
9	73	7	0	-5	y	74	6	n
10	59	8	13	-1	y	NA	NA	y
11	70	5	15	-6.33	y	72	3	y
12	68	12	0	-5.5	y	70	10	y
13	68	15	6	NA	y	NA	NA	NA
14	77	1	25	-1	y	77	1	n
15	72	6	NA	NA	y	77	1	n
16	61	6	0	NA	y	61	6	NA
mean (±SE)	68.5 (2.13)	7.5 (1.52)	8.43 (3.64)	-3.83 (0.94)		71.83 (2.44)	4.5 (1.43)	
Mixed AD/DLB- cPDD								
17	62	6	9	-4	y	60	8	y
18	63	12	15	-1	y	60	15	y
19	73	4	0	-5.5	y	72	5	y
mean (±SE)	66 (3.51)	7.33 (2.4)	8	-3.5 (1.32)		64.33 (4.33)	9 (3.21)	
Pure AD								
20	64	14	0	NA	n	NA	NA	n
21	77	6	10	-2.67	n	NA	NA	n
22	75	11	0	-0.5	n	NA	NA	n
23	75	9	0	NA	n	NA	NA	NA
24	80	1	27	NA	n	NA	NA	n
mean (±SE)	74.2 (2.71)	8.2 (2.22)	7.4 (5.27)	-1.59 (1.1)		NA	NA	
Pure DLB								
25	73	4	24	NA	NA	NA	NA	y
26	64	8	25	-1.8	y	64	8	y
27	64	7	1	-0.67	y	64	7	y
28	66	11	12	-0.5	y	70	8	y
mean (±SE)	66.75 (2.14)	7.5 (1.44)	13.5 (4.84)	-0.99 (0.41)		66.0 (2.0)	7.76 (0.33)	

Table 3.3 Clinical characteristics of the study cohort. Abbreviations: MMSE, Mini Mental State Examination; y, yes; n, no; AD, Alzheimer's disease; DLB, dementia with Lewy bodies; cAD, neuropathologically mixed AD/DLB presenting clinically with Alzheimer's disease NA, not available; SE, standard error, cDLB, neuropathologically mixed AD/DLB presenting clinically with dementia with Lewy bodies, cPDD, neuropathologically mixed AD/DLB presenting clinically with Parkinson's disease dementia.

3.4.4 Quantitative assessment of hyperphosphorylated tau loads

HP-τ load was higher in cAD compared to cDLB and cPDD in all regions except the frontal cortex where HP-τ load in cDLB was higher than in both cAD and cPDD (Table 3.4; Figure 3.1). Overall significant differences were detected (Kruskal–Wallis $p < 0.05$) and significant respective differences were seen only in the hippocampus ($p < 0.05$), striatum (putamen $p < 0.05$) and locus coeruleus ($p < 0.01$) of cAD when compared to cDLB and in hippocampus ($p < 0.05$), striatum (putamen $p < 0.05$), neocortical regions (frontal, temporal and parietal; $p < 0.05$), striatum (putamen $p < 0.05$) and cingulate cortex ($p < 0.05$) of cAD when compared to cPDD.

In cDLB, HP-τ load was significantly higher in frontal ($p < 0.05$) and cingulate cortices ($p < 0.05$) compared to cPDD, whilst HP-τ load was significantly higher in the LC in cPDD compared to cDLB.

When comparing HP-τ loads in limbic and cortical regions within the same clinical phenotype the cAD group showed highest HP-τ loads in the temporal cortex (mean 19.9 %, SE ±4.06), followed by hippocampus (mean 13.81 % SE ±2.58), occipital cortex (mean 13.14 %, SE ±3.68), parietal cortex (mean 12.04, SE ±2.67), cingulate gyrus (mean 10.5 %, SE ±2.7) and frontal cortex (mean 4.6 %, SE ±1.33; Figure 3.2a).

Interestingly, cDLB and cPDD displayed a different pattern of HP-τ distribution to the one observed in cAD. In cDLB, the occipital cortex exhibited the highest HP-τ load (mean 13.06 %, SE ±3.83) followed by temporal cortex (mean 11.38 %, SE ±2.62), parietal cortex (mean 10.49 %, SE ±3.19), cingulate cortex (mean 8.45 %, SE ±2.77), hippocampus (mean 7.72 %, SE ±1.36) and frontal cortex (mean 7.51 %, SE ±2.17; Figure 3.2a).

On the other hand, cPDD cases showed highest HP-τ loads in the hippocampus (mean 11.58 %, SE ±5.37), followed by occipital (mean 5.69 %, SE ±3.71), temporal (mean 3.49 %, SE ±2.04), parietal (mean 0.95 %, SE ±0.49), cingulate gyrus (mean 0.72 %, SE ±0.33) and frontal (mean 0.4 %, SE ±0.24; $p > 0.05$, Figure 3.2a)

Similar to cAD, pure AD showed highest HP-τ load in the temporal cortex (mean 18.45 %, SE ±5.48), but this was followed by occipital (mean 16.44 %, SE ±4.79), parietal (mean 13.19 %, SE ±5.65) and frontal (mean 11.68 %, SE ±5.83) cortices whilst lower loads were seen in the hippocampus (mean 11.12 %, SE ±5.02) and cingulate gyrus (mean 8.46 %, SE ±3.87; Figure 3.3a). HP-τ load did not differ significantly between pure AD and cAD, and HP-τ loads in cDLB and cPDD were significantly lower than in pure AD in those regions that showed significantly lower loads when cDLB and cPDD were compared with cAD (see above).

	cAD HP- τ (±SE)	cDLB HP- τ (±SE)	cPDD HP- τ (±SE)	pAD HP- τ (±SE)	pDLB HP- τ (±SE)	Statistic H_{df}, p value
Frontal	4.6 (1.33)	7.51 (2.17)	0.4 (0.24)	11.68 (5.83)	0.16 (0.07)	H_4 = 12.62, p = 0.013 [a]
Temporal	**19.9 (4.06)**	**11.38 (2.62)**	**3.49 (2.04)**	**18.45 (5.48)**	**0.24 (0.09)**	H_4 = 15.22, p = 0.004 [b]
Parietal	12.04 (2.67)	**10.49 (3.19)**	0.95 (0.49)	**13.19 (5.65)**	0.02 (0.01)	H_4 = 13.17, p = 0.01 [c]
Occipital	**13.14 (3.68)**	**13.06 (3.83)**	**5.69 (3.71)**	**16.44 (4.79)**	0	H_4 = 9.01, p = 0.061
Neocortex (mean of all cortical areas)	13.08 (2.53)	10.73 (1.96)	2.63 (0.68)	14.98 (4.74)	0.11 (0.03)	H_4 = 15.21, p = 0.004 [d]
Cingulate	10.50 (2.7)	8.45 (2.77)	0.72 (0.33)	8.46 (3.87)	**0.4 (0.34)**	H_4 = 12.66, p = 0.013 [e]
Hippocampus	**13.81 (2.58)**	7.72 (1.36)	**11.58 (5.37)**	11.12 (5.02)	**12.8 (4.1)**	H_4 = 9.6, p = 0.048 [f]
Caudate nucleus	2.94 (0.95)	0.95 (0.27)	0.65 (0.31)	1.7 (0.84)	0.04 (0.03)	H_4 = 9.42, p = 0.052
Putamen	3 (0.87)	0.68 (0.23)	0.18 (0.03)	2.77 (1.64)	0	H_4=15.2, p = 0.004 [g]
Striatum (mean of caudate nucleus and putamen)	2.97 (0.84)	0.77 (0.19)	0.42 (0.16)	1.55 (1.26)	0.02 (0.02)	H_4 = 14.11, p = 0.007 [h]
Amygdala	23.15 (7.31)	17.53 (5.83)	4.97 (4.97)	23.31 (7.15)	14.59 (7.72)	H_4 = 4.39, p = 0.355
Substantia Nigra	3.08 (1.02)	1.94 (0.4)	0.73 (0.14)	0.65 (0.22)	0.14 (0.06)	H_4 = 9.42, p = 0.056
Locus Coeruleus	4.02 (1.2)	0.8 (0.22)	2.75 (0.78)	1.68 (0.73)	1.5 (1.03)	H_4 = 9.6, p = 0.048 [i]

Table 3.4 Quantitative values for pathological burden of hyperphosphorylated tau All values are percentage area of the binary fraction covered by immunopositivity. Values expressed as mean. The highest values in each column are shown in bold lettering.
Abbreviations: cAD, neuropathologically mixed AD/DLB presenting clinically with Alzheimer's disease AD; HP-τ, hyperphosphorylated microtubule associated tau; standard error; cDLB, neuropathologically mixed AD/DLB presenting clinically with dementia with Lewy bodies; cPDD, neuropathologically mixed AD/DLB presenting clinically with Parkinson's disease dementia
Pairwise post hoc Mann Whitney U tests
[a] cPDD < cAD, cDLB and pAD p<0.05
[b] cPDD < cAD and pAD p<0.05
[c] cPDD < cAD and pAD p<0.05
[d] cPDD < cAD, and pAD p<0.05
[e] cPDD < cAD, cDLB and pAD p<0.05
[f] cAD and pAD > cDLB p<0.05
[g] cAD and pAD > cDLB and cPDD p<0.05
[h] cAD and pAD > cDLB and cPDD p<0.05
[i] cDLB < cAD and pAD p<0.01 and cPDD p<0.05

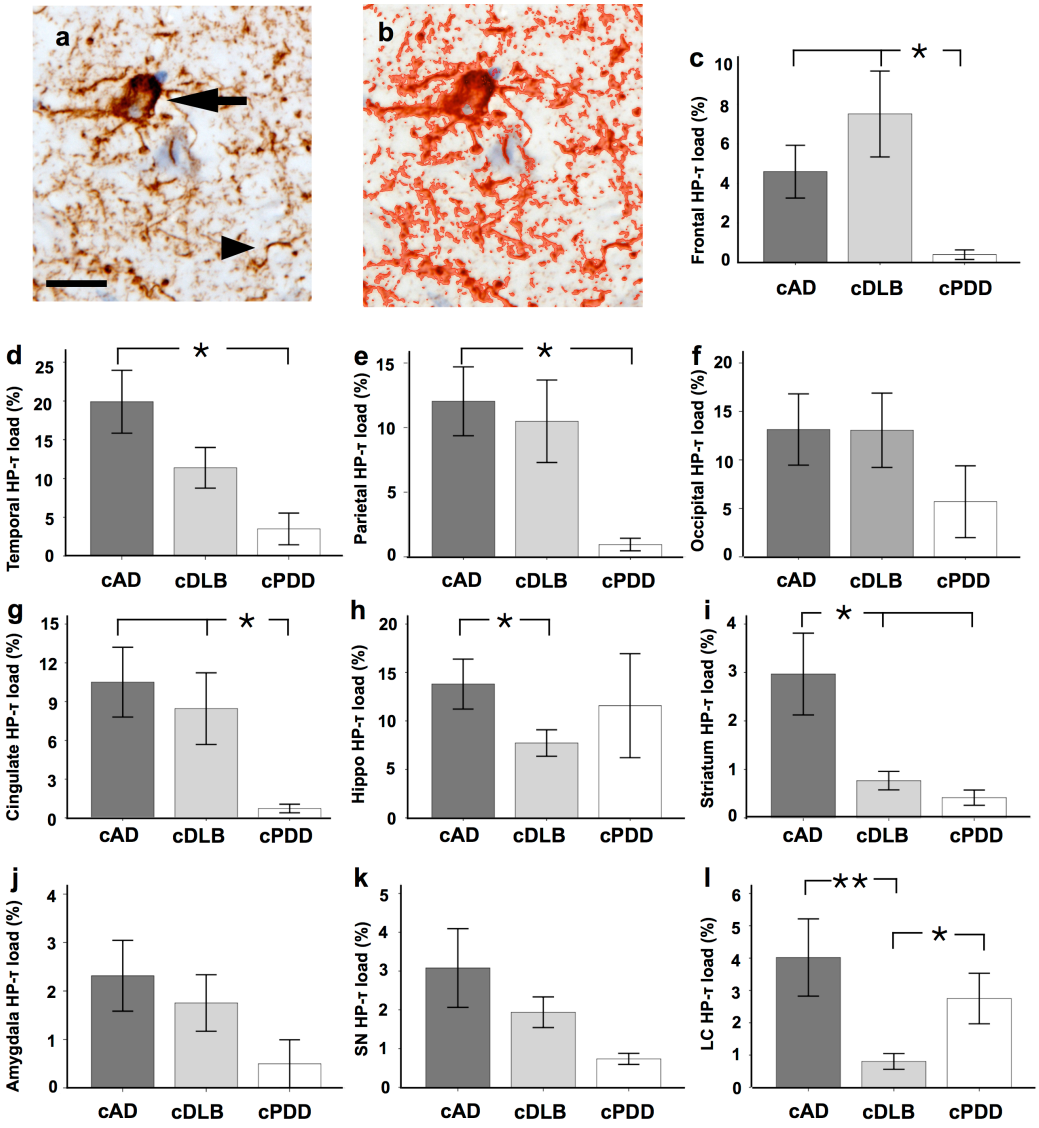

Figure 3.1 Hyperphosphorylated tau (HP-τ) load differs between clinical Alzheimer's disease (cAD) clinical dementia with Lewy bodies (cDLB) and clinical Parkinson's disease dementia (cPDD) cases. Neurofibrillary tangles (**(a)** NFTs - arrow) and neuropil threads (**(a)** NTs - arrowhead) immunopositive for AT8 antibody were included in the quantitative assessment. The area positive for AT8 immunoreactivity is shaded red in (**b**). Box plots show differences in HP-τ loads between clinical phenotypes in frontal cortex **(c)**, temporal cortex **(d)**, parietal cortex **(e)**, occipital cortex **(f)**, cingulate **(g)**, hippocampus **(h)**, striatum (i.e., mean of caudate and putamen values) **(i)**, amygdala **(j)**, substantia nigra (SN) **(k)** and locus coeruleus (LC) **(l)**. *, $p<0.05$; **, $p<0.01$; scale bar, 20μm, valid for **a** and **b**.

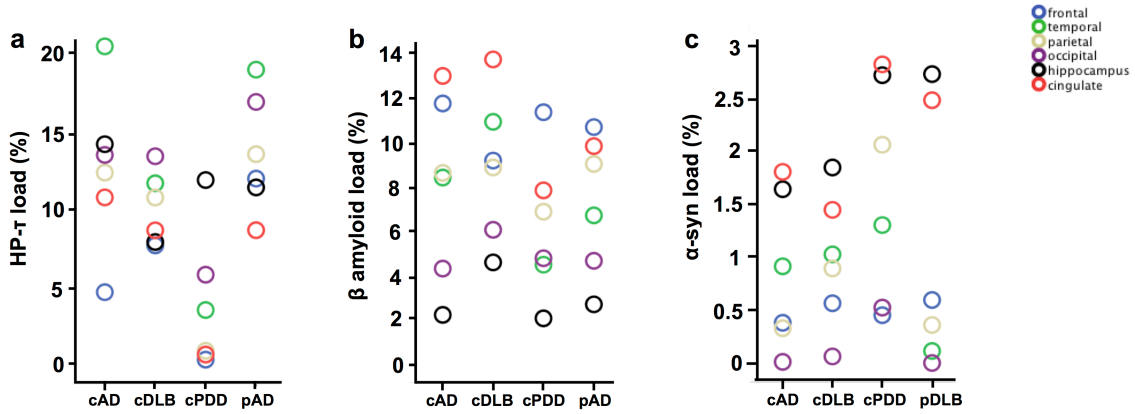

Figure 3.2 Scatter plots showing the hierarchical distribution of hyperphosphorylated tau (HP-τ), β-amyloid and α-synuclein (α-syn) loads of cortical and limbic regions in neuropathologically mixed AD/DLB cases which clinically either presented as Alzheimer's disease (cAD), dementia with Lewy bodies (cDLB) or Parkinson's disease dementia (cPDD) and in neuropathologically and clinical pure AD cases (pAD; **a** and **b**) or neuropathologically and clinical pure DLB cases (pDLB; **c**). cAD cases exhibited a similar pattern of HP-τ distribution to that observed pAD) cases with the temporal cortex being the most severely affected area in both, whilst the occipital cortex was the cortical region most severely affected by HP-τ in both clinical Dementia with Lewy bodies (cDLB) and clinical Parkinson's disease dementia (cPDD) **(a)**. β-amyloid displayed a different pattern of distribution with cAD displaying a similar hierarchical pattern of cortical distribution to pAD. This differed to that seen in cDLB and cPDD **(b)**. The limbic regions (hippocampus and cingulate) were most affected by α-synuclein (α-syn) and the occipital cortex was least affected in all phenotypes **(c)**.

3.4.5 Quantitative assessment of β-Amyloid loads

No significant differences were seen in Aβ loads between cAD and cDLB (Table 3.5; Figure 3.3). However, both cAD and cDLB showed significantly higher Aβ loads in the temporal cortex, and cDLB in the cingulate, when compared to cPDD ($p < 0.05$; Figure 3.3). In cAD, Aβ loads were highest in the cingulate cortex (mean 12.58 %, SE ±2.28) followed by frontal (mean 11.38 %, SE ±1.8), parietal (mean 8.35 %, SE ±1.95), temporal (mean 8.15 %, SE ±1.09) and occipital cortices (mean 4.18 %, SE ±0.65) and hippocampus (mean 2.16 %, SE ±0.44; Figure 3.3). Overall differences between lobes were observed (Friedman's $p < 0.05$). Here, cingulate, frontal, temporal and parietal Aβ loads were significantly higher than occipital Aβ load (cingulate: $p < 0.01$, all others: $p < 0.05$), whilst all cortical Aβ loads were significantly higher than hippocampal Aβ load ($p < 0.05$).

Aβ load in cDLB was highest in the cingulate cortex (mean 13.39 %, SE ±1.5) followed by temporal (mean 10.58 %, SE ±2.4), frontal (mean 8.89 %, SE ±1), parietal (mean 8.59 %, SE ±0.72) and occipital cortices (mean 5.87 %, SE ±0.7) and hippocampus (mean 4.45 %, SE ±1.34; Figure 3.3b). In cDLB cingulate

loads were significantly higher than parietal, occipital and hippocampal loads (p < 0.05). Overall differences between lobes were observed (Friedman's p < 0.05). Temporal Aβ loads were significantly higher than hippocampal and occipital ones as were parietal compared to occipital Aβ loads, respectively (p < 0.05).

In cPDD, highest Aβ loads were found in the frontal cortex (mean 11 %, SE ±1.87) followed by cingulate (mean 7.59 %, SE ±1.01), parietal (mean 6.66, SE ±2.26), occipital (mean 4.63 %, SE ±2.06) and temporal cortices (mean 4.35 %, SE ±0.93) and hippocampus (mean 2.01 %, SE ±0.7; p < 0.05; Figure 3.3b). Like in cAD, pure AD cases showed highest Aβ load in the frontal cortex (mean 10.35 %, SE ±1.58), followed by parietal (mean 8.74 %, SE ±1.39), cingulate (mean 8.46 %, SE ±3.87), temporal (mean 6.5 %, SE ±0.74), and occipital cortices (mean 4.52 %, SE ±1.08) and hippocampus (mean 2.62 %, SE ±0.67; Figure 3.3b). However, unlike cAD cases, in pure AD no significant differences in Aβ loads were observed between areas and regional Aβ loads in pure AD did not differ significantly from the ones seen in cAD, cDLB and cPDD.

	cAD β amyloid (±SE)	cDLB β amyloid (±SE)	cPDD β amyloid (±SE)	pAD β amyloid (±SE)	pDLB β amyloid (±SE)	Statistic H_{df}, p value
Frontal	**11.38 (1.8)**	**8.89 (1)**	**11 (1.87)**	**10.35 (1.58)**	**5.6 (3.21)**	H_4 = 3.2, p = 0.526
Temporal	8.15 (1.09)	**10.58 (2.4)**	4.35 (0.93) [a]	6.5 (0.74)	2.46 (1.43)	H_4 = 12.72, p = 0.013
Parietal	**8.35 (1.95)**	8.59 (0.72)	**6.66 (2.26)**	**8.74 (1.39)**	3.19 (1.98)	H_4 = 7.07, p = 0.132
Occipital	4.18 (0.65)	5.87 (0.7)	4.63 (2.06)	4.52 (1.08)	**4.19 (2.72)**	H_4 = 2.85, p = 0.584
Neocortex (mean of all cortical areas)	8.01 (1.01)	8.48 (0.88)	6.66 (1.54)	7.75 (0.68)	3.26 (2.03)	H_4 = 4.36, p = 0.359
Cingulate	**12.58 (2.28)**	**13.39 (1.5)** [b]	**7.59 (1.01)**	**9.52 (2.75)**	**3.74 (2.14)**	H_4 = 10.62, p = 0.031
Hippocampus	2.16 (0.44)	4.45 (1.34)	2.01 (0.7)	2.62 (0.67)	2.14 (1.06)	H_4 = 3.14, p = 0.534
Caudate nucleus	6.53 (0.91)	7.05 (0.77)	5.64 (2.19)	4.28 (0.52)	1.25 (0.71)	H_4 = 9.35, p = 0.054
Putamen	5.92 (0.88)	8.38 (1.15)	6.89 (1.69)	3.74 (0.55)	1.24 (0.62)	H_4 = 8.71, p = 0.064
Striatum (mean of caudate nucleus and putamen)	6.23 (0.86)	7.72 (0.76)	6.26 (1.79)	4 (0.51)	1.09 (0.45)	H_4 = 8.14, p = 0.08
Amygdala	4.33 (1.12)	4.86 (1.15)	2.29 (1.02)	3.07 (0.32)	4.83 (0)	H_4 = 3.49, p = 0.479
Substantia Nigra	2.78 (0.72)	2.13 (0.45)	1.73 (0.5)	1.48 (0.85)	0.23 (0.13)	H_4 = 9.17, p = 0.057
Locus Coeruleus	0.64 (0.15)	1.47 (0.63)	0.85 (0.46)	0.65 (0.57)	0.13 (0.13)	H_4 = 6.75, p = 0.15

Table 3.5 Quantitative values for pathological burden of β amyloid. All values are percentage area of the binary fraction covered by immunopositivity. Values expressed as mean. The highest values in each column are shown in bold lettering. Abbreviations: cAD, neuropathologically mixed AD/DLB presenting clinically with Alzheimer's disease AD; SE, standard error; cDLB, neuropathologically mixed AD/DLB presenting clinically with dementia with Lewy bodies; cPDD, neuropathologically mixed AD/DLB presenting clinically with Parkinson's disease dementia.

Pairwise post hoc Mann Whitney U tests

[a] cPDD < cAD and cDLB p<0.05
[b] cDLB > cPDD p<0.05

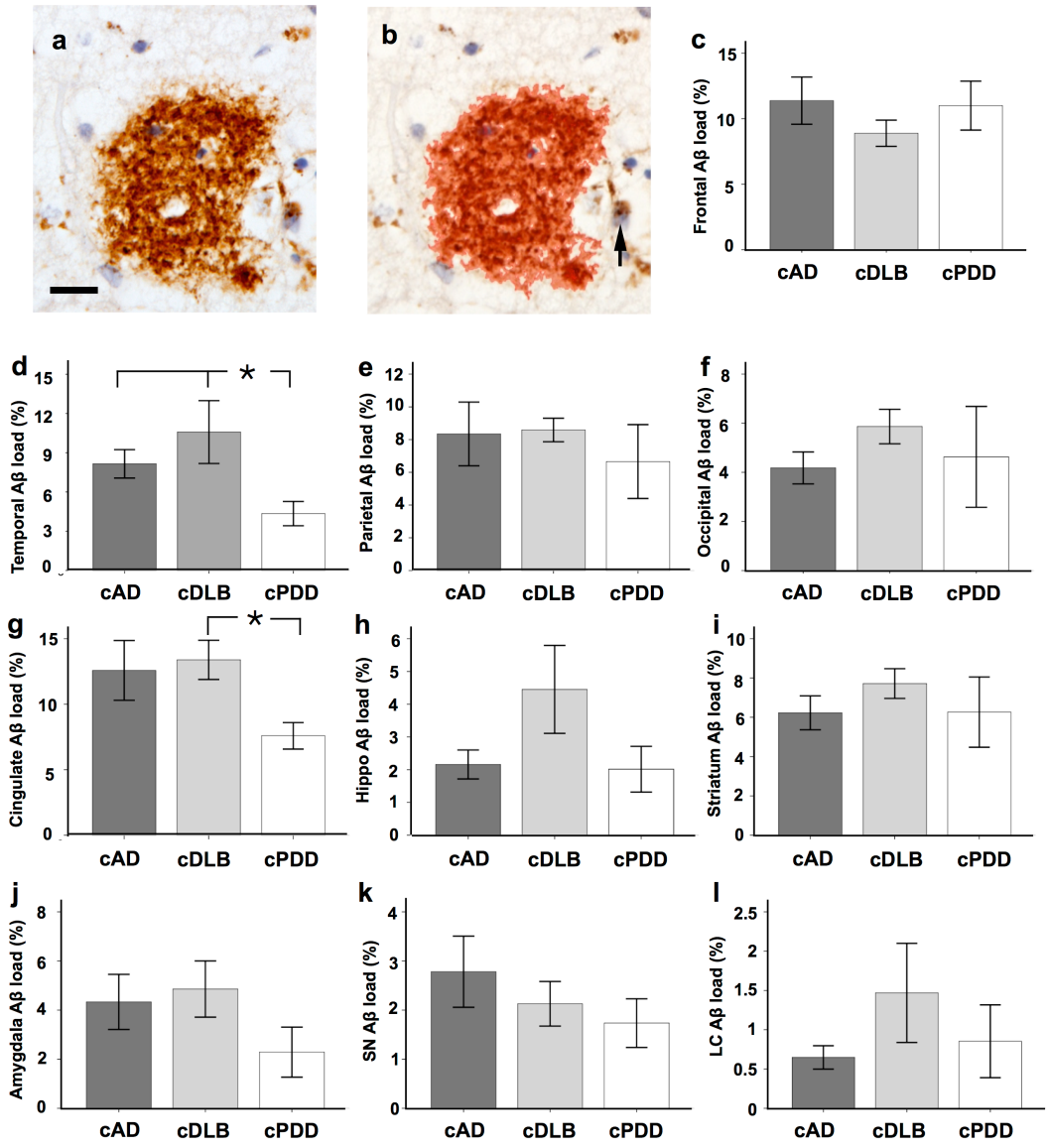

Figure 3.3 β-amyloid loads differ between clinical Alzheimer's disease (cAD) clinical dementia with Lewy bodies (cDLB) and clinical Parkinson's disease dementia (cPDD) in the mixed AD/ DLB cohort. All β-amyloid deposits immunopositive for 4G8 antibody **(a)** were included in the analysis (shaded in red (**b**)). Restriction thresholds (see materials and methods for details) were applied to include all pathological lesions in the assessment whilst excluding physiological cellular amyloid precursor protein (*APP*) (**b** - arrow). Differences in β-amyloid loads between the clinical phenotypes are illustrated in frontal cortex **(c)**, temporal cortex **(d)**, parietal cortex **(e)**, occipital cortex **(f)**, cingulate **(g)**, hippocampus **(h)**, striatum (i.e., mean of caudate and putamen values) **(i)**, amygdala **(j)**, substantia nigra (SN) **(k)** and locus coeruleus (LC) **(l)**. *, $p<0.05$; scale bar, 20μm, valid for **a** and **b**.

3.4.6 Quantitative assessment of α-Synuclein loads

α-Syn loads were highest in the amygdala and in the majority of areas analysed were comparable in all three mixed AD/LBD clinical phenotypes (Table 3.6; Figure 3.4). Overall differences were seen between clinical phenotypes (Kruskal–Wallis $p < 0.05$) with the α-syn load in the striatum being significantly higher in cPDD than in cAD ($p < 0.05$). In addition, although not significant, in cPDD α-syn load was higher in the hippocampus but lower in the SN compared to cAD and cDLB Figure 3.4; Table 3.6).

With regards to cortical and limbic areas, overall differences in α-syn loads between areas were observed (Friedmans $p < 0.05$). In the cAD cases, α-syn load was highest in the cingulate cortex (mean 1.77 %, SE ±0.65; $p < 0.05$ vs frontal, parietal and occipital cortices) followed by hippocampus (mean 1.61 %, SE ±0.76; $p < 0.05$ vs frontal and occipital cortices), temporal (mean 0.9 %, SE ±0.4; $p < 0.05$ vs parietal and occipital cortices), frontal (mean 0.38 %, SE ±0.18), parietal (mean 0.33 %, SE ±0.16) and occipital cortices (mean 0.02 %, SE ±0.01; Figure 3.2c).

cDLB cases showed highest cortico-limbic α-syn loads in the hippocampus (mean 1.81 %, SE ±0.72), followed by cingulate (mean 1.42 %, SE ±0.74), temporal (mean 1.01 %, SE ±0.44), parietal (mean 0.88 %, SE ±0.37), frontal (mean 0.56 %, SE ±0.34) and occipital cortices (mean 0.07 %, SE ±0.03; $p < 0.05$; Figure 3.2c).

Cortico-limbic α-syn loads in cPDD cases were highest in cingulate cortex (mean 2.76 %, SE ±2.15), followed by hippocampus (mean 2.66 %, SE ±0.98), parietal (mean 2.02 % SE ±1.4), temporal (mean 1.28 %, SE ±0.95), occipital (mean 0.52 %, SE ±0.3) and frontal cortices (mean 0.45 %, SE ±0.32; $p < 0.05$; Figure 3.2c).

Like cDLB, pure DLB cases showed highest cortico- limbic α-syn loads in the hippocampus (mean 2.68 %, SE ±0.67), followed by cingulate cortex (mean 2.43 %, SE ±1.67) but in pure DLB these were followed by frontal (mean 0.59 %, SE ±0.55), temporal (mean 0.12 %, SE ±0.03), parietal (mean 0.04 %, SE ±0.02) and occipital cortices (mean 0.01 %, SE ±0.00 %; $p < 0.05$; Figure 3.3c).

No significant differences were seen in α-syn loads between pure DLB and cAD, cDLB and cPDD.

	cAD α-synuclein (±SE)	cDLB α-synuclein (±SE)	cPDD α-synuclein (±SE)	pDLB α-synuclein (±SE)	Statistic H_{df}, p value
Frontal	0.38 (0.18)	0.56 (0.34)	0.45 (0.32)	**0.59 (0.55)**	H_3 = 5.52, p = 0.938
Temporal	**0.9 (0.4)**	**1.01 (0.44)**	1.28 (0.95)	0.12 (0.03)	H_3 = 8.76, p = 0.510
Parietal	0.33 (0.16)	0.88 (0.37)	**2.02 (1.4)**	0.04 (.02)	H_3 = 12.90, p = 0.064
Occipital	0.02 (0.01)	0.07 (0.03)	0.52 (0.3)	0.01 (0)	H_3 = 7.64, p = 0.365
Neocortex (mean of all cortical areas)	0.43 (0.17)	0.66 (0.26)	1.08 (0.32)	0.24 (0.13)	H_3 = 14.1, p = 0.225
Cingulate	**1.77 (0.65)**	**1.42 (0.74)**	**2.76 (2.15)**	**2.43 (1.67)**	H_3 = 10.51, p = 0.829
Hippocampus	**1.61 (0.76)**	**1.81 (0.72)**	**2.66 (0.98)**	**2.68 (0.67)**	H_3 = 7.69, p = 0.395
Caudate nucleus	0.34 (0.16)	0.2 (0.07)	(1.3) 0.64	0.65 (0.61)	H_3 = 11.85, p = 0.062
Putamen	0.49 (0.17)	0.96 (0.36)	1.52 (0.21)	0.36 (0.15)	H_3 = 13.24, p = 0.051
Striatum (mean of caudate nucleus and putamen)	0.57 (0.15)	0.75 (0.27)	1.41 (0.35)	0.51 (0.37)	H_3 = 12.55, p = 0.014 [a]
Amygdala	5.01 (1.27)	5.64 (2.16	3.79 (1.57)	4.71 (1.56)	H_3 = 9.6, p = 0.990
Substantia Nigra	3.04 (0.76)	2.87 (0.73)	0.55 (0.24)	1.33 (0.53)	H_3 = 15.06, p = 0.163
Locus Coeruleus	1.71 (0.76)	1.78 (0.58)	1.64 (0.99)	0.24 (0.13)	H_3 = 11.12, p = 0.355

Table 3.6 Quantitative values for pathological burden α-synuclein. All values are percentage area of the binary fraction covered by immunopositivity. Values expressed as mean. The highest values in each column are shown in bold lettering.

Abbreviations: cAD, neuropathologically mixed AD/DLB presenting clinically with Alzheimer's disease AD; SE, standard error; cDLB, neuropathologically mixed AD/DLB presenting clinically with dementia with Lewy bodies; cPDD, neuropathologically mixed AD/DLB presenting clinically with Parkinson's disease dementia.

Pairwise post hoc Mann Whitney U tests

[a] cPDD > cAD $p<0.05$

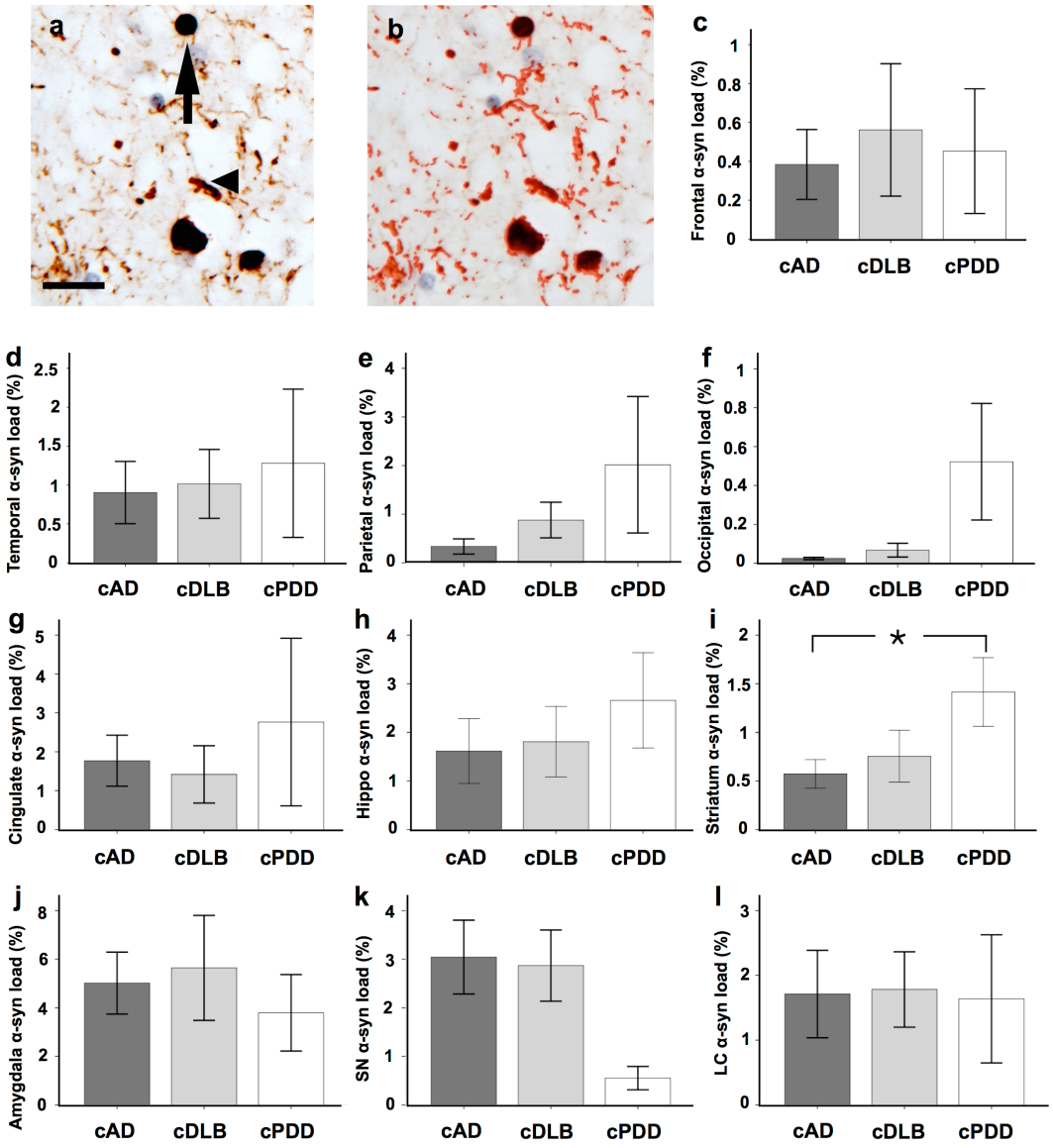

Figure 3.4 α-synuclein (α-syn) loads differ between clinical Alzheimer's disease (cAD) clinical dementia with Lewy bodies (cDLB) and clinical Parkinson's disease dementia (cPDD) in the mixed AD/DLB cohort. α-syn pathologies inclusive of Lewy bodies ((a) LBs - arrow) and Lewy neurites ((a) LNs - arrowhead) were included in the analysis. The area positive for α-syn immunoreactivity is highlighted in red (b). Differences in α-syn loads between the clinical phenotypes are illustrated in frontal cortex (c), temporal cortex (d), parietal cortex (e), occipital cortex (f), cingulate (g), hippocampus (h), striatum (i.e., mean of caudate and putamen values) (i), amygdala (j), substantia nigra (SN) (k) and locus coeruleus (LC) (l). *, $p<0.05$; scale bar, 20μm, valid for a and b.

3.4.7 Cortical thickness measurements

cDLB cases exhibited a significantly thinner cortex in the parietal region (2373.1μm ± 55.51) compared to control cases (2694.89μm ± 66.91; p<0.01) (Table 3.7). cPDD cases also displayed a thinner cortex in the parietal region (2450.21μm ± 2.14) compared to control cases (2694.89μm ± 66.91; p<0.05). No other differences were observed in other brain regions (Figure 3.6).

	cAD μm (μm±SE)	cDLB μm (±SE)	cPDD μm (±SE)	Control μm (±SE)	Statistic H_{df}, p value
Frontal	2455.8 (69.8)	2502.5 (60.5)	2560.8 (184.2)	2783.3 (102.5)	H_3 = 5.3, p = 0.15
Temporal	2473.7 (90.2)	2429.3 (76.7)	2643 (93.6)	2764.7 (98.8)	H_3 = 6.23, p = 0.1
Parietal	2396.2 (117.9)	2373.1 (55.5)	2450.2 (2.1)	2694.9 (66.9)	H_3 = 9.67, p = 0.02[ab]
Occipital	2114 (120.8)	2063.7 (96.4)	2335.3 (89.9)	2334.9 (134.7)	H_3 = 3.49, p = 0.32
Cingulate	2852.1 (156.3)	2706.4 (115.2)	2758.8 (156.1)	2717.2 (174)	H_3 = 0.52, p = 0.91

Table 3.7 Quantitative values for cortical thickness in frontal, temporal, parietal, occipital and cingulate as measured by the distance between the pial surface and the start of the white matter in cAD, cDLB, cPDD and control cases.

Abbreviations: Abbreviations: cAD, neuropathologically mixed AD/DLB presenting clinically with Alzheimer's disease AD; SE, standard error; cDLB, neuropathologically mixed AD/DLB presenting clinically with dementia with Lewy bodies; cPDD, neuropathologically mixed AD/DLB presenting clinically with Parkinson's disease dementia.

Pairwise post hoc Mann Whitney U tests

[a] cDLB < control p<0.01

[b] cPDD < control p<0.05

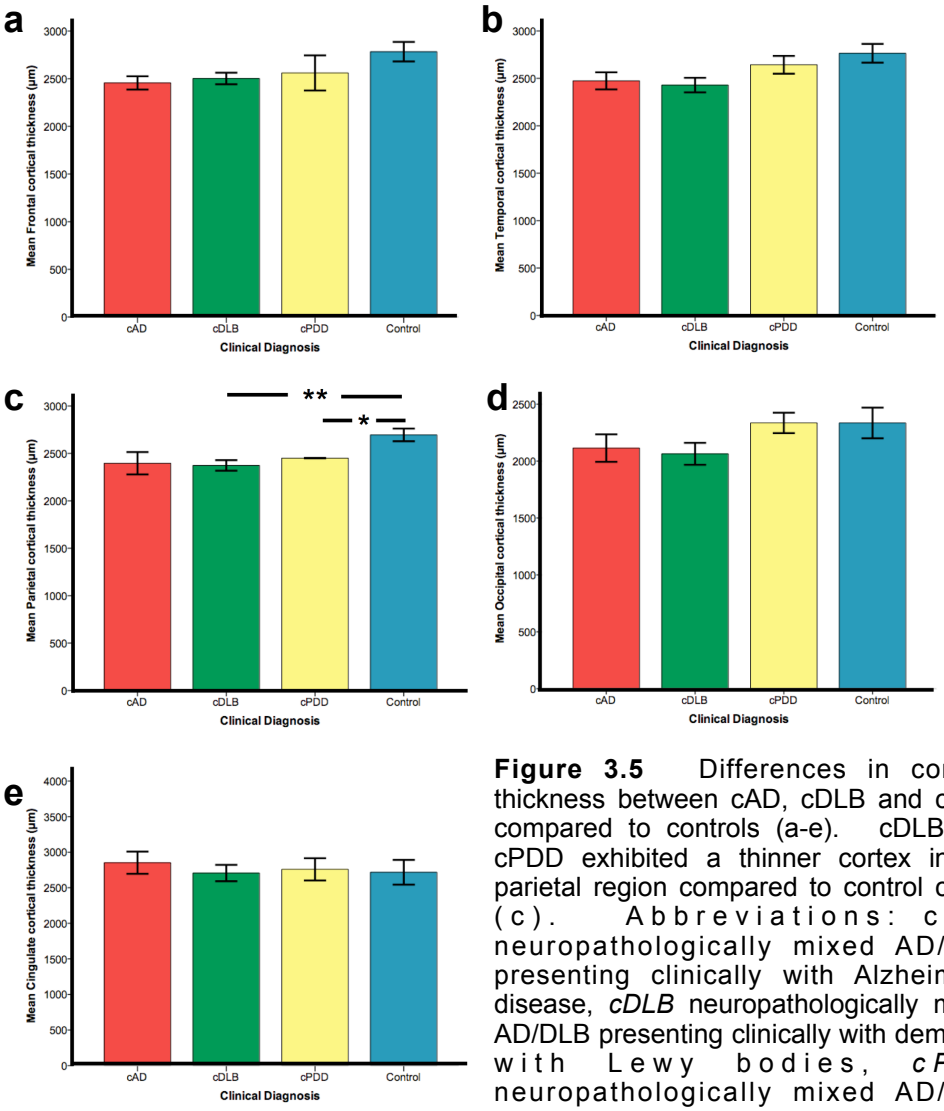

Figure 3.5 Differences in cortical thickness between cAD, cDLB and cPDD compared to controls (a-e). cDLB and cPDD exhibited a thinner cortex in the parietal region compared to control cases (c). Abbreviations: cAD; neuropathologically mixed AD/DLB presenting clinically with Alzheimer's disease, *cDLB* neuropathologically mixed AD/DLB presenting clinically with dementia with Lewy bodies, *cPDD* neuropathologically mixed AD/DLB presenting clinically with Parkinson's disease dementia. *p<0.05, **p<0.01.

3.4.8 APOE genotyping

APOE genotypes and allele frequencies for all cases are shown in Table 3.8. Two cases in the cAD group were homozygous for ε4, whilst there was one homozygous ε4 case in the cDLB group and none in the cPDD group.

The distribution of *APOE* allele frequency demonstrated that *APOE* ε4 allele frequencies were highest in the cDLB group (50 %) followed by the cAD group (43.75 %) and lowest in the cPDD group (33.33 %). Of note, none of the cases in this study had any *APOE* ε2 alleles.

	cAD (n=8)	cDLB (n=7)	cPDD (n=3)
APOE genotype			
ε3, ε3 n	3	1	1
ε3, ε4 n	3	5	2
ε4, ε4 n	2	1	0
APOE allele frequency			
ε3 n (%)	9 (56.25)	7 (50)	4 (66.66)
ε4 n (%)	7 (43.75)	7 (50)	2 (33.33)

Table 3.8 *APOE* genotype distribution * and allele frequencies † of the mixed AD/DLB cohort.

* Overall comparisons of *APOE* genotype demonstrated no significant differences between all three groups: Fisher's exact test p=0.649.

† Overall comparisons of APOE allele frequencies demonstrated no significant differences between all three groups: Fisher's exact test p=0.743.

Abbreviations: cAD, neuropathologically mixed AD/DLB presenting clinically with Alzheimer's disease; cDLB, neuropathologically mixed AD/DLB presenting clinically with dementia with Lewy bodies; cPDD, neuropathologically mixed AD/DLB presenting clinically with Parkinson's disease dementia.

3.5 Discussion

Using quantitative assessment to evaluate cases that neuropathologically fulfilled the criteria for both AD and DLB, I was able to detect significant differences in the amount of pathological protein aggregates between cases that clinically presented as either AD or DLB which were previously not seen using semi-quantitative neuropathological assessment.

3.5.1 cAD exhibited higher hyperphosphorylated tau loads compared to cDLB and cPDD.

HP-τ load (as measured by percentage area covered by immunopositivity) was higher in cAD cases than in cPDD cases in all assessed regions with significant higher loads seen in frontal, temporal, parietal and cingulate cortices as well as in the striatum. When compared to cDLB, cAD showed a significantly higher HP-τ load in the hippocampus, striatum and LC. This may suggest earlier involvement of these areas, as according to Braak stages of neurofibrillary pathology (Braak and Braak, 1991, Braak et al., 2006) the hippocampus is typically affected in stage II, the striatum in stage IV and the neocortex in stages V and VI. This may indicate that these cases originally started as AD cases and were following the typical course of AD, with LB pathology developing later, potentially even triggered by AD pathology.

Two recent studies by Braak and colleagues have demonstrated the presence of tau pathology can exist in the locus coruleus in individuals under the age of 30 (Braak and Del Tredici, 2011, Braak et al., 2011), and has been suggested to increase in line with the stepwise progression of pathology seen in Braak stages (Attems et al., 2012). The increase in tau pathology observed in the cAD cases may be attributed to an earlier progression in Braak staging in the cAD cases compared to cDLB and cPDD cases.

3.5.2 Differences in pathology loads between cDLB and cPDD

In the majority of regions cDLB showed higher Aβ loads than cPDD, confirming previous *post-mortem* studies (Jellinger and Attems, 2006, Halliday et al., 2011) demonstrating that DLB patients had higher striatal Aβ loads compared to PDD patients. This finding has been supported by imaging studies using Pittsburgh

compound B (PiB) to image Aβ where DLB patients exhibited higher neocortical, cingulate and striatal Aβ loads compared to PDD (Edison et al., 2008). In addition, in this study cPDD cases showed lower HP-τ loads than cDLB in all neocortical areas as well as in cingulate and striatum, further suggesting that the amount of AD pathology is generally lower in clinical PDD than in DLB even in PDD cases that neuropathologically fulfil the criteria for AD.

3.5.3 Differences in α-syn in the striatum and SN

Interestingly, except for the striatum where cPDD cases did show significantly higher α-syn loads than cAD cases, no significant respective differences were seen between cAD, cDLB and cPDD. Although not statistically significant, the latter group did exhibit less α-syn pathology in the SN than cAD and cDLB. This somewhat unexpected finding might be explained by severe loss of pigmented neurones in cPDD early in the disease, resulting in less LBs, which might contribute to an overall reduction in nigral α-syn burden. Due to time constraints, SN neuronal number scores were not available and would be required to support this hypothesis.

3.5.4 Comparisons to 'pure' cases suggest potential synergistic interactions between pathological protein aggregates

There were no significant differences in HP-τ load between cAD and pure AD and both showed highest HP-τ loads in the temporal cortex. However, although statistically not significant HP-τ loads in hippocampus and cingulate cortex were higher in cAD than in pure AD and this may have been influenced by concomitant α-syn pathology in cAD cases. Similarly, cingulate Aβ loads were higher in cAD than in pure AD, whilst the distribution of neocortical Aβ loads in cAD was identical to the one observed in pure AD (i.e. frontal > parietal > temporal > occipital). These findings suggest that AD pathology was the primary neurodegenerative change in cAD and represented the neuropathological correlate for the clinical AD phenotype in these cases. When comparing α-syn loads between mixed AD/DLB cases with pure DLB cases, we found mixed AD/DLB cases to have considerably higher α-syn loads in the temporal cortex, whilst no overt differences were seen in other areas. The temporal cortex in mixed AD/DLB cases did also show highest HP-τ loads and hence HP-τ might have promoted the aggregation and accumulation of α-syn. The notion of such

an interaction between HP-τ and α-syn has indeed been supported by data from transgenic animal studies (Clinton et al., 2010) and human *postmortem* studies found co-localisation of HP-τ and α-syn (Ishizawa et al., 2003, Colom-Cadena et al., 2013).

3.5.5 Concomitant pathology may exacerbate the existing clinical phenotype

cAD cases exhibited severe Lewy body pathology at *postmortem* examination, whilst no clinical symptoms suggestive for DLB were observed *ante mortem*; the impact of additional pathologies on the clinical phenotype is indeed of current interest. It has been suggested that concomitant AD pathology in DLB is associated with cognitive decline (Howlett et al., 2014) and concomitant TDP-43 pathology in AD exacerbates features associated with AD, i.e. greater cognitive impairment and medial temporal lobe atrophy (Josephs et al., 2014) but does not associate with behavioural features frequently associated with fronto-temporal lobar degeneration or amyotrophic lateral sclerosis (Jung et al., 2014), diseases in which TDP-43 inclusions are the characteristic pathological hallmark lesion. The latter is similar to the findings in the current study where in cAD, co-existing Lewy body pathology did not elicit symptoms associated with DLB and PDD (i.e. visual hallucinations and Parkinsonism).

The mean age of disease onset in cAD cases was considerably lower (65.75 years) than the mean age of onset in our pure AD cases (74.2 years) and the mean age of AD onset reported by others (Williams et al., 2006, Mandler et al., 2014). Likewise, the mean age of onset in cDLB (68.5 years) and cPDD (66 years) was low given that the mean age of onset in DLB is generally above 70 years (Kraybill et al., 2005, Williams et al., 2006, Gill et al., 2013). We observed a shorter survival time in the cDLB and cPDD patients compared to cAD patients, which is in agreement with studies comparing patients with AD and DLB alone (Singleton et al., 2002, Stubendorff et al., 2011, Brodaty et al., 2012, Garcia-Ptacek et al., 2014).

The rate of cognitive decline in cAD cases was considerably higher (mean: −7.17, SE ±2.8) compared to mean values of −3.5 (SE ±2.8) for AD, −3.4 (SE ±0.7) for DLB and −5.0 (SE ±0.5) for AD with varying degrees of Lewy body pathology which have been reported previously (Kraybill et al., 2005).

Therefore, additional Lewy body pathology in our cAD group possibly had an aggravating effect on the rate of cognitive decline.

3.5.6 cDLB and cPDD have increased cortical thinning in the parietal lobe

A reduction in cortical thickness was observed in the cDLB and cPDD groups compared to control cases in the parietal lobe. No other differences were observed with other clinical phenotypes in other brain regions. In 2014, Watson and colleagues used MRI to determine patterns of cortical thinning in DLB, AD and control subjects and found DLB cases displayed focal patches of cortical thinning mainly affecting posterior structures including inferior parietal, posterior cingulate and fusiform gyrus (Watson et al., 2014). Another MRI study demonstrated the susceptibility of the parietal lobe to cortical thinning in DLB, in addition to other regions such as pericalcarine and lingual gyri, cuneus, and precuneus (Delli Pizzi et al., 2014). Furthermore, comparisons between AD and DLB indicated an increased cortical thinning in the superior parietal gyrus in the DLB group compared to the control group. Although in the current study, the only difference in cortical thickness was observed between cDLB and cPDD in the parietal lobe when compared to controls, several explanations could account for this. Firstly, difference in study design may be a factor as the two studies described were both MRI studies whereas the current study is neuropathological, and while every effort was made to standardise tissue section preparation there may have been slight variation in processing the tissue which may have an impact on tissue shrinkage and therefore cortical thickness measurements. Cohort size may also explain lack of differences between cAD and control cases. Group sizes in the current study were: cAD n=8, cDLB n=8 and cPDD n=3 which is relatively small. Both MRI studies utilised cohort numbers more than double in size could account for the lack of differences observed. In the future, larger cohort size may reveal more differences in cortical thickness as measured neuropathological, between cAD, cDLB, cPDD and controls.

3.5.7 APOE genotype

No significant differences in were observed in *APOE* genotype or allele frequency between cAD, cDLB and cPDD groups. The *APOE* ε4 allele is the strongest genetic risk factor for the development of AD (Strittmatter et al., 1993, Farrer et al., 1997, Meyer et al., 1998). Up to 65 % of all pathologically confirmed AD cases carry at least one ε4 allele and 12–15 % are homozygous for ε4 compared to 1–3 % of healthy individuals (Farrer et al., 1997, Blacker and Tanzi, 1998). *APOE* ε4 has also been suggested as a risk factor for DLB (Tsuang et al., 2005, Berge et al., 2014) but there is a relative lack of ε4 homozygotes in DLB compared to AD (Singleton et al., 2002). In a large clinical cohort (n = 1318), Berge and colleagues recently reported a lower *APOE* ε4 allele frequency in DLB (32 %) than in AD (43 %) (Berge et al., 2014). By contrast in cases which show both AD and Lewy body pathology, *APOE* ε4 allele frequencies of up to 47 % have been reported (Tsuang et al., 2005) and the high *APOE* ε4 allele frequencies of 44.4 % in our mixed AD/DLB cases could at least partly explain the presence of AD pathology. Of note, none of our mixed AD/ DLB cases had an *APOE* ε2 allele.

3.5.8 Limitations

A limitation of this study is the small sample size (cAD n=8, cDLB n=8 and cPDD n=3). Concomitant pathology is frequent in brains diagnosed with neurodegenerative diseases, but cases that have sufficient pathology fulfil the criteria for both AD and DLB are limited. All of the cases from the NBTR that fulfilled neuropathological criteria for both AD and DLB were included in this study. Tissue from other brain banks was not requested as potential variability in gross dissection methods could not guarantee consistency in sampled regions.

Due to the population demographics of the North East of England being mainly white caucasian, the results of this study are not representative of a worldwide population. Indeed, differences have been found in the prevalence of mixed pathologies between different ethic groups, with a recent study by Barnes and colleagues reporting that mixed pathology is more likely in black descendants when matched for age, sex, education and cognition compared to white descendants (Barnes et al., 2015).

3.6 Conclusion

In conclusion, in cases that by semi-quantitative assessment showed severe degrees of both AD and Lewy body pathology and thus were neuropathologically diagnosed as mixed AD/DLB quantitative assessment revealed differences in the amount of pathological protein aggregates between different clinical phenotypes, in particular significantly higher HP-τ loads in cases with a clinical AD phenotype. Hence, our findings emphasise the important role of quantitative assessment in clinicopathological correlative studies as it is becoming increasingly clear that multiple pathological lesions frequently co-exist the brains of the ageing population (Ince, 2001, Jellinger, 2007a, Schneider et al., 2007, Kovacs et al., 2008, Sonnen et al., 2010, Attems and Jellinger, 2013a, Kovacs et al., 2013, Attems et al., 2014a). However, quantitative studies on larger cohorts are warranted to further elucidate the relative contribution of underlying neuropathological changes towards the clinical picture.

Chapter 4 - Investigating the pathological correlate of motor dysfunction in dementia with Lewy bodies and Parkinson's disease dementia

4.1 Introduction

Deficits in motor control as a result of degeneration of the nigro-striatal pathway and motor circuitry is common to both DLB and PDD. The loss of dopaminergic neurones in the SN pars compacta that project to the striatum, the loss of nerve terminals in the striatum (Bernheimer et al., 1973, Hornykiewicz and Kish, 1987) and the presence of LBs are all common neuropathological features of Lewy body diseases (Schulz-Schaeffer, 2010). In addition to α-syn inclusions, DLB and PDD exhibit co-pathologies more frequently associated with AD (i.e. HP-τ *and* Aβ) .

Dopaminergic abnormalities, including striatal transporter loss have been reported *in vivo* in DLB and PDD using PET (Hu et al., 2000) and SPECT (Donnemiller et al., 1997, O'Brien et al., 2004), and to date provide the best pathological correlate of motor dysfunction in LBD.

A previous study by Colloby and colleagues (Colloby et al., 2012) investigated the relative contributions of dopaminergic neuronal loss and the presence of pathologies associated with AD and LBD on imaging changes as seen in ^{123}I-N-fluoropropyl-2b-carbomethoxy-3b-(4-iodophenyl) nortropane single photon emission computed tomography (^{123}I-FP-CIT SPECT) in a cohort of LBD cases. Their results suggested that a reduced uptake in vivo was influenced by nigral dopaminergic neuronal loss (as measured by quantitatively assessing nigral neuronal density) rather than the presence of pathological lesions related to AD or LBD.

In 2002, Duda and colleagues proposed accumulation of α-syn in the striatum was the underlying pathology associated with parkinsonism seen in LB disorders (Duda et al., 2002) however, a semi-quantitative study conducted by Parkkinen and colleagues did not detect any associations between α-syn and motor dysfunction (Parkkinen et al., 2005).

It has been recently demonstrated that combined pathology scores of α-syn, Aβ and HP-τ contribute to cognitive decline as measured by MMSE in LBDs (Howlett et al., 2014). It is therefore hypothesised that as α-syn, Aβ and HP-τ can contribute to neural death in neurodegenerative diseases (Loo et al., 1993, Cookson and van der Brug, 2008, Di et al., 2016) the increased presence of all pathologies will have a detrimental effect on motor function. The motor circuit is comprised of multiple components including the SN, external globus pallidus, thalamus, striatum and motor cortex and so it is plausible that several of these regions may be affected by multiple pathologies and have downstream effects. Therefore, the aim of this study was to investigate if combined pathologies in the nigro-striatal pathway and associated brain regions are associated with motor dysfunction in DLB and PDD.

4.2 Aims

The specific aims of the study were:

- To investigate if quantification of individual pathology scores (IPS) or combined pathology scores (CPS) are associated with motor dysfunction as measured by UPDRS part III in DLB and PDD.

- To investigate the pathological burden of HP-τ, Aβ and α-syn in regions involved in the nigrostriatal pathway in relation to cortical and limbic pathology loads in DLB and PDD.

4.3 Methods

4.3.1 Study cohort

Brain tissue from 44 cases (mean age 76.40 SE: ±0.84 years; male 29; female 15) from the NBTR were used in this study; consisting of 23 DLB cases and 21 PDD cases. Patient demographics are available in table 4.1. UPDRS part III scores recorded closest to death were used in the analyses.

Case Number	Disease category	Age	Sex	PM delay (hours)	Fixation length (weeks)	Braak stage	Thal phase	CERAD	McKeith
25	DLB	89	M	88	85	3	NA	Sparse	Neocortical
26	DLB	88	F	16	12	3	NA	Moderate	Neocortical
27	DLB	78	F	120	7	5	NA	Frequent	Diffuse
28	DLB	75	F	64	5	6	NA	Frequent	Diffuse
29	DLB	75	M	18	3	2	NA	Negative	Limbic
30	DLB	77	M	29	4	2	NA	Moderate	Neocortical
31	DLB	78	F	96	5	3	NA	Sparse	Neocortical
32	DLB	91	F	84	3	5	NA	Frequent	Limbic
33	DLB	75	F	78	7	6	NA	Frequent	Neocortical
34	DLB	71	M	68	4	3	NA	Sparse	Neocortical
35	DLB	78	M	83	7	1	NA	Negative	Limbic
36	DLB	76	M	76	41	2	NA	Sparse	Neocortical
37	DLB	70	M	50	50	2	NA	Negative	Neocortical
38	DLB	74	M	42	8	4	NA	Sparse	Neocortical
39	DLB	77	M	8	4	2	0	Negative	Neocortical
40	DLB	71	M	8	10	2	1	Sparse	Neocortical
41	DLB	72	M	89	14	3	0	Negative	Neocortical
42	DLB	77	M	46	13	3	0	Negative	Neocortical
43	DLB	81	F	44	11	4	1	Moderate	Neocortical
44	DLB	73	F	99	9	3	3	Negative	Neocortical
45	DLB	78	M	8	13	3	3	Moderate	Neocortical
46	DLB	81	M	24	5	4	NA	Sparse	Neocortical
47	DLB	81	M	26	8	3	3	Moderate	Neocortical
48	PDD	69	M	17	6	2	NA	Negative	Limbic
49	PDD	69	F	46	6	2	NA	Negative	Neocortical
50	PDD	69	M	96	4	0	NA	Negative	Neocortical
51	PDD	81	M	40	10	2	NA	Negative	Neocortical
52	PDD	79	M	64	6	4	NA	Negative	Neocortical
53	PDD	75	M	40	5	3	NA	Sparse	Diffuse
54	PDD	78	M	48	6	3	NA	Negative	Limbic
55	PDD	79	M	30	4	3	NA	Sparse	Neocortical
56	PDD	77	M	17	6	2	NA	Negative	Neocortical
57	PDD	68	M	11	4	5	NA	Frequent	Neocortical
58	PDD	68	F	69	20	3	NA	Negative	Neocortical
59	PDD	75	M	28	18	5	NA	Frequent	Neocortical
60	PDD	73	M	31	5	0	NA	Negative	Limbic
61	PDD	75	M	83	5	1	NA	Negative	Neocortical
62	PDD	70	F	9	4	4	NA	Moderate	Neocortical
63	PDD	74	M	34	7	4	NA	Frequent	Neocortical
64	PDD	87	F	60	18	3	2	Negative	Neocortical
65	PDD	75	F	18	8	3	4	Moderate	Neocortical
66	PDD	83	M	71	9	4	5	Moderate	Neocortical
67	PDD	86	M	44	10	3	4	Moderate	Neocortical
68	PDD	76	M	68	8	3	1	Negative	Neocortical

Table 4.1 Demographics of the study cohort. Abbreviations: PM, post-mortem; CERAD, Consortium to Establish a Registry for Alzheimer's Disease; DLB, dementia with Lewy bodies; NA, not available; PDD, Parkinson's disease dementia.

4.3.2 Tissue preparation

An in-house TMA methodology was developed as described in section 2.6. The brain regions used specifically in this study were motor cortex, striatum (inclusive of caudate and putamen), external globus pallidus, thalamus and SN (diagnostic slide as described in section 2.4.2). To assess the distribution of pathology in the nigrostriatal pathway in relation to cortical and limbic pathology frontal, temporal, parietal and occipital cortices, cingulate cortex and entorhinal cortex were used included from the TMA block as described in section 2.6.

4.3.3 Immunohistochemistry

Tissue sections taken from the paraffin TMA block from each case were stained with antibodies against HP-τ (AT8), Aβ (4G8) and α-syn as described in section 2.9.

4.3.4 Quantification of pathological protein aggregates

TMA sections were analysed on a Nikon Eclipse 90i microscope coupled with NIS-Elements AR3.2 software as described in section 2.11.2. The diagnostic slides containing SN were analysed as described in section 2.11.1 The percentage are covered by immunopositivity was calculated all regions.

4.3.5 Calculation of IPS and CPS

The percentage area covered by immunopositivity for each aggregate was taken as the IPS for each region (i.e. % α-syn immunopositivity alone), and summation of 2 or 3 IPS were calculated of all possible pathology combinations to provide the CPS (i.e. % α-syn immunopositivity + % Aβ immunopositivity, see tables 4.2-4.4 for all pathology combinations).

4.3.6 Statistical analyses

Variables were tested for normality using the Kolmogorov-Smirnov Test test and visual inspection of variable histograms. As data was not normally distributed non-parametric tests were employed. To determine whether associations existed between IPS and CPS associated with end stage motor dysfunction as measured by UPDRS III, Spearman's rank correlation analyses were performed in the whole LBD cohort, then separately in PDD and DLB. Tissue sections containing SN was only available in 3 DLB cases that had corresponding

UPDRS scores, therefore correlations between IPS and CPS with UPDRS III were not investigated in this region. Finally, multiple regression analyses were performed to investigate the neuropathological predictors of motor dysfunction.

4.4 Results

4.4.1 No associations between IPS or CPS with UPDRS III in whole cohort

In the whole cohort, Spearman's rank correlation analysis revealed no correlation between any of the IPS or CPS with end stage UPDRS III in motor cortex, striatum, external globus pallidus, thalamus or SN (table 4.2). In addition, multiple regression analysis revealed no pathological predictors of end stage UPDRS III in the whole cohort.

Region	Pathology	Endstage UPDRS III
Motor cortex	α-syn	r_s = 0.186, p = 0.385
	HP-$_T$	r_s = -0.133, p = 0.518
	Aβ	r_s = 0.016, p = 0.937
	α-syn + HP-$_T$	r_s = 0.007, p = 0.976
	α-syn + Aβ	r_s = 0.288, p = 0.182
	Aβ + HP-$_T$	r_s = -0.050, p = 0.808
	α-syn + HP-$_T$ + Aβ	r_s = -0.017, p = 0.937
Striatum	α-syn	r_s = 0.019, p = 0.930
	HP-$_T$	r_s = -0.214, p = 0.294
	Aβ	r_s = 0.218, p = 0.274
	α-syn + HP-$_T$	r_s = -0.270, p = 0.194
	α-syn + Aβ	r_s = 0.159, p = 0.447
	Aβ + HP-$_T$	r_s = 0.022, p = 0.915
	α-syn + HP-$_T$ + Aβ	r_s = 0.031, p = 0.884
External globus pallidus	α-syn	r_s = 0.255, p = 0.265
	HP-$_T$	r_s = -0.214, p = 0.294
	Aβ	r_s = -0.177, p = 0.407
	α-syn + HP-$_T$	r_s = 0.064, p = 0.79
	α-syn + Aβ	r_s = 0.116, p = 0.618
	Aβ + HP-$_T$	r_s = -0.156, p = 0.5
	α-syn + HP-$_T$ + Aβ	r_s = -0.061, p = 0.799
Thalamus	α-syn	r_s = -0.14, p = 0.946
	HP-$_T$	r_s = -0.087, p = 0.661
	Aβ	r_s = 0.178, p = 0.374
	α-syn + HP-$_T$	r_s = -0.043, p = 0.478
	α-syn + Aβ	r_s = 0.124, p = 0.547
	Aβ + HP-$_T$	r_s = 0.041, p = 0.841
	α-syn + HP-$_T$ + Aβ	r_s = 0.06, p = 0.77
Substantia nigra	α-syn	r_s = -0.162, p = 0.728
	HP-$_T$	r_s = -0.144, p = 0.758
	Aβ	r_s = -0.491, p = 0.263
	α-syn + HP-$_T$	r_s = -0.257, p = 0.728
	α-syn + Aβ	r_s = -0.486, p = 0.329
	Aβ + HP-$_T$	r_s = -0.638, p = 0.173
	α-syn + HP-$_T$ + Aβ	r_s = -0.257, p = 0.623

Table 4.2 Spearman's rank (r_s) correlations between individual and combined pathology scores and end stage UPDRS III scores in the whole cohort. Abbreviations: UPDRS, Unified Parkinson's Disease Rating Scale; α-syn, α-synuclein; HP-$_T$, hyperphosphorylated tau; Aβ, amyloid β.

4.4.2 Associations of IPS snd CPS with UPDRS III in DLB cases

With respect the DLB group, significant positive correlations were seen between IPS of Aβ and UPDRS III in the striatum (r_s = 0.637, $p<0.05$) and thalamus (r_s = 0.725, $p<0.01$). A CPS of Aβ and α-syn also positively correlated with UPDRS III in the striatum (r_s = 0.636, $p<0.05$) and thalamus (r_s = 0.795, $p<0.01$). A positive correlation between a CPS of α-syn + HP-$_T$ + Aβ was observed in the thalamus (r_s = 0.585, $p<0.05$) Table 4.3

There were no pathological predictors of with IPS or CPS with UPDRS III in the DLB group.

4.4.3 Associations of IPS snd CPS with UPDRS III in PDD cases

In the PDD group only an IPS score of HP-$_T$ positively correlated with UPDRS III in the external globus pallidus (r_s = 0.678, $p<0.05$). No other associations were observed between IPS and CPS with UPDRS III in any other region Table 4.4

There were no pathological predictors (IPS or CPS) of UPDRS III in the PDD cohort.

Region	Pathology	Endstage UPDRS III
Motor cortex	α-syn	r_s = 0.288, p = 0.391
	HP-$_T$	r_s = -0.03, p = 0.927
	Aβ	r_s = 0.344, p = 0.274
	α-syn + HP-$_T$	r_s = -0.011, p = 0.973
	α-syn + Aβ	r_s = 0.470, p = 0.144
	Aβ + HP-$_T$	r_s = 0.924, p = 0.353
	α-syn + HP-$_T$ + Aβ	r_s = 0.278, p = 0.278
Striatum	α-syn	r_s = -0.060, p = 0.854
	HP-$_T$	r_s = -0.249, p = 0.412
	Aβ	r_s = 0.637, p = 0.014*
	α-syn + HP-$_T$	r_s = -0.11, p = 0.937
	α-syn + Aβ	r_s = 0.636, p = 0.026*
	Aβ + HP-$_T$	r_s = 0.466, p = 0.109
	α-syn + HP-$_T$ + Aβ	r_s = 0.438, p = 0.155
External globus pallidus	α-syn	r_s = 0.355, p = 0.314
	HP-$_T$	r_s = -0.229, p = 0.474
	Aβ	r_s = 0.014, p = 0.964
	α-syn + HP-$_T$	r_s = -0.132, p = 0.717
	α-syn + Aβ	r_s = 0.189, p = 0.601
	Aβ + HP-$_T$	r_s = -0.386, p = 0.241
	α-syn + HP-$_T$ + Aβ	r_s = -0.406, p = 0.244
Thalamus	α-syn	r_s = 0.117, p = 0.716
	HP-$_T$	r_s = -0.214, p = 0.482
	Aβ	r_s = 0.725, p = 0.005*
	α-syn + HP-$_T$	r_s = -0.320, p = 0.340
	α-syn + Aβ	r_s = 0.795, p = 0.002*
	Aβ + HP-$_T$	r_s = 0.492, p = 0.087
	α-syn + HP-$_T$ + Aβ	r_s = 0.585, p = 0.046*

Table 4.3 Spearman's rank (r_s) correlations between individual and combined pathology scores and end stage UPDRS III scores in DLB cases. Abbreviations: UPDRS, Unified Parkinson's Disease Rating Scale; α-syn, α-synuclein; HP-*T*, hyperphosphorylated tau; Aβ, amyloid β. * signifies a significant result.

Region	Pathology	Endstage UPDRS III
Motor cortex	α-syn	r_s = 0.102, p = 0.740
	HP-$_T$	r_s = -0.010, p = 0.973
	Aβ	r_s = 0.007, p = 0.982
	α-syn + HP-$_T$	r_s = 0.209, p = 0.492
	α-syn + Aβ	r_s = 0.396, p = 0.203
	Aβ + HP-$_T$	r_s = -0.085, p = 0.773
	α-syn + HP-$_T$ + Aβ	r_s = 0.088, p = 0.775
Striatum	α-syn	r_s = -0.011, p = 0.972
	HP-$_T$	r_s = 0.105, p = 0.733
	Aβ	r_s = 0.050, p = 0.872
	α-syn + HP-$_T$	r_s = -0.220, p = 0.470
	α-syn + Aβ	r_s = -0.036, p = 0.908
	Aβ + HP-$_T$	r_s = 0.044, p = 0.887
	α-syn + HP-$_T$ + Aβ	r_s = 0.11, p = 0.972
External globus pallidus	α-syn	r_s = 0.055, p = 0.872
	HP-$_T$	r_s = 0.678, p = 0.031*
	Aβ	r_s = -0.278, p = 0.382
	α-syn + HP-$_T$	r_s = 0.451, p = 0.191
	α-syn + Aβ	r_s = 0.187, p = 0.581
	Aβ + HP-$_T$	r_s = 0.506, p = 0.136
	α-syn + HP-$_T$ + Aβ	r_s = 0.620, p = 0.056
Thalamus	α-syn	r_s = -0.047, p = 0.868
	HP-$_T$	r_s = 0.298, p = 0.281
	Aβ	r_s = 0.18, p = 0.952
	α-syn + HP-$_T$	r_s = 0.197, p = 0.481
	α-syn + Aβ	r_s = 0.077, p = 0.794
	Aβ + HP-$_T$	r_s = 0.53, p = 0.858
	α-syn + HP-$_T$ + Aβ	r_s = 0.123, p = 0.675
Substantia nigra	α-syn	r_s = -0.4, p = 0.6
	HP-$_T$	r_s = -0.2, p = 0.8
	Aβ	r_s = -0.316, p = 0.684
	α-syn + HP-$_T$	r_s = -0.4, p = 0.6
	α-syn + Aβ	r_s = -0.8, p = 0.2
	Aβ + HP-$_T$	r_s = -0.4, p = 0.6
	α-syn + HP-$_T$ + Aβ	r_s = -0.4, p = 0.6

Table 4.4 Spearman's rank (r_s) correlations between individual and combined pathology scores and end stage UPDRS III scores in PDD cases. Abbreviations: UPDRS, Unified Parkinson's Disease Rating Scale; α-syn, α-synuclein; HP-$_T$, hyperphosphorylated tau; Aβ, amyloid β. * signifies a significant result.

4.4.4 Regional distribution of HP-$_T$ pathology

In DLB cases the highest HP-$_T$ load was in the entorhinal cortex (mean 25.37 %, SE ±5.2), followed by parietal cortex (mean 5.85 %, SE ±3.76), temporal cortex (mean 5.08 %, SE ±2.87), motor cortex (mean 4.5 %, SE ±3.27), occipital cortex (mean 4.24 %, SE ±3.31), cingulate cortex (mean 3.41 %, SE ±2.02), striatum (mean 2.68 %, SE ±2.14), thalamus (mean 1.8 %, SE ±1.24), frontal cortex (mean 1.71 %, SE ±1.5), external globus pallidus (mean 1.43 %, SE ±1.23) and SN (mean 0.4 %, SE ±0.07) Figure 4.1a

HP-$_T$ distribution was similar in PDD cases with entorhinal exhibiting the highest HP-$_T$ load (mean 15.14 %, SE ±4.98), followed by parietal cortex (mean 5.04 %, SE ±3.92), temporal cortex (mean 6.33 %, SE ±3.68), cingulate cortex (mean 3.48 %, SE ±3.1), occipital cortex (mean 2.79 %, SE ±2.68), frontal cortex (mean 2.59 %, SE ±2.49), striatum (mean 1.94 %, SE ±1.8), motor cortex (mean 0.4 %, SE ±0.21), external globus pallidus (mean 1.8 %, SE ±1.24), SN (mean 0.26 %, SE ±0.13) and thalamus (mean 0.24 %, SE ±0.13) Figure 4.1a.

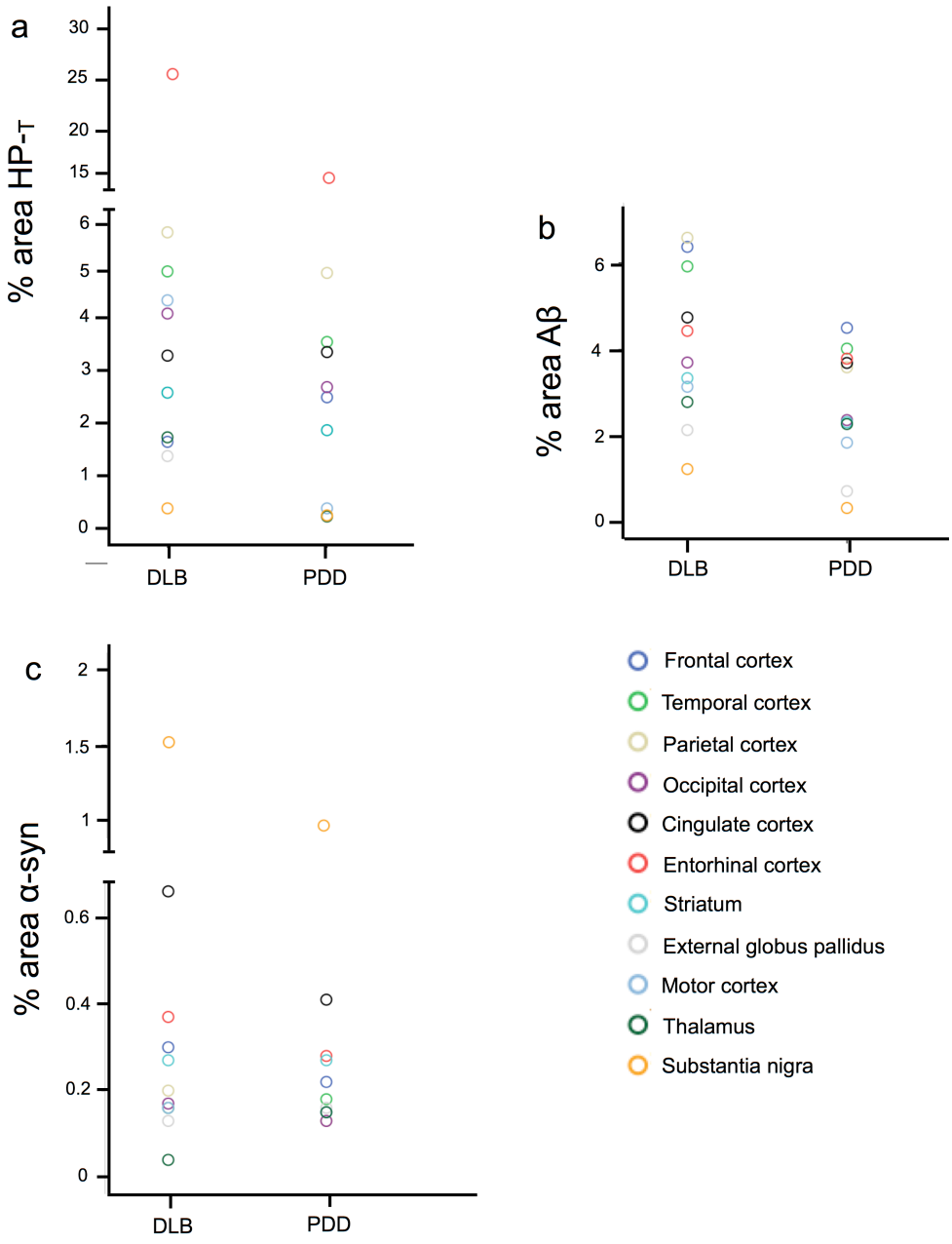

Figure 4.1 Regional distribution of HP-T, Aβ and α-syn pathologies in DLB and PDD.

4.4.5 Regional distribution of Aβ pathology

The parietal lobe exhibited the highest Aβ load in the DLB cases (mean 6.58 %, SE ±1.74) followed by frontal cortex (mean 6.37 %, SE ±1.36), temporal cortex (mean 5.09 %, SE ±1.56), cingulate cortex (mean 4.74 %, SE ±0.99), entorhinal cortex (mean 4.42 %, SE ±0.74), occipital cortex (mean 3.7 %, SE ±0.81), striatum (mean 3.34 %, SE ±0.98), thalamus (mean 3.14 %, SE ±1.21), motor cortex (mean 2.79 %, SE ±0.81), external globus pallidus (mean 2.12 %, SE ±1.29) and SN (mean 1.24 %, SE ±0.62) Figure 4.1b

In PDD cases frontal cortex exhibited the highest Aβ load (mean 4.9 %, SE ±1.0), temporal cortex (mean 4.02 %, SE ±0.87), entorhinal cortex (mean 3.78 %, SE ±0.71), cingulate cortex (mean 3.67 %, SE ±0.98), parietal cortex (mean 3.59 %, SE ±1.0), occipital cortex (mean 2.37 %, SE ±0.7), striatum (mean 2.32%, SE ±0.93), motor cortex (mean 2.28 %, SE ±0.95), thalamus (mean 1.85%, SE ±0.86), external globus pallidus (mean 0.73 %, SE ±0.44), and SN (mean 0.34 %, SE ±0.13) Figure 4.1b

4.4.6 Regional distribution of α-syn pathology

In DLB cases α-syn pathology was highest in the SN (mean 1.52 %, SE ±0.67) followed by cingulate cortex (mean 0.66 %, SE ±0.32), entorhinal cortex (mean 0.37 %, SE ±0.08), frontal cortex (mean 0.3 %, SE ±0.11), striatum (mean 0.27 %, SE ±0.07), parietal cortex (mean 0.2 %, SE ±0.06), occipital cortex (mean 0.17 %, SE ±0.06), temporal cortex (mean 0.16 %, SE ±0.04), motor cortex (mean 0.16 %, SE ±0.04), thalamus (mean 0.18 %, SE ±0.2), and external global pallidus (mean 0.13 %, SE ±0.02) Figure 4.1c

In PDD cases the SN exhibited the highest α-syn load (mean 0.97 %, SE ±0.39), followed by cingulate cortex (mean 0.41 %, SE ±0.11), entorhinal cortex (mean 0.28 %, SE ±0.06), striatum (mean 0.27 %, SE ±0.08), frontal cortex (mean 0.22 %, SE ±0.07), temporal cortex (mean 0.18 %, SE ±0.05), external globus pallidus (mean 0.16 %, SE ±0.03) motor cortex (mean 0.15 %, SE ±0.06), parietal cortex (mean 0.13 %, SE ±0.05), thalamus (mean 0.15 %, SE ±0.05) and lowest in the occipital cortex (mean 0.13 %, SE ±0.05). Figure 4.1c

4.5 Discussion

The present study revealed no relationship between single pathological lesions (α-syn, HP-$_T$ or Aβ) or a combination of pathologies on motor dysfunction as measured by UPDRS III in the combined cohort of LBD cases. However when looking at disease specific associations, in DLB cases, Aβ and a combination of Aβ + α-syn positively correlated with severity of motor impairment in the striatum and thalamus. Furthermore, a combination of all three pathologies (Aβ + α-syn and HP-$_T$) positively correlated with motor dysfunction in the thalamus. In contrast no such relationships between Aβ and Aβ + α-syn were observed in PDD where only HP-$_T$ was shown to positively correlate with motor impairment in the external globus pallidus.

Extrapyramidal symptoms are a cardinal feature of PDD and are a common occurrence in DLB cases, with severity of EPS correlating with age, duration of disease and cognitive impairment in PD but not DLB (Aarsland et al., 2001b). There is selective vulnerability of neuronal populations to degeneration and α-syn pathology. Projection neurones with long, thin and sparsely or unmyelinated axons in particular glutamatergic, GABAergic, dopaminergic, serotonergic and cholinergic populations are vulnerable (Dickson et al., 2009) in particular those encompassed in the nigro-striatal pathway.

4.5.1 α-syn in isolation does not associate with motor dysfunction

Accumulations of α-syn are the hallmark pathological lesions associated with LBD and are present in the nigro-striatal pathway. The role of α-syn in degeneration of the nigro-stiatal pathway is unclear. Kirk and colleagues expressed wild-type and A53T mutated α-syn in the nigro-striatal dopamine neurones of adult rats using recombinant adeno-associated viral vectors for up to six months (Kirik et al., 2002). Pathological alterations including cytoplasmic inclusions positive for α-syn developed in nigral dopaminergic neurones and motor impairments in combination with a dopaminergic neuronal cell loss exceeding 50-60%. Studies conducted in α-syn knockout mice demonstrated no changes in brain architecture or survival (Chandra et al., 2004) with mice possessing a normal complement of dopaminergic cell bodies, fibres and synapses (Abeliovich et al., 2000). However, α-syn null mice display functional deficits in the nigro-striatal dopamine system, suggesting physiological α-syn

may be a activity dependant negative regulator of dopamine (Abeliovich et al., 2000). Results from the current study suggest accumulation of α-syn in isolation in the nigrostriatal pathway and associated regions is not associated with motor impairments. It might therefore be more likely that loss of physiological α-syn may be responsible for impairments in the nigro-striatal pathway. Quantification of dopaminergic neurones and dopamine transporters were not included in this study and are required to further investigate this.

4.5.2 Aβ may associate with motor impairment in DLB

In the DLB cohort Aβ was found to correlate with motor impairment, although this association was not apparent in PDD cases. The association between between Aβ deposition and nigro-striatal degeneration is essentially unknown. Several studies have suggested Aβ may be related to EPS attributed to nigro-striatal dysfunction. Itoh and colleagues investigated the effects of Aβ protein infusion on neurotransmitter release by using an *in vivo* brain microdialysis method (Itoh et al., 1996). Dopamine release was found to be reduced in Aβ protein-infused rats compared to vehicle- infused rats. Furthermore, Perez and colleagues reported a close association between Aβ deposition and nigro-striatal pathology in transgenic mice harbouring familial AD (FAD)-linked *APP*swe/PS1ΔE9 (Perez et al., 2005). Using high performance liquid chromatography they found a reduction in the dopamine metabolite 3,4-dihydroxyphenylacetic acid (DOPAC) implicating a potential role for Aβ in nigral-striatal degeneration. In addition, it has been suggested that in LBD, the dying - back process originating in the striatum may contribute to neurodegeneration (Hornykiewicz, 1998, Cheng et al., 2010). Axonal transport dysfunction, which is highly associated with Aβ aggregates (Hiruma et al., 2003, Rui et al., 2006, Wang et al., 2010) is thought to activate the retrograde demyelination and fragmentation of the axon from the distal end and spreads retrogradely towards the cell soma (Coleman, 2005, Conforti et al., 2014). Loss of dopaminergic neurones by this mechanism might therefore contribute to EPS frequently seen in DLB cases in the presence of Aβ aggregates.

4.5.3 Combined pathologies may associate with motor impairment in DLB

The impact of multiple pathologies on the clinical phenotype is of current interest as Howlett and colleagues demonstrated the summation of semi-quantitative pathology scores in human cerebral cortex, particularly BA9 and BA21, is a better predictor of cognitive decline compared to the assessment of single lesions (Howlett et al., 2014). In the current study CPS of α-syn + Aβ in DLB cases associated with UPDRS III scores in the striatum and thalamus. In both regions this association is most likely driven by the Aβ IPS as the level of significance drops slightly with the addition of α-syn in the striatum ($p = 0.014$ to $p = 0.026$), however the association became slightly more significant with the addition of α-syn in the thalamus ($p = 0.005$ to $p = 0.002$). An association between and α-syn + Aβ + HP-$_T$ and UPDRS III was also observed in the thalamus in DLB cases, however the addition of HP-$_T$ to α-syn + Aβ lowered the significance level to $p=0.46$, questioning the contribution of HP-$_T$ to this association.

4.5.4 Regional distributions of pathologies in DLB and PDD

When assessing the regional distributions of pathologies in relation to cortical and limbic pathologies no differences were observed in the hierarchical distribution of regional pathologies of Aβ, HP-$_T$ and α-syn between DLB and PDD other than motor cortex exhibited the third highest HP-$_T$ burden whilst in PDD it exhibited the eighth highest HP-$_T$ load. In DLB, motor cortex was more affected by HP-$_T$ pathology than the striatum and other associated motor regions, whilst in PDD it was less affected by HP-$_T$ pathology than these regions although respective differences were not significant. It is therefore unlikely that insights into the differences of EPS onset in relation to dementia can be gained from assessing the quantitative pathological load of Aβ, HP-$_T$ and α-syn and DLB and PDD.

4.5.5 Limitations

The cohort used in this study was limited as it required tissue samples that had corresponding UPDRS III scores recorded during life. As it was a retrospective study not all of the cases had scores for motor dysfunction, and therefore not all of the cases were used in the correlation and regression analyses. UPDRS is used in standard clinical practice as a measure PD progression, however it

does not take into consideration the cognitive status of the patients. Severely demented individuals may have difficulty in following and carrying out commands when being tested with the UPDRS III, therefore UPDRS III scores can be subject to floor and ceiling effects. I have not considered the severity of cognitive decline in this study cohort therefore I cannot comment on their ability to complete the UPDRS III questionnaire, however a revision of the Unified Parkinson's Disease Rating Scale (MDS-UPDRS) by the Movement Disorder Society reported UPDRS was not limited by these floor and ceiling effects and is still considered a valuable tool in the clinical assessment of movement disorders (Goetz et al., 2008).

4.6 Conclusion

This study aimed to investigate the individual and combined effects of Aβ, HP-$_T$ and α-syn on motor dysfunction in LBD patients. Aβ was shown to correlate with UPDRS in DLB individually and in combination with α-syn. However, as none of these measures used in this study were able to independently predict UPDRS III scores, the pathological correlate of motor dysfunction in DLB and PDD is yet to be elucidated.

Chapter 5 - Associations between pyroglutamylated amyloid-β, hyperphosphorylated tau and total β amyloid with α-synuclein pSer-129 and disease severity in LBD

5.1 Introduction

The previous chapters demonstrated how quantitative neuropathological assessment can be a useful tool in clinico-pathological assessments, with the potential to detect previously unidentified subtypes of neurodegenerative diseases that could not be detected using semi-quantitative evaluation and ordinal-type parameters. In addition, results from chapter 4 suggested single types of pathological lesions as well as the combination of multiple pathological lesions may be associated with motor dysfunction in DLB and PDD.

The mechanism by which multiple pathological lesions affect clinical features of disease is poorly understood, however recent studies have suggested a synergistic relationship between HP-$_T$, Aβ and α-syn, hypothesising the mutual promotion and aggregation of each other (Giasson et al., 2003, Lee et al., 2004, Clinton et al., 2010) . Further studies have confirmed this with DLB and PD cases exhibiting a higher level of cortical α-syn aggregates in cases that have Aβ plaques in the cortex compared to those without (Pletnikova et al., 2005, Lashley et al., 2008).

Pyroglutamylated amyloid-β (pE(3)-Aβ) is a type of post-translationally modified Aβ, and research into its involvement in the pathogenesis of neurodegenerative diseases is gathering pace. A study by Nussbaum and colleagues suggested a functional connection between pE(3)-Aβ and HP-$_T$ by demonstrating Aβ oligomers containing pE(3)-Aβ might initiate tau-dependent cytotoxicity (Nussbaum et al., 2012). Furthermore, a study from our group in Newcastle demonstrated an association between pE(3)-Aβ and HP-$_T$ in human *post-mortem* tissue (Mandler et al., 2014). However, a putative association with other pathological protein aggregates has yet to be investigated.

α-syn phosphorylated at serine-129 (pSer129 α-syn) is the predominant post-translational modification of α-syn and has been found to strongly correlate with parenchymal Aβ loads assessed by immunohistochemistry and enzyme-linked immunosorbent assay (ELISA) (Obi et al., 2008, Swirski et al., 2014) .

Interestingly, a study by Swirski and colleagues also demonstrated that exposure of SH-SY5Y cells to Aβ42 significantly increased the proportion of α-syn that was phosphorylated at Ser129. As pE(3)-Aβ seems to be a highly pathogenic protein in AD I hypothesis that pE(3)-Aβ may associate with pSer129 α-syn and cognitive decline in LBD. Degeneration of the frontal and entorhinal cortices has been associated with cognitive decline (DeKosky and Scheff, 1990, Mufson et al., 1999) therefore I hypothesise pE(3)-Aβ may play a role in this. The aim of this investigation was to explore the relationship between Aβ and pSer129 α-syn further by examining relationships between pE(3)-Aβ and pSer129 α-syn and effects on cognitive decline as measured by MMSE in a cohort of LBD cases.

5.2 Aims

The specific aims of this study were: -

- To investigate the differences in pE(3)-Aβ loads between DLB, PDD and PD in multiple brain regions.

- To investigate the putative associations between HP-τ, pE(3)-Aβ, non-pE(3)-Aβ and total Aβ with pSer129 α-syn in multiple brain regions in an LBD cohort Frontal, cingulate and entorhinal cortices all display varying amounts of Aβ so these regions along with the thalamus which displays reduced Aβ pathology will be investigated.

- Determine whether pE(3)-Aβ loads are associated with cognitive decline as measured by MMSE in LBD cases.

5.3 Methods

5.3.1 Study cohort

Brain tissue from 41 donors (mean age 76.21 SE: ±0.97 years; male 30; female 11) from the NBTR were used in this study; consisting of 21 DLB cases, 13 PDD cases and 7 PD cases. Patient demographics are provided in Table 5.1. The final MMSE score recorded before death was used in the analyses.

Case Number	Disease category	Age	Sex	PM delay (hours)	Fixation length (weeks)	Braak stage	Thal phase	CERAD	McKeith
25	DLB	89	M	88	85	3	NA	Sparse	Neocortical
26	DLB	88	F	16	12	3	NA	Moderate	Neocortical
27	DLB	78	F	120	7	5	NA	Frequent	Diffuse
28	DLB	75	F	64	5	6	NA	Frequent	Diffuse
29	DLB	75	M	18	3	2	NA	Negative	Limbic
31	DLB	78	F	96	5	3	NA	Sparse	Neocortical
32	DLB	91	F	84	3	5	NA	Frequent	Limbic
33	DLB	75	F	78	7	6	NA	Frequent	Neocortical
34	DLB	71	M	68	4	3	NA	Sparse	Neocortical
35	DLB	78	M	83	7	1	NA	Negative	Limbic
36	DLB	76	M	76	41	2	NA	Sparse	Neocortical
37	DLB	70	M	50	50	2	NA	Negative	Neocortical
39	DLB	77	M	8	4	2	0	Negative	Neocortical
40	DLB	71	M	8	10	2	1	Sparse	Neocortical
41	DLB	72	M	89	14	3	0	Negative	Neocortical
42	DLB	77	M	46	13	3	0	Negative	Neocortical
43	DLB	81	F	44	11	4	1	Moderate	Neocortical
44	DLB	73	F	99	9	3	3	Negative	Neocortical
45	DLB	78	M	8	13	3	3	Moderate	Neocortical
46	DLB	81	M	24	5	4	NA	Sparse	Neocortical
47	DLB	81	M	26	8	3	3	Moderate	Neocortical
48	PDD	69	M	17	6	2	NA	Negative	Limbic
50	PDD	69	M	96	4	0	NA	Negative	Neocortical
51	PDD	81	M	40	10	2	NA	Negative	Neocortical
53	PDD	75	M	40	5	3	NA	Sparse	Diffuse
54	PDD	78	M	48	6	3	NA	Negative	Limbic
55	PDD	79	M	30	4	3	NA	Sparse	Neocortical
56	PDD	77	M	17	6	2	NA	Negative	Neocortical
57	PDD	68	M	11	4	5	NA	Frequent	Neocortical
58	PDD	68	F	69	20	3	NA	Negative	Neocortical
59	PDD	75	M	28	18	5	NA	Frequent	Neocortical
60	PDD	73	M	31	5	0	NA	Negative	Limbic
62	PDD	70	F	9	4	4	NA	Moderate	Neocortical
63	PDD	74	M	34	7	4	NA	Frequent	Neocortical
69	PD	76	M	49	7	1	NA	Sparse	Neocortical
70	PD	82	M	7	4	2	NA	None	Neocortical
71	PD	81	M	52	8	3	0	Negative	Limbic
72	PD	80	M	88	14	1	NA	Sparse	Limbic
73	PD	90	M	18	14	2	0	Negative	Limbic
74	PD	92	F	45	12	1	0	Negative	Limbic
75	PD	70	M	48	7	2	0	Negative	Limbic

Table 5.1 Patient demographics of the study cohort. Abbreviations: PM, *post-mortem*; CERAD, Consortium to Establish a Registry for Alzheimer's Disease; LB, Lewy body; DLB, dementia with Lewy bodies; M, male; NA, not available; F, female; PDD, Parkinson's disease dementia; PD, Parkinson's disease.

5.3.2 Tissue preparation

An in house TMA methodology was developed as described in section 2.6. The brain regions used specifically in this study were frontal, cingulate and entorhinal cortex and thalamus.

5.3.3 Immunohistochemistry

Tissue sections taken from the paraffin TMA block from each case were stained with antibodies against HP-$_T$ (AT8), pE(3)-Aβ (8/4D), total Aβ (4G8) and pSer129 α-syn as described in section 2.9. 8/4D antibody is not commercially available (kindly gifted by Dr M Mandler, Affiris, Vienna). Specificity for this antibody to pE(3)-Aβ was determined by binding to the epitope p(E)FRHDSC, pE(3)-Aβ and absence of reactivity to full length Aβ1-42 or truncated but unmodified Aβ3-42 using peptide ELISAs or Western blots. The 8/4D antibody strongly reacted with pE(3)-Aβ and displayed only minimal cross-reactivity with full length Aβ1-42 and truncated but unmodified Aβ3-42. This lack of reactivity strongly suggests that the 8/4D antibody is highly specific for the pyroglutamate modified AβpE3 peptides whereas other pyroglutamate containing peptides are not detectable (Mandler et al., 2012, Mandler et al., 2014).

5.3.4 Quantification of pathological protein aggregates

TMA sections were analysed on a Nikon Eclipse 90i microscope coupled with NIS-Elements AR3.2 software as described in section 2.11.2 The percentage area covered by immunopositivity was calculated in frontal, cingulate and entorhinal cortices and thalamus.

5.3.5 Immunofluoresence

To investigate if pE(3)-Aβ antibody 8/4D cross-reacts with pSer129 α-syn double immunofluoresence was performed. One fixed tissue section containing frontal cortex from a DLB case was subject to antigen retrieval and stained with both 8/4D and pSer129 α-syn as described in the protocol in section 2.10. Immunofluoresence was visualised using Nikon 90i microscope and DsFi1 camera (Nikon).

5.3.6 Statistical analyses

As data was not normally distributed non-parametric tests were employed. Kruskal-Wallis was employed to determine any group differences in the mean of HP-$_T$, pE(3)-Aβ, total Aβ and pSer129 α-syn between DLB, PDD and PD cases. Where significant differences were observed, post-hoc Mann-Whitney U tests determined specific differences between two groups. To determine whether associations existed between HP-$_T$, pE(3)-Aβ, total Aβ and pSer129 α-syn and cognitive decline as measured by MMSE, Spearman's rank correlation analyses were performed. Finally, multiple regression analyses were performed to investigate the neuropathological predictors of pSer129 α-syn.

5.4 Results

5.4.1 Differences in pE(3)-Aβ, HP-$_T$, total Aβ and pSer129 α-syn between DLB, PDD and PD cases.

Differences in pE(3)-Aβ loads between DLB, PDD and PD cases were investigated with respective differences between HP-$_T$, total Aβ and pSer129 α-syn included for comparison (Table 5.2).

	DLB pE(3)-Aβ (±SE)	PDD pE(3)-Aβ (±SE)	PD pE(3)-Aβ (±SE)	statistic H_{df}, p value
Frontal	0.44 (0.15)	0.26 (0.11)	0.04 (0.02)	H_2 = 6.02, p =0.049
Cingulate	0.54 (0.2)	0.22 (0.07)	0.06 (0.03)	H_2 = 3.71, p =0.157
Thalamus	0.15 (0.06)	0.1 (0.05)	0.11 (0.04)	H_2 = 1.6, p =0.45
Entorhinal	0.29 (0.1)	0.23 (0.06)	0.08 (0.22)	H_2 = 2.89, p =0.24
	DLB HP-$_T$ (±SE)	**PDD HP-$_T$ (±SE)**	**PD HP-$_T$ (±SE)**	**statistic H_{df}, p value**
Frontal	4.41 (2.82)	0.12 (0.04)	0.06 (0.03)	H_2 = 5.64, p =0.06
Cingulate	6.69 (3.62)	0.43 (0.14)	0.1 (0.03)	H_2 = 3.34, p =0.19
Thalamus	1.83 (1.17)	0.13 (0.03)	0.12 (0.06)	H_2 = 5.36, p =0.069
Entorhinal	29.91 (5.72)	15.23 (6.21)	11.09 (6.77)	H_2 = 6.57, p =0.037
	DLB Aβ (±SE)	**PDD Aβ (±SE)**	**PD Aβ (±SE)**	**statistic H_{df}, p value**
Frontal	7.13 (1.49)	3.71 (0.79)	0.28 (0.28)	H_2 = 8.22, p =0.016
Cingulate	5.56 (1.18)	2.92 (0.79)	0.3 (0.3)	H_2 = 6.57, p =0.037
Thalamus	3.59 (1.23)	1.51 (0.96)	0.01 (0.01)	H_2 = 6.08, p =0.048
Entorhinal	4.87 (0.85	3.44 (0.73)	0.36 (0.35)	H_2 = 7.55, p =0.023
	DLB pSer129 α-syn (±SE)	**PDD pSer129 α-syn (±SE)**	**PD pSer129 α-syn (±SE)**	**statistic H_{df}, p value**
Frontal	4.79 (2.18)	3.84 (1.8)	0.56 (0.14)	H_2 = 5.73, p =0.057
Cingulate	19.31 (4.84)	13.22 (4.79)	1.36 (0.31)	H_2 = 9.14, p =0.01
Thalamus	3.45 (1.03)	2.25 (0.23)	1.37 (0.29)	H_2 = 7.67, p =0.022
Entorhinal	15.13 (2.85)	10.9 (3.62)	1.94 (0.34)	H_2 = 12.42, p =0.002

Table 5.2 Overall group differences between pE(3)-Aβ, HP-$_T$, total Aβ and pSer129 α-syn loads between DLB, PDD and PD cases.

There were no differences in pE(3)-Aβ between DLB cases and PDD cases. However, pE(3)-Aβ loads were significantly higher in DLB cases compared to PD cases in the frontal cortex (mean 0.44% SE ±0.16 vs 0.04% SE ±0.02 $p<0.01$) (figure 5.1a). pE(3)-Aβ loads were also significantly higher in the frontal cortex in PDD cases compared to PD cases (mean 0.26% SE ±0.11 vs 0.04% SE ±0.02 $p<0.05$), (figure 5.1a).

HP-τ loads were significantly higher in DLB cases compared to PDD cases in the entorhinal cortex (mean 29.92% SE ±5.72 vs 15.24% SE ±6.21 $p<0.05$) (figure 5.1d)

Compared to PD cases, DLB cases exhibited significantly higher total Aβ loads in the frontal cortex (mean 7.13% SE ±1.49 vs 0.28 SE ±0.27 $p<0.01$), cingulate cortex (mean 5.56% SE ±1.18 vs 0.3% SE ±0.3 $p<0.05$), thalamus (mean 3.59% SE ±1.23 vs 0.01% vs SE ±0.01 $p<0.05$) and entorhinal cortex (mean 4.87% SE ±0.85 vs 0.36% SE ±0.35 $p<0.01$). PDD cases also exhibited significantly higher total Aβ loads in the entorhinal cortex compared to PD cases (mean 3.45% SE ±0.73 vs 0.36% SE ±0.35 $p<0.05$) (Figure 5.1a-d).

pSer129 α-syn loads were significantly higher in DLB compared to PD cases in the cingulate cortex (mean 19.31% SE ±4.83 vs 1.36% SE ±0.31 $p<0.01$), thalamus (mean 3.45% SE ±1.03 vs 1.37% SE ±0.28 $p<0.01$) and entorhinal cortex (mean 15.13% SE ±2.85 vs 1.94% SE ±0.34 $p<0.01$) PDD exhibited significantly higher pSer129 α-syn loads compared to PD cases in the cingulate cortex (mean 13.22% SE ± 4.79 vs 1.36% SE ±0.31 $p<0.05$) and entorhinal cortex (mean 10.9% SE ±3.62 vs 1.94% SE ±0.34 $p<0.01$) (Figure 5.1a-d)

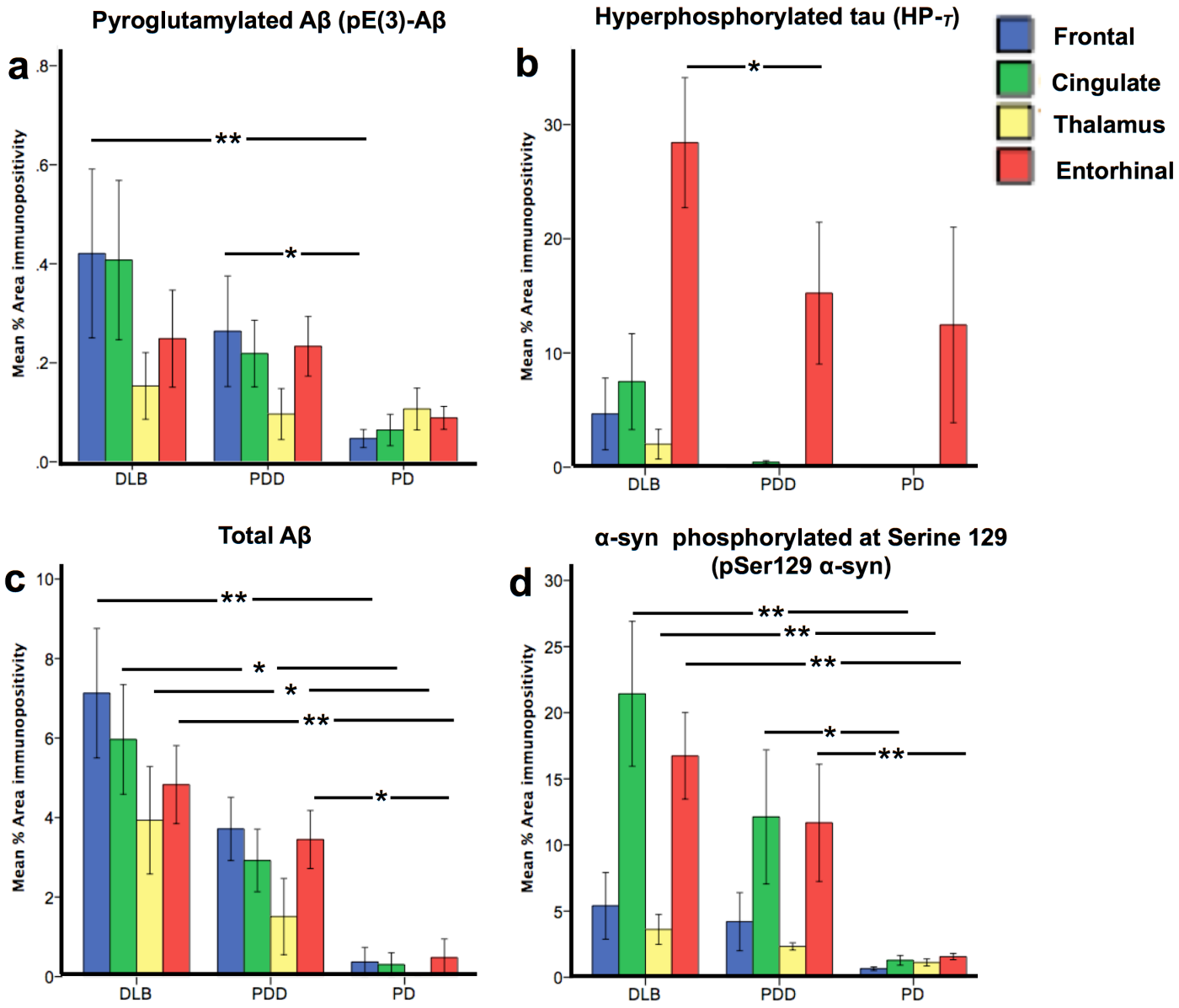

Figure 5.1 Regional differences of pE(3)-Aβ, HP-τ, total Aβ and pSer129 α-syn between DLB, PDD and PD cases.

5.4.2 Whole cohort

5.4.2.1 Correlations between HP-T, pE(3)-Aβ, non-pE(3)-Aβ and total Aβ with pSer129 α-syn.

To gain insight into putative associations between HP-*T*, pE(3)-Aβ and total Aβ with pSer129 α-syn across the whole LBD spectrum DLB, PDD, PD and PD-MCI cases were combined. Two-tailed Spearman's rank correlation analyses were performed in frontal cortex, cingulate cortex, thalamus and entorhinal cortex. To determine whether potential associations between pSer129 α-syn and pE(3)-Aβ were specific and to discount other modifications of Aβ, a non-pE(3)-Aβ fraction was calculated by subtracting regional specific pE(3)-Aβ loads from total Aβ (as measure by 4G8 antibody) and used in correlation analyses.

In the frontal cortex, analysis revealed HP-*T* positively correlated with pSer129 α-syn (r_s = 0.393, $p<0.05$) with no correlations between other aggregates and pSer129 α-syn observed; however an association between pE(3)-Aβ and pSer129 α-syn approached significance (r_s = 0.309, p = 0.056) (Figure 5.2 a-d). HP-*T*, pE(3)-Aβ, non-pE(3)-Aβ and total Aβ all positively correlated with pSer129 α-syn in the cingulate cortex (r_s = 0.645, $p<0.01$; r_s = 0.364, $p<0.05$; r_s = 0.427, $p<0.05$ and r_s = 0.429, $p<0.01$ respectively) (Figure 5.2 e-h). In the thalamus, non-pE(3)-Aβ (r_s = 0.607, $p<0.01$) and total Aβ (r_s = 0.603, $p<0.01$) positively correlated with pSer129 α-syn. An association between pE(3)-Aβ and pSer129 α-syn approached significance (r_s = 0.320, p = 0.05) and no correlation was observed between HP-*T* and pSer129 α-syn (Figure 5.3 a-d). In the entorhinal cortex, HP-*T,* non-pE(3)-Aβ and total Aβ positively correlated with pSer129 α-syn (r_s = 0.693, $p<0.01$; r_s = 0.366, $p<0.05$ and r_s = 0.370, $p<0.05$), however no association was observed between pE(3)-Aβ and pSer129 α-syn (Figure 5.3 e-h).

5.4.2.2 Neuropathological predictors of pSer129 α-syn

To investigate whether HP-*T*, pE(3)-Aβ, non-pE(3)-Aβ and total Aβ were independent predictors of pSer129 α-syn load, multiple regression analyses were performed with pSer129 α-syn as the dependant variable and HP-*T*, pE(3)-Aβ, non-pE(3)-Aβ and total Aβ as independent variables.

In the thalamus, pE(3)-Aβ, non-pE(3)-Aβ and total Aβ independently predicted pSer129 α-syn load (model R^2 = 0.956, F = $167.77_{(4)}$, p<0.01; pE(3)-Aβ β = 0.487, p<0.01; non-pE(3)-Aβ β = 10.45, p<0.01 and total Aβ = 10.68, p<0.01). Conversely, the only significant predictor of pSer129 α-syn load in the entorhinal cortex was HP-*T* pathology (model R^2 = 0.172, F = $2.716_{(4)}$ p<0.05; HP-*T* β = 0.57, p<0.01). No other predictors of pSer129 α-syn were observed in other brain regions within the whole cohort.

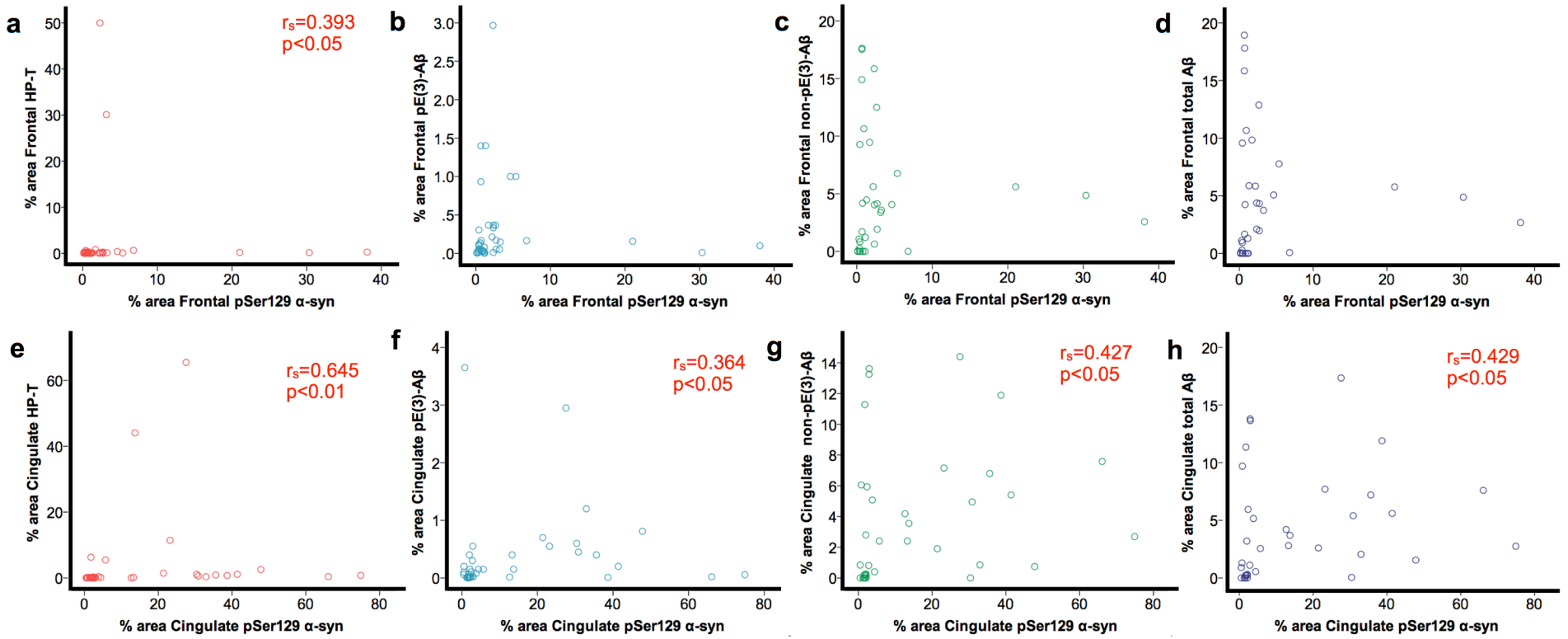

Figure 5.2 Overall cohort correlations between HP-τ, pE(3)-Aβ, non-pE(3)-Aβ and total Aβ with pSer129 α-syn in the frontal cortex **(a-d)** and cingulate cortex **(e-h)**. % area signifies percentage area covered by immunopositivity

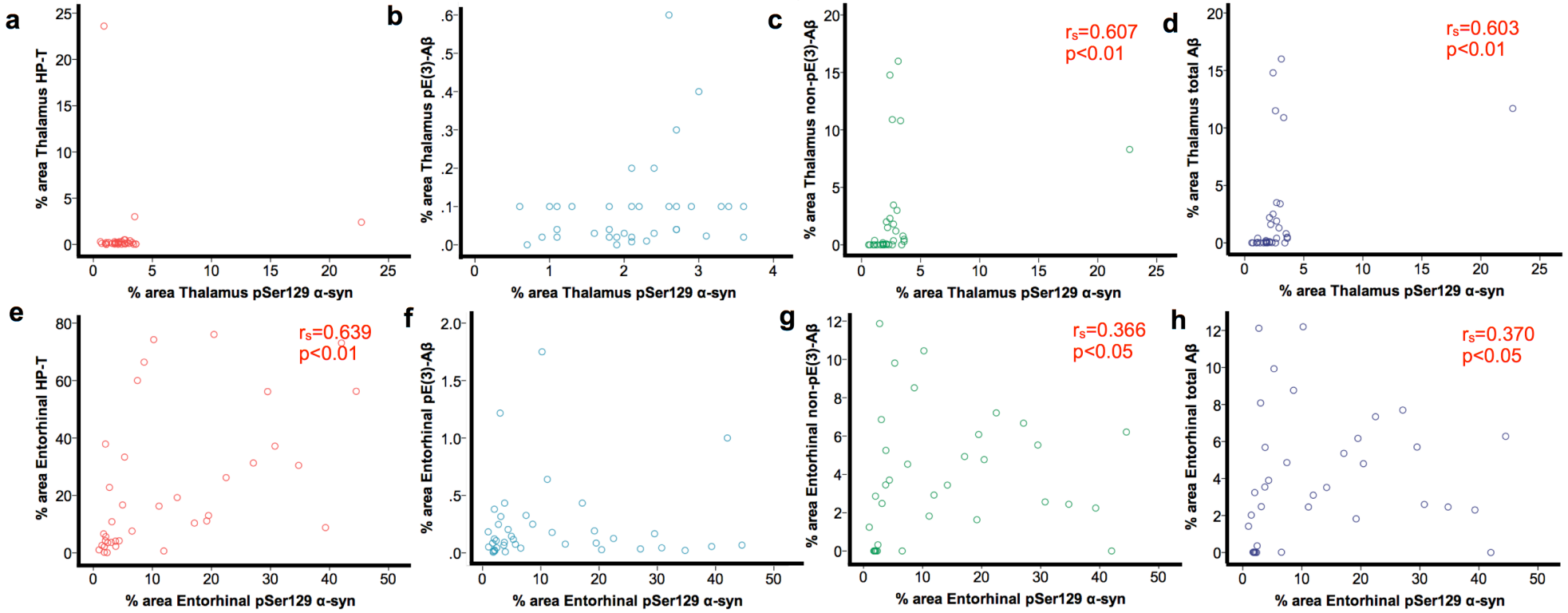

Figure 5.3 Overall cohort correlations between HP-$_T$, pE(3)-Aβ, non-pE(3)-Aβ and total Aβ with pSer129 α-syn in the thalamus **(a-d)** and entorhinal cortex **(e-h)**. % area signifies percentage area covered by immunopositivity

5.4.3 DLB cases

To investigate whether correlations between pathological protein aggregates were disease specific, DLB cases and PDD cases were analysed separately. As there were only 7 PD cases in the cohort, these were excluded form analyses.

5.4.3.1 Correlations between HP-T, pE(3)-Aβ, non-pE(3)-Aβ and total Aβ (Aβ) with pSer129 α-syn.

In the frontal cortex there were no correlations between HP-*T*, pE(3)-Aβ, non-pE(3)-Aβ and total Aβ with pSer129 α-syn, however the correlation between pE(3)-Aβ approached significance (r_s = 0.447, p = 0.055) (Figure 5.4 a-d). In the cingulate cortex only HP-*T* positively correlated with pSer129 α-syn (r_s = 0.483, $p<0.05$) as no other associations were observed between pE(3)-Aβ, non-pE(3)-Aβ and total Aβ with pSer129 α-syn (Figure 5.4 e-h). In the thalamus, positive correlations were observed between non-pE(3)-Aβ and total Aβ with pSer129 α-syn (r_s = 0.483, $p<0.05$ and r_s = 0.490 respectively), but not between HP-*T* and pE(3)-Aβ with pSer129 α-syn (Figure 5.5 a-d). Finally, in the entorhinal cortex a positive correlation was only observed between HP-*T* and pSer129 α-syn (r_s = 0.567, $p<0.05$) and not between pE(3)-Aβ, non-pE(3)-Aβ and total Aβ with pSer129 α-syn (Figure 5.5 e-h).

5.4.3.2 Neuropathological predictors of pSer129 α-syn

Multiple regression analyses revealed pSer129 α-syn load was only predicted by HP-*T* and this association was limited to the entorhinal cortex (model R^2 = 0.406, $F = 2.2254_{(4)}$ $p<0.05$; HP-*T* β = 0.529, $p<0.05$).

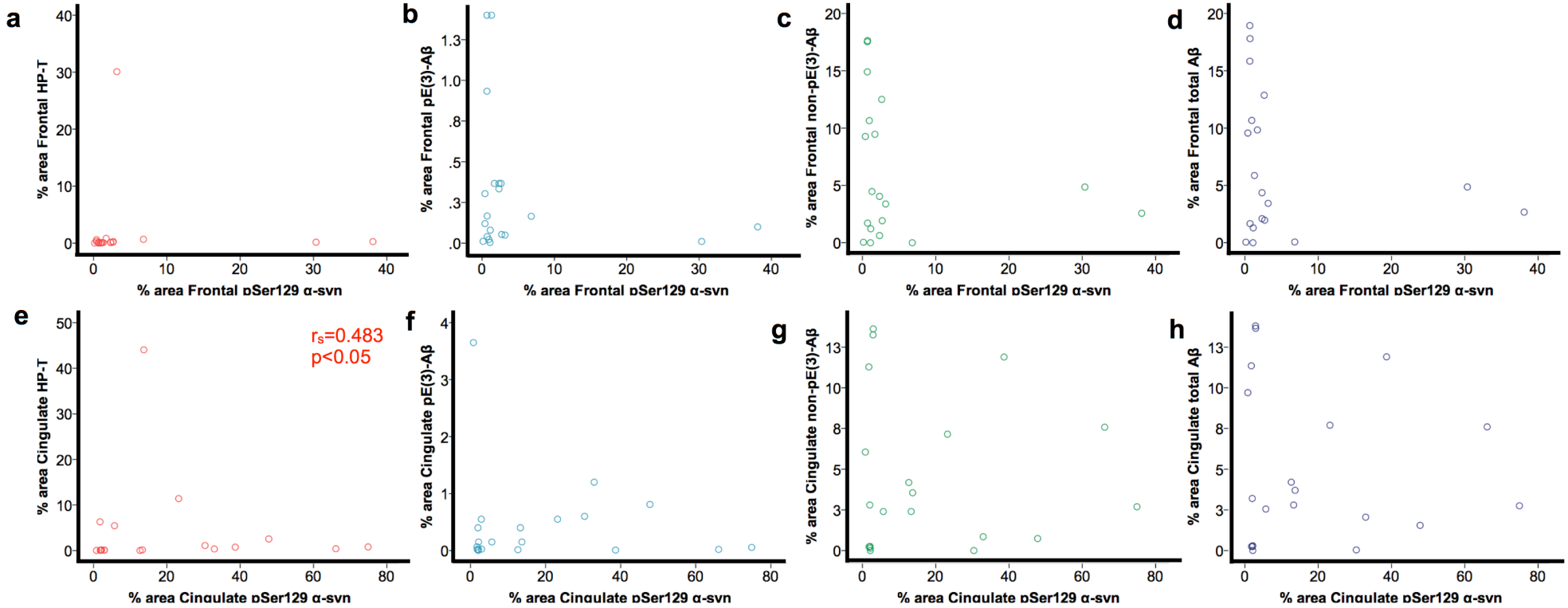

Figure 5.4 Correlations in DLB cases between HP-*T*, pE(3)-Aβ, non-pE(3)-Aβ and total Aβ with pSer129 α-syn in the frontal cortex **(a-d)** and cingulate cortex **(e-h)**. % area signifies percentage area covered by immunopositivity

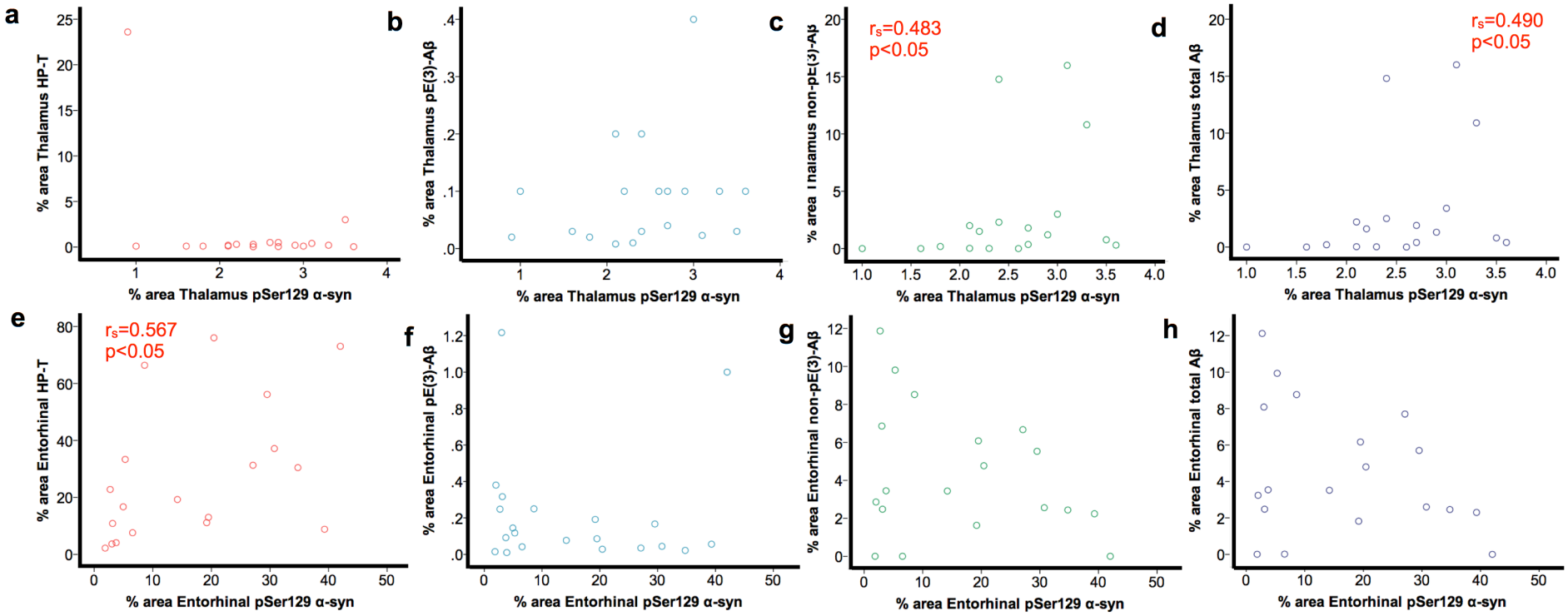

Figure 5.5 Correlations in DLB cases between HP-τ, pE(3)-Aβ, non-pE(3)-Aβ and total Aβ with pSer129 α-syn in the thalamus **(a-d)** and entorhinal cortex **(e-h)**. % area signifies percentage area covered by immunopositivity

5.4.4 PDD cases

5.4.4.1 Correlations between HP-$_T$, pE(3)-Aβ, non-pE(3)-Aβ and total Aβ (Aβ) with pSer129 α-syn.

In the frontal cortex, pE(3)-Aβ and total Aβ positively correlated with with pSer129 α-syn (r_s = 0.688, p<0.05 and r_s= 0.667, p<0.05 respectively). There were no associations observed between HP-$_T$ and non-pE(3)-Aβ with pSer129 α-syn (Figure 5.6 a-d). All proteins positively correlated with pSer129 α-syn in the cingulate cortex (HP-$_T$: r_s = 0.767, p<0.01; pE(3)-Aβ: r_s = 0.673, p<0.05; non-pE(3)-Aβ; r_s = 0.636, p<0.05 and total Aβ: r_s = 0.685, p<0.05) (Figure 5.6 e-h). No associations were observed between any of the pathological protein aggregates and pSer129 α-syn in the thalamus (Figure 5.7 a-d). In the entorhinal cortex HP-$_T$, non-pE(3)-Aβ and total Aβ positively correlated with pSer129 α-syn (r_s = 0.610, p<0.05; r_s = 0.676, p<0.05 and r_s = 0.709, p<0.01 respectively) (Figure 5.7 e-h).

5.4.4.2 Neuropathological predictors of pSer129 α-syn

Multiple regression analyses revealed HP-$_T$ and non-pE(3)-Aβ independently predicted pSer129 α-syn (model R^2 = 0.636, $F = 4.081_{(3)}$ p<0.05; HP-$_T$ β = 0.25, p<0.05; non-pE(3)-Aβ β = 0.923, p<0.05) in the cingulate cortex. No other variables predicted pSer129 α-syn in other brain regions.

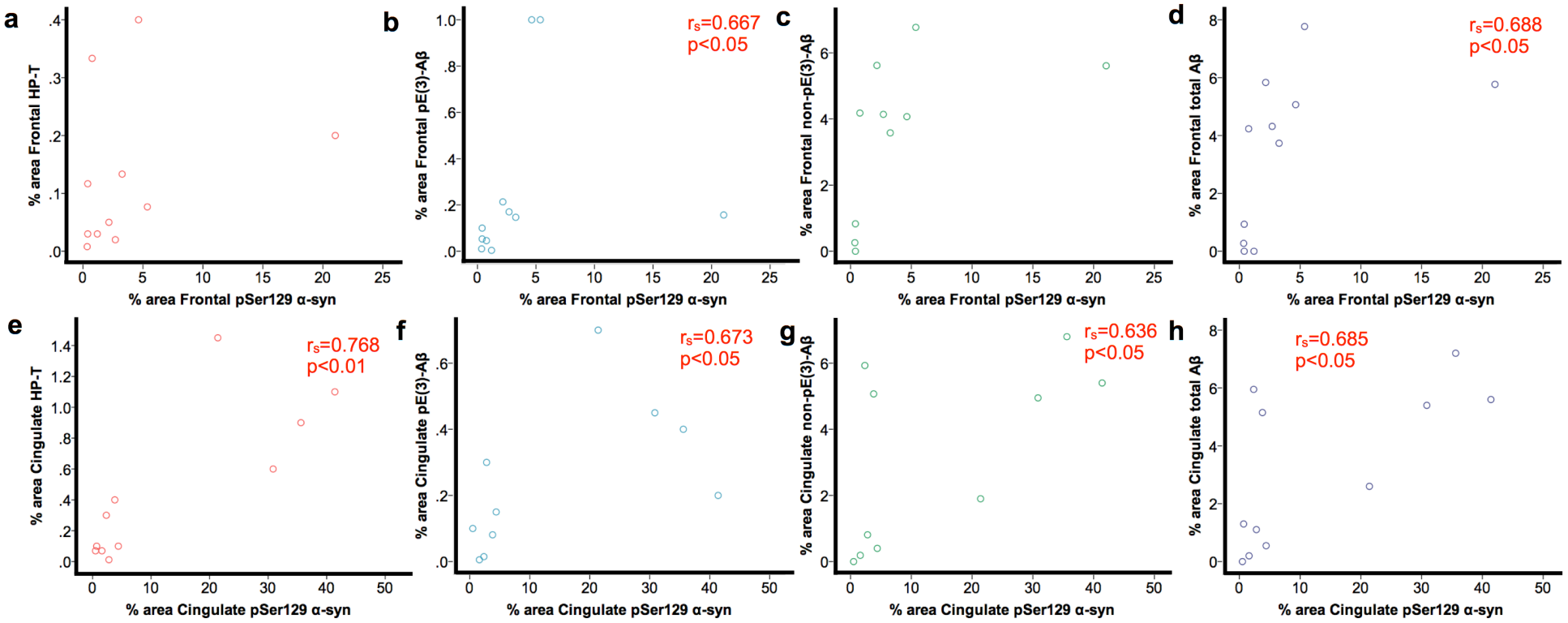

Figure 5.6 Correlations in PDD cases between HP-τ, pE(3)-Aβ, non-pE(3)-Aβ and total Aβ with pSer129 α-syn in the frontal cortex **(a-d)** and cingulate cortex **(e-h)**. % area signifies percentage area covered by immunopositivity

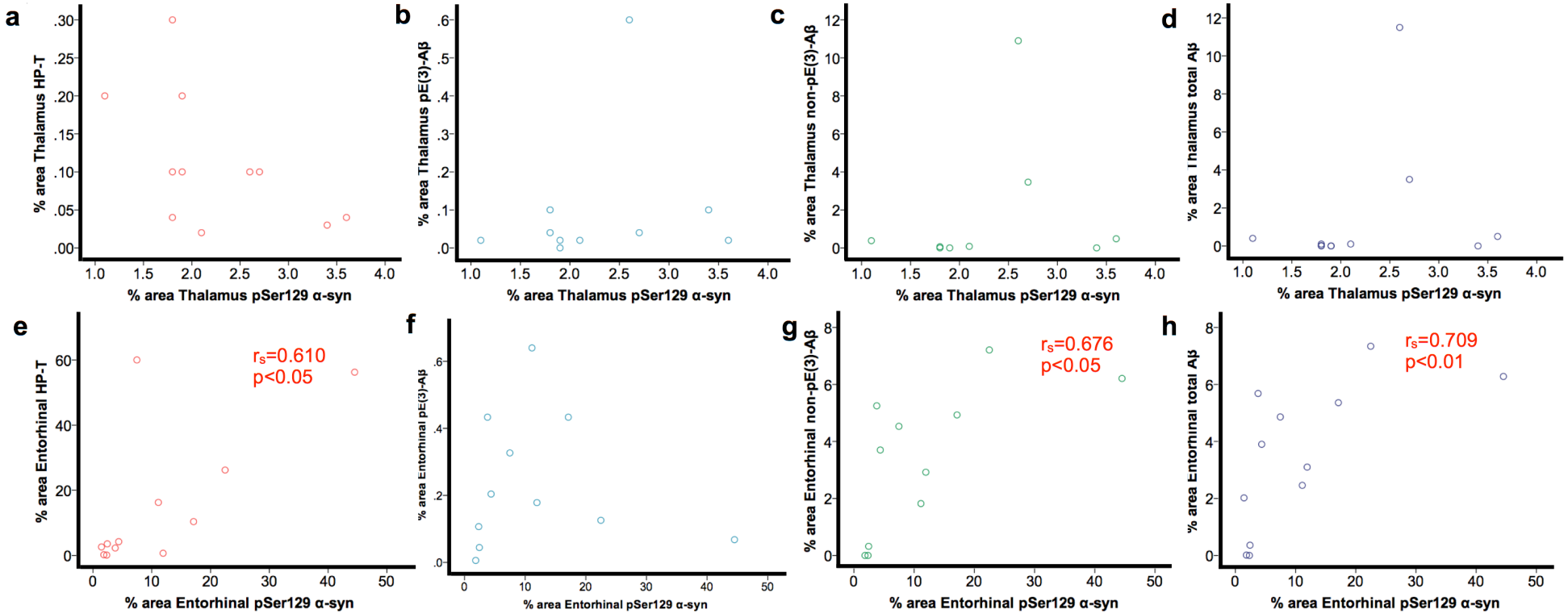

Figure 5.7 Correlations in PDD cases between HP-$_T$, pE(3)-Aβ, non-pE(3)-Aβ and total Aβ with pSer129 α-syn in the thalamus **(a-d)** and entorhinal cortex **(e-h)**. % area signifies percentage area covered by immunopositivity

5.4.5 8/4D antibody does not cross-react with pSer129 α-syn

Immunofluorescence staining demonstrated pyroglutamylated Aβ antibody 8/4D does not cross-react with pSer129 α-syn (Figure 5.8)

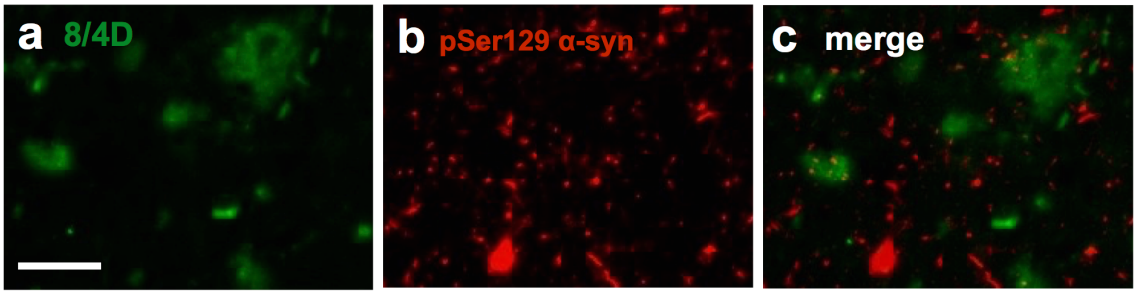

Figure 5.8 Pyroglutamylated Aβ antibody 8/4D does not cross-react with pSer129 α-syn. (a) 8/4D antibody labels a plaque and (b) Lewy body stained with pSer129 α-syn antibody. No staining of pSer129 α-syn with 8/4D antibody is seen indicating lack of cross-reactivity of 8/4D with pSer129 α-syn (c). Scale bar represents 50 μm and is valid for all photomicrographs.

5.4.6 Associations between pathologies and cognitive decline

In a subset of cases, where MMSE scores were available (n=16: DLB = 10; PDD = 6) Spearman's correlations were performed to determine if any relationships existed between each pathological protein aggregate and cognitive decline (Table 5.3). In the frontal cortex significant negative correlations were observed between non-pE(3)-Aβ and MMSE scores (r_s = -0.61, $p<0.05$), although a weak negative association between total Aβ approached significance (r_s = -0.47, $p = 0.077$). In the entorhinal cortex both non-pE(3)-Aβ and total Aβ negatively correlated with MMSE scores (r_s = -0.662, $p<0.01$ and r_s = -0.68, $p<0.01$ respectively). Regression analysis revealed only total Aβ was able to predict MMSE in the entorhinal cortex (model R^2 = 0.424, $F = 8.1_{(1)}$ $p<0.05$; β = -1.62, $p<0.05$). Disease specific correlations with MMSE were not performed as there were not sufficient numbers in each group to carry out the analysis.

	r_s	p value
Frontal HP-$_T$	0.32	0.913
Frontal pE(3)-Aβ	-0.014	0.96
Frontal non-pE(3)-Aβ	-0.61	0.021*
Frontal total Aβ	-0.47	0.077
Frontal pSer129 α-syn	0.047	0.867
Entorhinal HP-$_T$	-0.231	0.426
Entorhinal pE(3)-Aβ	-0.284	0.304
Entorhinal non-pE(3)-Aβ	-0.662	0.007*
Entorhinal total Aβ	-0.68	0.005*
Entorhinal pSer129 α-syn	0.075	0.79

Table 5.3 Spearman's rank correlations between HP-$_T$, pE(3)-Aβ, non-pE(3)-Aβ, total Aβ and pSer129 α-syn in brain regions with MMSE in the whole cohort. * signifies a significant correlation.

5.5 Discussion

It is well established that there is overlap in pathological protein aggregates between AD and LBD cases with LBs seen in up to 43% of AD cases (Uchikado et al., 2006), 95% of DLB cases exhibiting Aβ pathology and considerable HP-τ pathology present in up to 55% DLB cases (Jellinger and Attems, 2008). Previous studies have suggested the existence of a synergistic relationship between Aβ and pSer129 α-syn (Obi et al., 2008, Swirski et al., 2014), with the roles of other post-translational of Aβ i.e. pE(3)-Aβ yet to be investigated.

5.5.1 pE(3)-Aβ is higher in DLB and PDD compared to PD

DLB and PDD cases exhibited higher levels of pE(3)-Aβ compared to PD in all regions analysed, however significant increases was only observed in the frontal cortex. Although there were no significant differences in pE(3)-Aβ loads between DLB and PDD cases, overall DLB cases exhibited higher pE(3)-Aβ loads in all regions compared to PDD cases. The same hierarchical distribution between disease groups was observed with other pathologies (DLB>PDD>PD). There are no strict neuropathological differences distinguishing DLB from PDD however studies suggest that Aβ is higher in DLB cases compared to PDD cases in cortical association areas, cingulate cortex and striatum (Jellinger and Attems, 2006, Edison et al., 2008, Halliday et al., 2011).

To my knowledge this is the first study to investigate pE(3)-Aβ in human *post-mortem* tissue in patients with LBD, however a recent study by Becker and colleagues generated double transgenic ENTA-hQC mice to investigate the glutaminyl-cyclase mediated toxicity of pE(3)-Aβ *in vivo*. ETNA (E at the truncated N-terminus of Aβ) mice expressing truncated human Aβ(3-42) were crossed with transgenic mice over expressing human QC (hQC) and the resulting double transgenic mice demonstrated significant striatal neurodegeneration with considerable pE(3)-Aβ accumulation. In addition, behavioural alterations were observed, in particular impairments in sensorimotor gating, which argues the potential importance of pE(3)-Aβ playing a role in LBDs in which motor dysfunction is a cardinal feature (Becker et al., 2013).

Furthermore, Morawski and colleagues described glutaminyl cyclase expression (the enzyme responsible for catalysing the formation of pE(3)-Aβ) in the brain stem regions including the LC and nucleus basalis of Meynert (nbM) in AD cases (Morawski et al., 2010). As these regions are affected by pathology early in the disease course of PD (Braak et al., 2003) and as the nbM is the region where Friedrich Lewy first observed inclusions now known as Lewy bodies (Lewy, 1912), these findings may suggest that those subcortical regions demonstrate vulnerability to Aβ modifications in addition to α-syn.

5.5.2 pE(3)-Aβ is associated with pSer129 α-syn in LBD

In the overall cohort (DLB, PDD and PD) pE(3)-Aβ positively correlated with pSer129 α-syn in the cingulate cortex, however associations approached significance in the frontal cortex and thalamus. The cohort size in this study was limited, therefore with the addition of more cases associations observed the frontal cortex and thalamus may become significant. The exact pathomechanisms by which pE(3)-Aβ may be linked to pSer129 α-syn are yet to be elucidated, however it has been suggested pE(3)-Aβ may act as a seeding species of aggregate formation *in vitro* (Schilling et al., 2006). It has been demonstrated that pE(3)-Aβ acts as a seed for aggregation of several Aβ species (He and Barrow, 1999, D'Arrigo et al., 2009), and as a synergistic relationship between Aβ and pSer129 α-syn has been hypothesised (Obi et al., 2008, Marsh and Blurton-Jones, 2012, Swirski et al., 2014), it can be postulated that pE(3)-Aβ is related indirectly to pSer129 α-syn via the accumulation of multiple Aβ species. Results from the current study are in agreement with other studies regarding the relationship between Aβ and pSer129 α-syn, as significant positive correlations were observed between total Aβ in the cingulate cortex, thalamus and entorhinal cortex.

pE(3)-Aβ may also be associated with pSer129 α-syn via its relationship with HP-τ. Results from a study conduced by Nussbaum and colleagues supported the notion that pE(3)-Aβ might initiate tau-dependant cytotoxicity (Nussbaum et al., 2012) and work from our group in Newcastle also further supported this link, finding associations between pE(3)-Aβ and HP-τ in frontal and entorhinal cortices in AD cases (Mandler et al., 2014).

As both HP-τ and α-syn are phospho-proteins it is attractive to speculate similar modes of phosphorylation. Little is known about the phosphorylation of α-syn,

only that there are a limited number of phosphorylation sites including Serine 129 and 87 and very few kinases have been implicated in α-syn phosphorylation (Okochi et al., 2000). In contrast many kinases have been implicated in the phosphorylation of HP-*T*, including cyclin dependent kinase-2, cyclin dependent kinase-5 (Cdk 5), and glycogen synthase kinase-3β (Sperber et al., 1995, Vincent et al., 1997, Pei et al., 1998). However, a study conducted by Brion and colleagues demonstrated Cdk 5 has been detected in NFTs and LBs (Brion and Couck, 1995) making it an interesting target to study possible relationships between these proteins. In the current study, HP-*T* has been shown to correlate with pSer129 α-syn in the frontal, cingulate and entorhinal cortices supporting previous studies pertaining to a link between between pathological protein aggregates. An increase in pE(3)-Aβ may therefore be linked to increase in HP-*T* and subsequently pSer129 α-syn.

5.5.3 Non-pyroglutmylated Aβ is associated with pSer129 α-syn

Part of the aim of this study was to investigate associations between pE(3)-Aβ and pSer129 α-syn to the exclusion of other post-translational modifications that are stained with 4G8 and therefore can not be distinguished from total Aβ. However, the non-pE(3)-Aβ fraction (total Aβ minus pE(3)-Aβ) correlated with pSer129 α-syn in the cingulate cortex, thalamus and entorhinal cortex. Of note if the outlying case in the thalamus is removed this correlation becomes more significant (from $p<0.01$ to $p<0.001$). This indicates that other modifications of Aβ may contribute to a relationship with pSer129 α-syn i.e. Aβ phosphorylated at Serine 8 which shows enhanced aggregation into oligomers and fibrils and is present in the symptomatic stage of neurodegenerative diseases (Thal et al., 2015).

5.5.4 Disease specific associations with pSer129 α-syn

When investigating whether associations between pE(3)-Aβ, HP-*T* and total Aβ with pSer129 α-syn remained when the whole cohort was classified by disease category (DLB or PDD), fewer associations between pE(3)-Aβ, HP-*T*, and total Aβ with pSer129 α-syn were observed. pE(3)-Aβ failed to correlate with pSer129 α-syn in any region in the DLB cases (removing outlining cases failed to change this result) whilst pE(3)-Aβ did correlate with pSer129 α-syn in the frontal and cingulate cortices in PDD cases. This suggests the correlations

seen in the whole cohort were driven by those in the PDD group. The results for the whole cohort are consistent with those observed in the study by Swirski and colleagues (Swirski et al., 2014), who found that insoluble Aβ aggregates positively correlated with pSer129 α-syn in cingulate cortex, thalamus but not in the frontal cortex. They did not separate cases by disease category, but a larger proportion of the cohort was PDD cases compared to DLB cases (23 vs 10 respectively), and therefore it may be that results in their cohort are mostly be driven by associations in the PDD cases also. As there are no definitive neuropathological differences distinguishing DLB from PDD I can only speculate as to why there seems to be more associations between pathological aggregates in PDD cases. Although it is well established that both DLB and PDD cases have concomitant AD related pathology, the time course in the development of these lesions is less clear. Although not significant, the PDD cases in this study had lower HP-τ, pE(3)-Aβ and total Aβ loads compared to DLB cases, which could indicate pathology in the PDD cases had been accumulating for a shorter time period. Disease duration could be investigated in relation to pathology load in this cohort as a longer disease duration has been associated with global spread of pathology in both AD and LBD (Gomez-Tortosa et al., 1999, Armstrong, 2014). Early stages of aggregation formation may also have an influence in putative associations between pathologies. A study conducted by Ishizawa and colleagues investigating co-localisations between HP-τ and α-syn detected more co-localisations using TG3 and CP13 antibodies which target epitopes associated with early NFT development compared to Alz50 which targets late events in conformational changes involved in NFT development (Augustinack et al., 2002, Ishizawa et al., 2003, Luna-Munoz et al., 2007). This could suggest that early stage NFT formation is a key event in a putative interaction with α-syn. Stages in Aβ plaque and LB formation are less well described and this needs to be further elucidated to identify where interactions are likely to take place.

5.5.5 Aβ correlates with cognitive decline

Previous studies have implicated degeneration of the frontal and entorhinal cortices is associated with cognitive decline (DeKosky and Scheff, 1990, Mufson et al., 1999). Results from this study indicated a relationship between Aβ and cognitive decline as measured by MMSE. It is generally thought in AD

that HP-τ is the best pathological correlate of cognitive decline compared insoluble Aβ load in *post-mortem* tissue (Yamaguchi et al., 2001, Giannakopoulos et al., 2003). However, as suggested by Compta and colleagues (Compta et al., 2011) the relationship between Aβ and α-syn might play a part in the association between Aβ and cognitive dysfunction. MMSE is the most widely used cognitive test used in both clinical and epidemiological studies, however its sensitivity can decrease in mild cognitive impairment and established dementia (Benedict and Brandt, 1992, Nys et al., 2005, Franco-Marina et al., 2010). Patients with end-stage dementia my not be able to complete the test yielding low MMSE scores thus creating a floor effect. A more accurate reflection of cognitive status might be to calculate the rate of cognitive decline using multiple MMSE scores taken during the time course of the cognitive decline. However, multiple MMSE scores were not available for many of the cases used in this study therefore only final MMSE score was used in the analysis.

5.5.6 No cross-reaction with 8/4D and pSer129 α-syn

As the monoclonal 8/4D antibody that stains pE(3)-Aβ was not a commercially available antibody, double immunofluorescence was performed. No co-localisations were observed between 8/4D and pSer129 α-syn confirming there was no cross-reactivity of the 8/4D antibody, therefore any associations between pE(3)-Aβ and pSer129 α-syn were reflective of an association between pathologies.

5.5.7 Limitations

The most influential limiting factor of this study was the relatively small study cohort, with only 41 cases. Although quantitative assessment of neuropathological lesions provides an accurate reflection of the pathological load present in a given region, large cohorts are required to attain meaningful statistically significant results. Therefore, any conclusions drawn from this study should be treated with caution until more cases can be added to the study and the results can be confirmed. Correlations in this study were not corrected for multiple comparisons. Although such corrections such as Bonferonni adjustments will reduce type I error some consider it to be too conservative as it also increases the likelihood of type II error for associations that are not null

(Rothman, 1990, Perneger, 1998). Future studies including a much larger cohort are required to determine if associations reported in this study will stand up to robust statistical testing. In addition to the limited cohort size of this study, only 15 of the cases had MMSE scores recorded during life (DLB = 10; PDD = 6). Over 50% of the cases used in this study are lacking up to date neuropathological data specifically Braak LB staging for LB pathology (Braak et al., 2003) and Thal phases for the topographical distribution of Aβ deposits (Thal et al., 2002b). Brain tissue from these cases was donated to the NBTR prior to the implementation of these staging systems and work is ongoing to bring these cases up to current diagnostic standards.

This study did not measure the individual components that make up total pathological load, i.e. NFTs and NTs for HP-τ load and LBs and LNs for α-syn load, further clarification of these relationships is warranted.

The TMA methodology is an excellent tool to assess pathology across multiple brain regions in large-scale cohorts, in particular accurately reflecting cortical pathology load seen in diagnostic sections (Attems et al., 2014a, McAleese et al., 2015). However, other structures in the brain are more complex i.e. the thalamus, which is comprised of four parts: the hypothalamus, the epithalamus, the ventral thalamus, and the dorsal thalamus, encompassing 50-60 thalamic nuclei (Herrero et al., 2002). As only one 3mm tissue core is sampled for the TMA block, data from this will provide a basic overview of pathology in this structure but further analyses would be required to investigate individual nuclei.

5.6 Conclusion

This study supports previous data suggesting a synergistic relationship between Aβ and pSer129 α-syn and also introduces pE(3)-Aβ as a potential contributor, making it an interesting target for future study. In addition to Aβ, HP-τ may also play a role in a putative synergistic relationship and further investigations are warranted to unravel the effects these pathologies have on each other and the potential value of pE(3)-Aβ as a diagnostic marker and therapeutic target in LBD.

Chapter 6 - General Discussion

6.1 Introduction

The overall aims of this study were to investigate whether the use of quantitative neuropathological assessment is a useful tool in clinico-pathological correlative studies and then to investigate the impact that single and multiple pathological lesions have on the clinical and pathological phenotype of LBD. The key findings of this study are listed below and described in further detail: -

- Quantification of pathological lesions is a useful tool in clinico-pathological correlative studies and can detect subtle differences in pathology loads in cases that are classified as having 'severe' AD and LBD related pathology but different clinical phenotypes.
    - cAD cases had an increased HP-τ load in the majority of areas analysed compared to cDLB and cPDD cases.
    - Aβ loads were generally increased in cDLB cases compared to cPDD cases but only reached significance in the cingulate cortex.
    - Although not significant HP-τ loads were higher in hippocampus and cingulate in cAD compared to pAD.
- Mixed cases have higher rates of cognitive decline compared to 'pure' cases
- α-syn *per se* is not a pathological correlate of motor dysfunction in LBD.
- Aβ may be related to end stage motor dysfunction in DLB as measured by UPDRS III.
- Combined pathologies may associate with motor impairment in DLB.
- Hierarchical distribution of HP-τ, Aβ and α-syn does not differ between DLB and PDD.
- pE(3)-Aβ is associated with pSer129 α-syn in LBD

6.2 Quantitative methodologies in clinico-pathological correlative studies

The study described in Chapter 3 aimed to investigate the potential use of quantification techniques in clinico-pathological correlative studies. Many current studies rely on semi-quantitative methodologies which only provide an estimate on pathological burden and can be subject to inter-rater reliability issues. For the assessment of HP-τ and α-syn, this entails four-tiered ordinal scales (absent, mild, moderate and severe) (Alafuzoff et al., 2008, Alafuzoff et

al., 2009a) however, such is the diverse nature of Aβ deposits, a dichotomous scale is most frequently preferred to describe the presence or absence of Aβ pathology (Thal et al., 2002b, Alafuzoff et al., 2009b). This may have implications when analysing data from large cohorts across multiple centres when cases may fall on the border line between two categories. In addition, cases within the same category may differ considerably in their respective pathological loads. This was demonstrated by Attems and Jellinger who found in cases semi-quantitatively assessed as having 'severe' HP-τ pathology, significant differences were observed between cases when area covered by immunopositivity was measured (Attems and Jellinger, 2013a). Furthermore, in a large cohort of AD cases that all exhibited 'severe' entorhinal HP-τ pathology using quantitative neuropathological techniques, Murray and colleagues were able to determine three subtypes of AD (Murray et al., 2011). In addition to typical AD, hippocampal sparing and limbic predominant cases have been identified. In a subsequent radiological study, the authors were able to predict these subtypes on MRI during life (Whitwell et al., 2012). Using quantitative techniques in Chapter 3, I was able to determine differences in the pathological aggregate burden between cases that fulfilled neuropathological criteria for mixed AD/LBD but with different clinical presentations. Semi-quantitative scoring failed to detect such differences as all cases exhibited 'severe' pathology, however quantitative methods removed the 'ceiling effect' which is created by the constraints of semi-quantitative assessment.

6.2.1 Differences in pathology burden in mixed AD/LBD cases with different clinical phenotypes

As highlighted above, the quantitative assessment of pathological lesions detected differences in pathology load in mixed AD/LBD cases with different clinical phenotypes (Chapter 3). cAD cases exhibited higher HP-τ loads and the regional distributions of pathologies followed the same hierarchical pattern to that that observed in 'pure' AD cases suggesting the primary pathological correlate for dementia might have been AD related pathology later followed by Lewy body related pathology. Furthermore, cDLB cases had a significant increase in Aβ load in the cingulate compared to cPDD cases which has been a reported difference between 'pure' DLB and PDD using neuro-imaging techniques (Edison et al., 2008). A surprising finding from this study was the

decrease in α-syn in the SN of cPDD cases in comparison to the cDLB cases. One could speculate that the loss of dopaminergic neurones was greater in the the SN in the cPDD cases compared to cDLB therefore there are fewer neurones for α-syn to aggregate in. Increasing evidence has suggested a role for inflammation in the brain in the pathogenesis of PD. A study by Geo and colleagues demonstrated that microglial activation induced by a chronic infusion of an inflammagen lipopolysaccharide resulted in the gradual cell loss of dopaminergic neurones in a rat model (Gao et al., 2002). Inflammatory markers were not considered in this study but, an increase in activated microglia and subsequent dopaminegic cell loss could account for the relative lack of α-syn in cPDD cases.

6.2.2 Clinical implications of mixed dementia

In the current study cAD cases exhibited severe Lewy body pathology at *post-mortem* examination, while no clinical symptoms suggestive for DLB were observed *ante mortem*. Previous studies have suggested that concomitant AD pathology in DLB is associated with cognitive decline (Howlett et al., 2014) and concomitant TDP-43 pathology in AD exacerbates features associated with AD (Josephs et al., 2014) but does not associate with behavioural features frequently associated with frontotemporal lobar degeneration or amyotrophic lateral sclerosis (Jung et al., 2014), diseases in which TDP-43 inclusions are the characteristic pathological hallmark lesion. The latter is similar to our findings in cAD where co-existing Lewy body pathology did not elicit symptoms associated with DLB and PDD. However, all mixed AD/LBD cases, irrespective of clinical diagnosis, had lower MMSE and higher rates of cognitive decline compared to 'pure' AD and 'pure' DLB which is in agreement with previous work (Olichney et al., 1998).

6.3 The pathological correlates of motor dysfunction in DLB and PDD

The study described in Chapter 4 study builds on previous work by Parkkinen and colleagues (Parkkinen et al., 2005) who reported that α-syn does not predict EPS, incorporating more of the nigro-striatal pathway and associated regions in addition to investigating the impact of combined pathologies EPS in DLB and PDD. This study is in agreement with the previous study in that α-syn did not independently associate with EPS, however results suggested there

may be an association between Aβ, and Aβ in combination with α-syn with motor dysfunction in DLB cases. A potential pathomechamism of nigral-striatal degeneration in DLB cases could involve the dying-back process triggered by Aβ accumulation in the striatum. The proximal part of the lesioned neurone i.e Aβ accumulation surrounding synaptic connection onto the striatum, may undergo degeneration resulting in increased calcium (Ca^{++}) influx (LoPachin and Lehning, 1997) and disruptions in axonal transport (Coleman, 2005). Increased influx of Ca^{++} into the cell is a prerequisite for many cytological changes including fragmentation of the axon (Carafoli, 1987). Axonal degeneration in response to Aβ accumulation has been demonstrated in a drosophila model (Zhao et al., 2010) as Aβ expression in a small number of neurones induced intracellular accumulation of Aβ and age dependant depletion of mitochondria. Moreover, intracellular axonal Aβ disrupted the axonal transport mitochondria essential to maintain the functionality of the neurone. Further studies investigating striatal dopamine transporters may start to unravel this. Several studies have investigated the degeneration of SN neurones in PD and incidental Lewy body disease (iLBD - cases with abundant LB pathology but lacking dementia or Parkinsonism). Iacono and colleagues reported an 82% and 40% loss in nigral neurones in PD and iLBD respectively compared to controls (Iacono et al., 2015). Whilst Milber and colleagues found a decrease in tyrosine hydroxylse in neurones in the SN of iLBD categorised at Braak LB 1/2 compared to controls (Milber et al., 2012). iLBD is speculated to be an intermediate stage before PD, however if the degeneration of nigral neurones precedes the temporal appearance of LB in the SN it is tempting to speculate that degeneration of dopaminergic neurones is not a result of α-syn accumulation in the SN but dysfunction of neurones originating further up the nigro-striatal pathway in the striatum.

6.4 Synergistic relationships between protein aggregates

Results from this study supports others suggesting a synergistic relationship between Aβ, HP-τ and α-syn and introduces pE(3)-Aβ as a potential contributor. Despite associations between the aggregates being well documented, little is known about the patho-mechanisms driving these interactions.

6.4.1 Direct interactions

In healthy neurones Aβ and α-syn do not exist in the same sub-cellular compartment therefore limiting the potential for direct interaction. However, in pathological states both have been detected in mitochondria, lysosomes and autophagosomes (Hansson Petersen et al., 2008, Chinta et al., 2010). Most of the studies supporting a direct interaction between Aβ and α-syn are from *in vitro* experiments i.e. α-syn can promote conformational changes in Aβ detected by NMR spectroscopy (Mandal et al., 2006). Cell models have also demonstrated that HP-τ can enhance aggregation and toxicity of α-syn (Badiola et al., 2011).

6.4.2 Indirect interactions

6.4.2.1 Inflammation

Aβ induced inflammation can affect aggregation of α-syn i.e. Aβ-induced release of pro-inflammatory cytokines can activate cytokines such as Cdk5 that induces tau formation (Waxman and Giasson, 2011) and has also been implicated in Lewy body formation (Takahashi et al., 2000).

6.4.2.2 Impaired protein degradation

Both Aβ and α-syn are degraded by autophagy, therefore this pathway could be affected by interactions between these aggregates. Uptake of Aβ via lysosomal degradation induces lysosomal leakage providing a mechanism for interactions between Aβ and α-syn (Masliah et al., 2001).

Future studies are warranted to elucidate potential patho-mechanisms linking pE(3)-Aβ and pSer129 α-syn.

6.5 Potential translational impact

Results from this study further highlight the importance of co-morbid pathologies in LBDs in particular Aβ and pE(3)-Aβ. Mixed dementias are difficult to diagnose during life as symptoms are indistinguishable from single neurodegenerative diseases and as such the prevalence of mixed dementias are under reported. Although not significant, results from Chapter 3 suggest mixed cases have an increased pathology load compared to pure cases, caused by potential synergistic relationship between co-existing aggregates. Corroboration of these

findings using neuro-imaging techniques could aid the diagnosis of mixed pathologies which would help clinicians when deciding on which treatment pathway to follow. Current biomarkers for LBD include neuro-imaging and detection of pathological proteins in cerebral spinal fluid (CSF). Studies investigating α-syn as a CSF biomarker have had conflicting results; some have reported a decrease in α-syn compared to AD and controls (Shi et al., 2011, van Dijk et al., 2014) whilst others have demonstrated no difference (Ohrfelt et al., 2009, Reesink et al., 2010). HP-τ CSF levels have been reported to be lower in DLB in relation to AD but higher compared to PDD cases (Parnetti et al., 2008). Future development of a pE(3)-Aβ CSF test could add to and complement current CSF biomarkers and potentially become part of a diagnostic panel to aid the diagnoses of LBDs during life.

6.6 General strengths and limitations

The primary strength of this project is the NIS-Elements quantification software attached to the microscope. This software enables the use of automated quantification to assess the amount of pathology within cases and comparison between cases. Semi-quantification is a very useful tool that has allowed neuropathologists to diagnose dementing disorders for many years. However, as more research is being conducted in neurodegenerative diseases it is becoming increasingly clear that complex synergistic relationships exist between hallmark pathologies within the human brain. A quantification system that can detect subtle differences in the amount of pathology that cannot be detected by semi-quantification may help direct future imaging and drug therapy studies. In addition to quantification of pathologic lesions providing an accurate reflection of pathology load, the automated microscope and software provides the possibility to perform large-scale quantitative assessment using standardised inclusion thresholds designed to detect specific pathological lesions. TMA is most commonly used in cancer studies however, this methodology can be applied in the assessment of human *post-mortem* cerebral tissue allowing the analysis of up to 40 tissue samples on one slide (Attems et al., 2014a) allowing efficient assessment.

The most recent and prominent clinico-pathological correlative studies in AD include cohort sizes ranging between 122 and 652 (Bancher et al., 1996,

Bennett et al., 2005, Petrovitch et al., 2005), and LBD studies include between 90 and 872 participants (Lewis et al., 2005, Schneider et al., 2009, Selikhova et al., 2009, Dugger et al., 2012). In comparison, the current study is most likely underpowered and an increased cohort number is required to ensure significant results are robust and reproducible.

I am fortunate that I have had access to human *post-mortem* brain tissue, which is an invaluable resource in dementia research. The Newcastle Brain Tissue Resource (NBTR) is an excellent facility, which houses both fresh and formalin fixed tissues. Along with high quality tissue the NBTR holds medical notes on each of the donors and as many of the patients are signed up to research studies within Newcastle University during their lifetime, the NBTR records additional clinical information i.e. MMSE and UPDRS scores. However, as this study was retrospective not all of the cases included had corresponding clinical data available for motor impairment or MMSE.

In addition to AD related pathologies, LBDs also exhibit vascular pathologies that are significantly more extensive than controls but less extensive than AD cases (Barber et al., 1999). Assessment of vascular pathologies were not included in this study but should be considered in future investigations as a co-morbidity of LBD.

6.7 Future directions

6.7.1 Short-term studies

- Results form this study were obtained using a very limited cohort size (in particular the cohort used in Chapter 3 where only a total of 19 cases fulfilled neuropathological criteria for both AD and DLB). Therefore to make the analyses more robust, other brain banks should be contacted to potentially increase the cohort number.
- HP-τ and α-syn have been shown to co-localise in the same neurones (Ishizawa et al., 2003, Colom-Cadena et al., 2013). Measuring co-localisations in the mixed AD/LBD cases may give insights as to which brain regions are susceptible to HP-τ and α-syn interactions promoting the aggregation, accumulation and potential spreading to other brain regions.

- Quantifying microglial activation in the SN by immunostaining with CD68 could help to determine whether an elevated immune response and subsequent dopaminergic cell loss is responsible for the relative lack of α-syn in the SN in cPDD cases in Chapter 3.
- This study did not include dopaminergic cell counts in the SN. Therefore, density of neuromelanin containing and tyrosine hydroxylase positive neurones should be quantified. This will help to test the hypothesis that Aβ contributes to degeneration of the nigral-striatal pathway via the dying back process originating in the striatum in DLB cases as hypothesised in Chapter 4.

6.7.2 Medium-term and long-term studies

- The development of a CSF test for pE(3)-Aβ would add to the diagnostic panel of aggregates that are currently being investigated as potential biomarkers. Initially this would entail the development of an ELISA capable of detecting pE(3)-Aβ in *post-mortem* CSF. These results would then be compared to quantitative immunohistochemical and biochemical data taken from *post-mortem* brain samples to elucidate how pE(3)-Aβ relates to pE(3)-Aβ deposits in cerebral tissue. Following this, detection of pE(3)-Aβ can then be tested in CSF taken at lumbar puncture.
- In addition to CSF biomarkers, neuro-imaging is a useful tool to assess accumulations of proteins to neurodegeneration in living patients. Currently 11C-PIB PET imaging is available to assess Aβ deposits *intra-vitam*. The development of pE(3)-Aβ ligands would give insight into the accumulation of pE(3)-Aβ over time.
- *In vitro* experiments can be designed using mouse neuronal cell cultures or human induced pluripotent stem cells derived from patients with familial forms of the disease to investigate putative associations between pE(3)-Aβ and α-syn.
- Aβ phosphorylated at serine 8 (AβSer8) is another post-translational modification of Aβ that has been found to be significantly elevated in AD and associates with later Braak stages (Ashby et al., 2015). AβSer8 could be another interesting sub-type of Aβ to investigate in regards to potential associations with α-syn.

6.8 Conclusion

This study aimed to investigate the feasibility of the use of digital quantitative neuropathological assessment in clinico-pathological correlative studies and to implement this method in the subsequent studies which investigated the impact of multiple pathological lesions on the aggregation and accumulation of each and the clinical features associated with LBDs.

Quantitative methods provided the accuracy required to detect subtle changes in pathological burden of HP-τ, Aβ and α-syn in a cohort of cases that fulfil the neuropatholoiglcal criteria for mixed AD/LBD with different clinical presentations. In addition, this study highlighted the importance of AD related pathologies in particular Aβ and pE(3)-Aβ and their putative relationships with Lewy body pathology and clinical symptoms associated with LBDs.

Future studies are required to elucidate patho-mechanisms responsible for interactions of AD related and Lewy body pathologies and the combined effect they exert on neurodegeneration in LBDs.

Better stratification of patients and an understanding of relationships between pathologies, in particular in patients with mixed pathologies, may lead to better outcomes in clinical trials, targeted therapeutic design and ultimately tailored treatment options for patients with neurodegenerative diseases.

References

AARSLAND, D., ANDERSEN, K., LARSEN, J. P., LOLK, A. & KRAGH-SORENSEN, P. 2003. Prevalence and characteristics of dementia in Parkinson disease: an 8-year prospective study. *Arch Neurol,* 60**,** 387-92.

AARSLAND, D., ANDERSEN, K., LARSEN, J. P., LOLK, A., NIELSEN, H. & KRAGH-SORENSEN, P. 2001a. Risk of dementia in Parkinson's disease: a community-based, prospective study. *Neurology,* 56**,** 730-6.

AARSLAND, D., BALLARD, C., MCKEITH, I., PERRY, R. H. & LARSEN, J. P. 2001b. Comparison of extrapyramidal signs in dementia with Lewy bodies and Parkinson's disease. *J Neuropsychiatry Clin Neurosci,* 13**,** 374-9.

AARSLAND, D., LARSEN, J. P., TANDBERG, E. & LAAKE, K. 2000. Predictors of nursing home placement in Parkinson's disease: a population-based, prospective study. *J Am Geriatr Soc,* 48**,** 938-42.

ABELIOVICH, A., SCHMITZ, Y., FARINAS, I., CHOI-LUNDBERG, D., HO, W. H., CASTILLO, P. E., SHINSKY, N., VERDUGO, J. M., ARMANINI, M., RYAN, A., HYNES, M., PHILLIPS, H., SULZER, D. & ROSENTHAL, A. 2000. Mice lacking alpha-synuclein display functional deficits in the nigrostriatal dopamine system. *Neuron,* 25**,** 239-52.

ALAFUZOFF, I. 2013. Alzheimer's disease-related lesions. *J Alzheimers Dis,* 33 Suppl 1**,** S173-9.

ALAFUZOFF, I., ARZBERGER, T., AL-SARRAJ, S., BODI, I., BOGDANOVIC, N., BRAAK, H., BUGIANI, O., DEL-TREDICI, K., FERRER, I., GELPI, E., GIACCONE, G., GRAEBER, M. B., INCE, P., KAMPHORST, W., KING, A., KORKOLOPOULOU, P., KOVACS, G. G., LARIONOV, S., MEYRONET, D., MONORANU, C., PARCHI, P., PATSOURIS, E., ROGGENDORF, W., SEILHEAN, D., TAGLIAVINI, F., STADELMANN, C., STREICHENBERGER, N., THAL, D. R., WHARTON, S. B. & KRETZSCHMAR, H. 2008. Staging of neurofibrillary pathology in Alzheimer's disease: a study of the BrainNet Europe Consortium. *Brain Pathol,* 18**,** 484-96.

ALAFUZOFF, I., INCE, P. G., ARZBERGER, T., AL-SARRAJ, S., BELL, J., BODI, I., BOGDANOVIC, N., BUGIANI, O., FERRER, I., GELPI, E., GENTLEMAN, S., GIACCONE, G., IRONSIDE, J. W., KAVANTZAS, N., KING, A., KORKOLOPOULOU, P., KOVACS, G. G., MEYRONET, D., MONORANU, C., PARCHI, P., PARKKINEN, L., PATSOURIS, E., ROGGENDORF, W., ROZEMULLER, A., STADELMANN-NESSLER, C., STREICHENBERGER, N., THAL, D. R. & KRETZSCHMAR, H. 2009a. Staging/typing of Lewy body related alpha-synuclein pathology: a study of the BrainNet Europe Consortium. *Acta Neuropathol,* 117**,** 635-52.

ALAFUZOFF, I. & PARKKINEN, L. 2014. Staged pathology in Parkinson's disease. *Parkinsonism Relat Disord,* 20 Suppl 1**,** S57-61.

ALAFUZOFF, I., THAL, D. R., ARZBERGER, T., BOGDANOVIC, N., AL-SARRAJ, S., BODI, I., BOLUDA, S., BUGIANI, O., DUYCKAERTS, C., GELPI,

E., GENTLEMAN, S., GIACCONE, G., GRAEBER, M., HORTOBAGYI, T., HOFTBERGER, R., INCE, P., IRONSIDE, J. W., KAVANTZAS, N., KING, A., KORKOLOPOULOU, P., KOVACS, G. G., MEYRONET, D., MONORANU, C., NILSSON, T., PARCHI, P., PATSOURIS, E., PIKKARAINEN, M., REVESZ, T., ROZEMULLER, A., SEILHEAN, D., SCHULZ-SCHAEFFER, W., STREICHENBERGER, N., WHARTON, S. B. & KRETZSCHMAR, H. 2009b. Assessment of beta-amyloid deposits in human brain: a study of the BrainNet Europe Consortium. *Acta Neuropathol,* 117**,** 309-20.

ALVAREZ, P. & SQUIRE, L. R. 1994. Memory consolidation and the medial temporal lobe: a simple network model. *Proc Natl Acad Sci U S A,* 91**,** 7041-5.

ALVAREZ-ERVITI, L., RODRIGUEZ-OROZ, M. C., COOPER, J. M., CABALLERO, C., FERRER, I., OBESO, J. A. & SCHAPIRA, A. H. 2010. Chaperone-mediated autophagy markers in Parkinson disease brains. *Arch Neurol,* 67**,** 1464-72.

ALZHEIMER'S SOCIETY 2014. Dementia 2014: opportunity for change. London UK: Alzheimer's society.

AMIEVA, H., MOKRI, H., LE GOFF, M., MEILLON, C., JACQMIN-GADDA, H., FOUBERT-SAMIER, A., ORGOGOZO, J. M., STERN, Y. & DARTIGUES, J. F. 2014. Compensatory mechanisms in higher-educated subjects with Alzheimer's disease: a study of 20 years of cognitive decline. *Brain,* 137**,** 1167-75.

ANDERSON, J. P., WALKER, D. E., GOLDSTEIN, J. M., DE LAAT, R., BANDUCCI, K., CACCAVELLO, R. J., BARBOUR, R., HUANG, J., KLING, K., LEE, M., DIEP, L., KEIM, P. S., SHEN, X., CHATAWAY, T., SCHLOSSMACHER, M. G., SEUBERT, P., SCHENK, D., SINHA, S., GAI, W. P. & CHILCOTE, T. J. 2006. Phosphorylation of Ser-129 is the dominant pathological modification of alpha-synuclein in familial and sporadic Lewy body disease. *J Biol Chem,* 281**,** 29739-52.

ANDRES, P. 2003. Frontal cortex as the central executive of working memory: time to revise our view. *Cortex,* 39**,** 871-95.

ARMSTRONG, R. A. 2012. On the 'classification' of neurodegenerative disorders: discrete entities, overlap or continuum? *Folia Neuropathol,* 50**,** 201-8.

ARMSTRONG, R. A. 2014. Factors determining disease duration in Alzheimer's disease: a postmortem study of 103 cases using the Kaplan-Meier estimator and Cox regression. *Biomed Res Int,* 2014**,** 623487.

ARMSTRONG, R. A., LANTOS, P. L. & CAIRNS, N. J. 2005. Overlap between neurodegenerative disorders. *Neuropathology,* 25**,** 111-24.

ARNOLD, S. E., HYMAN, B. T., FLORY, J., DAMASIO, A. R. & VAN HOESEN, G. W. 1991. The topographical and neuroanatomical distribution of neurofibrillary tangles and neuritic plaques in the cerebral cortex of patients with Alzheimer's disease. *Cereb Cortex,* 1**,** 103-16.

ASHBY, E. L., MINERS, J. S., KUMAR, S., WALTER, J., LOVE, S. & KEHOE, P. G. 2015. Investigation of Abeta phosphorylated at serine 8 (pAbeta) in

Alzheimer's disease, dementia with Lewy bodies and vascular dementia. *Neuropathol Appl Neurobiol,* 41**,** 428-44.

ATTEMS, J. & JELLINGER, K. 2013a. Neuropathological correlates of cerebral multimorbidity. *Curr Alzheimer Res,* 10**,** 569-77.

ATTEMS, J. & JELLINGER, K. 2013b. Neuropathology. *In:* DENING, T. T., A.J. (ed.) *Oxford Textbook of Old Age Psychiatry.* New York: Oxford Unversity Press.

ATTEMS, J., JELLINGER, K. A. & LINTNER, F. 2005. Alzheimer's disease pathology influences severity and topographical distribution of cerebral amyloid angiopathy. *Acta Neuropathol,* 110**,** 222-31.

ATTEMS, J., NELTNER, J. H. & NELSON, P. T. 2014a. Quantitative neuropathological assessment to investigate cerebral multi-morbidity. *Alzheimers Res Ther,* 6**,** 85.

ATTEMS, J., QUASS, M., JELLINGER, K. A. & LINTNER, F. 2007. Topographical distribution of cerebral amyloid angiopathy and its effect on cognitive decline are influenced by Alzheimer disease pathology. *J Neurol Sci,* 257**,** 49-55.

ATTEMS, J., THAL, D. R. & JELLINGER, K. A. 2012. The relationship between subcortical tau pathology and Alzheimer's disease. *Biochem Soc Trans,* 40**,** 711-5.

ATTEMS, J., WALKER, L. & JELLINGER, K. A. 2014b. Olfactory bulb involvement in neurodegenerative diseases. *Acta Neuropathol,* 127**,** 459-75.

AUGUSTINACK, J. C., SCHNEIDER, A., MANDELKOW, E. M. & HYMAN, B. T. 2002. Specific tau phosphorylation sites correlate with severity of neuronal cytopathology in Alzheimer's disease. *Acta Neuropathol,* 103**,** 26-35.

BADIOLA, N., DE OLIVEIRA, R. M., HERRERA, F., GUARDIA-LAGUARTA, C., GONCALVES, S. A., PERA, M., SUAREZ-CALVET, M., CLARIMON, J., OUTEIRO, T. F. & LLEO, A. 2011. Tau enhances alpha-synuclein aggregation and toxicity in cellular models of synucleinopathy. *PLoS One,* 6**,** e26609.

BAGYINSZKY, E., YOUN, Y. C., AN, S. S. & KIM, S. 2014. The genetics of Alzheimer's disease. *Clin Interv Aging,* 9**,** 535-51.

BANCHER, C., BRUNNER, C., LASSMANN, H., BUDKA, H., JELLINGER, K., WICHE, G., SEITELBERGER, F., GRUNDKE-IQBAL, I., IQBAL, K. & WISNIEWSKI, H. M. 1989. Accumulation of abnormally phosphorylated tau precedes the formation of neurofibrillary tangles in Alzheimer's disease. *Brain Res,* 477**,** 90-9.

BANCHER, C., JELLINGER, K., LASSMANN, H., FISCHER, P. & LEBLHUBER, F. 1996. Correlations between mental state and quantitative neuropathology in the Vienna Longitudinal Study on Dementia. *Eur Arch Psychiatry Clin Neurosci,* 246**,** 137-46.

BARBER, R., SCHELTENS, P., GHOLKAR, A., BALLARD, C., MCKEITH, I., INCE, P., PERRY, R. & O'BRIEN, J. 1999. White matter lesions on magnetic resonance imaging in dementia with Lewy bodies, Alzheimer's disease, vascular dementia, and normal aging. *J Neurol Neurosurg Psychiatry,* 67**,** 66-72.

BARNES, L. L., LEURGANS, S., AGGARWAL, N. T., SHAH, R. C., ARVANITAKIS, Z., JAMES, B. D., BUCHMAN, A. S., BENNETT, D. A. & SCHNEIDER, J. A. 2015. Mixed pathology is more likely in black than white decedents with Alzheimer dementia. *Neurology,* 85**,** 528-34.

BEACH, T. G., ADLER, C. H., LUE, L., SUE, L. I., BACHALAKURI, J., HENRY-WATSON, J., SASSE, J., BOYER, S., SHIROHI, S., BROOKS, R., ESCHBACHER, J., WHITE, C. L., 3RD, AKIYAMA, H., CAVINESS, J., SHILL, H. A., CONNOR, D. J., SABBAGH, M. N. & WALKER, D. G. 2009. Unified staging system for Lewy body disorders: correlation with nigrostriatal degeneration, cognitive impairment and motor dysfunction. *Acta Neuropathol,* 117**,** 613-34.

BECKER, A., KOHLMANN, S., ALEXANDRU, A., JAGLA, W., CANNEVA, F., BAUSCHER, C., CYNIS, H., SEDLMEIER, R., GRAUBNER, S., SCHILLING, S., DEMUTH, H. U. & VON HORSTEN, S. 2013. Glutaminyl cyclase-mediated toxicity of pyroglutamate-beta amyloid induces striatal neurodegeneration. *BMC Neurosci,* 14**,** 108.

BENDOR, J. T., LOGAN, T. P. & EDWARDS, R. H. 2013. The function of alpha-synuclein. *Neuron,* 79**,** 1044-66.

BENEDICT, R. H. & BRANDT, J. 1992. Limitation of the Mini-Mental State Examination for the detection of amnesia. *J Geriatr Psychiatry Neurol,* 5**,** 233-7.

BENNETT, D. A., SCHNEIDER, J. A., BIENIAS, J. L., EVANS, D. A. & WILSON, R. S. 2005. Mild cognitive impairment is related to Alzheimer disease pathology and cerebral infarctions. *Neurology,* 64**,** 834-41.

BERGE, G., SANDO, S. B., RONGVE, A., AARSLAND, D. & WHITE, L. R. 2014. Apolipoprotein E {varepsilon}2 genotype delays onset of dementia with Lewy bodies in a Norwegian cohort. *J Neurol Neurosurg Psychiatry,* 85**,** 1227-31.

BERNHEIMER, H., BIRKMAYER, W., HORNYKIEWICZ, O., JELLINGER, K. & SEITELBERGER, F. 1973. Brain dopamine and the syndromes of Parkinson and Huntington. Clinical, morphological and neurochemical correlations. *J Neurol Sci,* 20**,** 415-55.

BEYDOUN, M. A., BEYDOUN, H. A. & WANG, Y. 2008. Obesity and central obesity as risk factors for incident dementia and its subtypes: a systematic review and meta-analysis. *Obes Rev,* 9**,** 204-18.

BEYER, K. 2006. Alpha-synuclein structure, posttranslational modification and alternative splicing as aggregation enhancers. *Acta Neuropathol,* 112**,** 237-51.

BIESSELS, G. J., STAEKENBORG, S., BRUNNER, E., BRAYNE, C. & SCHELTENS, P. 2006. Risk of dementia in diabetes mellitus: a systematic review. *Lancet Neurol,* 5**,** 64-74.

BINDER, L. I., FRANKFURTER, A. & REBHUN, L. I. 1985. The distribution of tau in the mammalian central nervous system. *J Cell Biol,* 101**,** 1371-8.

BLACKER, D. & TANZI, R. E. 1998. The genetics of Alzheimer disease: current status and future prospects. *Arch Neurol,* 55**,** 294-6.

BLENNOW, K., DE LEON, M. J. & ZETTERBERG, H. 2006. Alzheimer's disease. *Lancet,* 368**,** 387-403.

BLOCH, A., PROBST, A., BISSIG, H., ADAMS, H. & TOLNAY, M. 2006. Alpha-synuclein pathology of the spinal and peripheral autonomic nervous system in neurologically unimpaired elderly subjects. *Neuropathol Appl Neurobiol,* 32**,** 284-95.

BOESVELDT, S., VERBAAN, D., KNOL, D. L., VISSER, M., VAN ROODEN, S. M., VAN HILTEN, J. J. & BERENDSE, H. W. 2008. A comparative study of odor identification and odor discrimination deficits in Parkinson's disease. *Mov Disord,* 23**,** 1984-90.

BOOT, B. P., ORR, C. F., AHLSKOG, J. E., FERMAN, T. J., ROBERTS, R., PANKRATZ, V. S., DICKSON, D. W., PARISI, J., AAKRE, J. A., GEDA, Y. E., KNOPMAN, D. S., PETERSEN, R. C. & BOEVE, B. F. 2013. Risk factors for dementia with Lewy bodies: a case-control study. *Neurology,* 81**,** 833-40.

BRAAK, H., ALAFUZOFF, I., ARZBERGER, T., KRETZSCHMAR, H. & DEL TREDICI, K. 2006. Staging of Alzheimer disease-associated neurofibrillary pathology using paraffin sections and immunocytochemistry. *Acta Neuropathol,* 112**,** 389-404.

BRAAK, H. & BRAAK, E. 1991. Neuropathological stageing of Alzheimer-related changes. *Acta Neuropathol,* 82**,** 239-59.

BRAAK, H. & DEL TREDICI, K. 2008. Invited Article: Nervous system pathology in sporadic Parkinson disease. *Neurology,* 70**,** 1916-25.
BRAAK, H. & DEL TREDICI, K. 2011. The pathological process underlying Alzheimer's disease in individuals under thirty. *Acta Neuropathol,* 121**,** 171-81.

BRAAK, H., DEL TREDICI, K., RUB, U., DE VOS, R. A., JANSEN STEUR, E. N. & BRAAK, E. 2003. Staging of brain pathology related to sporadic Parkinson's disease. *Neurobiol Aging,* 24**,** 197-211.

BRAAK, H., THAL, D. R., GHEBREMEDHIN, E. & DEL TREDICI, K. 2011. Stages of the pathologic process in Alzheimer disease: age categories from 1 to 100 years. *J Neuropathol Exp Neurol,* 70**,** 960-9.

BRION, J. P. & COUCK, A. M. 1995. Cortical and brainstem-type Lewy bodies are immunoreactive for the cyclin-dependent kinase 5. *Am J Pathol,* 147**,** 1465-76.

BRODATY, H., SEEHER, K. & GIBSON, L. 2012. Dementia time to death: a systematic literature review on survival time and years of life lost in people with dementia. *Int Psychogeriatr,* 24**,** 1034-45.

BRUNNSTROM, H. R. & ENGLUND, E. M. 2009. Cause of death in patients with dementia disorders. *Eur J Neurol,* 16**,** 488-92.

BUBENDORF, L., NOCITO, A., MOCH, H. & SAUTER, G. 2001. Tissue microarray (TMA) technology: miniaturized pathology archives for high-throughput in situ studies. *J Pathol,* 195**,** 72-9.

BURTON, E. J., BARBER, R., MUKAETOVA-LADINSKA, E. B., ROBSON, J., PERRY, R. H., JAROS, E., KALARIA, R. N. & O'BRIEN, J. T. 2009. Medial temporal lobe atrophy on MRI differentiates Alzheimer's disease from dementia with Lewy bodies and vascular cognitive impairment: a prospective study with pathological verification of diagnosis. *Brain,* 132**,** 195-203.

CALERO, O., HORTIGUELA, R., BULLIDO, M. J. & CALERO, M. 2009. Apolipoprotein E genotyping method by real time PCR, a fast and cost-effective alternative to the TaqMan and FRET assays. *J Neurosci Methods,* 183**,** 238-40.

CAMPION, D., DUMANCHIN, C., HANNEQUIN, D., DUBOIS, B., BELLIARD, S., PUEL, M., THOMAS-ANTERION, C., MICHON, A., MARTIN, C., CHARBONNIER, F., RAUX, G., CAMUZAT, A., PENET, C., MESNAGE, V., MARTINEZ, M., CLERGET-DARPOUX, F., BRICE, A. & FREBOURG, T. 1999. Early-onset autosomal dominant Alzheimer disease: prevalence, genetic heterogeneity, and mutation spectrum. *Am J Hum Genet,* 65**,** 664-70.

CARAFOLI, E. 1987. Intracellular calcium homeostasis. *Annu Rev Biochem,* 56**,** 395-433.

CARRELL, R. W. & LOMAS, D. A. 1997. Conformational disease. *Lancet,* 350**,** 134-8.

CHANDRA, S., FORNAI, F., KWON, H. B., YAZDANI, U., ATASOY, D., LIU, X., HAMMER, R. E., BATTAGLIA, G., GERMAN, D. C., CASTILLO, P. E. & SUDHOF, T. C. 2004. Double-knockout mice for alpha- and beta-synucleins: effect on synaptic functions. *Proc Natl Acad Sci U S A,* 101**,** 14966-71.

CHAUDHURI, K. R., HEALY, D. G. & SCHAPIRA, A. H. 2006. Non-motor symptoms of Parkinson's disease: diagnosis and management. *Lancet Neurol,* 5**,** 235-45.

CHENG, H. C., ULANE, C. M. & BURKE, R. E. 2010. Clinical progression in Parkinson disease and the neurobiology of axons. *Ann Neurol,* 67**,** 715-25.

CHIEN, D. T., BAHRI, S., SZARDENINGS, A. K., WALSH, J. C., MU, F., SU, M. Y., SHANKLE, W. R., ELIZAROV, A. & KOLB, H. C. 2013. Early clinical PET imaging results with the novel PHF-tau radioligand [F-18]-T807. *J Alzheimers Dis,* 34**,** 457-68.

CHINTA, S. J., MALLAJOSYULA, J. K., RANE, A. & ANDERSEN, J. K. 2010. Mitochondrial alpha-synuclein accumulation impairs complex I function in dopaminergic neurons and results in increased mitophagy in vivo. *Neurosci Lett,* 486**,** 235-9.

CIECHANOVER, A. 2005. Proteolysis: from the lysosome to ubiquitin and the proteasome. *Nat Rev Mol Cell Biol,* 6**,** 79-87.

CLINTON, L. K., BLURTON-JONES, M., MYCZEK, K., TROJANOWSKI, J. Q. & LAFERLA, F. M. 2010. Synergistic Interactions between Abeta, tau, and alpha-synuclein: acceleration of neuropathology and cognitive decline. *J Neurosci,* 30**,** 7281-9.

COLEMAN, M. 2005. Axon degeneration mechanisms: commonality amid diversity. *Nat Rev Neurosci,* 6**,** 889-98.

COLLOBY, S. J., MCPARLAND, S., O'BRIEN, J. T. & ATTEMS, J. 2012. Neuropathological correlates of dopaminergic imaging in Alzheimer's disease and Lewy body dementias. *Brain,* 135**,** 2798-808.

COLOM-CADENA, M., GELPI, E., CHARIF, S., BELBIN, O., BLESA, R., MARTI, M. J., CLARIMON, J. & LLEO, A. 2013. Confluence of alpha-synuclein, tau, and beta-amyloid pathologies in dementia with Lewy bodies. *J Neuropathol Exp Neurol,* 72**,** 1203-12.

COMPTA, Y., PARKKINEN, L., O'SULLIVAN, S. S., VANDROVCOVA, J., HOLTON, J. L., COLLINS, C., LASHLEY, T., KALLIS, C., WILLIAMS, D. R., DE SILVA, R., LEES, A. J. & REVESZ, T. 2011. Lewy- and Alzheimer-type pathologies in Parkinson's disease dementia: which is more important? *Brain,* 134**,** 1493-505.

CONFORTI, L., GILLEY, J. & COLEMAN, M. P. 2014. Wallerian degeneration: an emerging axon death pathway linking injury and disease. *Nat Rev Neurosci,* 15**,** 394-409.

CONVIT, A., DE ASIS, J., DE LEON, M. J., TARSHISH, C. Y., DE SANTI, S. & RUSINEK, H. 2000. Atrophy of the medial occipitotemporal, inferior, and middle temporal gyri in non-demented elderly predict decline to Alzheimer's disease. *Neurobiol Aging,* 21**,** 19-26.

COOK, C. N., MURRAY, M. E. & PETRUCELLI, L. 2015. Understanding Biomarkers of Neurodegeneration: Novel approaches to detecting tau pathology. *Nat Med,* 21**,** 219-20.

COOKSON, M. R. & VAN DER BRUG, M. 2008. Cell systems and the toxic mechanism(s) of alpha-synuclein. *Exp Neurol,* 209**,** 5-11.

CORDER, E. H., SAUNDERS, A. M., STRITTMATTER, W. J., SCHMECHEL, D. E., GASKELL, P. C., SMALL, G. W., ROSES, A. D., HAINES, J. L. & PERICAK-VANCE, M. A. 1993. Gene dose of apolipoprotein E type 4 allele and the risk of Alzheimer's disease in late onset families. *Science,* 261**,** 921-3.

CRYSTAL, H. A., DICKSON, D. W., SLIWINSKI, M. J., LIPTON, R. B., GROBER, E., MARKS-NELSON, H. & ANTIS, P. 1993. Pathological markers associated with normal aging and dementia in the elderly. *Ann Neurol,* 34**,** 566-73.

CUERVO, A. M., STEFANIS, L., FREDENBURG, R., LANSBURY, P. T. & SULZER, D. 2004. Impaired degradation of mutant alpha-synuclein by chaperone-mediated autophagy. *Science,* 305**,** 1292-5.

D'ARRIGO, C., TABATON, M. & PERICO, A. 2009. N-terminal truncated pyroglutamyl beta amyloid peptide Abetapy3-42 shows a faster aggregation kinetics than the full-length Abeta1-42. *Biopolymers,* 91**,** 861-73.

DAAR, A. S., SINGER, P. A., PERSAD, D. L., PRAMMING, S. K., MATTHEWS, D. R., BEAGLEHOLE, R., BERNSTEIN, A., BORYSIEWICZ, L. K., COLAGIURI, S., GANGULY, N., GLASS, R. I., FINEGOOD, D. T., KOPLAN, J., NABEL, E. G., SARNA, G., SARRAFZADEGAN, N., SMITH, R., YACH, D. & BELL, J. 2007. Grand challenges in chronic non-communicable diseases. *Nature,* 450**,** 494-6.

DAHLSTROEM, A. & FUXE, K. 1964. Evidence for the existence of monoamine-containing neurons in the central nervous system. I. Demonstration of monoamines in the cell bodies of brain stem neurons. *Acta Physiol Scand Suppl***,** Suppl 232:1-55.

DAMIER, P., HIRSCH, E. C., AGID, Y. & GRAYBIEL, A. M. 1999. The substantia nigra of the human brain. II. Patterns of loss of dopamine-containing neurons in Parkinson's disease. *Brain,* 122 (Pt 8)**,** 1437-48.

DANZER, K. M., HAASEN, D., KAROW, A. R., MOUSSAUD, S., HABECK, M., GIESE, A., KRETZSCHMAR, H., HENGERER, B. & KOSTKA, M. 2007. Different species of alpha-synuclein oligomers induce calcium influx and seeding. *J Neurosci,* 27**,** 9220-32.

DE FELICE, F. G., VIEIRA, M. N., SARAIVA, L. M., FIGUEROA-VILLAR, J. D., GARCIA-ABREU, J., LIU, R., CHANG, L., KLEIN, W. L. & FERREIRA, S. T. 2004. Targeting the neurotoxic species in Alzheimer's disease: inhibitors of Abeta oligomerization. *Faseb j,* 18**,** 1366-72.

DE LA TORRE, J. C. 2004. Alzheimer's disease is a vasocognopathy: a new term to describe its nature. *Neurol Res,* 26**,** 517-24.

DE LAU, L. M. & BRETELER, M. M. 2006. Epidemiology of Parkinson's disease. *Lancet Neurol,* 5**,** 525-35.

DEHAY, B., BOVE, J., RODRIGUEZ-MUELA, N., PERIER, C., RECASENS, A., BOYA, P. & VILA, M. 2010. Pathogenic lysosomal depletion in Parkinson's disease. *J Neurosci,* 30**,** 12535-44.

DEKOSKY, S. T. & SCHEFF, S. W. 1990. Synapse loss in frontal cortex biopsies in Alzheimer's disease: correlation with cognitive severity. *Ann Neurol,* 27**,** 457-64.

DELLI PIZZI, S., FRANCIOTTI, R., TARTARO, A., CAULO, M., THOMAS, A., ONOFRJ, M. & BONANNI, L. 2014. Structural alteration of the dorsal visual network in DLB patients with visual hallucinations: a cortical thickness MRI study. *PLoS One,* 9**,** e86624.

DEPARTMENT OF HEALTH 2012. Prime Minister's challenge on dementia: delivering major improvements in dementia care and research by 2015. London, UK: Department of Health.

DERAMECOURT, V., SLADE, J. Y., OAKLEY, A. E., PERRY, R. H., INCE, P. G., MAURAGE, C. A. & KALARIA, R. N. 2012. Staging and natural history of cerebrovascular pathology in dementia. *Neurology,* 78**,** 1043-50.

DI, J., COHEN, L. S., CORBO, C. P., PHILLIPS, G. R., EL IDRISSI, A. & ALONSO, A. D. 2016. Abnormal tau induces cognitive impairment through two different mechanisms: synaptic dysfunction and neuronal loss. *Sci Rep,* 6**,** 20833.

DICKSON, D. W., BRAAK, H., DUDA, J. E., DUYCKAERTS, C., GASSER, T., HALLIDAY, G. M., HARDY, J., LEVERENZ, J. B., DEL TREDICI, K., WSZOLEK, Z. K. & LITVAN, I. 2009. Neuropathological assessment of Parkinson's disease: refining the diagnostic criteria. *Lancet Neurol,* 8**,** 1150-7.

DOBSON, C. M. 1999. Protein misfolding, evolution and disease. *Trends Biochem Sci,* 24**,** 329-32.

DOCHERTY, M. J. & BURN, D. J. 2010. Parkinson's disease dementia. *Curr Neurol Neurosci Rep,* 10**,** 292-8.

DONNEMILLER, E., HEILMANN, J., WENNING, G. K., BERGER, W., DECRISTOFORO, C., MONCAYO, R., POEWE, W. & RANSMAYR, G. 1997. Brain perfusion scintigraphy with 99mTc-HMPAO or 99mTc-ECD and 123I-beta-CIT single-photon emission tomography in dementia of the Alzheimer-type and diffuse Lewy body disease. *Eur J Nucl Med,* 24**,** 320-5.

DOPPLER, K., EBERT, S., UCEYLER, N., TRENKWALDER, C., EBENTHEUER, J., VOLKMANN, J. & SOMMER, C. 2014. Cutaneous neuropathy in Parkinson's disease: a window into brain pathology. *Acta Neuropathol,* 128**,** 99-109.

DOTY, R. L., BROMLEY, S. M. & STERN, M. B. 1995. Olfactory testing as an aid in the diagnosis of Parkinson's disease: development of optimal discrimination criteria. *Neurodegeneration,* 4**,** 93-7.

DUDA, J. E., GIASSON, B. I., MABON, M. E., LEE, V. M. & TROJANOWSKI, J. Q. 2002. Novel antibodies to synuclein show abundant striatal pathology in Lewy body diseases. *Ann Neurol,* 52**,** 205-10.

DUGGER, B. N., ADLER, C. H., SHILL, H. A., CAVINESS, J., JACOBSON, S., DRIVER-DUNCKLEY, E. & BEACH, T. G. 2014. Concomitant pathologies among a spectrum of parkinsonian disorders. *Parkinsonism Relat Disord*.

DUGGER, B. N., BOEVE, B. F., MURRAY, M. E., PARISI, J. E., FUJISHIRO, H., DICKSON, D. W. & FERMAN, T. J. 2012. Rapid eye movement sleep behavior

disorder and subtypes in autopsy-confirmed dementia with Lewy bodies. *Mov Disord,* 27**,** 72-8.

DUM, R. P. & STRICK, P. L. 1991. The origin of corticospinal projections from the premotor areas in the frontal lobe. *J Neurosci,* 11**,** 667-89.

DUYCKAERTS, C., DELATOUR, B. & POTIER, M. C. 2009. Classification and basic pathology of Alzheimer disease. *Acta Neuropathol,* 118**,** 5-36.

EDISON, P., ROWE, C. C., RINNE, J. O., NG, S., AHMED, I., KEMPPAINEN, N., VILLEMAGNE, V. L., O'KEEFE, G., NAGREN, K., CHAUDHURY, K. R., MASTERS, C. L. & BROOKS, D. J. 2008. Amyloid load in Parkinson's disease dementia and Lewy body dementia measured with [11C]PIB positron emission tomography. *J Neurol Neurosurg Psychiatry,* 79**,** 1331-8.

EL-AGNAF, O. M., JAKES, R., CURRAN, M. D., MIDDLETON, D., INGENITO, R., BIANCHI, E., PESSI, A., NEILL, D. & WALLACE, A. 1998. Aggregates from mutant and wild-type alpha-synuclein proteins and NAC peptide induce apoptotic cell death in human neuroblastoma cells by formation of beta-sheet and amyloid-like filaments. *FEBS Lett,* 440**,** 71-5.

ELBAZ, A., DUFOUIL, C. & ALPEROVITCH, A. 2007. Interaction between genes and environment in neurodegenerative diseases. *C R Biol,* 330**,** 318-28.
EMRE, M., AARSLAND, D., BROWN, R., BURN, D. J., DUYCKAERTS, C., MIZUNO, Y., BROE, G. A., CUMMINGS, J., DICKSON, D. W., GAUTHIER, S., GOLDMAN, J., GOETZ, C., KORCZYN, A., LEES, A., LEVY, R., LITVAN, I., MCKEITH, I., OLANOW, W., POEWE, W., QUINN, N., SAMPAIO, C., TOLOSA, E. & DUBOIS, B. 2007. Clinical diagnostic criteria for dementia associated with Parkinson's disease. *Mov Disord,* 22**,** 1689-707; quiz 1837.

FARRER, L. A., CUPPLES, L. A., HAINES, J. L., HYMAN, B., KUKULL, W. A., MAYEUX, R., MYERS, R. H., PERICAK-VANCE, M. A., RISCH, N. & VAN DUIJN, C. M. 1997. Effects of age, sex, and ethnicity on the association between apolipoprotein E genotype and Alzheimer disease. A meta-analysis. APOE and Alzheimer Disease Meta Analysis Consortium. *JAMA,* 278**,** 1349-56.

FEARNLEY, J. M. & LEES, A. J. 1991. Ageing and Parkinson's disease: substantia nigra regional selectivity. *Brain,* 114 (Pt 5)**,** 2283-301.

FODERO-TAVOLETTI, M. T., OKAMURA, N., FURUMOTO, S., MULLIGAN, R. S., CONNOR, A. R., MCLEAN, C. A., CAO, D., RIGOPOULOS, A., CARTWRIGHT, G. A., O'KEEFE, G., GONG, S., ADLARD, P. A., BARNHAM, K. J., ROWE, C. C., MASTERS, C. L., KUDO, Y., CAPPAI, R., YANAI, K. & VILLEMAGNE, V. L. 2011. 18F-THK523: a novel in vivo tau imaging ligand for Alzheimer's disease. *Brain,* 134**,** 1089-100.

FOLSTEIN, M. F., FOLSTEIN, S. E. & MCHUGH, P. R. 1975. "Mini-mental state". A practical method for grading the cognitive state of patients for the clinician. *J Psychiatr Res,* 12**,** 189-98.

FOLTYNIE, T., BRAYNE, C. E., ROBBINS, T. W. & BARKER, R. A. 2004. The cognitive ability of an incident cohort of Parkinson's patients in the UK. The CamPaIGN study. *Brain,* 127**,** 550-60.

FORMAN, M. S., TROJANOWSKI, J. Q. & LEE, V. M. 2004. Neurodegenerative diseases: a decade of discoveries paves the way for therapeutic breakthroughs. *Nat Med,* 10**,** 1055-63.

FOSTER, V., OAKLEY, A. E., SLADE, J. Y., HALL, R., POLVIKOSKI, T. M., BURKE, M., THOMAS, A. J., KHUNDAKAR, A., ALLAN, L. M. & KALARIA, R. N. 2014. Pyramidal neurons of the prefrontal cortex in post-stroke, vascular and other ageing-related dementias. *Brain,* 137**,** 2509-21.

FRANCO-MARINA, F., GARCIA-GONZALEZ, J. J., WAGNER-ECHEAGARAY, F., GALLO, J., UGALDE, O., SANCHEZ-GARCIA, S., ESPINEL-BERMUDEZ, C., JUAREZ-CEDILLO, T., RODRIGUEZ, M. A. & GARCIA-PENA, C. 2010. The Mini-mental State Examination revisited: ceiling and floor effects after score adjustment for educational level in an aging Mexican population. *Int Psychogeriatr,* 22**,** 72-81.

FRIEDLANDER, R. M. 2003. Apoptosis and caspases in neurodegenerative diseases. *N Engl J Med,* 348**,** 1365-75.

FUJIWARA, H., HASEGAWA, M., DOHMAE, N., KAWASHIMA, A., MASLIAH, E., GOLDBERG, M. S., SHEN, J., TAKIO, K. & IWATSUBO, T. 2002. alpha-Synuclein is phosphorylated in synucleinopathy lesions. *Nat Cell Biol,* 4**,** 160-4.

GAO, H. M., JIANG, J., WILSON, B., ZHANG, W., HONG, J. S. & LIU, B. 2002. Microglial activation-mediated delayed and progressive degeneration of rat nigral dopaminergic neurons: relevance to Parkinson's disease. *J Neurochem,* 81**,** 1285-97.

GARCIA-PTACEK, S., FARAHMAND, B., KAREHOLT, I., RELIGA, D., CUADRADO, M. L. & ERIKSDOTTER, M. 2014. Mortality risk after dementia diagnosis by dementia type and underlying factors: a cohort of 15,209 patients based on the Swedish Dementia Registry. *J Alzheimers Dis,* 41**,** 467-77.

GENTLEMAN, S. M., ALLSOP, D., BRUTON, C. J., JAGOE, R., POLAK, J. M. & ROBERTS, G. W. 1992. Quantitative differences in the deposition of beta A4 protein in the sulci and gyri of frontal and temporal isocortex in Alzheimer's disease. *Neurosci Lett,* 136**,** 27-30.

GERTZ, H. J., XUEREB, J. H., HUPPERT, F. A., BRAYNE, C., KRUGER, H., MCGEE, M. A., PAYKEL, E. S., HARRINGTON, C. R., MUKAETOVA-LADINSKA, E. B., O'CONNOR, D. W. & WISCHIK, C. M. 1996. The relationship between clinical dementia and neuropathological staging (Braak) in a very elderly community sample. *Eur Arch Psychiatry Clin Neurosci,* 246**,** 132-6.

GIANNAKOPOULOS, P., HERRMANN, F. R., BUSSIERE, T., BOURAS, C., KOVARI, E., PERL, D. P., MORRISON, J. H., GOLD, G. & HOF, P. R. 2003. Tangle and neuron numbers, but not amyloid load, predict cognitive status in Alzheimer's disease. *Neurology,* 60**,** 1495-500.

GIASSON, B. I., DUDA, J. E., MURRAY, I. V., CHEN, Q., SOUZA, J. M., HURTIG, H. I., ISCHIROPOULOS, H., TROJANOWSKI, J. Q. & LEE, V. M. 2000. Oxidative damage linked to neurodegeneration by selective alpha-synuclein nitration in synucleinopathy lesions. *Science,* 290**,** 985-9.

GIASSON, B. I., FORMAN, M. S., HIGUCHI, M., GOLBE, L. I., GRAVES, C. L., KOTZBAUER, P. T., TROJANOWSKI, J. Q. & LEE, V. M. 2003. Initiation and synergistic fibrillization of tau and alpha-synuclein. *Science,* 300**,** 636-40.

GIBB, W. R. & LEES, A. J. 1988. The relevance of the Lewy body to the pathogenesis of idiopathic Parkinson's disease. *J Neurol Neurosurg Psychiatry,* 51**,** 745-52.

GILL, D. P., HUBBARD, R. A., KOEPSELL, T. D., BORRIE, M. J., PETRELLA, R. J., KNOPMAN, D. S. & KUKULL, W. A. 2013. Differences in rate of functional decline across three dementia types. *Alzheimers Dement,* 9**,** S63-71.
GOEDERT, M., SPILLANTINI, M. G., DEL TREDICI, K. & BRAAK, H. 2013. 100 years of Lewy pathology. *Nat Rev Neurol,* 9**,** 13-24.

GOETZ, C. G., TILLEY, B. C., SHAFTMAN, S. R., STEBBINS, G. T., FAHN, S., MARTINEZ-MARTIN, P., POEWE, W., SAMPAIO, C., STERN, M. B., DODEL, R., DUBOIS, B., HOLLOWAY, R., JANKOVIC, J., KULISEVSKY, J., LANG, A. E., LEES, A., LEURGANS, S., LEWITT, P. A., NYENHUIS, D., OLANOW, C. W., RASCOL, O., SCHRAG, A., TERESI, J. A., VAN HILTEN, J. J. & LAPELLE, N. 2008. Movement Disorder Society-sponsored revision of the Unified Parkinson's Disease Rating Scale (MDS-UPDRS): scale presentation and clinimetric testing results. *Mov Disord,* 23**,** 2129-70.

GOETZ, C. G. E. A. 2003. The Unified Parkinson's Disease Rating Scale (UPDRS): status and recommendations. *Mov Disord,* 18**,** 738-50.

GOLD, G., BOURAS, C., KOVARI, E., CANUTO, A., GLARIA, B. G., MALKY, A., HOF, P. R., MICHEL, J. P. & GIANNAKOPOULOS, P. 2000. Clinical validity of Braak neuropathological staging in the oldest-old. *Acta Neuropathol,* 99**,** 579-82; discussion 583-4.

GOLD, G., GIANNAKOPOULOS, P., HERRMANN, F. R., BOURAS, C. & KOVARI, E. 2007. Identification of Alzheimer and vascular lesion thresholds for mixed dementia. *Brain,* 130**,** 2830-6.

GOLDMAN, J. G. & LITVAN, I. 2011. Mild cognitive impairment in Parkinson's disease. *Minerva Med,* 102**,** 441-59.

GOMEZ-TORTOSA, E., NEWELL, K., IRIZARRY, M. C., ALBERT, M., GROWDON, J. H. & HYMAN, B. T. 1999. Clinical and quantitative pathologic correlates of dementia with Lewy bodies. *Neurology,* 53**,** 1284-91.

GONG, C. X., SHAIKH, S., WANG, J. Z., ZAIDI, T., GRUNDKE-IQBAL, I. & IQBAL, K. 1995. Phosphatase activity toward abnormally phosphorylated tau: decrease in Alzheimer disease brain. *J Neurochem,* 65**,** 732-8.

GRAEBER, M. B. & MORAN, L. B. 2002. Mechanisms of cell death in neurodegenerative diseases: fashion, fiction, and facts. *Brain Pathol,* 12**,** 385-90.

GRAYBIEL, A. M., AOSAKI, T., FLAHERTY, A. W. & KIMURA, M. 1994. The basal ganglia and adaptive motor control. *Science,* 265**,** 1826-31.

GREFFARD, S., VERNY, M., BONNET, A. M., SEILHEAN, D., HAUW, J. J. & DUYCKAERTS, C. 2010. A stable proportion of Lewy body bearing neurons in the substantia nigra suggests a model in which the Lewy body causes neuronal death. *Neurobiol Aging,* 31**,** 99-103.

GRUNDKE-IQBAL, I., IQBAL, K., TUNG, Y. C., QUINLAN, M., WISNIEWSKI, H. M. & BINDER, L. I. 1986. Abnormal phosphorylation of the microtubule-associated protein tau (tau) in Alzheimer cytoskeletal pathology. *Proc Natl Acad Sci U S A,* 83**,** 4913-7.

GUILLOZET, A. L., WEINTRAUB, S., MASH, D. C. & MESULAM, M. M. 2003. Neurofibrillary tangles, amyloid, and memory in aging and mild cognitive impairment. *Arch Neurol,* 60**,** 729-36.

HAASS, C. & SELKOE, D. J. 2007. Soluble protein oligomers in neurodegeneration: lessons from the Alzheimer's amyloid beta-peptide. *Nat Rev Mol Cell Biol,* 8**,** 101-12.

HADLAND, K. A., RUSHWORTH, M. F., GAFFAN, D. & PASSINGHAM, R. E. 2003. The effect of cingulate lesions on social behaviour and emotion. *Neuropsychologia,* 41**,** 919-31.

HALLIDAY, G. M., DOUBLE, K. L., MACDONALD, V. & KRIL, J. J. 2003. Identifying severely atrophic cortical subregions in Alzheimer's disease. *Neurobiol Aging,* 24**,** 797-806.

HALLIDAY, G. M., K. CARTWRIGHT, H. 2014. Pathology of Parkinson's disease. *In:* WOLTERS, E. B., C. (ed.) *Parkinsin's disease and Other Movement Disorders.* Chicago, USA: Independant publishers.

HALLIDAY, G. M., SONG, Y. J. & HARDING, A. J. 2011. Striatal beta-amyloid in dementia with Lewy bodies but not Parkinson's disease. *J Neural Transm,* 118**,** 713-9.

HAMPEL, H., SHEN, Y., WALSH, D. M., AISEN, P., SHAW, L. M., ZETTERBERG, H., TROJANOWSKI, J. Q. & BLENNOW, K. 2010. Biological markers of amyloid beta-related mechanisms in Alzheimer's disease. *Exp Neurol,* 223**,** 334-46.

HAN, L., COLE, M., BELLAVANCE, F., MCCUSKER, J. & PRIMEAU, F. 2000. Tracking cognitive decline in Alzheimer's disease using the mini-mental state examination: a meta-analysis. *Int Psychogeriatr,* 12**,** 231-47.

HANGER, D. P. 2015. *Tau phosphorylation sites* [Online]. Available: http://cnr.iop.kcl.ac.uk/hangerlab/tautable [Accessed 31/7/15 2015].

HANGER, D. P., ANDERTON, B. H. & NOBLE, W. 2009. Tau phosphorylation: the therapeutic challenge for neurodegenerative disease. *Trends Mol Med,* 15**,** 112-9.

HANSSON PETERSEN, C. A., ALIKHANI, N., BEHBAHANI, H., WIEHAGER, B., PAVLOV, P. F., ALAFUZOFF, I., LEINONEN, V., ITO, A., WINBLAD, B., GLASER, E. & ANKARCRONA, M. 2008. The amyloid beta-peptide is imported into mitochondria via the TOM import machinery and localized to mitochondrial cristae. *Proc Natl Acad Sci U S A,* 105**,** 13145-50.

HARDY, J. A. & HIGGINS, G. A. 1992. Alzheimer's disease: the amyloid cascade hypothesis. *Science,* 256**,** 184-5.

HAROUTUNIAN, V., PUROHIT, D. P., PERL, D. P., MARIN, D., KHAN, K., LANTZ, M., DAVIS, K. L. & MOHS, R. C. 1999. Neurofibrillary tangles in nondemented elderly subjects and mild Alzheimer disease. *Arch Neurol,* 56**,** 713-8.

HASHIMOTO, M., TAKEDA, A., HSU, L. J., TAKENOUCHI, T. & MASLIAH, E. 1999. Role of cytochrome c as a stimulator of alpha-synuclein aggregation in Lewy body disease. *J Biol Chem,* 274**,** 28849-52.

HASSLER, R. 1938. Zur Pathologie der paralysis agitans und des postenzephalitischen Parkinsonismmus. *J Psychol Neurol,* 48**,** 387-476.

HAWKES, C. A., JAYAKODY, N., JOHNSTON, D. A., BECHMANN, I. & CARARE, R. O. 2014. Failure of perivascular drainage of beta-amyloid in cerebral amyloid angiopathy. *Brain Pathol,* 24**,** 396-403.

HAWKES, C. H., DEL TREDICI, K. & BRAAK, H. 2010. A timeline for Parkinson's disease. *Parkinsonism Relat Disord,* 16**,** 79-84.

HE, W. & BARROW, C. J. 1999. The A beta 3-pyroglutamyl and 11-pyroglutamyl peptides found in senile plaque have greater beta-sheet forming and aggregation propensities in vitro than full-length A beta. *Biochemistry,* 38**,** 10871-7.

HELY, M. A., REID, W. G., ADENA, M. A., HALLIDAY, G. M. & MORRIS, J. G. 2008. The Sydney multicenter study of Parkinson's disease: the inevitability of dementia at 20 years. *Mov Disord,* 23**,** 837-44.

HERNANDEZ, D. G., REED, X. & SINGLETON, A. B. 2016. Genetics in Parkinson disease: Mendelian versus non-Mendelian inheritance. *J Neurochem*. (epub ahead of print).

HERRERO, M. T., BARCIA, C. & NAVARRO, J. M. 2002. Functional anatomy of thalamus and basal ganglia. *Childs Nerv Syst,* 18**,** 386-404.

HIRUMA, H., KATAKURA, T., TAKAHASHI, S., ICHIKAWA, T. & KAWAKAMI, T. 2003. Glutamate and amyloid beta-protein rapidly inhibit fast axonal transport in cultured rat hippocampal neurons by different mechanisms. *J Neurosci,* 23**,** 8967-77.

HOEHN, M. M. & YAHR, M. D. 1967. Parkinsonism: onset, progression and mortality. *Neurology,* 17**,** 427-42.

HOLMES, C., BOCHE, D., WILKINSON, D., YADEGARFAR, G., HOPKINS, V., BAYER, A., JONES, R. W., BULLOCK, R., LOVE, S., NEAL, J. W., ZOTOVA, E. & NICOLL, J. A. 2008. Long-term effects of Abeta42 immunisation in Alzheimer's disease: follow-up of a randomised, placebo-controlled phase I trial. *Lancet,* 372**,** 216-23.

HONG, M., ZHUKAREVA, V., VOGELSBERG-RAGAGLIA, V., WSZOLEK, Z., REED, L., MILLER, B. I., GESCHWIND, D. H., BIRD, T. D., MCKEEL, D., GOATE, A., MORRIS, J. C., WILHELMSEN, K. C., SCHELLENBERG, G. D., TROJANOWSKI, J. Q. & LEE, V. M. 1998. Mutation-specific functional impairments in distinct tau isoforms of hereditary FTDP-17. *Science,* 282**,** 1914-7.

HORNYKIEWICZ, O. 1998. Biochemical aspects of Parkinson's disease. *Neurology,* 51**,** S2-9.

HORNYKIEWICZ, O. & KISH, S. J. 1987. Biochemical pathophysiology of Parkinson's disease. *Adv Neurol,* 45**,** 19-34.

HOWLETT, D. R., WHITFIELD, D., JOHNSON, M., ATTEMS, J., O'BRIEN, J. T., AARSLAND, D., LAI, M. K., LEE, J. H., CHEN, C., BALLARD, C., HORTOBAGYI, T. & FRANCIS, P. T. 2014. Regional Multiple Pathology Scores are Associated with Cognitive Decline in Lewy Body Dementias. *Brain Pathol,* [Epub ahead of print].

HU, X. S., OKAMURA, N., ARAI, H., HIGUCHI, M., MATSUI, T., TASHIRO, M., SHINKAWA, M., ITOH, M., IDO, T. & SASAKI, H. 2000. 18F-fluorodopa PET study of striatal dopamine uptake in the diagnosis of dementia with Lewy bodies. *Neurology,* 55**,** 1575-7.

HURTIG, H. I., TROJANOWSKI, J. Q., GALVIN, J., EWBANK, D., SCHMIDT, M. L., LEE, V. M., CLARK, C. M., GLOSSER, G., STERN, M. B., GOLLOMP, S. M. & ARNOLD, S. E. 2000. Alpha-synuclein cortical Lewy bodies correlate with dementia in Parkinson's disease. *Neurology,* 54**,** 1916-21.

HUTCHINSON, J. B., UNCAPHER, M. R., WEINER, K. S., BRESSLER, D. W., SILVER, M. A., PRESTON, A. R. & WAGNER, A. D. 2014. Functional heterogeneity in posterior parietal cortex across attention and episodic memory retrieval. *Cereb Cortex,* 24**,** 49-66.

HYMAN, B. T., PHELPS, C. H., BEACH, T. G., BIGIO, E. H., CAIRNS, N. J., CARRILLO, M. C., DICKSON, D. W., DUYCKAERTS, C., FROSCH, M. P., MASLIAH, E., MIRRA, S. S., NELSON, P. T., SCHNEIDER, J. A., THAL, D. R., THIES, B., TROJANOWSKI, J. Q., VINTERS, H. V. & MONTINE, T. J. 2012. National Institute on Aging-Alzheimer's Association guidelines for the neuropathologic assessment of Alzheimer's disease. *Alzheimers Dement,* 8**,** 1-13.

IACONO, D., GERACI-ERCK, M., RABIN, M. L., ADLER, C. H., SERRANO, G., BEACH, T. G. & KURLAN, R. 2015. Parkinson disease and incidental Lewy body disease: Just a question of time? *Neurology,* 85**,** 1670-9.

IMHOF, A., KOVARI, E., VON GUNTEN, A., GOLD, G., RIVARA, C. B., HERRMANN, F. R., HOF, P. R., BOURAS, C. & GIANNAKOPOULOS, P. 2007. Morphological substrates of cognitive decline in nonagenarians and centenarians: a new paradigm? *J Neurol Sci,* 257**,** 72-9.

INCE, P. G. 2001. Pathological correlates of late-onset dementia in a multicentre, community-based population in England and Wales. Neuropathology Group of the Medical Research Council Cognitive Function and Ageing Study (MRC CFAS). *Lancet,* 357**,** 169-75.

INGRAM, E. M. & SPILLANTINI, M. G. 2002. Tau gene mutations: dissecting the pathogenesis of FTDP-17. *Trends Mol Med,* 8**,** 555-62.

IRWIN, D. J., WHITE, M. T., TOLEDO, J. B., XIE, S. X., ROBINSON, J. L., VAN DEERLIN, V., LEE, V. M., LEVERENZ, J. B., MONTINE, T. J., DUDA, J. E., HURTIG, H. I. & TROJANOWSKI, J. Q. 2012. Neuropathologic substrates of Parkinson disease dementia. *Ann Neurol,* 72**,** 587-98.

ISHIZAWA, T., MATTILA, P., DAVIES, P., WANG, D. & DICKSON, D. W. 2003. Colocalization of tau and alpha-synuclein epitopes in Lewy bodies. *J Neuropathol Exp Neurol,* 62**,** 389-97.

ITOH, A., NITTA, A., NADAI, M., NISHIMURA, K., HIROSE, M., HASEGAWA, T. & NABESHIMA, T. 1996. Dysfunction of cholinergic and dopaminergic neuronal systems in beta-amyloid protein--infused rats. *J Neurochem,* 66**,** 1113-7.

JACK, C. R., JR., ALBERT, M. S., KNOPMAN, D. S., MCKHANN, G. M., SPERLING, R. A., CARRILLO, M. C., THIES, B. & PHELPS, C. H. 2011. Introduction to the recommendations from the National Institute on Aging-Alzheimer's Association workgroups on diagnostic guidelines for Alzheimer's disease. *Alzheimers Dement,* 7**,** 257-62.

JANKOVIC, J. 2008. Parkinson's disease: clinical features and diagnosis. *J Neurol Neurosurg Psychiatry,* 79**,** 368-76.

JAUNMUKTANE, Z., MEAD, S., ELLIS, M., WADSWORTH, J. D., NICOLL, A. J., KENNY, J., LAUNCHBURY, F., LINEHAN, J., RICHARD-LOENDT, A., WALKER, A. S., RUDGE, P., COLLINGE, J. & BRANDNER, S. 2015. Evidence for human transmission of amyloid-beta pathology and cerebral amyloid angiopathy. *Nature,* 525**,** 247-50.

JELLINGER, K. A. 2001. Small concomitant cerebrovascular lesions are not important for cognitive decline in severe Alzheimer disease. *Arch Neurol,* 58**,** 520-1.

JELLINGER, K. A. 2002. Alzheimer disease and cerebrovascular pathology: an update. *J Neural Transm,* 109**,** 813-36.

JELLINGER, K. A. 2003. General aspects of neurodegeneration. *J Neural Transm Suppl*, 101-44.

JELLINGER, K. A. 2007a. The enigma of mixed dementia. *Alzheimers Dement,* 3, 40-53.

JELLINGER, K. A. 2007b. The enigma of vascular cognitive disorder and vascular dementia. *Acta Neuropathol,* 113, 349-88.

JELLINGER, K. A. 2009. Recent advances in our understanding of neurodegeneration. *J Neural Transm,* 116, 1111-62.

JELLINGER, K. A. & ATTEMS, J. 2003. Incidence of cerebrovascular lesions in Alzheimer's disease: a postmortem study. *Acta Neuropathol,* 105, 14-7.

JELLINGER, K. A. & ATTEMS, J. 2005. Prevalence and pathogenic role of cerebrovascular lesions in Alzheimer disease. *J Neurol Sci,* 229-230, 37-41.

JELLINGER, K. A. & ATTEMS, J. 2006. Does striatal pathology distinguish Parkinson disease with dementia and dementia with Lewy bodies? *Acta Neuropathol,* 112, 253-60.

JELLINGER, K. A. & ATTEMS, J. 2007. Neuropathological evaluation of mixed dementia. *J Neurol Sci,* 257, 80-7.

JELLINGER, K. A. & ATTEMS, J. 2008. Prevalence and impact of vascular and Alzheimer pathologies in Lewy body disease. *Acta Neuropathol,* 115, 427-36.
JELLINGER, K. A. & ATTEMS, J. 2010. Prevalence of dementia disorders in the oldest-old: an autopsy study. *Acta Neuropathol,* 119, 421-33.

JONES, E. G. 1998. A new view of specific and nonspecific thalamocortical connections. *Adv Neurol,* 77, 49-71; discussion 72-3.

JOSEPHS, K. A., WHITWELL, J. L., WEIGAND, S. D., MURRAY, M. E., TOSAKULWONG, N., LIESINGER, A. M., PETRUCELLI, L., SENJEM, M. L., KNOPMAN, D. S., BOEVE, B. F., IVNIK, R. J., SMITH, G. E., JACK, C. R., JR., PARISI, J. E., PETERSEN, R. C. & DICKSON, D. W. 2014. TDP-43 is a key player in the clinical features associated with Alzheimer's disease. *Acta Neuropathol,* 127, 811-24.

JUNG, Y., DICKSON, D. W., MURRAY, M. E., WHITWELL, J. L., KNOPMAN, D. S., BOEVE, B. F., JACK, C. R., JR., PARISI, J. E., PETERSEN, R. C. & JOSEPHS, K. A. 2014. TDP-43 in Alzheimer's disease is not associated with clinical FTLD or Parkinsonism. *J Neurol,* 261, 1344-1348.

KANG, J., LEMAIRE, H. G., UNTERBECK, A., SALBAUM, J. M., MASTERS, C. L., GRZESCHIK, K. H., MULTHAUP, G., BEYREUTHER, K. & MULLER-HILL, B. 1987. The precursor of Alzheimer's disease amyloid A4 protein resembles a cell-surface receptor. *Nature,* 325, 733-6.

KATZENSCHLAGER, R., ZIJLMANS, J., EVANS, A., WATT, H. & LEES, A. J. 2004. Olfactory function distinguishes vascular parkinsonism from Parkinson's disease. *J Neurol Neurosurg Psychiatry,* 75**,** 1749-52.

KAWAMATA, T., AKIYAMA, H., YAMADA, T. & MCGEER, P. L. 1992. Immunologic reactions in amyotrophic lateral sclerosis brain and spinal cord tissue. *Am J Pathol,* 140**,** 691-707.

KEMPSTER, P. A., O'SULLIVAN, S. S., HOLTON, J. L., REVESZ, T. & LEES, A. J. 2010. Relationships between age and late progression of Parkinson's disease: a clinico-pathological study. *Brain,* 133**,** 1755-62.

KIRIK, D., ROSENBLAD, C., BURGER, C., LUNDBERG, C., JOHANSEN, T. E., MUZYCZKA, N., MANDEL, R. J. & BJORKLUND, A. 2002. Parkinson-like neurodegeneration induced by targeted overexpression of alpha-synuclein in the nigrostriatal system. *J Neurosci,* 22**,** 2780-91.

KLOPPENBORG, R. P., VAN DEN BERG, E., KAPPELLE, L. J. & BIESSELS, G. J. 2008. Diabetes and other vascular risk factors for dementia: which factor matters most? A systematic review. *Eur J Pharmacol,* 585**,** 97-108.

KLUNK, W. E., ENGLER, H., NORDBERG, A., WANG, Y., BLOMQVIST, G., HOLT, D. P., BERGSTROM, M., SAVITCHEVA, I., HUANG, G. F., ESTRADA, S., AUSEN, B., DEBNATH, M. L., BARLETTA, J., PRICE, J. C., SANDELL, J., LOPRESTI, B. J., WALL, A., KOIVISTO, P., ANTONI, G., MATHIS, C. A. & LANGSTROM, B. 2004. Imaging brain amyloid in Alzheimer's disease with Pittsburgh Compound-B. *Ann Neurol,* 55**,** 306-19.

KOFFIE, R. M., HASHIMOTO, T., TAI, H. C., KAY, K. R., SERRANO-POZO, A., JOYNER, D., HOU, S., KOPEIKINA, K. J., FROSCH, M. P., LEE, V. M., HOLTZMAN, D. M., HYMAN, B. T. & SPIRES-JONES, T. L. 2012. Apolipoprotein E4 effects in Alzheimer's disease are mediated by synaptotoxic oligomeric amyloid-beta. *Brain,* 135**,** 2155-68.

KOLASINSKI, J., STAGG, C. J., CHANCE, S. A., DELUCA, G. C., ESIRI, M. M., CHANG, E. H., PALACE, J. A., MCNAB, J. A., JENKINSON, M., MILLER, K. L. & JOHANSEN-BERG, H. 2012. A combined post-mortem magnetic resonance imaging and quantitative histological study of multiple sclerosis pathology. *Brain,* 135**,** 2938-51.

KONONEN, J., BUBENDORF, L., KALLIONIEMI, A., BARLUND, M., SCHRAML, P., LEIGHTON, S., TORHORST, J., MIHATSCH, M. J., SAUTER, G. & KALLIONIEMI, O. P. 1998. Tissue microarrays for high-throughput molecular profiling of tumor specimens. *Nat Med,* 4**,** 844-7.

KOPEIKINA, K. J., HYMAN, B. T. & SPIRES-JONES, T. L. 2012. Soluble forms of tau are toxic in Alzheimer's disease. *Transl Neurosci,* 3**,** 223-233.

KOPKE, E., TUNG, Y. C., SHAIKH, S., ALONSO, A. C., IQBAL, K. & GRUNDKE-IQBAL, I. 1993. Microtubule-associated protein tau. Abnormal phosphorylation of a non-paired helical filament pool in Alzheimer disease. *J Biol Chem,* 268**,** 24374-84.

KOVACS, G. G., ALAFUZOFF, I., AL-SARRAJ, S., ARZBERGER, T., BOGDANOVIC, N., CAPELLARI, S., FERRER, I., GELPI, E., KOVARI, V.,

KRETZSCHMAR, H., NAGY, Z., PARCHI, P., SEILHEAN, D., SOININEN, H., TROAKES, C. & BUDKA, H. 2008. Mixed brain pathologies in dementia: the BrainNet Europe consortium experience. *Dement Geriatr Cogn Disord,* 26**,** 343-50.

KOVACS, G. G., MILENKOVIC, I., WOHRER, A., HOFTBERGER, R., GELPI, E., HABERLER, C., HONIGSCHNABL, S., REINER-CONCIN, A., HEINZL, H., JUNGWIRTH, S., KRAMPLA, W., FISCHER, P. & BUDKA, H. 2013. Non-Alzheimer neurodegenerative pathologies and their combinations are more frequent than commonly believed in the elderly brain: a community-based autopsy series. *Acta Neuropathol,* 126**,** 365-84.

KRAYBILL, M. L., LARSON, E. B., TSUANG, D. W., TERI, L., MCCORMICK, W. C., BOWEN, J. D., KUKULL, W. A., LEVERENZ, J. B. & CHERRIER, M. M. 2005. Cognitive differences in dementia patients with autopsy-verified AD, Lewy body pathology, or both. *Neurology,* 64**,** 2069-73.

KSIEZAK-REDING, H., LIU, W. K. & YEN, S. H. 1992. Phosphate analysis and dephosphorylation of modified tau associated with paired helical filaments. *Brain Res,* 597**,** 209-19.

KUNZLE, H. 1977. Projections from the primary somatosensory cortex to basal ganglia and thalamus in the monkey. *Exp Brain Res,* 30**,** 481-92.
LAFERLA, F. M., GREEN, K. N. & ODDO, S. 2007. Intracellular amyloid-beta in Alzheimer's disease. *Nat Rev Neurosci,* 8**,** 499-509.

LARGE, P. 2014. Annual Mid-year Population Estimates, 2013. Office for National Statistics.

LASHLEY, T., HOLTON, J. L., GRAY, E., KIRKHAM, K., O'SULLIVAN, S. S., HILBIG, A., WOOD, N. W., LEES, A. J. & REVESZ, T. 2008. Cortical alpha-synuclein load is associated with amyloid-beta plaque burden in a subset of Parkinson's disease patients. *Acta Neuropathol,* 115**,** 417-25.

LEE, J. H., OLICHNEY, J. M., HANSEN, L. A., HOFSTETTER, C. R. & THAL, L. J. 2000. Small concomitant vascular lesions do not influence rates of cognitive decline in patients with Alzheimer disease. *Arch Neurol,* 57**,** 1474-9.

LEE, V. M., GIASSON, B. I. & TROJANOWSKI, J. Q. 2004. More than just two peas in a pod: common amyloidogenic properties of tau and alpha-synuclein in neurodegenerative diseases. *Trends Neurosci,* 27**,** 129-34.

LEVERENZ, J. B., HAMILTON, R., TSUANG, D. W., SCHANTZ, A., VAVREK, D., LARSON, E. B., KUKULL, W. A., LOPEZ, O., GALASKO, D., MASLIAH, E., KAYE, J., WOLTJER, R., CLARK, C., TROJANOWSKI, J. Q. & MONTINE, T. J. 2008. Empiric refinement of the pathologic assessment of Lewy-related pathology in the dementia patient. *Brain Pathol,* 18**,** 220-4.

LEVY, G., SCHUPF, N., TANG, M. X., COTE, L. J., LOUIS, E. D., MEJIA, H., STERN, Y. & MARDER, K. 2002a. Combined effect of age and severity on the risk of dementia in Parkinson's disease. *Ann Neurol,* 51**,** 722-9.

LEVY, G., TANG, M. X., COTE, L. J., LOUIS, E. D., ALFARO, B., MEJIA, H., STERN, Y. & MARDER, K. 2000. Motor impairment in PD: relationship to incident dementia and age. *Neurology,* 55**,** 539-44.

LEVY, G., TANG, M. X., LOUIS, E. D., COTE, L. J., ALFARO, B., MEJIA, H., STERN, Y. & MARDER, K. 2002b. The association of incident dementia with mortality in PD. *Neurology,* 59**,** 1708-13.

LEWIS, S. J., FOLTYNIE, T., BLACKWELL, A. D., ROBBINS, T. W., OWEN, A. M. & BARKER, R. A. 2005. Heterogeneity of Parkinson's disease in the early clinical stages using a data driven approach. *J Neurol Neurosurg Psychiatry,* 76**,** 343-8.

LEWY, F. H. 1912. Paralysis Agitans Pathologische Anatomie. *In:* LEWANDOWSKI, M. (ed.) *Handbuch der Neurologie.* Berlin: Springer.

LIPPA, C. F., DUDA, J. E., GROSSMAN, M., HURTIG, H. I., AARSLAND, D., BOEVE, B. F., BROOKS, D. J., DICKSON, D. W., DUBOIS, B., EMRE, M., FAHN, S., FARMER, J. M., GALASKO, D., GALVIN, J. E., GOETZ, C. G., GROWDON, J. H., GWINN-HARDY, K. A., HARDY, J., HEUTINK, P., IWATSUBO, T., KOSAKA, K., LEE, V. M., LEVERENZ, J. B., MASLIAH, E., MCKEITH, I. G., NUSSBAUM, R. L., OLANOW, C. W., RAVINA, B. M., SINGLETON, A. B., TANNER, C. M., TROJANOWSKI, J. Q. & WSZOLEK, Z. K. 2007. DLB and PDD boundary issues: diagnosis, treatment, molecular pathology, and biomarkers. *Neurology,* 68**,** 812-9.

LITVAN, I., GOLDMAN, J. G., TROSTER, A. I., SCHMAND, B. A., WEINTRAUB, D., PETERSEN, R. C., MOLLENHAUER, B., ADLER, C. H., MARDER, K., WILLIAMS-GRAY, C. H., AARSLAND, D., KULISEVSKY, J., RODRIGUEZ-OROZ, M. C., BURN, D. J., BARKER, R. A. & EMRE, M. 2012. Diagnostic criteria for mild cognitive impairment in Parkinson's disease: Movement Disorder Society Task Force guidelines. *Mov Disord,* 27**,** 349-56.

LIU, F., GRUNDKE-IQBAL, I., IQBAL, K. & GONG, C. X. 2005a. Contributions of protein phosphatases PP1, PP2A, PP2B and PP5 to the regulation of tau phosphorylation. *Eur J Neurosci,* 22**,** 1942-50.

LIU, F., IQBAL, K., GRUNDKE-IQBAL, I., ROSSIE, S. & GONG, C. X. 2005b. Dephosphorylation of tau by protein phosphatase 5: impairment in Alzheimer's disease. *J Biol Chem,* 280**,** 1790-6.

LOO, D. T., COPANI, A., PIKE, C. J., WHITTEMORE, E. R., WALENCEWICZ, A. J. & COTMAN, C. W. 1993. Apoptosis is induced by beta-amyloid in cultured central nervous system neurons. *Proc Natl Acad Sci U S A,* 90**,** 7951-5.

LOPACHIN, R. M. & LEHNING, E. J. 1997. Mechanism of calcium entry during axon injury and degeneration. *Toxicol Appl Pharmacol,* 143**,** 233-44.

LUE, L. F., WALKER, D. G., ADLER, C. H., SHILL, H., TRAN, H., AKIYAMA, H., SUE, L. I., CAVINESS, J., SABBAGH, M. N. & BEACH, T. G. 2012. Biochemical increase in phosphorylated alpha-synuclein precedes histopathology of Lewy-type synucleinopathies. *Brain Pathol,* 22**,** 745-56.

LUNA-MUNOZ, J., CHAVEZ-MACIAS, L., GARCIA-SIERRA, F. & MENA, R. 2007. Earliest stages of tau conformational changes are related to the appearance of a sequence of specific phospho-dependent tau epitopes in Alzheimer's disease. *J Alzheimers Dis,* 12**,** 365-75.

LUNKES, A. & MANDEL, J. L. 1998. A cellular model that recapitulates major pathogenic steps of Huntington's disease. *Hum Mol Genet,* 7**,** 1355-61.

MACKENZIE, I. R. 2001. The pathology of Parkinson's disease. *BC Medical Journal,* 43**,** 142-147.

MANDAL, P. K., PETTEGREW, J. W., MASLIAH, E., HAMILTON, R. L. & MANDAL, R. 2006. Interaction between Abeta peptide and alpha synuclein: molecular mechanisms in overlapping pathology of Alzheimer's and Parkinson's in dementia with Lewy body disease. *Neurochem Res,* 31**,** 1153-62.

MANDLER, M., ROCKENSTEIN, E., UBHI, K., HANSEN, L., ADAME, A., MICHAEL, S., GALASKO, D., SANTIC, R., MATTNER, F. & MASLIAH, E. 2012. Detection of peri-synaptic amyloid-beta pyroglutamate aggregates in early stages of Alzheimer's disease and in AbetaPP transgenic mice using a novel monoclonal antibody. *J Alzheimers Dis,* 28**,** 783-94.

MANDLER, M., WALKER, L., SANTIC, R., HANSON, P., UPADHAYA, A. R., COLLOBY, S. J., MORRIS, C. M., THAL, D. R., THOMAS, A. J., SCHNEEBERGER, A. & ATTEMS, J. 2014. Pyroglutamylated amyloid-beta is associated with hyperphosphorylated tau and severity of Alzheimer's disease. *Acta Neuropathol,* 128**,** 67-79.

MANN, D. M. & JONES, D. 1990. Deposition of amyloid (A4) protein within the brains of persons with dementing disorders other than Alzheimer's disease and Down's syndrome. *Neurosci Lett,* 109**,** 68-75.

MARSH, S. E. & BLURTON-JONES, M. 2012. Examining the mechanisms that link beta-amyloid and alpha-synuclein pathologies. *Alzheimers Res Ther,* 4**,** 11.

MASELLIS, M., SHERBORN, K., NETO, P., SADOVNICK, D. A., HSIUNG, G. Y., BLACK, S. E., PRASAD, S., WILLIAMS, M. & GAUTHIER, S. 2013. Early-onset dementias: diagnostic and etiological considerations. *Alzheimers Res Ther,* 5**,** S7.

MASLIAH, E., ROCKENSTEIN, E., VEINBERGS, I., SAGARA, Y., MALLORY, M., HASHIMOTO, M. & MUCKE, L. 2001. beta-amyloid peptides enhance alpha-synuclein accumulation and neuronal deficits in a transgenic mouse model linking Alzheimer's disease and Parkinson's disease. *Proc Natl Acad Sci U S A,* 98**,** 12245-50.

MASLIAH, E., TERRY, R. D., DETERESA, R. M. & HANSEN, L. A. 1989. Immunohistochemical quantification of the synapse-related protein synaptophysin in Alzheimer disease. *Neurosci Lett,* 103**,** 234-9.

MATA, I. F., SAMII, A., SCHNEER, S. H., ROBERTS, J. W., GRIFFITH, A., LEIS, B. C., SCHELLENBERG, G. D., SIDRANSKY, E., BIRD, T. D.,

LEVERENZ, J. B., TSUANG, D. & ZABETIAN, C. P. 2008. Glucocerebrosidase gene mutations: a risk factor for Lewy body disorders. *Arch Neurol,* 65**,** 379-82.

MAYEUX, R. & STERN, Y. 2012. Epidemiology of Alzheimer disease. *Cold Spring Harb Perspect Med,* 2.

MCALEESE, K. E., FIRBANK, M., DEY, M., COLLOBY, S. J., WALKER, L., JOHNSON, M., BEVERLEY, J. R., TAYLOR, J. P., THOMAS, A. J., O'BRIEN, J. T. & ATTEMS, J. 2015. Cortical tau load is associated with white matter hyperintensities. *Acta Neuropathol Commun,* 3**,** 60.

MCGEER, P. L., ITAGAKI, S., BOYES, B. E. & MCGEER, E. G. 1988. Reactive microglia are positive for HLA-DR in the substantia nigra of Parkinson's and Alzheimer's disease brains. *Neurology,* 38**,** 1285-91.
MCGEER, P. L. & MCGEER, E. G. 1995. The inflammatory response system of brain: implications for therapy of Alzheimer and other neurodegenerative diseases. *Brain Res Brain Res Rev,* 21**,** 195-218.
MCKEITH, I. G. 2002. Dementia with Lewy bodies. *Br J Psychiatry,* 180**,** 144-7.

MCKEITH, I. G., DICKSON, D. W., LOWE, J., EMRE, M., O'BRIEN, J. T., FELDMAN, H., CUMMINGS, J., DUDA, J. E., LIPPA, C., PERRY, E. K., AARSLAND, D., ARAI, H., BALLARD, C. G., BOEVE, B., BURN, D. J., COSTA, D., DEL SER, T., DUBOIS, B., GALASKO, D., GAUTHIER, S., GOETZ, C. G., GOMEZ-TORTOSA, E., HALLIDAY, G., HANSEN, L. A., HARDY, J., IWATSUBO, T., KALARIA, R. N., KAUFER, D., KENNY, R. A., KORCZYN, A., KOSAKA, K., LEE, V. M., LEES, A., LITVAN, I., LONDOS, E., LOPEZ, O. L., MINOSHIMA, S., MIZUNO, Y., MOLINA, J. A., MUKAETOVA-LADINSKA, E. B., PASQUIER, F., PERRY, R. H., SCHULZ, J. B., TROJANOWSKI, J. Q. & YAMADA, M. 2005. Diagnosis and management of dementia with Lewy bodies: third report of the DLB Consortium. *Neurology,* 65**,** 1863-72.

MCKEITH, I. G., GALASKO, D., KOSAKA, K., PERRY, E. K., DICKSON, D. W., HANSEN, L. A., SALMON, D. P., LOWE, J., MIRRA, S. S., BYRNE, E. J., LENNOX, G., QUINN, N. P., EDWARDSON, J. A., INCE, P. G., BERGERON, C., BURNS, A., MILLER, B. L., LOVESTONE, S., COLLERTON, D., JANSEN, E. N., BALLARD, C., DE VOS, R. A., WILCOCK, G. K., JELLINGER, K. A. & PERRY, R. H. 1996. Consensus guidelines for the clinical and pathologic diagnosis of dementia with Lewy bodies (DLB): report of the consortium on DLB international workshop. *Neurology,* 47**,** 1113-24.

MCKHANN, G., DRACHMAN, D., FOLSTEIN, M., KATZMAN, R., PRICE, D. & STADLAN, E. M. 1984. Clinical diagnosis of Alzheimer's disease: report of the NINCDS-ADRDA Work Group under the auspices of Department of Health and Human Services Task Force on Alzheimer's Disease. *Neurology,* 34**,** 939-44.

MCKHANN, G. M., KNOPMAN, D. S., CHERTKOW, H., HYMAN, B. T., JACK, C. R., JR., KAWAS, C. H., KLUNK, W. E., KOROSHETZ, W. J., MANLY, J. J., MAYEUX, R., MOHS, R. C., MORRIS, J. C., ROSSOR, M. N., SCHELTENS, P., CARRILLO, M. C., THIES, B., WEINTRAUB, S. & PHELPS, C. H. 2011. The diagnosis of dementia due to Alzheimer's disease: recommendations from the National Institute on Aging-Alzheimer's Association workgroups on diagnostic guidelines for Alzheimer's disease. *Alzheimers Dement,* 7**,** 263-9.

MCLEAN, C. A., CHERNY, R. A., FRASER, F. W., FULLER, S. J., SMITH, M. J., BEYREUTHER, K., BUSH, A. I. & MASTERS, C. L. 1999. Soluble pool of Abeta amyloid as a determinant of severity of neurodegeneration in Alzheimer's disease. *Ann Neurol,* 46**,** 860-6.

MCNAUGHT, K. S., BELIZAIRE, R., ISACSON, O., JENNER, P. & OLANOW, C. W. 2003. Altered proteasomal function in sporadic Parkinson's disease. *Exp Neurol,* 179**,** 38-46.

MCPARLAND, S., MCALEESE, K., WALKER, L., JOHNSON, M., FIELDER, E., KNOWLES I., ATTEMS J. 2013. Tissue microarray in the quantification of hyperphosphorylated tau, amyloid-beta and alpha-synuclein. *Neuropathology and Applied Neurobiology.*

MEYER, M. R., TSCHANZ, J. T., NORTON, M. C., WELSH-BOHMER, K. A., STEFFENS, D. C., WYSE, B. W. & BREITNER, J. C. 1998. APOE genotype predicts when--not whether--one is predisposed to develop Alzheimer disease. *Nat Genet,* 19**,** 321-2.

MIKI, Y., TOMIYAMA, M., UENO, T., HAGA, R., NISHIJIMA, H., SUZUKI, C., MORI, F., KAIMORI, M., BABA, M. & WAKABAYASHI, K. 2010. Clinical availability of skin biopsy in the diagnosis of Parkinson's disease. *Neurosci Lett,* 469**,** 357-9.

MILBER, J. M., NOORIGIAN, J. V., MORLEY, J. F., PETROVITCH, H., WHITE, L., ROSS, G. W. & DUDA, J. E. 2012. Lewy pathology is not the first sign of degeneration in vulnerable neurons in Parkinson disease. *Neurology,* 79**,** 2307-14.

MILLER, D. L., PAPAYANNOPOULOS, I. A., STYLES, J., BOBIN, S. A., LIN, Y. Y., BIEMANN, K. & IQBAL, K. 1993. Peptide compositions of the cerebrovascular and senile plaque core amyloid deposits of Alzheimer's disease. *Arch Biochem Biophys,* 301**,** 41-52.

MIRRA, S. S., HEYMAN, A., MCKEEL, D., SUMI, S. M., CRAIN, B. J., BROWNLEE, L. M., VOGEL, F. S., HUGHES, J. P., VAN BELLE, G. & BERG, L. 1991. The Consortium to Establish a Registry for Alzheimer's Disease (CERAD). Part II. Standardization of the neuropathologic assessment of Alzheimer's disease. *Neurology,* 41**,** 479-86.

MONTINE, T., PHELPS, C., BEACH, T., BIGIO, E., CAIRNS, N., DICKSON, D., DUYCKAERTS, C., FROSCH, M., MASLIAH, E., MIRRA, S., NELSON, P., SCHNEIDER, J., THAL, D., TROJANOWSKI, J., VINTERS, H. & HYMAN, B. 2012. National Institute on Aging–Alzheimer’s Association guidelines for the neuropathologic assessment of Alzheimer’s disease: a practical approach. *Acta Neuropathologica***,** 1-11.

MORAWSKI, M., HARTLAGE-RUBSAMEN, M., JAGER, C., WANIEK, A., SCHILLING, S., SCHWAB, C., MCGEER, P. L., ARENDT, T., DEMUTH, H. U. & ROSSNER, S. 2010. Distinct glutaminyl cyclase expression in Edinger-

Westphal nucleus, locus coeruleus and nucleus basalis Meynert contributes to pGlu-Abeta pathology in Alzheimer's disease. *Acta Neuropathol,* 120**,** 195-207.

MORI, H., TAKIO, K., OGAWARA, M. & SELKOE, D. J. 1992. Mass spectrometry of purified amyloid beta protein in Alzheimer's disease. *J Biol Chem,* 267**,** 17082-6.

MORLEY, J. E., FARR, S. A., BANKS, W. A., JOHNSON, S. N., YAMADA, K. A. & XU, L. 2010. A physiological role for amyloid-beta protein:enhancement of learning and memory. *J Alzheimers Dis,* 19**,** 441-9.

MORRISON, I. & DOWNING, P. E. 2007. Organization of felt and seen pain responses in anterior cingulate cortex. *Neuroimage,* 37**,** 642-51.

MUFSON, E. J., CHEN, E. Y., COCHRAN, E. J., BECKETT, L. A., BENNETT, D. A. & KORDOWER, J. H. 1999. Entorhinal cortex beta-amyloid load in individuals with mild cognitive impairment. *Exp Neurol,* 158**,** 469-90.

MULLAN, M. & CRAWFORD, F. 1993. Genetic and molecular advances in Alzheimer's disease. *Trends Neurosci,* 16**,** 398-403.

MURRAY, M. E., GRAFF-RADFORD, N. R., ROSS, O. A., PETERSEN, R. C., DUARA, R. & DICKSON, D. W. 2011. Neuropathologically defined subtypes of Alzheimer's disease with distinct clinical characteristics: a retrospective study. *Lancet Neurol,* 10**,** 785-96.

MURRAY, M. E., LOWE, V. J., GRAFF-RADFORD, N. R., LIESINGER, A. M., CANNON, A., PRZYBELSKI, S. A., RAWAL, B., PARISI, J. E., PETERSEN, R. C., KANTARCI, K., ROSS, O. A., DUARA, R., KNOPMAN, D. S., JACK, C. R., JR. & DICKSON, D. W. 2015. Clinicopathologic and 11C-Pittsburgh compound B implications of Thal amyloid phase across the Alzheimer's disease spectrum. *Brain,* 138**,** 1370-81.

NAGATA, K., TAKANO, D., YAMAZAKI, T., MAEDA, T., SATOH, Y., NAKASE, T. & IKEDA, Y. 2012. Cerebrovascular lesions in elderly Japanese patients with Alzheimer's disease. *J Neurol Sci,* 322**,** 87-91.

NAGY, Z., ESIRI, M. M., JOBST, K. A., MORRIS, J. H., KING, E. M., MCDONALD, B., LITCHFIELD, S., SMITH, A., BARNETSON, L. & SMITH, A. D. 1995. Relative roles of plaques and tangles in the dementia of Alzheimer's disease: correlations using three sets of neuropathological criteria. *Dementia,* 6**,** 21-31.

NALLS, M. A., DURAN, R., LOPEZ, G., KURZAWA-AKANBI, M., MCKEITH, I. G., CHINNERY, P. F., MORRIS, C. M., THEUNS, J., CROSIERS, D., CRAS, P., ENGELBORGHS, S., DE DEYN, P. P., VAN BROECKHOVEN, C., MANN, D. M., SNOWDEN, J., PICKERING-BROWN, S., HALLIWELL, N., DAVIDSON, Y., GIBBONS, L., HARRIS, J., SHEERIN, U. M., BRAS, J., HARDY, J., CLARK, L., MARDER, K., HONIG, L. S., BERG, D., MAETZLER, W., BROCKMANN, K., GASSER, T., NOVELLINO, F., QUATTRONE, A., ANNESI, G., DE MARCO, E. V., ROGAEVA, E., MASELLIS, M., BLACK, S. E., BILBAO, J. M., FOROUD, T., GHETTI, B., NICHOLS, W. C., PANKRATZ, N., HALLIDAY, G., LESAGE, S.,

KLEBE, S., DURR, A., DUYCKAERTS, C., BRICE, A., GIASSON, B. I., TROJANOWSKI, J. Q., HURTIG, H. I., TAYEBI, N., LANDAZABAL, C., KNIGHT, M. A., KELLER, M., SINGLETON, A. B., WOLFSBERG, T. G. & SIDRANSKY, E. 2013. A Multicenter Study of Glucocerebrosidase Mutations in Dementia With Lewy Bodies. *JAMA Neurol*, 1-9.

NASLUND, J., HAROUTUNIAN, V., MOHS, R., DAVIS, K. L., DAVIES, P., GREENGARD, P. & BUXBAUM, J. D. 2000. Correlation between elevated levels of amyloid beta-peptide in the brain and cognitive decline. *JAMA,* 283, 1571-7.

NELSON, P. T., ALAFUZOFF, I., BIGIO, E. H., BOURAS, C., BRAAK, H., CAIRNS, N. J., CASTELLANI, R. J., CRAIN, B. J., DAVIES, P., DEL TREDICI, K., DUYCKAERTS, C., FROSCH, M. P., HAROUTUNIAN, V., HOF, P. R., HULETTE, C. M., HYMAN, B. T., IWATSUBO, T., JELLINGER, K. A., JICHA, G. A., KOVARI, E., KUKULL, W. A., LEVERENZ, J. B., LOVE, S., MACKENZIE, I. R., MANN, D. M., MASLIAH, E., MCKEE, A. C., MONTINE, T. J., MORRIS, J. C., SCHNEIDER, J. A., SONNEN, J. A., THAL, D. R., TROJANOWSKI, J. Q., TRONCOSO, J. C., WISNIEWSKI, T., WOLTJER, R. L. & BEACH, T. G. 2012. Correlation of Alzheimer disease neuropathologic changes with cognitive status: a review of the literature. *J Neuropathol Exp Neurol,* 71, 362-81.

NELTNER, J. H., ABNER, E. L., SCHMITT, F. A., DENISON, S. K., ANDERSON, S., PATEL, E. & NELSON, P. T. 2012. Digital pathology and image analysis for robust high-throughput quantitative assessment of Alzheimer disease neuropathologic changes. *J Neuropathol Exp Neurol,* 71, 1075-85.

NORTON, H. W. & NEEL, J. V. 1965. Hardy-Weinberg equilibrium and primitive populations. *Am J Hum Genet,* 17, 91-2.

NUSSBAUM, J. M., SCHILLING, S., CYNIS, H., SILVA, A., SWANSON, E., WANGSANUT, T., TAYLER, K., WILTGEN, B., HATAMI, A., RONICKE, R., REYMANN, K., HUTTER-PAIER, B., ALEXANDRU, A., JAGLA, W., GRAUBNER, S., GLABE, C. G., DEMUTH, H. U. & BLOOM, G. S. 2012. Prion-like behaviour and tau-dependent cytotoxicity of pyroglutamylated amyloid-beta. *Nature,* 485, 651-5.

NYS, G. M., VAN ZANDVOORT, M. J., DE KORT, P. L., JANSEN, B. P., KAPPELLE, L. J. & DE HAAN, E. H. 2005. Restrictions of the Mini-Mental State Examination in acute stroke. *Arch Clin Neuropsychol,* 20, 623-9.

O'BRIEN, J. T., COLLOBY, S., FENWICK, J., WILLIAMS, E. D., FIRBANK, M., BURN, D., AARSLAND, D. & MCKEITH, I. G. 2004. Dopamine transporter loss visualized with FP-CIT SPECT in the differential diagnosis of dementia with Lewy bodies. *Arch Neurol,* 61, 919-25.

O'BRIEN, J. T. & HERHOLZ, K. 2015. Amyloid imaging for dementia in clinical practice. *BMC Med,* 13, 163.

OBI, K., AKIYAMA, H., KONDO, H., SHIMOMURA, Y., HASEGAWA, M., IWATSUBO, T., MIZUNO, Y. & MOCHIZUKI, H. 2008. Relationship of

phosphorylated alpha-synuclein and tau accumulation to Abeta deposition in the cerebral cortex of dementia with Lewy bodies. *Exp Neurol,* 210**,** 409-20.

OHM, T. G., BUSCH, C. & BOHL, J. 1997. Unbiased estimation of neuronal numbers in the human nucleus coeruleus during aging. *Neurobiol Aging,* 18**,** 393-9.

OHRFELT, A., GROGNET, P., ANDREASEN, N., WALLIN, A., VANMECHELEN, E., BLENNOW, K. & ZETTERBERG, H. 2009. Cerebrospinal fluid alpha-synuclein in neurodegenerative disorders-a marker of synapse loss? *Neurosci Lett,* 450**,** 332-5.

OKOCHI, M., WALTER, J., KOYAMA, A., NAKAJO, S., BABA, M., IWATSUBO, T., MEIJER, L., KAHLE, P. J. & HAASS, C. 2000. Constitutive phosphorylation of the Parkinson's disease associated alpha-synuclein. *J Biol Chem,* 275**,** 390-7.

OLANOW, C. W. & MCNAUGHT, K. S. 2006. Ubiquitin-proteasome system and Parkinson's disease. *Mov Disord,* 21**,** 1806-23.

OLANOW, C. W., PERL, D. P., DEMARTINO, G. N. & MCNAUGHT, K. S. 2004. Lewy-body formation is an aggresome-related process: a hypothesis. *Lancet Neurol,* 3**,** 496-503.

OLICHNEY, J. M., GALASKO, D., SALMON, D. P., HOFSTETTER, C. R., HANSEN, L. A., KATZMAN, R. & THAL, L. J. 1998. Cognitive decline is faster in Lewy body variant than in Alzheimer's disease. *Neurology,* 51**,** 351-7.

OLICHNEY, J. M., HANSEN, L. A., HOFSTETTER, C. R., GRUNDMAN, M., KATZMAN, R. & THAL, L. J. 1995. Cerebral infarction in Alzheimer's disease is associated with severe amyloid angiopathy and hypertension. *Arch Neurol,* 52**,** 702-8.

ONITSUKA, T., SHENTON, M. E., SALISBURY, D. F., DICKEY, C. C., KASAI, K., TONER, S. K., FRUMIN, M., KIKINIS, R., JOLESZ, F. A. & MCCARLEY, R. W. 2004. Middle and inferior temporal gyrus gray matter volume abnormalities in chronic schizophrenia: an MRI study. *Am J Psychiatry,* 161**,** 1603-11.

PAPEZ, J. W. 1995. A proposed mechanism of emotion. 1937. *J Neuropsychiatry Clin Neurosci,* 7**,** 103-12.

PARKKINEN, L., KAUPPINEN, T., PIRTTILA, T., AUTERE, J. M. & ALAFUZOFF, I. 2005. Alpha-synuclein pathology does not predict extrapyramidal symptoms or dementia. *Ann Neurol,* 57**,** 82-91.

PARKKINEN, L., O'SULLIVAN, S. S., COLLINS, C., PETRIE, A., HOLTON, J. L., REVESZ, T. & LEES, A. J. 2011. Disentangling the relationship between lewy bodies and nigral neuronal loss in Parkinson's disease. *J Parkinsons Dis,* 1**,** 277-86.

PARKKINEN, L., PIRTTILA, T. & ALAFUZOFF, I. 2008. Applicability of current staging/categorization of alpha-synuclein pathology and their clinical relevance. *Acta Neuropathol,* 115**,** 399-407.

PARNETTI, L., TIRABOSCHI, P., LANARI, A., PEDUCCI, M., PADIGLIONI, C., D'AMORE, C., PIERGUIDI, L., TAMBASCO, N., ROSSI, A. & CALABRESI, P. 2008. Cerebrospinal fluid biomarkers in Parkinson's disease with dementia and dementia with Lewy bodies. *Biol Psychiatry,* 64**,** 850-5.

PEI, J. J., GRUNDKE-IQBAL, I., IQBAL, K., BOGDANOVIC, N., WINBLAD, B. & COWBURN, R. F. 1998. Accumulation of cyclin-dependent kinase 5 (cdk5) in neurons with early stages of Alzheimer's disease neurofibrillary degeneration. *Brain Res,* 797**,** 267-77.

PEREZ, S. E., LAZAROV, O., KOPRICH, J. B., CHEN, E. Y., RODRIGUEZ-MENENDEZ, V., LIPTON, J. W., SISODIA, S. S. & MUFSON, E. J. 2005. Nigrostriatal dysfunction in familial Alzheimer's disease-linked APPswe/ PS1DeltaE9 transgenic mice. *J Neurosci,* 25**,** 10220-9.

PERNEGER, T. V. 1998. What's wrong with Bonferroni adjustments. *Bmj,* 316**,** 1236-8.

PERRY, R. H. & OAKLEY, A. E. 1993. Coronal map of Brodmann areas in the human brian. *In:* ROBERTS, G. W., LEIGH, N. & WEINBERGER, D. R. (eds.) *Neuropsychiatric Disorders.* London: Wolfe.

PETROVITCH, H., ROSS, G. W., STEINHORN, S. C., ABBOTT, R. D., MARKESBERY, W., DAVIS, D., NELSON, J., HARDMAN, J., MASAKI, K., VOGT, M. R., LAUNER, L. & WHITE, L. R. 2005. AD lesions and infarcts in demented and non-demented Japanese-American men. *Ann Neurol,* 57**,** 98-103.

PEYRIN, J. M., LASMEZAS, C. I., HAIK, S., TAGLIAVINI, F., SALMONA, M., WILLIAMS, A., RICHIE, D., DESLYS, J. P. & DORMONT, D. 1999. Microglial cells respond to amyloidogenic PrP peptide by the production of inflammatory cytokines. *Neuroreport,* 10**,** 723-9.

PHELPS, E. A. 2004. Human emotion and memory: interactions of the amygdala and hippocampal complex. *Curr Opin Neurobiol,* 14**,** 198-202.
PLETNIKOVA, O., WEST, N., LEE, M. K., RUDOW, G. L., SKOLASKY, R. L., DAWSON, T. M., MARSH, L. & TRONCOSO, J. C. 2005. Abeta deposition is associated with enhanced cortical alpha-synuclein lesions in Lewy body diseases. *Neurobiol Aging,* 26**,** 1183-92.

POLYMENIDOU, M., LAGIER-TOURENNE, C., HUTT, K. R., HUELGA, S. C., MORAN, J., LIANG, T. Y., LING, S. C., SUN, E., WANCEWICZ, E., MAZUR, C., KORDASIEWICZ, H., SEDAGHAT, Y., DONOHUE, J. P., SHIUE, L., BENNETT, C. F., YEO, G. W. & CLEVELAND, D. W. 2011. Long pre-mRNA depletion and RNA missplicing contribute to neuronal vulnerability from loss of TDP-43. *Nat Neurosci,* 14**,** 459-68.

POSTUMA, R. B. 2014. Prodromal Parkinson's disease - Using REM sleep behavior disorder as a window. *Parkinsonism Relat Disord,* 20 Suppl 1**,** S1-4.

POSTUMA, R. B., AARSLAND, D., BARONE, P., BURN, D. J., HAWKES, C. H., OERTEL, W. & ZIEMSSEN, T. 2012. Identifying prodromal Parkinson's disease: pre-motor disorders in Parkinson's disease. *Mov Disord,* 27**,** 617-26.

PRELLI, F., CASTANO, E., GLENNER, G. G. & FRANGIONE, B. 1988. Differences between vascular and plaque core amyloid in Alzheimer's disease. *J Neurochem,* 51**,** 648-51.

PRINCE, M., BRYCE, R., ALBANESE, E., WIMO, A., RIBEIRO, W. & FERRI, C. P. 2013. The global prevalence of dementia: a systematic review and metaanalysis. *Alzheimers Dement,* 9**,** 63-75 e2.

PRINCE, M. J., J. 2009. World Alzheimer's report 2009. London: Alzheimer's disease International.

PRINCE, M. J., WU, F., GUO, Y., GUTIERREZ ROBLEDO, L. M., O'DONNELL, M., SULLIVAN, R. & YUSUF, S. 2015. The burden of disease in older people and implications for health policy and practice. *Lancet,* 385**,** 549-62.
RAHIMI, J. & KOVACS, G. G. 2014. Prevalence of mixed pathologies in the aging brain. *Alzheimers Res Ther,* 6**,** 82.

RAKSHI, J. S., UEMA, T., ITO, K., BAILEY, D. L., MORRISH, P. K., ASHBURNER, J., DAGHER, A., JENKINS, I. H., FRISTON, K. J. & BROOKS, D. J. 1999. Frontal, midbrain and striatal dopaminergic function in early and advanced Parkinson's disease A 3D [(18)F]dopa-PET study. *Brain,* 122 (Pt 9)**,** 1637-50.

RAO, G., FISCH, L., SRINIVASAN, S., D'AMICO, F., OKADA, T., EATON, C. & ROBBINS, C. 2003. Does this patient have Parkinson disease? *JAMA,* 289**,** 347-53.

REESINK, F. E., LEMSTRA, A. W., VAN DIJK, K. D., BERENDSE, H. W., VAN DE BERG, W. D., KLEIN, M., BLANKENSTEIN, M. A., SCHELTENS, P., VERBEEK, M. M. & VAN DER FLIER, W. M. 2010. CSF alpha-synuclein does not discriminate dementia with Lewy bodies from Alzheimer's disease. *J Alzheimers Dis,* 22**,** 87-95.
REVESZ, T., GHISO, J., LASHLEY, T., PLANT, G., ROSTAGNO, A., FRANGIONE, B. & HOLTON, J. L. 2003. Cerebral amyloid angiopathies: a pathologic, biochemical, and genetic view. *J Neuropathol Exp Neurol,* 62**,** 885-98.

RIZZARDI, A. E., JOHNSON, A. T., VOGEL, R. I., PAMBUCCIAN, S. E., HENRIKSEN, J., SKUBITZ, A. P., METZGER, G. J. & SCHMECHEL, S. C. 2012. Quantitative comparison of immunohistochemical staining measured by digital image analysis versus pathologist visual scoring. *Diagn Pathol,* 7**,** 42.

ROBINSON, J. L., GESER, F., CORRADA, M. M., BERLAU, D. J., ARNOLD, S. E., LEE, V. M., KAWAS, C. H. & TROJANOWSKI, J. Q. 2011. Neocortical and hippocampal amyloid-beta and tau measures associate with dementia in the oldest-old. *Brain,* 134**,** 3708-15.

ROGERS, J. & MORRISON, J. H. 1985. Quantitative morphology and regional and laminar distributions of senile plaques in Alzheimer's disease. *J Neurosci,* 5**,** 2801-8.

ROTHMAN, K. J. 1990. No adjustments are needed for multiple comparisons. *Epidemiology,* 1**,** 43-6.

RUBINSZTEIN, D. C. 2006. The roles of intracellular protein-degradation pathways in neurodegeneration. *Nature,* 443**,** 780-6.

RUI, Y., TIWARI, P., XIE, Z. & ZHENG, J. Q. 2006. Acute impairment of mitochondrial trafficking by beta-amyloid peptides in hippocampal neurons. *J Neurosci,* 26**,** 10480-7.

RUSSO, C., VIOLANI, E., SALIS, S., VENEZIA, V., DOLCINI, V., DAMONTE, G., BENATTI, U., D'ARRIGO, C., PATRONE, E., CARLO, P. & SCHETTINI, G. 2002. Pyroglutamate-modified amyloid beta-peptides--AbetaN3(pE)--strongly affect cultured neuron and astrocyte survival. *J Neurochem,* 82**,** 1480-9.

SAITO, Y., KAWASHIMA, A., RUBERU, N. N., FUJIWARA, H., KOYAMA, S., SAWABE, M., ARAI, T., NAGURA, H., YAMANOUCHI, H., HASEGAWA, M., IWATSUBO, T. & MURAYAMA, S. 2003. Accumulation of phosphorylated alpha-synuclein in aging human brain. *J Neuropathol Exp Neurol,* 62**,** 644-54.

SAMUELS, E. R. & SZABADI, E. 2008. Functional neuroanatomy of the noradrenergic locus coeruleus: its roles in the regulation of arousal and autonomic function part II: physiological and pharmacological manipulations and pathological alterations of locus coeruleus activity in humans. *Curr Neuropharmacol,* 6**,** 254-85.

SAVICA, R., GROSSARDT, B. R., BOWER, J. H., BOEVE, B. F., AHLSKOG, J. E. & ROCCA, W. A. 2013. Incidence of dementia with Lewy bodies and Parkinson disease dementia. *JAMA Neurol,* 70**,** 1396-402.

SCHEFF, S. W., PRICE, D. A. & SPARKS, D. L. 2001. Quantitative assessment of possible age-related change in synaptic numbers in the human frontal cortex. *Neurobiol Aging,* 22**,** 355-65.

SCHELTENS, P., BLENNOW, K., BRETELER, M. M., DE STROOPER, B., FRISONI, G. B., SALLOWAY, S. & VAN DER FLIER, W. M. 2016. Alzheimer's disease. *Lancet*. (epub ahead of print)

SCHEUNER, D., ECKMAN, C., JENSEN, M., SONG, X., CITRON, M., SUZUKI, N., BIRD, T. D., HARDY, J., HUTTON, M., KUKULL, W., LARSON, E., LEVY-LAHAD, E., VIITANEN, M., PESKIND, E., POORKAJ, P., SCHELLENBERG, G., TANZI, R., WASCO, W., LANNFELT, L., SELKOE, D. & YOUNKIN, S. 1996. Secreted amyloid beta-protein similar to that in the senile plaques of Alzheimer's disease is increased in vivo by the presenilin 1 and 2 and APP mutations linked to familial Alzheimer's disease. *Nat Med,* 2**,** 864-70.

SCHILLING, S., LAUBER, T., SCHAUPP, M., MANHART, S., SCHEEL, E., BOHM, G. & DEMUTH, H. U. 2006. On the seeding and oligomerization of pGlu-amyloid peptides (in vitro). *Biochemistry,* 45**,** 12393-9.

SCHNEIDER, J. A., AGGARWAL, N. T., BARNES, L., BOYLE, P. & BENNETT, D. A. 2009. The neuropathology of older persons with and without dementia from community versus clinic cohorts. *J Alzheimers Dis,* 18**,** 691-701.

SCHNEIDER, J. A., ARVANITAKIS, Z., BANG, W. & BENNETT, D. A. 2007. Mixed brain pathologies account for most dementia cases in community-dwelling older persons. *Neurology,* 69**,** 2197-204.

SCHNEIDER, J. A., ARVANITAKIS, Z., YU, L., BOYLE, P. A., LEURGANS, S. E. & BENNETT, D. A. 2012. Cognitive impairment, decline and fluctuations in older community-dwelling subjects with Lewy bodies. *Brain,* 135**,** 3005-14.

SCHULZ-SCHAEFFER, W. J. 2010. The synaptic pathology of alpha-synuclein aggregation in dementia with Lewy bodies, Parkinson's disease and Parkinson's disease dementia. *Acta Neuropathol,* 120**,** 131-43.

SELIKHOVA, M., WILLIAMS, D. R., KEMPSTER, P. A., HOLTON, J. L., REVESZ, T. & LEES, A. J. 2009. A clinico-pathological study of subtypes in Parkinson's disease. *Brain,* 132**,** 2947-57.

SELKOE, D. J. 2000. Toward a comprehensive theory for Alzheimer's disease. Hypothesis: Alzheimer's disease is caused by the cerebral accumulation and cytotoxicity of amyloid beta-protein. *Ann N Y Acad Sci,* 924**,** 17-25.
SELKOE, D. J. 2001a. Alzheimer's disease results from the cerebral accumulation and cytotoxicity of amyloid beta-protein. *J Alzheimers Dis,* 3**,** 75-80.

SELKOE, D. J. 2001b. Alzheimer's disease: genes, proteins, and therapy. *Physiol Rev,* 81**,** 741-66.

SELKOE, D. J. 2004. Cell biology of protein misfolding: the examples of Alzheimer's and Parkinson's diseases. *Nat Cell Biol,* 6**,** 1054-61.

SERBY, M., BRICKMAN, A. M., HAROUTUNIAN, V., PUROHIT, D. P., MARIN, D., LANTZ, M., MOHS, R. C. & DAVIS, K. L. 2003. Cognitive burden and excess Lewy-body pathology in the Lewy-body variant of Alzheimer disease. *Am J Geriatr Psychiatry,* 11**,** 371-4.

SERPELL, L. C., BERRIMAN, J., JAKES, R., GOEDERT, M. & CROWTHER, R. A. 2000. Fiber diffraction of synthetic alpha-synuclein filaments shows amyloid-like cross-beta conformation. *Proc Natl Acad Sci U S A,* 97**,** 4897-902.

SHANKAR, G. M., LI, S., MEHTA, T. H., GARCIA-MUNOZ, A., SHEPARDSON, N. E., SMITH, I., BRETT, F. M., FARRELL, M. A., ROWAN, M. J., LEMERE, C. A., REGAN, C. M., WALSH, D. M., SABATINI, B. L. & SELKOE, D. J. 2008. Amyloid-beta protein dimers isolated directly from Alzheimer's brains impair synaptic plasticity and memory. *Nat Med,* 14**,** 837-42.

SHI, M., BRADNER, J., HANCOCK, A. M., CHUNG, K. A., QUINN, J. F., PESKIND, E. R., GALASKO, D., JANKOVIC, J., ZABETIAN, C. P., KIM, H. M., LEVERENZ, J. B., MONTINE, T. J., GINGHINA, C., KANG, U. J., CAIN, K. C.,

WANG, Y., AASLY, J., GOLDSTEIN, D. & ZHANG, J. 2011. Cerebrospinal fluid biomarkers for Parkinson disease diagnosis and progression. *Ann Neurol,* 69**,** 570-80.

SINGLETON, A. B., WHARTON, A., O'BRIEN, K. K., WALKER, M. P., MCKEITH, I. G., BALLARD, C. G., O'BRIEN, J., PERRY, R. H., INCE, P. G., EDWARDSON, J. A. & MORRIS, C. M. 2002. Clinical and neuropathological correlates of apolipoprotein E genotype in dementia with Lewy bodies. *Dement Geriatr Cogn Disord,* 14**,** 167-75.

SKOOG, I., KALARIA, R. N. & BRETELER, M. M. 1999. Vascular factors and Alzheimer disease. *Alzheimer Dis Assoc Disord,* 13 Suppl 3**,** S106-14.

SMID, L. M., KEPE, V., VINTERS, H. V., BRESJANAC, M., TOYOKUNI, T., SATYAMURTHY, N., WONG, K. P., HUANG, S. C., SILVERMAN, D. H., MILLER, K., SMALL, G. W. & BARRIO, J. R. 2013. Postmortem 3-D Brain Hemisphere Cortical Tau and Amyloid-beta Pathology Mapping and Quantification as a Validation Method of Neuropathology Imaging. *J Alzheimers Dis*.

SMITH, E. E. & JONIDES, J. 1999. Storage and executive processes in the frontal lobes. *Science,* 283**,** 1657-61.

SNOWDON, D. A. 2003. Healthy aging and dementia: findings from the Nun Study. *Ann Intern Med,* 139**,** 450-4.

SONNEN, J. A., POSTUPNA, N., LARSON, E. B., CRANE, P. K., ROSE, S. E., MONTINE, K. S., LEVERENZ, J. B. & MONTINE, T. J. 2010. Pathologic correlates of dementia in individuals with Lewy body disease. *Brain Pathol,* 20**,** 654-9.

SOTO, C. 2003. Unfolding the role of protein misfolding in neurodegenerative diseases. *Nat Rev Neurosci,* 4**,** 49-60.

SPERBER, B. R., LEIGHT, S., GOEDERT, M. & LEE, V. M. 1995. Glycogen synthase kinase-3 beta phosphorylates tau protein at multiple sites in intact cells. *Neurosci Lett,* 197**,** 149-53.

SPILLANTINI, M. G., CROWTHER, R. A., JAKES, R., HASEGAWA, M. & GOEDERT, M. 1998. alpha-Synuclein in filamentous inclusions of Lewy bodies from Parkinson's disease and dementia with lewy bodies. *Proc Natl Acad Sci U S A,* 95**,** 6469-73.

SPILLANTINI, M. G., SCHMIDT, M. L., LEE, V. M., TROJANOWSKI, J. Q., JAKES, R. & GOEDERT, M. 1997. Alpha-synuclein in Lewy bodies. *Nature,* 388**,** 839-40.

SQUIRE, L. R., STARK, C. E. & CLARK, R. E. 2004. The medial temporal lobe. *Annu Rev Neurosci,* 27**,** 279-306.

STERN, Y. 2006. Cognitive reserve and Alzheimer disease. *Alzheimer Dis Assoc Disord,* 20**,** S69-74.

STRITTMATTER, W. J., SAUNDERS, A. M., SCHMECHEL, D., PERICAK-VANCE, M., ENGHILD, J., SALVESEN, G. S. & ROSES, A. D. 1993. Apolipoprotein E: high-avidity binding to beta-amyloid and increased frequency of type 4 allele in late-onset familial Alzheimer disease. *Proc Natl Acad Sci U S A,* 90**,** 1977-81.

STUBENDORFF, K., HANSSON, O., MINTHON, L. & LONDOS, E. 2011. Differences in survival between patients with dementia with Lewy bodies and patients with Alzheimer's disease--measured from a fixed cognitive level. *Dement Geriatr Cogn Disord,* 32**,** 408-16.

STUSS, D. T. 2011. Functions of the frontal lobes: relation to executive functions. *J Int Neuropsychol Soc,* 17**,** 759-65.

STUSS, D. T. & ALEXANDER, M. P. 2000. Executive functions and the frontal lobes: a conceptual view. *Psychol Res,* 63**,** 289-98.

SWANSON, L. W. 2003. The amygdala and its place in the cerebral hemisphere. *Ann N Y Acad Sci,* 985**,** 174-84.

SWIRSKI, M., MINERS, J. S., DE SILVA, R., LASHLEY, T., LING, H., HOLTON, J., REVESZ, T. & LOVE, S. 2014. Evaluating the relationship between amyloid-beta and alpha-synuclein phosphorylated at Ser129 in dementia with Lewy bodies and Parkinson's disease. *Alzheimers Res Ther,* 6**,** 77.

TAKAHASHI, M., ISEKI, E. & KOSAKA, K. 2000. Cyclin-dependent kinase 5 (Cdk5) associated with Lewy bodies in diffuse Lewy body disease. *Brain Res,* 862**,** 253-6.

TERRY, R. D., MASLIAH, E., SALMON, D. P., BUTTERS, N., DETERESA, R., HILL, R., HANSEN, L. A. & KATZMAN, R. 1991. Physical basis of cognitive alterations in Alzheimer's disease: synapse loss is the major correlate of cognitive impairment. *Ann Neurol,* 30**,** 572-80.

THAL, D. R., GHEBREMEDHIN, E., RUB, U., YAMAGUCHI, H., DEL TREDICI, K. & BRAAK, H. 2002a. Two types of sporadic cerebral amyloid angiopathy. *J Neuropathol Exp Neurol,* 61**,** 282-93.

THAL, D. R., RUB, U., ORANTES, M. & BRAAK, H. 2002b. Phases of A beta-deposition in the human brain and its relevance for the development of AD. *Neurology,* 58**,** 1791-800.

THAL, D. R., RUB, U., SCHULTZ, C., SASSIN, I., GHEBREMEDHIN, E., DEL TREDICI, K., BRAAK, E. & BRAAK, H. 2000. Sequence of Abeta-protein deposition in the human medial temporal lobe. *J Neuropathol Exp Neurol,* 59**,** 733-48.

THAL, D. R., WALTER, J., SAIDO, T. C. & FANDRICH, M. 2015. Neuropathology and biochemistry of Abeta and its aggregates in Alzheimer's disease. *Acta Neuropathol,* 129**,** 167-82.

TOMLINSON, B. E., BLESSED, G. & ROTH, M. 1970. Observations on the brains of demented old people. *J Neurol Sci,* 11**,** 205-42.

TSUANG, D. W., WILSON, R. K., LOPEZ, O. L., LUEDECKING-ZIMMER, E. K., LEVERENZ, J. B., DEKOSKY, S. T., KAMBOH, M. I. & HAMILTON, R. L. 2005. Genetic association between the APOE*4 allele and Lewy bodies in Alzheimer disease. *Neurology,* 64**,** 509-13.

UCHIHARA, T. 2014. Pretangles and neurofibrillary changes: similarities and differences between AD and CBD based on molecular and morphological evolution. *Neuropathology,* 34**,** 571-7.

UCHIKADO, H., LIN, W. L., DELUCIA, M. W. & DICKSON, D. W. 2006. Alzheimer disease with amygdala Lewy bodies: a distinct form of alpha-synucleinopathy. *J Neuropathol Exp Neurol,* 65**,** 685-97.

VAN DIJK, K. D., BIDINOSTI, M., WEISS, A., RAIJMAKERS, P., BERENDSE, H. W. & VAN DE BERG, W. D. 2014. Reduced alpha-synuclein levels in cerebrospinal fluid in Parkinson's disease are unrelated to clinical and imaging measures of disease severity. *Eur J Neurol,* 21**,** 388-94.

VANN JONES, S. A. & O'BRIEN, J. T. 2014. The prevalence and incidence of dementia with Lewy bodies: a systematic review of population and clinical studies. *Psychol Med,* 44**,** 673-83.

VENDA, L. L., CRAGG, S. J., BUCHMAN, V. L. & WADE-MARTINS, R. 2010. alpha-Synuclein and dopamine at the crossroads of Parkinson's disease. *Trends Neurosci,* 33**,** 559-68.

VERGHESE, P. B., CASTELLANO, J. M. & HOLTZMAN, D. M. 2011. Apolipoprotein E in Alzheimer's disease and other neurological disorders. *Lancet Neurol,* 10**,** 241-52.

VINCENT, I., JICHA, G., ROSADO, M. & DICKSON, D. W. 1997. Aberrant expression of mitotic cdc2/cyclin B1 kinase in degenerating neurons of Alzheimer's disease brain. *J Neurosci,* 17**,** 3588-98.

VOLLES, M. J., LEE, S. J., ROCHET, J. C., SHTILERMAN, M. D., DING, T. T., KESSLER, J. C. & LANSBURY, P. T., JR. 2001. Vesicle permeabilization by protofibrillar alpha-synuclein: implications for the pathogenesis and treatment of Parkinson's disease. *Biochemistry,* 40**,** 7812-9.

VONSATTEL, J. P., MYERS, R. H., HEDLEY-WHYTE, E. T., ROPPER, A. H., BIRD, E. D. & RICHARDSON, E. P., JR. 1991. Cerebral amyloid angiopathy without and with cerebral hemorrhages: a comparative histological study. *Ann Neurol,* 30**,** 637-49.

WALKER, D. G., LUE, L. F., ADLER, C. H., SHILL, H. A., CAVINESS, J. N., SABBAGH, M. N., AKIYAMA, H., SERRANO, G. E., SUE, L. I. & BEACH, T. G. 2013. Changes in properties of serine 129 phosphorylated alpha-synuclein with progression of Lewy-type histopathology in human brains. *Exp Neurol,* 240**,** 190-204.

WANG, X., PERRY, G., SMITH, M. A. & ZHU, X. 2010. Amyloid-beta-derived diffusible ligands cause impaired axonal transport of mitochondria in neurons. *Neurodegener Dis,* 7**,** 56-9.

WATSON, R., COLLOBY, S. J., BLAMIRE, A. M. & O'BRIEN, J. T. 2014. Assessment of Regional Gray Matter Loss in Dementia with Lewy Bodies: A Surface-Based MRI Analysis. *Am J Geriatr Psychiatry*.

WATTS, R. L. & MANDIR, A. S. 1992. The role of motor cortex in the pathophysiology of voluntary movement deficits associated with parkinsonism. *Neurol Clin,* 10**,** 451-69.

WAXMAN, E. A. & GIASSON, B. I. 2011. Induction of intracellular tau aggregation is promoted by alpha-synuclein seeds and provides novel insights into the hyperphosphorylation of tau. *J Neurosci,* 31**,** 7604-18.

WEBB, J. L., RAVIKUMAR, B., ATKINS, J., SKEPPER, J. N. & RUBINSZTEIN, D. C. 2003. Alpha-Synuclein is degraded by both autophagy and the proteasome. *J Biol Chem,* 278**,** 25009-13.

WELLER, R. O., DJUANDA, E., YOW, H. Y. & CARARE, R. O. 2009. Lymphatic drainage of the brain and the pathophysiology of neurological disease. *Acta Neuropathol,* 117**,** 1-14.

WELLER, R. O., MASSEY, A., KUO, Y. M. & ROHER, A. E. 2000. Cerebral amyloid angiopathy: accumulation of A beta in interstitial fluid drainage pathways in Alzheimer's disease. *Ann N Y Acad Sci,* 903**,** 110-7.

WHEELER, M. E. & BUCKNER, R. L. 2004. Functional-anatomic correlates of remembering and knowing. *Neuroimage,* 21**,** 1337-49.

WHITFIELD, D. R., VALLORTIGARA, J., ALGHAMDI, A., HOWLETT, D., HORTOBAGYI, T., JOHNSON, M., ATTEMS, J., NEWHOUSE, S., BALLARD, C., THOMAS, A. J., O'BRIEN, J. T., AARSLAND, D. & FRANCIS, P. T. 2014. Assessment of ZnT3 and PSD95 protein levels in Lewy body dementias and Alzheimer's disease: association with cognitive impairment. *Neurobiol Aging,* 35**,** 2836-44.

WHITWELL, J. L., DICKSON, D. W., MURRAY, M. E., WEIGAND, S. D., TOSAKULWONG, N., SENJEM, M. L., KNOPMAN, D. S., BOEVE, B. F., PARISI, J. E., PETERSEN, R. C., JACK, C. R., JR. & JOSEPHS, K. A. 2012. Neuroimaging correlates of pathologically defined subtypes of Alzheimer's disease: a case-control study. *Lancet Neurol,* 11**,** 868-77.

WILLIAMS, M. M., XIONG, C., MORRIS, J. C. & GALVIN, J. E. 2006. Survival and mortality differences between dementia with Lewy bodies vs Alzheimer disease. *Neurology,* 67**,** 1935-41.

WIRTHS, O., BREYHAN, H., CYNIS, H., SCHILLING, S., DEMUTH, H. U. & BAYER, T. A. 2009. Intraneuronal pyroglutamate-Abeta 3-42 triggers

neurodegeneration and lethal neurological deficits in a transgenic mouse model. *Acta Neuropathol,* 118**,** 487-96.

WITTNAM, J. L., PORTELIUS, E., ZETTERBERG, H., GUSTAVSSON, M. K., SCHILLING, S., KOCH, B., DEMUTH, H. U., BLENNOW, K., WIRTHS, O. & BAYER, T. A. 2012. Pyroglutamate amyloid beta (Abeta) aggravates behavioral deficits in transgenic amyloid mouse model for Alzheimer disease. *J Biol Chem,* 287**,** 8154-62.

WONG, K., SIDRANSKY, E., VERMA, A., MIXON, T., SANDBERG, G. D., WAKEFIELD, L. K., MORRISON, A., LWIN, A., COLEGIAL, C., ALLMAN, J. M. & SCHIFFMANN, R. 2004. Neuropathology provides clues to the pathophysiology of Gaucher disease. *Mol Genet Metab,* 82**,** 192-207.

WORLD HEALTH ORGANISATION AND ALZHEIMER'S DISEASE INTERNATIONAL 2012. Dementia: a public health priority. Geneva, Switzerland: World Health Organisation.

WYSS-CORAY, T. & MUCKE, L. 2002. Inflammation in neurodegenerative disease--a double-edged sword. *Neuron,* 35**,** 419-32.

WYSS-CORAY, T., YAN, F., LIN, A. H., LAMBRIS, J. D., ALEXANDER, J. J., QUIGG, R. J. & MASLIAH, E. 2002. Prominent neurodegeneration and increased plaque formation in complement-inhibited Alzheimer's mice. *Proc Natl Acad Sci U S A,* 99**,** 10837-42.

XU, Z. S. 2012. Does a loss of TDP-43 function cause neurodegeneration? *Mol Neurodegener,* 7**,** 27.

YAMAGUCHI, H., SUGIHARA, S., OGAWA, A., OSHIMA, N. & IHARA, Y. 2001. Alzheimer beta amyloid deposition enhanced by apoE epsilon4 gene precedes neurofibrillary pathology in the frontal association cortex of nondemented senior subjects. *J Neuropathol Exp Neurol,* 60**,** 731-9.

YATES, S. L., BURGESS, L. H., KOCSIS-ANGLE, J., ANTAL, J. M., DORITY, M. D., EMBURY, P. B., PIOTRKOWSKI, A. M. & BRUNDEN, K. R. 2000. Amyloid beta and amylin fibrils induce increases in proinflammatory cytokine and chemokine production by THP-1 cells and murine microglia. *J Neurochem,* 74**,** 1017-25.

YORK, D. H. 1970. Possible dopaminergic pathway from substantia nigra to putamen. *Brain Res,* 20**,** 233-49.

YOSHIYAMA, Y., HIGUCHI, M., ZHANG, B., HUANG, S. M., IWATA, N., SAIDO, T. C., MAEDA, J., SUHARA, T., TROJANOWSKI, J. Q. & LEE, V. M. 2007. Synapse loss and microglial activation precede tangles in a P301S tauopathy mouse model. *Neuron,* 53**,** 337-51.

ZHAO, X. L., WANG, W. A., TAN, J. X., HUANG, J. K., ZHANG, X., ZHANG, B. Z., WANG, Y. H., YANGCHENG, H. Y., ZHU, H. L., SUN, X. J. & HUANG, F. D. 2010. Expression of beta-amyloid induced age-dependent presynaptic and axonal changes in Drosophila. *J Neurosci,* 30**,** 1512-22.